Investigation and Disruption of *Baker's Yeast / Chlorella Vulgaris* in High-Pressure Homogenizer (HPH) to Improve Cost-Effective Protein Yield

A thesis submitted for the degree of

Doctor of Philosophy

by

LEONARD EGHOSA NKEM EKPENI

[B.ENG. (HONS), M.SC., MIEI, AMIMECHE]

School of Mechanical and Manufacturing Engineering

Faculty of Engineering and Computing

Dublin City University

September 2015

Supervisors

Prof Abdul-Ghani Olabi

Dr Joseph Stokes

PhD   2015

Preface

This thesis describes original work which has not previously been submitted for a degree in Dublin City University or at any other University. The investigations were carried out in the School of Mechanical and Manufacturing Engineering, Dublin City University, during the period October 2010 to December 2014, under the supervision of Prof Abdul-Ghani Olabi and Dr Joseph Stokes. This work has been disseminated through the following publications.

Journal Articles/Publication

Journal Articles:

1. **Ekpeni, L. E. N.,** Benyounis, K. Y., Nkem-Ekpeni, Fehintola F., Stokes, J., Olabi, A.G., (2015). Underlying factors to consider in improving energy yield from biomass source through yeast use on high-pressure homogenizer (HPH), ***Energy,*** *Volume 81, 2015, pp. 74-83,* ISSN 0360-5442, *DOI:10.1016/j.energy.2014.11.038*

2. **Ekpeni, L. E. N.**, Nkem-Ekpeni, F. F., Benyounis, K. Y., Aboderheeba, A. K. M., Stokes, J., Olabi, A. G. (2014). Yeast: A Potential Biomass Substrate for the Production of Cleaner Energy (Biogas). ***Energy Procedia,*** *Volume 61, 2014, pp. 1718-1731* *DOI:10.1016/j.egypro.2014.12.199*

3. **Ekpeni, L. E. N.,** Benyounis, K. Y., Nkem-Ekpeni, F. F., Stokes, J., Olabi, A. G. (2014), Energy Diversity through Renewable Energy Source (RES) – A Case Study of Biomass. ***Energy Procedia,*** *Volume 61, 2014, pp. 1740-1747* *DOI:10.1016/j.egypro.2014.12.202*

4. **Ekpeni, L. E. N** and Olabi, A. G. (2013). A Change in the Transportation Needs Today, a Better Future for Tomorrow: Climate Change Review. In *Causes, Impacts and Solutions to Global Warming. Part II* (pp. 933-947). ***Springer New York,*** *DOI 10.1007/978-1-4614-7588-0_49* (Online ISBN 978-1-4614-7588-0)

5. **Ekpeni, L. E. N** and Olabi, A. G., (2012). Energy Sustainability – An Issue for Today. *Journal of Sustainable Development and Environmental Protection, 2 (2),* Apr – Jun. 2012. ***ierdafrica.org.***

6. **Ekpeni, L. E. N.,** Benyounis, K. Y., Stokes, J., and Olabi, A. G, Improved disruption technique for biomass substrates using high-pressure homogenizer (HPH) as an efficient means for protein production *(Submitted to Applied Energy Journal - Elsevier)*

7. **Ekpeni, L. E. N.,** Benyounis, K. Y., Stokes, J., and Olabi, A. G, Baker's yeast homogenization - An effective energy conversion process for higher protein concentration yield *(Submitted to Energy Conversion and Management Journal - Elsevier)*

International Conference Papers:

1. **Ekpeni, L. E. N.** and Olabi, A. G., Biogas Improvement Through Yeast Use in High-Pressure Homogenizer, 3rd International Symposium on Environmental Management (SEM2011), Zagreb, Croatia, October 26 – 28, 2011.

2. **Ekpeni, L. E. N.,** and Olabi, A. G., (2012). Energy Sustainability – An Issue for Today. 2012 International Conference on Sustainable Development and Environmental Protection. Bell University of Technology, Ota near Lagos, Nigeria, March 20 – 22, 2012.

3. **Ekpeni, L. E. N.,** Benyounis, K. Y., and Olabi, A. G., Gap Sizes Effects on Homogenized Yeast and its Efficiency on Biogas Production. DCU 5th International Conference on Sustainable Energy and Environmental Protection (SEEP 2012), Dublin City University, Dublin, Ireland, June 5 – 8, 2012.

4. **Ekpeni, L. E. N** and Olabi, A. G. A Change in the Transportation Needs Today, a Better Future for Tomorrow - Climate Change Review. Global Conference on Global Warming (GCGW-12), Istanbul Technical University, Maslak, Istanbul, Turkey, July 8 -12, 2012.

5. **Ekpeni, L. E. N.,** Nkem-Ekpeni, F. F., and Olabi, A. G., Climate change effects and its continuous environmental impacts on the developing nations, World Climate 2013 World Conference on Climate Change and Humanity, Vienna, Austria, May 25 – 26, 2013

6. **Ekpeni, L. E. N.,** Benyounis, K. Y., Nkem-Ekpeni, F. F., Aidarous, H., and Olabi, A. G., Viscosity of Yeast Suspension and the Effect of its Flow Rate in High Pressure Homogenizer (HPH), CLIMA 2013 - 11th REHVA World Congress and the 8th International Conference on Indoor Air Quality, Ventilation and Energy

Conservation in Buildings (IAQVEC), Prague, Czech Republic, June 16 – 19, 2013.

7. **Ekpeni, L. E. N.,** Benyounis, K. Y., Stokes, J., and Olabi, A. G., Underlying Factors to Consider in Improving Energy Yield from Biomass Source through Yeast Use on High-Pressure Homogenizer (HPH), 6th International Conference on Sustainable Energy and Environmental Protection (SEEP) 2013, Maribor, Slovenia, August 20 – 23, 2013.

8. **Ekpeni, L. E. N.,** Bobadilla, M. C., González, E. P. V., and Lostado Lorza, R., Modification and Partial Elimination of Isocyanuric Acid from Swimming Pool Water through Melamine Additives. The 8th Conference on Sustainable Development of Energy, Water and Environment Systems (SDEWES), Dubrovnik, Croatia, September 22 – 27, 2013

9. **Ekpeni, L. E. N.,** Benyounis, K. Y., Nkem-Ekpeni, F. F., Stokes, J., Olabi, A. G, Yeast: A Potential Biomass Substrate for the Production of Cleaner Energy (Biogas). The 6th International Conference on Applied Energy (ICAE2014), Taipei, Taiwan, May 30th – June 2nd, 2014.

10. **Ekpeni, L. E. N.,** Benyounis, K. Y., Nkem-Ekpeni, F. F., Stokes, J., Olabi, A. G. Energy Diversity through Renewable Energy Source (RES) – A Case Study of Biomass. The 6th International Conference on Applied Energy (ICAE2014), Taipei, Taiwan, May 30th – June 2nd, 2014.

11. **Ekpeni, L. E. N.,** Benyounis, K. Y., Nkem-Ekpeni, F. F., Stokes, J., Olabi, A. G. Improving and Optimizing Protein Concentration Yield from Homogenized Baker's Yeast at Different Ratios of Buffer Solution. 8th International Conference on Sustainable Energy and Environmental Protection (SEEP2015), University of the West of Scotland, Paisley, Scotland, UK, August 11th – 14th, 2015.

Seminars and Posters:

1. **Ekpeni, L. E. N.,** Olabi, A. G., Effects of Pressure Increase on Yeast Usage in High-Pressure Homogenizer, Faculty Research Day, Dublin City University, May 12th, 2011.

2. **Ekpeni, L. E. N.,** Olabi, A. G., Biogas Improvement Through Yeast Use in High-Pressure Homogenizer, Faculty Research Day, Dublin City University, September 12th, 2012.

3. **Ekpeni, L. E. N.,** Martínez R. F., Bobadilla, M. C., Lostado Lorza, R., Olabi, A. G., Stokes, J. Using R-Software to Statistically Determine the Effects of Temperature, Pressure and Number of Cycles on Partially Diluted Yeast from High-Pressure Homogenizer (HPH). The 8th Conference on Sustainable Development of Energy, Water and Environment Systems (SDEWES), Dubrovnik, Croatia, September 22 – 27, 2013

4. **Ekpeni, L. E. N.,** Benyounis, K. Y., Stokes, J., Olabi, A. G. Effect of Homogenized Baker's Yeast Concentration on Protein in the Production of Biogas Using High-Pressure Homogenizer (HPH). Sir Bernard Crossland Symposium, National University of Ireland Galway, Galway, Ireland**.** April 28 - 29, 2014

Special Invitation to Attend Conference:

1. **Ekpeni, L. E. N.,** Benyounis, K. Y., Stokes, J., Olabi, A. G. Protein Concentration Yield from Treated and Untreated Samples of Homogenized Baker's Yeast Using High-Pressure Homogenizer (HPH). 28th VH-Yeast Conference in Berlin, Germany. April 13th – 14th, 2015.

Declaration

I hereby certify that this material, which I now submit for assessment on the programme of study leading to the award of Doctor of Philosophy is entirely my own work, that I have exercised reasonable care to ensure that the work is original, and does not to the best of my knowledge breach any law of copyright, and has not been taken from the work of others save and to the extent that such work has been cited and acknowledged within the text of my work.

Signed: ……………….....

             (Leonard Eghosa Nkem Ekpeni)

ID No.   10100156

Date: 10th September 2015

Dedication

To my darling Wife (Fehintola), & my lovely Children; (Leonard Jnr., Lennox, Laura & Lynton):

For being part of my life and standing by me all through these years of struggle and perseverance

To my great and precious Mother:

For nurturing and teaching me all the good deeds of the world from childhood. I would have been nothing today without her

And to the memory of my great and precious Mother-in-law:

For her kindness, prayers, and being a perfect mother-in-law. May her gentle soul rest in perfect peace, Amen

Acknowledgements

Abstract

Leonard E. N. Ekpeni
BEng (Hons.), MSc, MIEI, AMIMechE

Investigation and Disruption of *Baker's Yeast / Chlorella Vulgaris* in High-Pressure Homogenizer (HPH) to Improve Cost-Effective Protein Yield

The presented work investigated two biomasses Baker's yeast (*Saccharomyces cerevisiae*) and microalgae (*Chlorella vulgaris*), through characterisation of their cell disruptions in a high-pressure homogenizer (HPH).

As energy producing biomasses, emphasis has been placed on optimizing the yeast/microalgae through determining the protein concentration yields and associated cost to determine its economic feasibility. Through a One-Variable-At-a-Time (OVAT) approach the dataset range was established for the parameters. The results presented show yeast/microalgae homogenized at various pressures (30 - 90 MPa), temperature (15 - 25 °C) as well as (30 - 50 °C), and the number of cycles (passes) (1 - 5) against two responses; protein concentration yield and cost. The high-pressure homogenizer (HPH), GYB40-10S (with a two stage homogenizing valves pressure with a maximum pressure of 100 MPa) was used to cause cell disruption. The homogenate in categorical ratio to buffer solution (Solution C) of 10:90; 20:80 and 30:70 was centrifuged. *Design Expert Software; Design of Experiment (DOE)* was used in establishing the design matrix and to also analyse the experimental data. The relationships between the yeast/microalgae homogenizing parameters (pressure, number of cycles, temperature, and ratio) and the two responses (protein concentration and operating cost) were established. Also, the optimization capabilities in *Design-Expert software* were used to optimize the homogenizing process.

The mathematical models developed were tested for adequacy through the analysis of variance (ANOVA) and other adequacy measures. In this investigation, the optimal homogenizing conditions were identified at a pressure of 90MPa, 5 cycles, a temperature of 20 °C and a buffer solution ratio of 30:70 which yielded a maximum protein concentration of 1.7694 mg/mL, and a minimum total operating cost of 0.28 Euro/hr for a 15 to 25 °C temperature range for Baker's yeast (*Saccharomyces cerevisiae*) as biomass.

Table of Contents

CHAPTER 1: INTRODUCTION

CHAPTER 2: REVIEW OF LITERATURE

X

CHAPTER 3: EXPERIMENTAL AND ANALYTICAL PROCEDURES

CHAPTER 4: RESULTS AND DISCUSSION

CHAPTER 5: CONCLUSION AND FUTURE WORK

XIV

LIST OF FIGURES

XVIII

XIX

List of Tables

Nomenclature

MSW	Municipal Solid Waste
EU	European Union
GHGs	Greenhouse Gases
RES	Renewable Energy Sources
CO_2	Carbon Dioxide
AD	Anaerobic Digestion
WWTP	Waste Water Treatment Plant
OFMSW	Organic Fraction of Municipal Solid Waste
VS	Volatile Solid
SS	Sewage Sludge
RSM	Response Surface Methodology
DOE	Design of Experiment
V.8	Version 8
ANOVA	Analysis of Variance
SEM	Scanning Electron Microscope
OPEC	Organization of Petroleum Exporting Countries
'DOE'	Department of Energy
ASP	Aquatic Special Program
XP	Crude Protein

XL	Crude Fat
Cel	Cellulose
CHP	Combined Heat and Power
SCP	Single Cell Protein
NH_3	Ammonia
H_2S	Hydrogen Sulphide
H_2O	Water
C/N	Carbon to Nitrogen ratio
FDA	Food and Drug Administration
GRAS	Generally Regarded As Safe
DP	Degree of Polymerization
WAS	Waste Activated Sludge
COD	Chemical Oxygen Demand
TOC	Total Organic Chemical
Solution C	Prepared Buffer Solution
BSA	Bicinchoninic Acid Assay
mg/mL	Milligram/Millilitre (Protein Concentration Unit)
OVAT	One-Variable-At-a-Time
ε	Extinction Coefficient
UV	Ultra-Violet Absorbance Rate
M	Mole

BBD	Box-Behnken Design
CCD	Central Composite Design
Prob > F	p-value
α	Level of Significance
D	Desirability Function
PDI	Poly Dispersity Index
CFD	Computational Fluid Dynamics
HHP	High Hydrostatic Pressure
CW	Cheese Whey
CCAP	Culture Collection of Algae and Protozoa
$\mu mol/m^2 s$	Culture Intensity
CH_4, NaCl	Methane, Sodium Chloride
μm, μl	Microns in metre, Microns in litre
Kwh/m^3	Kilowatt hour per cubic metre
Euro/h	Euro per hour (Energy Cost for Protein Yield)
pH	Concentration of Hydrogen ions
K_2CO_3	Potassium Carbonate
KH_2PO_4	Potassium Phosphate Monobasic
K_2HPO_4	Potassium Phosphate Monobasic Trihydrate
D	Categorical Factor
ρ, v, d, x	Density, Velocity jet, Distance, Impingement wall

Chapter 1
Introduction

1.1.   Introduction

Energy is a vital input for social and economic development and affects all aspects of modern life. Its demand is continually increasing at an exponential rate due to the exponential growth of the world population [1, 2]. This means that the demand for energy has been considered proportional to the growth of the population size worldwide. Transportation, industrial activities, communication, health, and education are some of the areas where energy cannot be substituted [3]. As the world faces problems due to growing energy consumption and decline in the supply of fossil fuels at this present time, this has inevitably led to the development of energy from other sources. Sustainable energy has been perceived as the ultimate solution to the current energy crisis being faced globally. Therefore energy must be renewable, sustainable and economically viable to meet the needs of the world's growing population.

Currently, energy demand has been proposed to exceed the supply sources at an exponential rate. By 2050, it is predicted to double or even triple, as the global population rises and developing countries expand their economies [4]. Figure 1 - 1 shows the world energy demand on long term energy sources and Figure 1 - 2 shows the world's rising population, predicted up to 2050. Based on these available facts and figures, fossil fuels are not sustainable, and as such will not be able to support the economic growth and energy security in the long term. The volatility in the oil producing region and instability of the oil prices, along with uncertainty in the supply, has resulted in some environmental factors that have proven to be risky in the exploitation of fossil fuel.
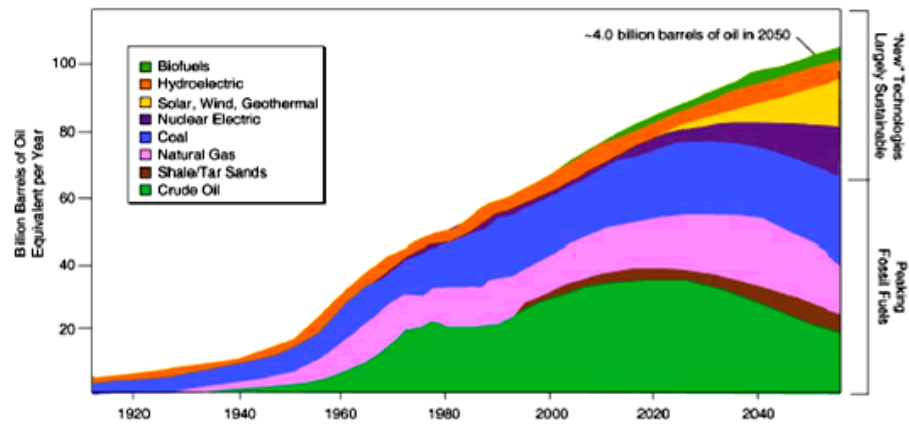
Figure 1 - 1: World Energy Demand - Long Term Sources [5]
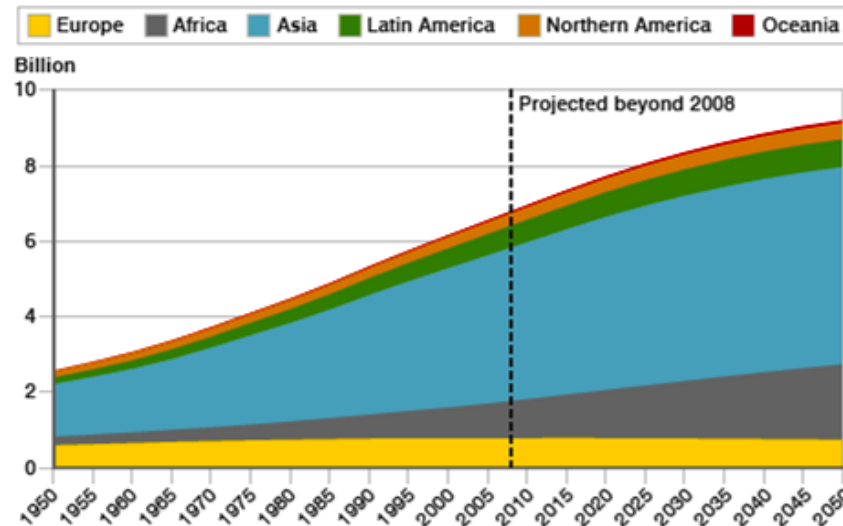
Figure 1 - 2: World Rising Population as Predicted to 2050 [6]

On the other hand, there has been growing concern regarding waste production across the globe as seen within the developed and developing countries. A report from the World Bank [7] shows that the current global municipal solid waste (MSW) generation levels are approximately 1.3 billion tonnes per year, and are expected to increase to approximately 2.2 billion tonnes per year by 2025. This means an increment in waste generation from 1.2 to 1.42 kg per person per day within the next 15 years (see Figure 1 - 3). In Ireland, the total waste generated was estimated at 19.8 million tonnes during the last full survey, which is equivalent of 4.3 tonnes per person. In 2011 alone, household waste generated per person amounted to 367 kg per year (equivalently 1.01 kg/day) which is considerably less than the European Union (EU) average of 438 kg per year [8].

2
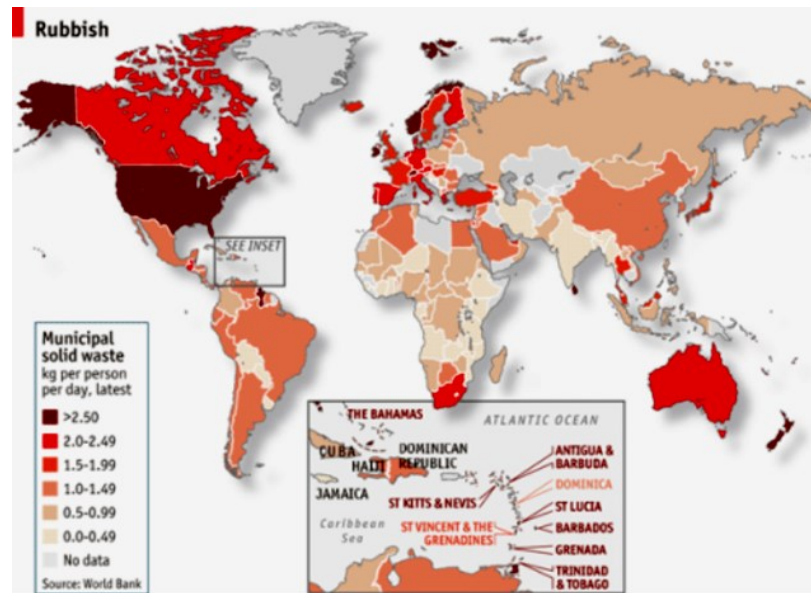
Figure 1 - 3: Municipal solid waste (MSW) production, kg per person per day [7]

Since the proposition of Kyoto Protocol in 1997 [9], EU member states as a nation and part of the world communities, have initiated plans towards tackling of these energy issues. As set out in the 2005 Green paper on energy efficiency, this has become the cornerstone of EU energy policy contributing to all three main energy policy objectives; competitiveness, energy security as well as environmental protection. This was aimed at having emission of GHG down by 20% by 2020 compared to the 1990 record. If achieved this will save primary energy by 20% and therefore increase the renewable energy share to 20% of energy consumption across the EU. Particularly, this will include 10% share of renewable energy in the transport sector with legally binding national targets and action plans [10].

In response to the issues raised above, it is expected that alternative energy will increase in the future, as the world has shown interest in renewable energy and related conversion technologies over the last 20 - 25 years. This is aimed at correcting the aftermath or devastating effects that have arisen as a result of the use of fossil fuel. From a scholarly point of view and research to date, one possible solution to the current energy issue is biomass. It is considered to be one of the most important Renewable Energy Sources (RES) this century [11], to replace fossil fuels without increasing greenhouse gas emissions [12]. As biomass is a widely available renewable resource, its utilisation for energy production has great potential in reducing CO_2 emissions and thereby preventing global warming [13].

3

In addition, using waste agricultural biomass does not compromise the production of main food or non-food crops [14]. Biomass energy has been referred to as any source of heat energy produced from non-fossil biological materials; this can come from ocean and freshwater habitats as well as from land [15]. It is one of the renewable energy sources capable of making a large contribution to the future world's energy supply. Although the role of bio-energy will depend on its competitiveness with fossil fuels and on agricultural policies worldwide, it is expected that the current bio-energy contribution of 40-55 10^{18}J per year will increase considerably [16]. Different technologies are in place in the conversion of biomass into energy using form. These are as detailed below.

1.1.1 Biochemical Conversion

Biochemical conversion uses biocatalysts such as enzymes coupled with heat and other chemicals to convert the carbohydrate portion of biomass (hemicelluloses and cellulose) into an intermediate sugar stream (see Figure 1 - 4). This have gained more popularity than ever before in the last few years and requires a different technology (such as anaerobic digestion) in the pretreatment of the different biomasses into biogas as part of the conversion processes.
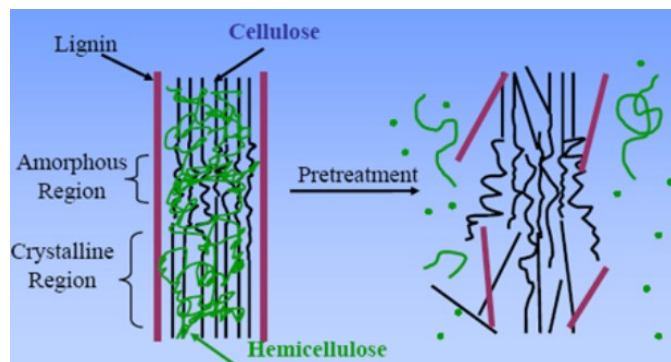
Figure 1 - 4: Pre-treatment of biomass by different methods removes hemicelluloses and lignin from the polymer matrix [17]

1.1.2   Anaerobic Digestion

Anaerobic digestion (AD) is the decomposition of biomass through bacterial action in the absence of oxygen; it is essentially a fermentation process that produces a mixed gas output of methane and carbon dioxide [18, 19]. Once broken down, it reduces to simpler chemical components other than just methane and carbon dioxide. The process is applicable to all biomass resources including wood and wood wastes, agricultural crops and their waste by-products, municipal solid waste (MSW), animal wastes, waste from food processing and aquatic plants and algae [20]. Energy produced from the majority of biomass on average are rated at 64% for wood and wood wastes, MSW at 24%, agricultural waste at 5% and landfill gases at 5% [21-23]. Agricultural biogas plants are considered most suitable for digestion because they have lignocellulosic materials. But there are more abundant raw materials from hardwood, softwood, grasses and agricultural residues along with newsprint, office paper and municipal solid wastes [24]. These are thought to consist of three types of polymers; lignin, cellulose and hemicelluloses which are associated with each other [25], along with fractions of other inner materials such as proteins and extractives

1.1.3   Fermentation

Another well-known biochemical process is fermentation. This is used commercially on a large scale in various countries in the production of ethanol from sugar crops and starch crops. This is ground down and the starch is converted by enzymes to sugars with yeast converting the sugars to ethanol [26]. Mosier *et al.* [17] have highlighted the four major units of operation in the processing of lignocellulosics material as pretreatment, hydrolysis, fermentation, and product separation. Hayes *et al.* [27], and Balat *et al.* [28] have indicated the complexity of the substrate and the need for many different enzymes before these substrates can be hydrolysed completely and effectively. The structure of lignocelluloses resists degradation as result of cross linking between the polysaccharides (cellulose and hemicelluloses) along with the lignin via ester and ether linkages. While Hendriks and Zeeman [29], and Puri [30] viewed factors limiting hydrolysis as: degree of polymerization, crystallinity, accessible surface area, and lignin distribution. Pre-

treatments are therefore considered as a prerequisite in the improvement of cellulosic material degradation. This pre-treatment which could be physio-chemical, biological, chemical or mechanical [31], is to enhance the overall yield of methane.

1.1.4 Mechanical pre-treatment

This is the method employed in such pre-treatments as milling, irradiation, heat treatment, liquid shear lysis-centrifuge, sonication, high-pressure homogenizer (HPH), collision, maceration, and chipping. Ariunbaatar *et al.* [32] studied maceration, sonication and HPH, and therefore reported these as the simplest mechanical pre-treatments for organic solid waste (OSW) such as waste water treatment plant (WWTP) sludge and lignocellulosic substrates. Size reduction of lignocellulosic substrates therefore resulted in a 5 – 25% increase in hydrolysis yield, depending on the mechanical methods used [29]. Whereas for WWTP sludge and manure, the effects of pre-treatments significantly differ and applying maceration pre-treatment enhances biogas production by 10–60% [33]. High pressure homogenizer (HPH) increases the pressure up to several hundred bars, and then homogenizes the substrates under strong depressurization [34]. These pre-treatments methods are not common for the organic fraction of municipal solid waste (OFMSW) but are to other substrates such as lignocellulosic materials, manures and WWTP sludge. Engelhart *et al.* [35] studied the effect of HPH on the AD of sewage sludge (SS), and achieved a 25% increased volatile solid (VS) reduction. Overall, these pre-treatment methods are used to reduce crystallinity but more importantly to give a reduction of particle size, to ease make material handling, alongside increasing surface/volume ratio. This improvement was achieved by an increase of soluble protein, lipid, and carbohydrate concentration.

1.2. Research Approach

In this research, a mechanical pre-treatment technique has been utilized, employing a high-pressure homogenizer device in the treatment of biomass substrates. This device also called a homogenizer machine, has the name "*Cell*

Disruption Machine" given to this method. Homogenizing lignocellulosic materials result in decreased particle size and increased surface area. This will also damage and change the structure of the component and then improve the high recovery of protein yield. The homogenizing of the treated and untreated sets of biomass materials with buffer solution were carried out and are presented within this report.

Furthermore, so as to optimise the cell disruption process after homogenization, statistical optimization work was carried out using Design of Experiment (DOE) - Response Surface Methodology (RSM) techniques. In this part, Box Behnken Design (BBD) was used to develop the experimental design (design matrix). After this study was concluded, the optimum combinations of homogenization parameters can be selected and used to achieve high levels of protein yield at a minimal cost on energy usage.

1.3   Statement of Investigation

A high pressure homogenizer plays a dual role, it reduces the particle size and increases the surface area. This is aimed at damaging and disrupting the cell walls to improve the release of yeast/microalgae inner components [36-40]. The main objectives of this study were:

- To introduce a mechanical pre-treatment technique through employing a high-pressure homogenizer device *Cell Disruption Machine* to treat cellulosic as well as lignocellulosic materials. The use of this equipment has been achievable by considering and investigating the biomass substrates through their pre-treatments in the determining of material structures and the treatment effect on protein concentration yields which is known to aid the production of biogas. This study also investigated the behaviour and rheological properties of the substrates and the consequent effect on the biomass parameters during homogenization. A cost effectiveness energy analysis was also conducted so as to ascertain the economic feasibility of the treatment technique.
- To predict and optimise the homogenizing process after treating yeast and the micro algae using Response Surface Methodology (RSM) via the

Design Expert STATEASE Software to develop mathematical models that relate the process input parameters to their output responses. Based on this study, the three most important input parameters of the homogenization process considered were the number of cycle (passes), temperature and pressure. These were thoroughly investigated to determine their effects on the homogenized substrates. The investigated output features are protein concentration and cost for the energy consumption.

The following points further elucidate and summarise the second objective of this study:

- Applying Response Surface Methodology (RSM) to develop mathematical models for the materials mentioned above through using Design Expert V.8 statistical software to predict and optimise the following process responses;
  - ➢ Protein concentration
  - ➢ Energy cost
- Present the developed models graphically to demonstrate the effect of each homogenizing parameter selected on the responses as mentioned above.
- Analysis of variance (ANOVA) was applied to have the adequacy of the developed model tested, and also to have each term in the developed models examined using statistical significance tools.
- Determining the optimal combinations of input homogenizing factors, using the developed models with numerical and graphical optimization, to achieve the desired criterion for the responses listed above.
- To investigate particle size effects of the biomass substrates particularly on the effect of the process performance thus improving protein concentration yield.

The present study is not limited to the aforementioned processing parameters in HPH. Previous work has demonstrated a correlation between homogenization of biomass substrates and the processing parameter for higher protein yields. To facilitate higher protein production yields and quality of target protein, the production process should be optimised [41]. The work presented in this thesis provides new insights into the investigation of biomasses in improvement of protein production through their uses in high-pressure homogenizer (HPH).

1.4 Thesis Outline

The thesis has been laid out in a progressive manner that initially introduces the reader to the problem at hand. This provides an introduction to the work as well as the thesis statement of investigation and the thesis outline. Background knowledge relating to the subject is then presented, followed by the detailed study of the cell disruption machine (HPH), as well as the material and methods used in the work. The results from the study are then elucidated followed by discussions, and finally conclusions with recommendation for future work. The contents of each chapter are highlighted below:

Chapter 2 – The aim of the chapter is to introduce the reader to the several subjects the thesis encompasses. The chapter reviews the necessary background and literature review on yeast *(Saccharomyces Cerevisiae)* and microalgae *(Chlorella Vulgaris)*, pre-treatment methods, high-pressure homogenizer and the operating parameters. The reasons behind the choice of materials and processes used in this research were considered also. This chapter also reveals previous work carried out in this field, highlighting the short-comings that need improvements and further study.

In addition, this chapter also details research on high-pressure homogenizer as the main mechanical treatment (cell disruption machine) for this research with details about how the device works, which in essence reflect the mechanism of the technique.

Chapter 3 – The chapter aims at revealing the instrumentation and equipment used, as well as the biomass substrates and their compositions which are detailed in the experimental procedures in this study. This allows for experimental repeatability by readers. This chapter also detailed the software package applicable to the research; *Design Expert V.8*

Chapter 4 – This chapter presents the results and discussion from the experimental findings. As the first step, it considered the one-variable-at-a-time approach (OVAT) which determines the data range of the experiments conducted. Trial experiments were conducted to showcase the workability of the experimentation plans with data range for the parameters considered based on the trial experiments.

Particle size analysis was also considered in this chapter as size reduction means in the liberation of the inner contents of substrates. The particle size measurements were conducted using the Delsa Nano C equipment and Scanning Electron Microscope (SEM) was also used in checking the deformation of substrates after treatments.

Through the software, the chapter explains how the *Design of Experiments* (DOE) and *Response Surface Methodology* (RSM) were implemented in this research for optimization of the homogenized substrates. This involved the gradation and how the experimental work has been sectioned in terms of result and analyses. Baker's yeast was used as the substrate, homogenized at temperature ranges 15 - 25 °C and 30 - 50 °C. While the microalgae experimental work was only considered at temperature ranges 15 - 25 °C. The results therefore presented and discussed are within the dataset of temperature indicated above. The chapter also contains the optimization of experimental work using *Design of Experiments* (DOE) with particular consideration of the responses, the protein concentration yield, and the energy cost.

Chapter 5 – This chapter concludes by highlighting the most important findings and recommendations for future research work.

1.5. Summary

This chapter has provided the general introductory note into the conducted research topic with emphasis on the current energy trends coupled with the world growing population, which is expected to double or even triple in the next 35 years. The areas of greater difficulties have been highlighted as the world faces problems due to growing energy consumption and the decline in the supply of fossil fuels at this present time. This coupled with climate change and energy security poses a higher threat to the future energy need. However, renewable energy has been foreseen as part solution to the current problem, and in line with the current research biomass is ranked favourably for the provision of lasting solution to the problem.

Based on this study, some biomass contributions have been highlighted in the chapter, where energy saving opportunities is possible and as such will contribute to enhancing future energy needs/trends. The chapter highlighted the steps involved in complete disruption of biomass substrate in order to release protein concentration keeping in mind cost effectiveness.

Chapter 2
Review of Literature

2.1 Introduction

This chapter introduces the reader to the literature review as it pertains to the research topic. In this chapter the substrates, Baker's yeast and microalgae will be critically analysed and considered through protein yield when homogenized under high pressure. The high-pressure homogenizer disruption equipment will also be reviewed with emphasis on the mechanism, operation and its usefulness, in comparison to other equipment for recovery intracellular product of microorganisms.

2.1.1 Background

The view of energy in the 21st century has taken a dramatic change in terms of energy demand and this has been accounted for due to population growth. This growth in global energy demand is projected to rise sharply over the coming years [42]. The continuous use of fossil fuels has been a leading cause of the current global paradigm resulting in the emission of greenhouse gases, effects of global warming as well as changes in the climate. Hall *et al.* [43] have related civilization to technology. They indicated that technology has generally led to a greater use of hydrocarbon fuels for most human activities. This then makes civilization vulnerable to decreases in supply. Because our civilization has been heavily dependent on the enormous flows of cheap hydrocarbons, many of our once-proud ancient cultures have collapsed due to their inability to maintain energy resources and societal complexity [44]. Accomplishing civilizations have largely advanced through increased efficiencies and the extensive harnessing of the various forms of energy as the result of human ingenuity [42]. Growing energy and environmental concerns have become important issues amid concerns about high energy prices and the occurrence of regional supply shortfalls [45-48]. An assessment of the current state of oil security indicates that the risks of supply disruption have not diminished [48]. Von Hippel *et al.* [49] reported the energy security concept as

being based on the concept of security in general. Energy as a crucial feature of human life has evolved in to matching with contemporary human development and requirements [42]. Historical experience has suggested energy transitions to have been characterized by major increases in energy consumption [50], and looking at trends in global energy consumption have shown that each energy transition has led to greater energy consumption since 1800 (see Figure 2-1). Energy related challenges, such as greenhouse gas emission, fossil fuel depletion, rising oil prices and global warming are some of environmental concerns that need urgent attention.
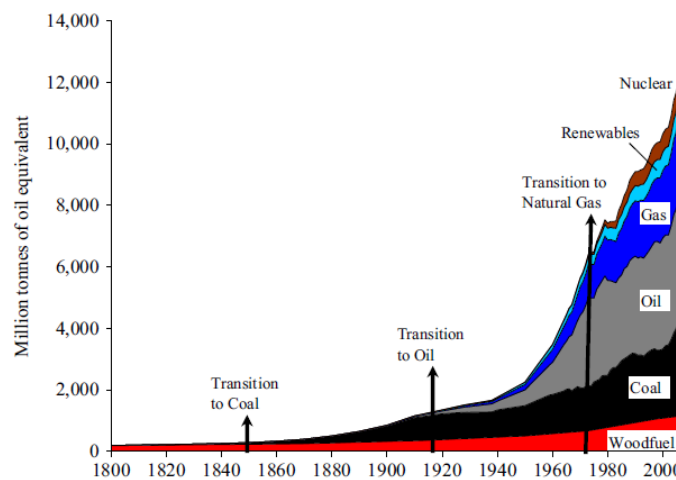
Figure 2 - 1: Global energy consumption and transitions, 1800-2010 [51]

2.2 Biomass Energy and Its Substrates

Field *et al.* (2008) [15] researched and considered biomass energy sources as amongst the most promising, most hyped and most heavily subsidized renewable energy sources. They have real potential to heighten energy security in regions without abundant fossil fuel reserves. This will increase the supplies of liquid transportation fuels along with decreasing the net emissions of carbon into the atmosphere per unit of energy delivered. Biomass comprises all living matter present on earth [52]. It is derived from growing plants that includes algae, trees, and crops or from animal manure [53]. Biomass as a carbon resource in its life cycle is the primary contributor to the greenhouse effect. It accounts for 14% of the world's primary energy consumption and the fourth largest source of energy

after coal, petroleum, and natural gas. As an important energy resource globally, it is used in meeting variety of energy needs and that includes electricity generation, fuelling vehicles, and providing heat for industrial uses [53-55]. Özbay *et al.* [56] and Demirbas, (2001) [57] have demonstrated biomass as the only renewable energy source of carbon which can be converted into convenient solid, liquid and gaseous fuels through different conversion processes. Based on their findings, Sheth and Babu [58] showcased biomass as a unique renewable form of energy with many ecological advantages. Through thermochemical conversion, they were able to illustrate biomass as one of the promising routes amongst the renewable energy options of future energy. Biomass with such substrates as wood, were considered as predominant fuel in many non-OPEC (Organization of the Petroleum Exporting Countries), tropical, developing countries and its use will continue to be used for many years. Wood is used as a fuel in the domestic (for cooking and water heating), commercial (water heating) and industrial (for water heating and process heat) sector. Demirbas, (2000) [20] evaluated wood as it competes well with fossil fuels due to its being renewable and with soft energies like solar and wind, on account of its energy storage capability. Saxena *et al.* [52] in their paper therefore evaluated biomass as being able to be converted into three main types of products; electrical/heat energy, fuel for the transport sector, and feedstock for chemical products.

Another area of great concern is the conversion technologies for utilizing biomass and these can be separated into four basic categories: direct combustion, thermochemical processes, biochemical processes, and agrochemical processes. Biological processes are essentially microbial digestion and biochemical processes convert biomass to ethanol and methane [59].

2.2.1 Microbes

Microbes are tiny single-cell organisms and are considered the oldest form of life on earth. They form a most vital part of human existence as without them, no human activities can take place. They can be divided into six main types such as; archaea, bacteria, fungi, protista, viruses and microbial merger and are collectively

useful in all parts of human life in one form or another. The current surge in food and fuel prices has sounded an alarm showing why providing a sustainable global energy supply and minimizing climate change and are arguably two of the greatest challenges facing 21st century society. Bacteria, yeasts, fungi and archaea as unseen inhabitants of the microbial world have proven to be helpful in addressing these challenges according to Wolin *et al.* [60]. To harness microbial activities in the address of these challenges, much remains to be learned about the chemical space these occupy. It is estimated that 10^{30} of these microbes exist on earth, vast majority are still not known. Most microbes are beneficial, and their combined activities positively affect numerous aspects of the biosphere inhabitants. Other areas of great importance are the production of renewable energy which is now serving a purpose in meeting the needs of our population worldwide.

2.2.2 Yeast as a Biomass

Baker's yeast, whose scientific name is known as *Saccharomyces cerevisiae* has been in use for a long time [61]. It is widely available in a number of forms, including cake yeast known as wet, fresh or compressed yeast (see Figure 2-2), active dry yeast, and instant or fast-rising yeast. It is a common name for the strains of yeast commonly used as a leavening agent in baking bread and bakery products where it converts the fermentable sugars present in the dough into carbon dioxide and ethanol. Yeasts are single-cell organisms found to have extensive use in the food and beverage industries [62-63]. Alais and Linden [64] and Reed and Nagodawithana [65] have found yeast to be important as a raw material for the food, pharmaceutical, and cosmetic industries, in addition to being an excellent source of nutrients, mainly protein, vitamins of the B complex and essential minerals. Inactivated yeast cells have also been used for animal feeding and as a nutritional complement for humans [66-67].

Mostly widely used amongst microorganisms for ethanol fermentation is *Saccharomyces cerevisiae;* this is due to its ability to hydrolyse cane sucrose into fermentable sugars. This yeast has the ability to grow under anaerobic conditions, and a certain amount of oxygen is necessary to synthesize essential fatty acids and

other compounds [68] contained in it to form energy. Yeast may be defined as microorganisms in which the unicellular form is conspicuous, but belongs to fungi. Most yeast cells are colourless and transparent, while some produces carotenoid pigments like *Rhodotorula*. Beudeker *et al.* [69] elucidated and considered Baker's yeast (*S. cerevisiae*) as one of the most important biotechnological products due to its several industrial applications. As a commercial product, it has several formulations; hence it can be grouped into two main types: compressed yeast (fresh yeast) in block forms along with the other kinds; active dry yeast, and instant or fast-rising yeast. Apart from yeast uses in the industry for energy production, its uses have been prominent as experimental models since the very beginning of microbiology and biochemistry.

2.2.3 Classification of Yeasts

Phaff and Macmillan [70] classified yeasts into four groups;

1. Ascomycetous yeasts – capable of forming ascospores in asci.
2. Basidiomycetous yeast – those having a lifecycle similar to those of order Ustilaginales or Basidiomycetes.
3. Ballistosporogenous yeasts – those that forcibly discharge spores by the mechanism of excretion.
4. Asporogeneous yeasts (or Deuteromycetes or false yeasts) – these are otherwise known as *Fungi imperfecti* members. They are incapable of producing ascospores, ballistospores, or sporidia, since sexual lifecycle does not occur or has not been observed so far.

Reed and Peppler [71] in their studies, named and classified yeasts into two classes of fungi based on their spore-forming capabilities and industrial importance. The true yeast and the false yeast which are known respectively to be ascomycetes (or ascorporogeneous) and asexual deuteromycetes or (asporogeneous) and based on this research, focus will only be on the species, *Saccharomyces cerevisiae* also known as the Baker's yeast. Species were named on the basis of fermentation that they have always been associated with, like *Saccharomyces cerevisiae, Saccharomyces vinii* or *Saccharomyces sake*. Since

their morphological and physiological properties show no difference, their strain differentiation should therefore be more valuable than just the species classification as separate names have shown no justification from a taxonomic point of view [72].

2.2.4 Yeast Cell wall and Plasma Membrane

Yeast cell wall structure and organization along with the nature of the cell surface have been investigated based on the composition of the wall, the structure of the components, and the immunochemistry of the cell surface. The investigation of the cell has been necessitated due to the great importance attached to yeast in practice. Little progress has been made in the understanding of yeast cytology through ordinary light microscope examination. The chemical composition of the yeast cell wall was first studied by Salkowski in 1894, who investigated the polysaccharide material which remained after cells had been digested with dilute sodium hydroxide solution [73]. In the continuation of the study by Zechmeister and Toth [74] in 1934, the cells were disrupted by various rigorous chemical actions. They therefore suggested that an enzymic method might do less damage to the cell wall. Glucan component of the cell wall was later isolated through the action of pepsin and amylase on an autolysed yeast suspension [74]. Halász and Lásztity [63] revealed electron micrographs of thin sections of yeast cell showing the existence of a membranous system along with the fine structure. This has related many metabolic functions of the inner structure and chemical composition of the yeast cell. Yeast cell wall and the schematic cross-section are shown in Figures 2-2 and 2-3 respectively.

Based on their findings on the chemical and enzymic investigations, it has been indicated that several polysaccharides may be present in the cell wall. This suggests that apart from glucan, mannan [75] and possibly a glycogen [76] all may be part of the structure but has not been proven.

The yeast cells are covered by an envelope known as plasma membrane, and the cell wall. The cell wall forms 15 – 20% of the dry weight of the cell and mainly consists of mannanproteins along with a certain amount of chitin. The middle

17

layer consists of glucan, while the innermost layer contains more protein including enzymic protein [63]. Cell wall proportional weight usually decreases during the growth phase and increases while in the stationary phase. The native cell wall represents a very complex heterogeneous polymer. Fractions are obtained in the form of complex macromolecular and structural fragments of the cell wall when treated with a weak alkali, or some form of digestive enzymes. In contrast, glucose, mannose, glucosamine, amino acids, phosphates and lipids are obtained when hydrolysed with strong acid. These compounds originate from the main components of the cell wall; the polysaccharides glucan and mannan, chitin, protein, and lipids.
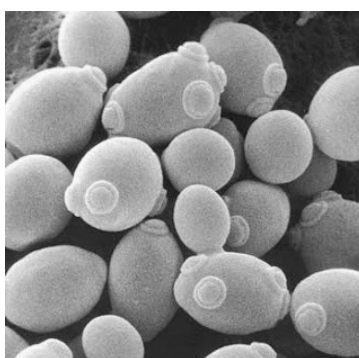
Figure 2 - 2: Scanning electronic microscope image of yeast cell wall [77]
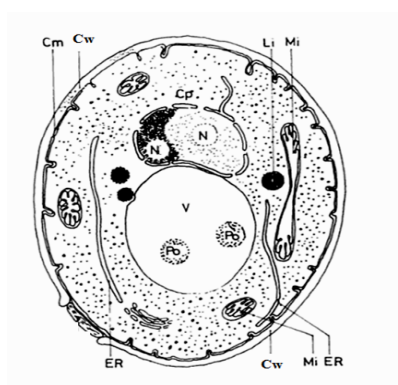
Figure 2 - 3: Schematic cross-section of yeast cell [78]

Cm – cell membrane; Cw – cell wall; Li – Lipid; Mi – Mitochondrium; V – Vacuole; Cp – Cytoplasm; Po – Polyphosphate; ER – Endoplasmatic reticulum

Other internal structures of the yeast include the nucleus, mitochondria, and vacuoles (Figure 2-3). The nuclei are surrounded by an envelope which is characterized by the presence of many pores [78]. The size, shape, number, and the composition of mitochondria vary widely under different conditions of growth.

Under anaerobic conditions of growth, the unsaturated fatty acids within are replaced by saturated fatty acids and the sterol content is significantly reduced. These are in abundance in all fungi. Vacuoles are present in both the vegetative and reproductive cells and vary significantly in size. They are important subcellular organelles in yeasts and contain degrading intracellular substances with variety of hydrolytic enzymes like proteases.

2.2.5 Baker's Yeast (Saccharomyces Cerevisiae) Cell Wall

Baker's yeast whose scientific name is *Saccharomyces cerevisiae* was previously been dealt with in Sections 2.2.3 and 2.24. Published data for the chemical composition of the cell wall of *Saccharomyces cerevisiae* shows a great variability as carbohydrates vary 60 to 91%, proteins 6 to 13% and lipids 2 to 8.5% [77]. The significant differences is as a result of the different isolation methods and clean up procedures of the different research groups, or caused by different growth conditions. The basic structural components of the yeast cell wall are identified as glucans, mannans, and proteins. The overall structures are thicker than in Grampositive bacteria, and based on this, many of the proteins found in yeast cell walls are to be considered enzymes rather than structural components. Glucan fibrils constitute the innermost part of the cell wall and result in the formation of the cell shape [40, 78, 79]. Halász and Lásztity [63] have indicated the glucan to be highly branched polysaccharide with β(1-3) and β(1-6) linked glucose residues. The main chain is built up entirely of glucose linked by β(1-6); the (1-3) linkages are in the side chains. The mannan is alkali soluble with a highly branched mannose polymer of β(1-6) main chain alongside α(1-4) and some α(1-3) linked side chains. Also, chitin is a polymer of β(1-4) linked N-acetyl glucosamine though not all of the glucosamine contents are located in the bud scar region. The structural protein of the cell wall is mainly bound to polysaccharides to form a complex structure in which glucosamine is suggested as a connecting link between polysaccharide and protein [78]. The cell wall lipid content varies both with species and growth conditions. From published data, there are indications which show that great variations could probably be due to incomplete removal of the

lipid rich plasma membrane (see Figure 2-4). While some are strongly bound to the cell, these may play roles in maintaining the ordered structure of the wall.
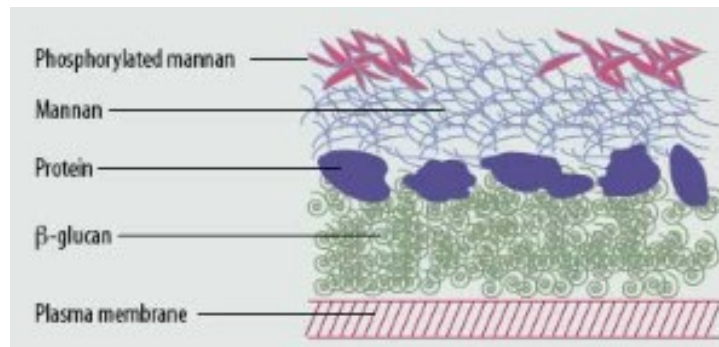
Figure 2 - 4: Saccharomyces cerevisiae cell wall showing the inner structure [80]

2.2.6 Micro Algae as a Biomass

The utilization of microalgae lipids has been of interest since the proposal of mass cultivation of diatoms required to produce urgently needed fat in the World War II by Harder and von Witsch in 1942. For example in the United States alone, the US Department of Energy ('DOE') has dedicated $25 million to the aquatic Special Program (ASP) between 1978 and 1996. This was aimed at identifying high lipid yielding strains and the development of technologies for producing an algal-derived liquid fuel [81]. Oswald and Golueke [82] and Benemann *et al.* [83] have proposed algae before 1978 in particular green unicellular microalgae with potential as a renewable energy source. Pittman *et al.* [84] also contributed through their studies that microalgae have the potential in generating significant quantities of biomass and oil suitable for biodiesel conversion. Brennan and Owende [85] and Brune *et al.* [86] researched and estimated microalgae to have higher biomass productivity than crops in terms of land area required for cultivation. They predicted microalgae to have lower cost per yield along with the potential to reduce GHG emissions through fossil fuels replacement. This will certainly have the potential of reducing the GHG emissions and tackling of other climate and environmental issues, but the associated cost-effectiveness of the process is yet to be fully proven. This has still to this day been a matter of great concern for researchers who are at same time thinking and worried about the

gradually depleting fossil fuels. This and other worrying issues have led to alternatives in terms of energy development and generation that will continue to meet the growing population. Microalgae as biomass substrates have been developed by researchers over the years to serve one of these purposes.

Microalgae belong to the green algae and based on a number of biochemical and cellular differences, two major groups of green microalgae have been identified. These are Chlorophyta and Conjugaphyta. Conjugaphyta which has never been employed for biotechnological applications is known to be five times larger in size than the Chlorophyta [87]. Chlorophyta are subdivided into 4 groups. These are Prasinophyceae, Chlorophyceae, Ulvophyceae and Charophyceae [87].

Prasinophyceae are flagellated unicellular algae, covered with organic scales and are only about 10 – 15 μm in diameter. They inhabit marine and brackish environments, as other species prefer freshwater. Chlorophyceae is considered the largest group, with about 2,500 species in 350 genera. The majority of these are unicellular filamentous freshwater forms and the best among the algal in this group are the *Chlorella, Chlamydomonas, Dunaliella* and *Haematococcus*. While Ulvophyceae and Charophyceae belong to macroalgae and none of the unicellular or filamentous forms are of biotechnological importance.

Table 2 - 1: Microalgal species with high relevance for biotechnology applications [87]

Species/group	Product	Application areas
Spirulina platensis/Cyanobacteria	Phycocyanin, Biomass	Health food, cosmetics
Chlorella vulgaris / Chlorophyta	Biomass	Health food, food supplement, feed surrogates
Dunaliella salina/Chlorophyta	Carotenoids, β-carorene	Health food, food supplement, feed
Haematococcus pluvialis/Chlorophyta	Carotenoids, astaxanthin	Health food, pharmaceutical, feed additives
Odontella aurita/Bacillariophyta	Fatty acids	Pharmaceuticals, cosmetics, baby food
Porphyridium cruentum /Rhodophyta	Polysaccharides	Pharmaceuticals, cosmetics, nutrition
Isochrysis galbana /Chlorophyta	Fatty acids	Animal nutrition
Phaeodactylum tricornutum /Bacillariophyta	Lipids, Fatty acids	Nutrition, fuel production
Lyngbya majuscule/ Cyanobacteria	Immune modulators	Pharmaceuticals, nutrition

Table 2-1 showcases the microalgae species with high relevance for biotechnology applications, with Chlorella vulgaris highlighted for this research. The market for microalgal biomass is assumed to have a size of about 5000 tonnes per year of dry matter and generates a turnover of US$ 1.25×10^9 per year, and this excludes the processed products. Algal biotechnology success is dependent on choosing the right algae with relevant properties for specific conditions and products. This also includes the rate of production worldwide of various algae (see Table 2-2).

Table 2 - 2: Various algae production rates worldwide [87]

Alga	Production (t/year)
Spirulina	3000
Chlorella	2000
Dunaliella	1200
Nostoc	600
Aphanizomenon	500

2.2.7 Relationship between Protein Yield and Biogas

Biogas is known to be a combustible mixture of gases consisting mainly of methane (CH_4) and (CO_2) and is formed from the anaerobic bacteria decomposition of organic compounds (without oxygen). The resultant gases are the waste products of the respiration of these decomposer microorganisms and the composition of the gases is dependent on the substance being decomposed [88]. Based on the substrates, methane is likely to be high when the fat content is high and then low if the materials are mainly of carbohydrates. The complete biological decomposition of organic matter to methane (CH_4) and carbon dioxide (CO_2) under anaerobic conditions is complicated. The interactions between the numbers of different bacteria are each responsible for their part of the task and what may be a waste product from some bacteria could be a substrate or food for others. Balsari *et al.* [89] and Amon *et al.* [90] found crude protein, crude fat, crude fibre, cellulose, hemicellulose, starch, and sugar to markedly influence methane formation. The production of methane from organic substrates mainly depends on their content that can be degraded to CH_4 and CO_2. Weiland [91] investigated and showed that all types of biomass can be used as substrates for biogas production as long as they contain carbohydrates, proteins, fats, cellulose, and hemicelluloses as the main components. This was further proven by showing that fats provide the highest biogas yield but will require a long time for retention due to their poor bioavailability.
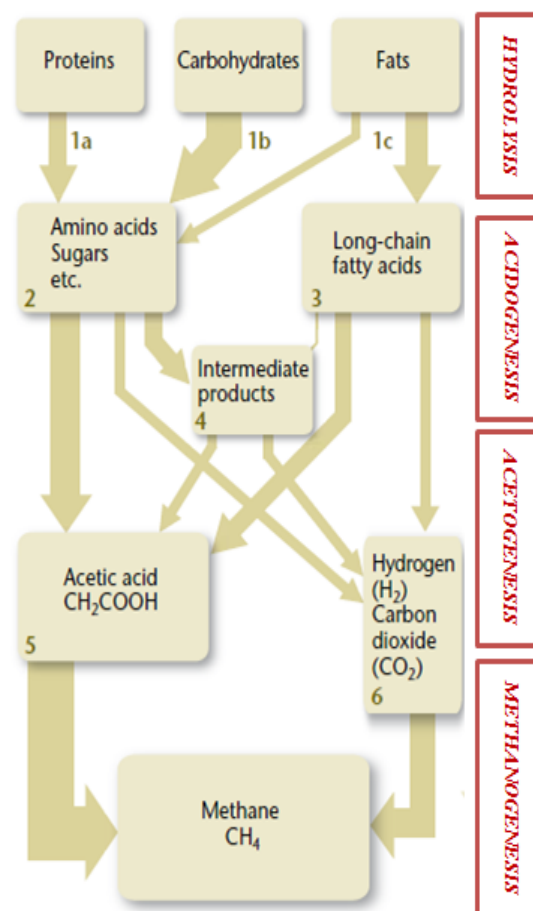
Figure 2 - 5: Biogas production process showing the different stages [54]

Carbohydrates and proteins show much faster conversion rates but with lower gas yields. Protein yield influences biogas production, as researched by [91-95], Oslaj *et al.* [95] concluded that biogas production depended on the content of crude protein. Sialve *et al.* [94] highlighted that the high proportion in proteins for several species of microalgal composition was characterized by a low C/N (carbon-Nitrogen ratio), especially if compared with terrestrial plants. Amon *et al.* [92] researched on "Biogas production from maize and dairy cattle manure - Influence of biomass composition on the methane yield", and in their findings, realized that the nutrients crude protein (XP), crude fat (XL), cellulose (Cel) and hemi-cellulose (Hem), all proved to have significant influence on methane production. They showed the contribution of each nutrient to the net total methane yield. This therefore supported the previous work carried out by Amon *et al.* [96] in their 2004 paper wherein crude fat (27.73) and crude protein (19.05) contributed most to the net total methane energy value of maize silage. The biogas production

process is depicted in (Figure 2-5) showing the contribution of protein and other constituents.

2.2.8 Choices of Yeast and Micro algae substrates

The use of Baker's yeast (*Saccharomyces Cerevisiae*) and microalgae (*Chlorella Vulgaris*) are fundamental to this research. Biomass has shown to have largest potential which can only be considered as the best option in the meeting the demand and insurance of future energy/fuel supply in a sustainable manner. Chandra *et al.* [97] have clarified and suggested that the modernization of biomass technologies have led to more efficient biomass production. They have further stressed conversion as one possible direction for biomass resource efficient utilization. The direct combustion of residues and wastes for electricity generation, ethanol, biogas, and biodiesel as liquid fuels, and combined heat and power (CHP) production from energy crops have all been considered as the main biomass processes that will be expected to be utilized in the future. Biomass resources from agriculture are considered and classified as either the food based portion, or the non-food based portion. Chandra *et al.* [97] viewed oil and simple carbohydrates of crops such as corn, sugarcane, beets as food based portion and complex carbohydrates of crops such as the leaves, stalks, and cobs of corn stover, orchard trimmings, rice husk, straw, along with perennial grasses, and animal waste as non-food based.

Algae and yeast, amongst others, are microorganisms which utilize inexpensive feedstocks and wastes as sources of carbon and energy for growth in the production of biomass, protein concentrate, or amino acids. Due to protein accounting for the quantitatively important part of the microbial cells, they are therefore known as single cell protein (SCP) as natural protein concentrate [98]. Based on this nature of theirs, microbial biomass has been considered as an alternative to conventional sources of food or feed. *Saccharomyces Cerevisiae* and *Chlorella Vulgaris* choices as biomass substrates cannot be overemphasized.

On the other hand, microalgae species choices of Chlorella vulgaris is considered commercially important because of its green nature and own its potential to serve

as a food and energy source as a result of their high photosynthetic efficiency. This in theory can reach 8% and can be grown with autotropic and heterotrophic modes [99]. Algal proteins are of high quality and comparable to conventional vegetable proteins and Rasoul-Amini *et al.* [100] therefore concluded that due to their high production costs and technical difficulties, its cultivation as protein is still under evaluation. Kim *et al.* [101] were particularly concerned with yeast small particle size, high protein content as SCP and their relatively low production costs, resulting in their cells being substituted. For ease of cell wall disruption, several methods such as; mechanical disruption, autolysis and enzymatic treatment have been used in the improvement of the digestibility of SCP products [102].

2.2.9 Biogas properties/Composition and Uses

Biogas is composed of methane (CH_4), carbon dioxide (CO_2) and water (H_2O) as the main constituents. It is also constituted by a minority of other gases in which some are considered toxic and thus be monitored due to their toxic nature. Such gases are ammonia (NH_3) and hydrogen sulphide (H_2S). Biogas is a flammable gas and the proportions of the biogas components depend directly on the substrates being decomposed (see Table 2-3). It can be exploited in variety of ways and the direct approach in the production of energy from biogas is through burning it in chambers or boilers to produce both heat and electricity. Energy produced from such means does not require any upgrade of biogas as long as emission limitations are observed [103]. The composition of biogas varies and is dependent upon the origin of the anaerobic digestion or conversion processes that are involved. Landfill gas typically has methane concentrations around 50%. Advanced waste treatment technologies can produce biogas with 55-75% CH_4 [104].

Table 2 - 3: Biogas composition (Actual (%) depends on substrate being decomposed) [88]

Gas	Percentage (%)
Methane (CH_4)	55 – 70
Carbon dioxide (CO_2)	30 – 45
Water Vapour (H_2O)	6 (40 °C)
Hydrogen sulphide (H_2S)	
Hydrogen (H_2)	1 – 2
Ammonia (NH_3)	
Carbon monoxide (CO)	Trace
Nitrogen (N_2)	Trace
Oxygen (O_2)	Trace

The characteristic properties of biogas, just as in any pure gas are, pressure and temperature dependent. Moisture content has a very great effect on these and therefore shows up a factor. The factors are; (1) change in volume as a function of temperature and pressure, (2) change in calorific value as a function of temperature, pressure and water vapour content, and (3) change in water vapour content as a function of temperature and pressure. The calorific value of biogas is around 6 kWh/m^3 and therefore corresponds to about half a litre of diesel oil. The net calorific value depends on the efficiency of the burners/appliances and methane is therefore the valuable component under the aspect of using biogas as a fuel. In other words, the biogas produced from other sources is different from one another in terms of their volume contents in percentage of their components value.

2.2.10 Baker's Yeast/ Microalgae Compositions and Constituents

Baker's yeast (*Saccharomyces cerevisiae*) and microalgae (*Chlorella vulgaris*) will be of greater emphasis in this discussion. The reason for this is due to their being biomass substrates in this work. The choice of *Saccharomyces cerevisiae* and of *Chlorella vulgaris* as biomass substrates have already been discussed in section 2.2.9. Baker's yeast study as analyzed by Schaffner and Matile [105] showed that lipid globules isolated from Baker's yeast cells contain mainly sterol esters, triacyalglycerols, and phospholipids as well as sterols, free fatty acids, and diacylglycerides as minor components. Table 2-4 shows the components of lipid particles of yeast *Saccharomyces cerevisiae* with steryl esters and triacylglycerols constituting the major constituents of yeast lipid particles [106].

Sialve *et al.* [94] analysed that determining the composition of microalgae is a way to apprehend their digestion potential. They reiterated that microalgae mineral composition meets the nutritional requirements of the anaerobic microflora.

Table 2 - 4: Components of lipid particles of yeast *Saccharomyces cerevisiae* **[107]**

Components	Percent (w/w)
Protein	2.6
Steryl esters	44.4
Triacylglycerols	51.2
Sterols	<0.3
Squalene	0.5
Phospholipids	1.3

Brown *et al.* [108] numerated these organisms to have a proportion of protein of 6-52%, lipids 7-23%, and carbohydrates 5-23%, and the proportions are strongly species dependent. It is therefore evident that a high proportion in protein characterizes several species by a low carbon-nitrogen (C/N) ratio, especially when compared with terrestrial plants. They found freshwater microalgae to have an average ratio of 10.2 as against that of terrestrial plants which is considered as 36.

Table 2-5 depicts the general composition of different human food sources and algae as percentage of dry matter [109]. To completely characterize protein and determine the amino acid content of microalgae, information on the nutritive value of the protein and the degree of availability of amino acids should be given [110]. Hence the high protein content of various microalgal species is one of the main reasons to consider them as an unconventional source of protein [111]. Becker [109] explained that carbohydrates in microlagae can be found in the form of starch, glucose, sugars and other polysaccharides. Their overall digestibility is high, which is why there is no limitation to using dried whole microalgae in foods or feeds.

Table 2 - 5: General composition of different human food sources and of algae (%) of dry matter [109]

Commodity	Protein	Carbohydrate	Lipids
Synechococcus sp.	63	15	11
Meat	43	1	34
Milk	26	38	28
Baker's yeast (Saccharomyces cerevisiae)	39	38	1
Soybean	37	30	20
Anabaena cylindrical	43-56	25-30	4-7
Chlamydomonas rheinhardii	48	17	21
Microalgae (Chlorella vulgaris)	51-58	12-17	14-22
Dunaliella salina	57	32	6
Porphyridium cruetum	28-39	40-57	9-14

2.2.11 Release of Protein from Biological Host

Biological hosts such as microalgae and yeast produce protein in different quantities. Gaining access to the product from a biological source is the primary consideration during downstream processing of proteins. Hatti-Kaul and

Mattiasson [112] and Porro *et al.* [113] elucidated that microorganisms clearly constitute the most common production systems for industrial enzymes and other proteins. Production of protein at a higher level from engineered organisms provides an alternative to protein extraction from natural sources. This has led to yeast as microbial eukaryotic host systems combine the advantages of unicellular organisms with the capability of a protein processing typical for eukaryotic organisms for higher yield. Based on this fact, *Saccharomyces cerevisae* use by the US Food and Drug Administration (FDA) as an organism is generally regarded as safe (GRAS) [113]. This however is not an optimal host for large-scale production of foreign protein due to the technical fermentation needs that require highly sophisticated equipment. The similarities between yeast and microalgae considered in this study make them a better biological host for protein production. The choice of yeast is of paramount importance for the success of the whole process [113].

Several protein products are still produced economically from animal and plant materials despite the advantages of microorganisms being considered as a protein source. This is because of the fact that high sufficient amounts are produced from these sources.

2.2.12 Why Pre-Treat Biomass

Figure 1-4 in Chapter 1 depicted the pre-treatment of biomass by different methods in the removal of hemicelluloses and lignin from the polymer matrix. High-pressure homogenization is used extensively in improving the degradability and the rate of cell wall breakage within the biomass material to improve and increase the protein concentration yield. Biomass materials like lignocellulosic plant residues contains up to 70% carbohydrates as cellulose and hemicelluloses. These are prominent substrates for cheap ethanol production, and due to the closeness of lignin in the plant cell wall, pre-treatment is necessary to make the carbohydrates available for enzymatic hydrolysis and fermentation [114]. As in the case of substrates considered for this research, the inner contents of protein are coated with hard cell wall. These need to be completely homogenized over some passes to liberate the protein inside. Most researchers in their conclusion show that

the barrier to the production and recovery of lignocellulosic material is the lignocelluloses structure [31, 59]. Laureano-Perez *et al.* [115] pointed out that several structural and compositional factors affect the enzymatic digestibility of lignocellulosic materials and Hendriks and Zeeman [29] concluded that cellulose crystallinity is just one of the factors that make hydrolysis of lignocelluloses limited. As different feedstocks contain different amounts of lignin, Agbor *et al.* [116] stressed the need for them to be removed via pre-treatment so as to enhance biomass digestibility in both cases; homogenization and anaerobic digestion.

Based on the consistency that has been reported by several researchers, the main factors for consideration in the pre-treatment of biomass are therefore highlighted below [17];

- To improve the rate of enzymatic hydrolysis,
- To degrade so as to improve digestibility enhancement,
- To aid in the intended product yields
- To also alter the structural and compositional impediments to the hydrolysis and homogenization processes

2.3 Buffer Solution and Contents

Buffer solution is an aqueous solution consisting of a mixture of weak acid and its conjugate base or a weak base and its conjugate acid. Weak acids and bases do not completely dissociate in water, and instead exist in solution as equilibrium of dissociated and un-dissociated species. It has the property that the pH of the solution changes very little when a small amount of strong acid or base is added to it. All buffers have an optimal pH range over which they are able to moderate changes in hydrogen ion concentration. This range is a factor of the dissociation constant of the acid of the buffer (K_a). This is generally defined as the pK_a ($-\log K_a$) value plus or minus one pH unit [117].

Buffer solutions are used as a means of keeping pH at nearly constant value in a wide variety of chemical applications. Buffer solutions in this study has become necessitated as the pH values of biomass substrates will constantly need to be monitored and maintained for higher protein yield during and after homogenization of the substrates.

2.3.1 Properties of a Buffer

Buffer solutions are known to be solutions that resist changes to pH. It is considered as one of the more important properties of an aqueous solution, which is its concentration of hydronium ion. This ion has great effect on the solubility of many inorganic and organic species, as well as on the nature of complex metallic cations in the solutions and on the rates of many chemical reactions. Determining pH value of a solution can be done in two ways; this is determined through the use of a chemical called indicator. This is sensitive to pH. These substances have colours that change over a relatively short pH range and can, when properly chosen through its use determine the pH of a solution to an estimated value.

The other method for finding pH is a device called the pH meter. This device have two electrodes, one of which is sensitive to $[H_3O^+]$, are immersed in a solution. The potential between the two electrodes is related to the pH. This is designed so that the scale will directly furnish the pH of the solution and gives much more precise measurement of pH than does a typical indicator [117]. Its use is required when accuracy of pH value is needed and will be discussed further in chapter 3 under experimental and analytical procedures.

2.4 Mechanical Pre-treatment Methods

Other than mechanical pre-treatment which is also known as physical pre-treatment, other known pre-treatment methods for the conversion of lignocellulosic and biomass materials into biogas are the chemical and biological pre-treatments. But for the purpose of this study, emphasis will be placed only on the mechanical pre-treatment methods. This method is aimed at reducing the particle size and crystallinity of the substrates, which in effect increases the digestibility of the cellulose and hemicellulose in the biomass material. This

therefore also increases the performance of the digestion along with the protein yield. Though Kumar *et al.* [118] have emphasized the digestibility of the cellulose present in lignocellulosic biomass being hindered by many physicochemical, structural, and compositional factors. The biomass needs to be treated so that the cellulose in the plant fibres is exposed in the conversion of lignocellulosic biomass to other useful products.

2.4.1 Milling

Palmowski and Miller [119] categorized coarse size reduction, chipping, shredding, grinding and milling as amongst the different mechanical size reduction methods that have been used in the enhancement of digestibility of lignocellulosic biomass. Milling is aimed at improving the susceptibility of enzymatic hydrolysis through the reduction of particle size and lignocellulosic crystallinity in the material. Apart from the reduction of particle size and lignocellulosic crystallinity; these treatments increase the available specific surface area and reduce the degree of polymerization (DP) [120]. Agbor *et al*. [116] investigated that harvesting and preconditioning reduces lignocellulosic biomass from logs to coarse sizes of about 10-50 mm and chipping reduces the size of the biomass to 10-30 mm. Grinding and milling show better action and result as they are more effective at reducing the particle size and cellulose crystallinity than chipping; this is probably as a result of the shear forces generated during milling [116]. Figure 2-6 shows a typical ball milling in operation.
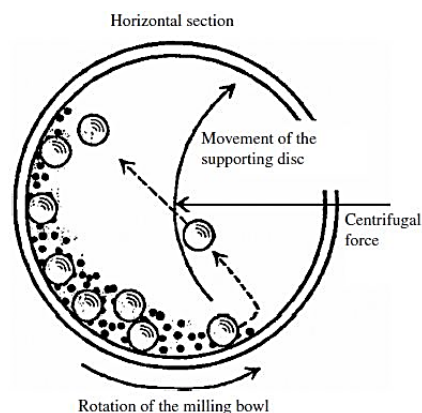
Figure 2 - 6: Cross sectional view of the ball milling [121]

2.4.2 Extrusion

Another mechanical technique involved in the reduction of biomass materials particle size is extrusion. Its processing can provide a unique continuous reactor environment for a combination of thermo-mechanical and chemical pre-treatment of lignocellulosic biomass at higher throughput and solid levels. Alvira *et al.* [122] have indicated that the extrusion process is a novel and promising physical pre-treatment method for biomass conversion. Particularly, recent studies have shown the extrusion process being considered as a promising technology in the production of ethanol. This is based on the fact that with extrusion, the materials are subjected to heating, mixing and shearing, thereby resulting in physical and chemical modifications during the passage through the extruder. Extrusion as a pre-treatment method used in waste treatment and other biomasses for energy extraction has the name "pressure extrusion" and has recently been employed for a plant in the waste treatment in Italy and other European countries [123]. Novarino and Zanetti [123] in their paper used organic fraction of municipal solid waste (OFMSW) as the biomass resource. The system of pressure extrusion employed in their work has guaranteed the satisfaction of producing a clean organic fraction which has been characterised by a reduced and uniform particle size distribution. Figure 2-7 shows the extruded material using the two different sizes of hole grates. The extruded organic material appearance shows a kind of jam which can be simply used in co-digestion or alone, diluted or not, in an anaerobic digestion plants.
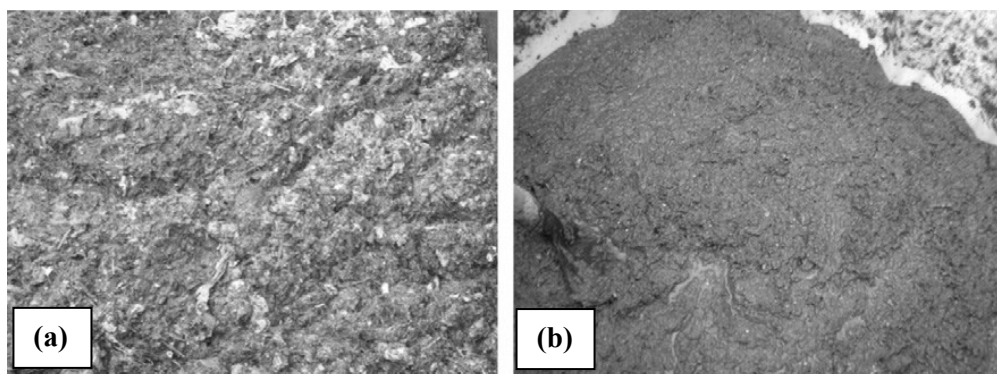
Figure 2 - 7: Extruded material obtained with: (a) 16 mm holes grate; (b) 8 mm holes grate [123]

2.4.3 Ultrasonic

Tyagi and Lo [124] highlighted on ultrasonic pre-treatment method being investigated by researchers, among other physical and chemical pre-treatment methods in the acceleration of the hydrolysis step, as well as to increase the digestion rate. The application of this pre-treatment method to waste activated sludge (WAS) improved sludge reduction and increases methane production. Ultrasonic as a mechanical pre-treatment means relies on the cavitation process of disintegrated cell walls. Wang *et al*. [125] and Benabdallah El-Hadj *et al*. [126] demonstrated the pre-treatment of WAS by ultrasonic disintegration significantly improved microbial cell lysis and increased volatile solids degradation as well as biogas production. Based on this, researchers found that the disintegration of particulate being enhanced by high energy intensity. This has been evident through the reduction in particle size along with soluble matter fraction increment [127], and ultrasound which is a sound wave at a frequency range from 20 KHz to 10 MHz, has a wide range of environmental applications. Likewise, low frequency ultrasonic pre-treatment prior to anaerobic sludge digestion has been considered as one of the most promising recent technologies that have been extensively investigated for wastewater sludge management [127, 128]. The majority of the effects of ultrasonic treatment are in the disruption of the physical, chemical and biological properties of sludge, the reduction of the floc size, along with biodegradability improvement. Pre-treatment of sludge could increase its biodegradability through the hydrolysis stages enhancement, and as a result leads to enhanced anaerobic digestion. Tiehm *et al*. [127] showcased that the most efficient solubilisation was achieved by the lowest frequency. This works by ultrasound waves propagating in the sludge medium. The compression cycle makes positive pressure on the liquid by pushing the molecules together and the rarefaction cycle makes a negative pressure by pulling the molecules from one another (see Figure 2-8).
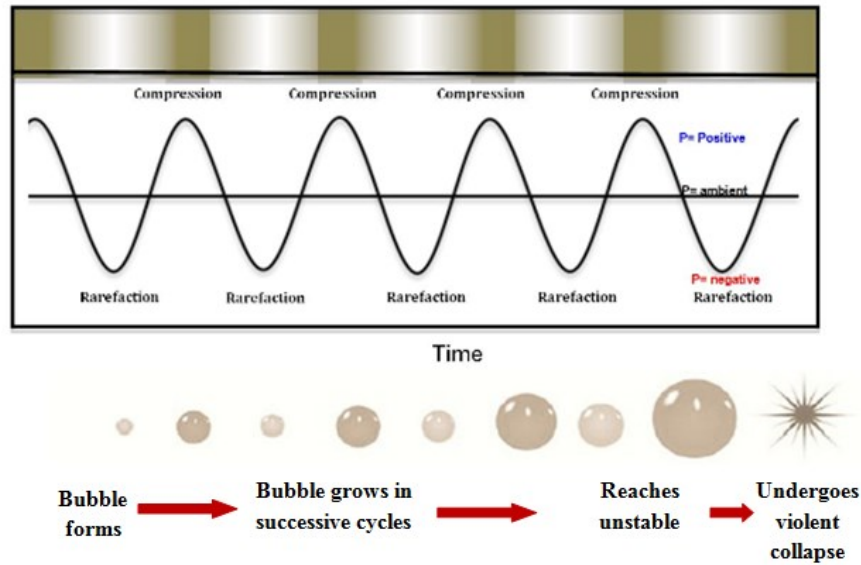
Figure 2 - 8: Sound waves interaction with a liquid medium and the bubble growth due to the expansion-compression cycles resulting in the localized "hot spots" formation [129]

2.4.4 Lysis-Centrifuge

This is operational by directly working on the thickened sludge stream in a dewatering centrifuge and it is then suspended again with the liquid stream thereon.
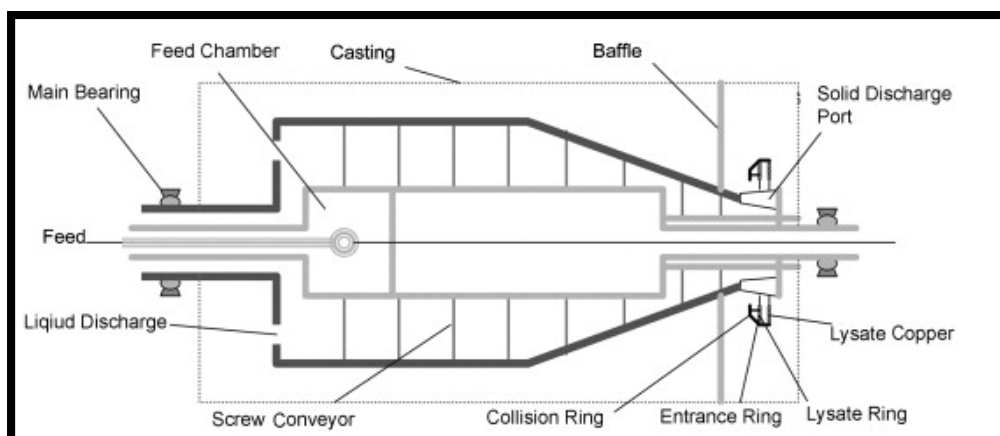
Figure 2 - 9: Lysate-thickening centrifuge. Adapted from [130]

Figure 2-9 shows the schematic view of lysate-thickening centrifuge and contained within the bacterial cells are enzymes, part of enzymes and cofactors, through these cellular degradation can result after the initial lyses. Improvement of the performance of anaerobic digestion will require the use of altered centrifuges in the enhancement of cell lyses to produce lysate rich in cellular degradation. The goal with using lysate-thickening centrifuge is in the partial disintegration of cells during thickening through kinetic energy generated by the centrifuge without additional energy. The addition of aerobic cell lysate with waste activated sludge (WAS) thickened to 6% has proven to increase anaerobic digestion performance, as indicated by increased biogas production by as much as 86% [131]. Dohanyos *et al*. [131] reiterated also that the higher disintegration effect was achieved with a lower WAS age, shorter retention time in digesters, along with a higher anaerobic microorganism activity in the digesting sludge. Based on these, Zabranska *et al*. [132] had a similar view through their findings on the long-term monitoring results from three full-scale installations of lysate-thickening centrifuges. They showed that anaerobic digestion could be improved by this process as organic matter in the digested sludge significantly decreased to 48-49% while there was a substantial increment in the biogas production by 15-26%. The good use that has resulted from this equipment has enabled it to be patented worldwide with its major licensee based in Germany.

2.4.5 Collision Plate

Figure 2-10 shows the schematic view of collision plate pre-mechanical treatment system and is mainly used in wastewater treatment. This collision plate mechanical treatment as conducted by Nah *et al*. [133], the municipal aerobic was mechanically disrupted by jetting the sludge to collide with a collision plate at 30 bar pressure and rising up to 50 bar. The Waste Activated Sludge (WAS) jet pressure was controlled through regulating the by-pass WAS flux in the high-pressure pump and the mechanical pre-treatment and digestion experiment procedures carried out resulted in WAS consistency between 1.4% and 1.8%. This therefore showed that the treated sludge characteristics were six-fold more in terms of soluble matter in Chemical Oxygen Demand (COD) and Total Organic

Carbon (TOC). These on the whole resulted in soluble proteins increment by two and half times with 20% more alkalinity, ammonia, and phosphorus produced along with a decrease in AD from 13 to 6 days [134]. These are as a result of losses in suspended solids.
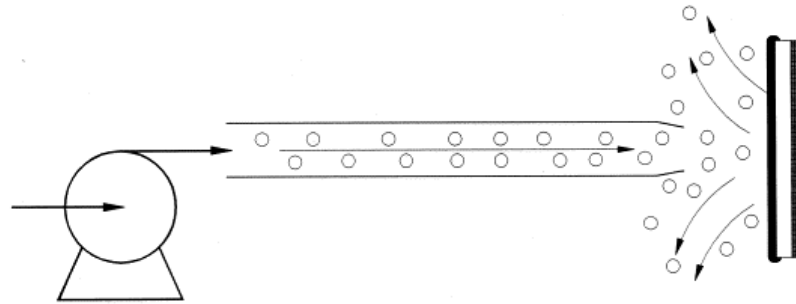
Figure 2 - 10: Schematic view of Collision Plate mechanical pre-treatment of WAS [133]

In the experimental work carried out by Nah *et al.* [133] after the disruption resulting from the mechanical treatment of WAS at 30 bar, it showed that there were some changes in the microstructure. It is thought that part of the intracellular substance has been released from the inner part of the aerobic microorganisms to the outside. This therefore indicates that most of the microorganisms were hydrolytically converted to low-molecular-weight components [133-134] (see Figure 2-11).
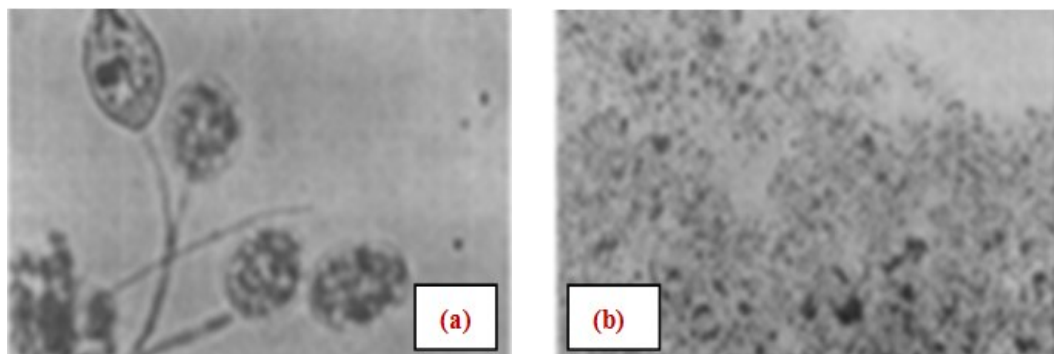
Figure 2 - 11: Microphotograph of WAS before (a) and after (b) pre-treatment at 30 bar (x400) using the collision plate. Adapted from [133]

2.4.6 Hollander Beater

Hollander beater as shown in the figure (Figure 2-12) was first introduced and developed by the Dutch in the 17th century. Its purpose was to produce paper pulp from cellulose containing plant fibres. Hollander beater machines are used for beating and the process can increase the strength of the product through flattening of the cellulosic fibres which will increase the area for fibre bonding. This has since changed as it is also now being used in the bioenergy sector in the beating of biomass substrates as well as other lignocellulosic materials. This works by allowing the substrate to go through the gap with water and then result in the decrease of the particle size and the increase of the surface area. As the lignocellulosic material pass under the blades on their path of circulation, they rub between the blades of the beater roll and another stationary set of blades on the base of the tub known as bedplate where the refining is known to take place. The bedplate is adjustable to control the amount of shearing in the gap between the blades [135]. This process therefore damage and change the structural components of the substrate, thereby reducing the cellulose crystallinity. The principles employed in the Hollander beater is similar to that in milling wherein the objective of a mechanical treatment is to reduce the particle size and crystallinity of the substrate. Hendriks and Zeeman [29] have found milling as a mechanical pre-treatment of the lignocellulosic biomass; a process that requires cutting the lignocellulosic biomass into smaller pieces as a pretreatment method.
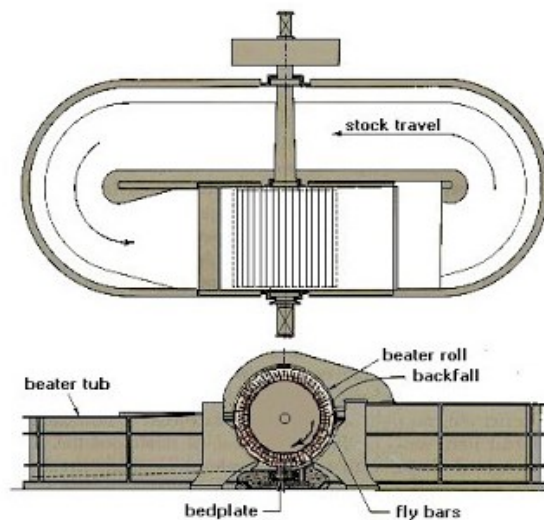
Figure 2 - 12: Schematic view of Hollander Beater [135]

2.5 Other Mechanical Pre-treatment Method

The previous section has discussed the most up to date mechanical pre-treatment methods used in the treatment of substrates to enhance biomass-biogas conversion including cell wall disruption of substrates. Based on these ideas of cell disruption in biomass, a mechanical treatment employing a high-pressure homogenizer is therefore introduced for the work in this research. This homogenizes and ruptures the cell wall to liberate the intracellular products, including proteins which in turn are designed to improve protein production after centrifugation where the supernatant is separated from the solid. Homogenizing biomass materials result in the decrease in particle size and increment in the surface area; these then results in the damage and change in the component microstructure and which, as a result, improves the yield in proteins.

2.5.1 High-Pressure Homogenizer (HPH)

Cell rupture is required in the recovering of biological products that are located inside cells. This is required to be done either mechanically or non-mechanically [136]. There are other methods, as well as those which are non-mechanical, which could either be the physical way or the enzymatic way. In general, De Boer *et al.* [137] emphasized mechanical methods being non-specific, but their efficiency is considered higher with broader application in comparison to any of the other methods. Ahmad-Raus *et al.* [138] have rated this as highly dependent on the nature of the product of interest, the cell or tissue itself, like the extent of the cell's fragility. Cell disruption is otherwise considered as the isolation and preparation of intercellular products which is important for use in research and in the industries for manufacturing end products for consumers. In the industries, HPH application is linked to the production of stable emulsions; hence it is widely used in such areas [40, 137, 139, 140], and apart from it being able to emulsify it disrupts particles into a disperse phase of suspension. It has also extensively proven to be suitable for the inactivation of the microbial flora occurring in fruit juices and milk-based beverages [141] especially contributing to the preservation of the freshness and texture attributes, coupled with antioxidant capacity and the polyphenols, vitamins, and flavonoids contents of the product [142]. HPH is

therefore used in the disruption of cell walls of biological matter including biomass substrates, organic matters and industrial products through pumping the sludge under high pressure (though most homogenizer today are known to exceed 150 MPa [139]). This product passes through homogenizing valves at high velocity against an impact ring with a decrease in pressure. The homogenized product then liberates the intracellular matter by reducing the particle size and increasing the surface area of the homogenized product. A typical example of a high-pressure homogenizer is given in Figure 2-13 which shows the three main functionalities of valve seat, impact ring, and the valve head during the operation of the high pressure homogenizer.
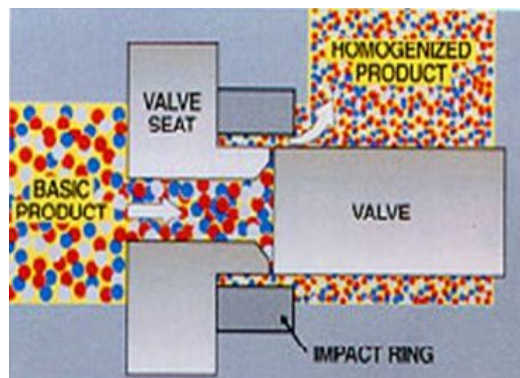
Figure 2 - 13: Typical example of high-pressure homogenizer [143]

2.5.2 Different Types of High-Pressure Homogenizer

High-pressure homogenizer come in different designs, sizes, forms, geometries, and shapes, but technically these works the same way in principles. The particle size trends for the different high pressure homogenizers [144] show the sizes of the homogenized particles ranging from nano size to over 100 micron (Figure 2-14). This wide range of sizes is particularly suitable for a broad range of applications such as; cell disruption, particle size reduction, nano/micro emulsions and dispersion. The minimum size of the droplets that can be produced using each approach is dependent on many different factors. Qian and McClements [145] explained previous studies that the minimum particle size achievable using the high-energy approach depends on homogenizer type, its operating conditions (for

example; energy intensity, time and temperature) and sample composition (for example; oil type, emulsifier type, and relative concentrations). The physicochemical properties of the component phases (for example; interfacial tension and viscosity) were also considered.

The geometries of the homogenizing valves make a difference also in determining the type of HPH in operation. The processed liquid in any type of homogenizer valve passes under high pressure through a convergent section called the "homogenizing gap" and then expands.
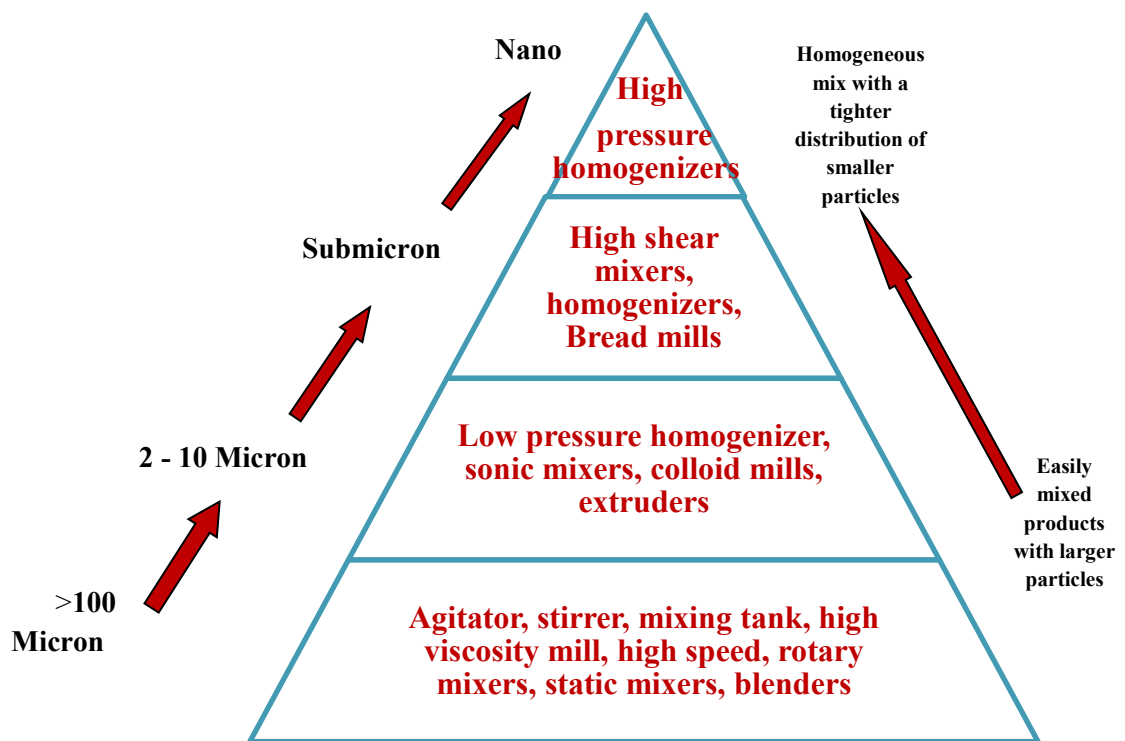
Figure 2 - 14: Particle size trends for the different high pressure homogenizers [144]

For example, Floury *et al.* [146] have compared the APV-Gaulin valve against the Stansted valve in their work, and have confirmed that the Stansted homogenizing valve technology using ceramic material will withstand ultra-high pressure levels. This shows that that the geometry has been modified as compared to that of APV-Gaulin. Of ultimate consideration here is the flow direction which is reversed. In

the classical valve design, the fluid is fed axially into the valve seat and then accelerates radially into a region between the valve head and valve seat. Kleinig and Middelberg [147] found that the fluid becomes a radial jet that stagnates on collision with the impact ring before leaving the homogenizer at atmospheric pressure after leaving the gap (see Figure 2-15 [A]). The Stansted valve shows a different form; the fluid is fed in axially first through the mobile part of the valve and then accelerates radially through the narrow gap between valve head and valve seat. Floury *et al.* [148] revealed from the numerical simulation that the radial jets leave the valve seat without impinging on the valve point, but re-circulates downstream the slit of the valve before flowing out of the valve seat (Figure 2-15 [B]). Another applicable difference between both (HPH) is in their pressures. Stansted is able to reach much higher pressure (350 MPa) than the APV-Gaulin type which rated between (70 – 100 MPa). When in operation, it can be controlled by adjusting the gap (h) between the valve head and the valve seat; the valve gaps involved in the ultra-high pressure valve are considered lower (h = 2 – 5 µm) as against APV-Gaulin type (10 – 30 µm) [146].
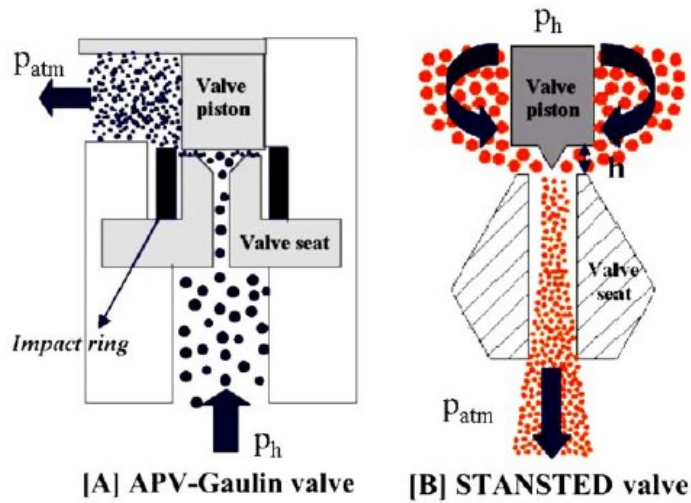
Figure 2 - 15: Homogenizing valve geometries (A) APV-Gaulin valve and (B) Stansted valve as adapted from [146]

2.5.3 GYB40-10S /GYB60-6S 2-Stage Homogenizing Valve HPH

The GYB40-10S high pressure homogenizer has been employed in this research for the mechanical treatment of biomass substrates. The GYB series high pressure homogenizer is general-purpose equipment for the preparation of superfine liquid-liquid emulsion or liquid-solid dispersion. It is widely used in the production and research areas including food, beverage, pharmacy, chemical industries, biotechnologies, and others not mentioned here. All parts with direct contact with fluid media are made from materials of super abrasion durability and excellent corrosion resistance, to avoid any adverse impact on the fluid to be handled.

The machine is made of a reciprocating plunger pump and a homogenizing valve, with its homogenizing portion made up of a double stage homogenizing system which includes a 1st stage homogenizing valve and a 2nd stage homogenizing valve. The two stage homogenizing valve pressures are adjustable under the scope of nominal pressure, and at the same time can also be used separately due to the high-low of homogenizing pressure which directly relates to the speed of materials through the homogenizing valve. The material particle size is considered to be less than 2 μm. The GYB series HPH therefore makes the incompatibility in liquid-liquid or liquid-solid materials to be compatible, superfine, and homogenous. The stability in the liquid-liquid or solid-liquid under the multiple actions of cavitations effect can result in high speed impact and shearing through the adjustment of pressure homogenizing valve of the HPH [149]. Figure 2-16 with the operating units depict the 2-stage homogenizing valve HPH with the serial name as GYB40-10S /GYB60-6S, and this has been employed in this study based on the technical specification as indicated in the Table 2-6. The high-pressure homogenizer (HPH) has the same features as others, but its unique feature is in its operation during homogenization in 2- stages with the different hand wheels for raising pressure and stabilizing it at that point. This enables the homogenization pressure to be read at any point during cell disruption.

Connector pipe for rotational fluid flow into the feeders tank

Pressure Dial Gauge

Feeders tank for mixed soluble yeast

Exit pipe for homogenized yeast release

Directional tap lock for fluid flow either to the connector or exit pipe during homogenization

1st Hand wheel for increasing pressure build up

2nd Hand wheel for balancing pressure

Lock for dropping down the pressure on the gauge after homogenization and trapped air exit

Figure 2 - 16: GYB40-10S 2-Stage Homogenizing Valves HPH [149]

Table 2 - 6: GYB40-10S / GYB 60-6S High Pressure Homogenizer technical specification [149]

Technical Data (Item)	Specification	
	GYB40-10S	GYB 60-6S
Pressure (MPa) **Maximum Pressure (MPa)** **Working Pressure (MPa)**	One grade 0 ~ 100 Two grade 0 ~ 20 100 90	One grade 0 ~ 60 Two grade 0 ~ 20 100 90
Flow Rate (L/h)	40	60
Volume efficiency (%)	≥ 85	≥ 85
Motor Power (Kw)	3 (380V, 50 HZ, 3 Phase)	3 (380V, 50 HZ, 3 Phase)
Material Temperature (°C)	0 ~ 120	0 ~ 120
Noise (Db)	≤80	≤80
Corrosive-proof (PH)	2 ~ 10	2 ~ 10
Dimension (mm)	920 x 445 x 1220	920 x 445 x 1220
Weight (kg)	265	265

2.5.4 Mechanism of the HPH Technique and Homogenization Process

High-pressure homogenization is the most commonly employed method for large scale disruption of microbial cells in the industry. In other words, it is considered as an essential step in commercial processing of diary, pharmaceutical, biotechnological, food, and chemical products as well as microorganism cell wall disruption through the provision of improved functional properties [150]. Briñez *et al.* [151] and Kheadr *et al.* [152] have found high pressure homogenization to be one of the most promising new food processing technologies due to the recent improvements in high-pressure homogenizers along with the acceptance by consumers of pressure processed foods. For example, milk homogenized at 10 – 20 MPa under temperatures of 55 – 65 °C is done to prevent fat separation or gel formation during storage [153]. Several papers have reported the effectiveness of HPH in deactivating pathogenic and spoilage microorganisms in model systems

and real foods and thus stimulating investigations on the application of HPH so as to improve food safety and shelf-life [151, 154-156]. This method has been found to be generally suitable for a variety of bacteria, yeast, and mycelia including algae. The homogenization technique works by forcing cell suspensions through a very narrow channel or orifice under pressure. Depending on the type of HPH, the suspension may or may not impinge at high velocity on a hard-impact ring or against another high velocity stream of cells coming from the opposite direction. As the process requires the disruption of biomass substrates before homogenization can take place, the cell wall of the microbial products are broken down to release the proteins which are a great source and at the same time aid biogas production.

2.5.4.1 Effects of Valve Head, Valve Seat and Impact Ring on Substrates

Homogenization considerations have shown high pressure homogenizers consisting of a positive displacement pump and a homogenizing valve. And as previously indicated, the pump is used to force the fluid into the homogenizing valve where the work is done [157]. The three main components with useful value and functionalities in the HPH are the valve head, valve seat, and impact ring. These are within the internal structure of the designed HPH and are often regarded as the powerhouse of the machine. In the homogenizing valve, the fluid is forced under pressure through a small orifice between the valve head and valve seat (as depicted in the Figures 2-15 [A] and [B]. The fluid leaves the gap in the form of a radial jet that stagnates on an impact ring [157]. It therefore exits the homogenizer finally at low velocity and atmospheric pressure. During operation, higher pressure on the hand wheel compresses the valve seat against the valve head through the impact ring. This, as a result reduces the gap size wherein the homogenized suspension/emulsion flows through at a very low velocity. The disruption of the cell wall leads to a large drop in pressure, and results in highly focussed turbulent eddies along with strong shearing forces to occur. Effluent from the homogenizer is normally chilled to minimise thermal damage to the product caused as a result of the frictional heat which is generated due to the high fluid velocity that elevates

the product temperature, considered to be between 2 - 2.5 J per units 10 MPa [158-159].

2.5.4.2 The Effects of Homogenizing Valves Parts on GYB40-10S HPH

The homogenization using the GYB40-10S HPH is in two parts. This is as a result of the double hand wheel (Figure 2-16). The inner components are shown separately in Figure 2-17; these work together in one piece for complete homogenization of the biomass substrate. The first hand wheel is used to increase the pressure build up with the second one set to normalise and balance the set working pressure required before the homogenized substrate exits through the exit pipe. This is represented in Figures 2-18 and 2-19 wherein the flow part is indicated before and after cell disruption during the homogenization process. The silt size along with the resulting stream velocity and pressure of the liquid ahead of the valve depends on the force acting on the valve piston, and can be adjusted to regulate the homogenizing intensity. During this process of homogenization of the biomass substrates, the pressure drop in the valve is otherwise known as the homogenizing pressure and termed the working pressure of the fluid.
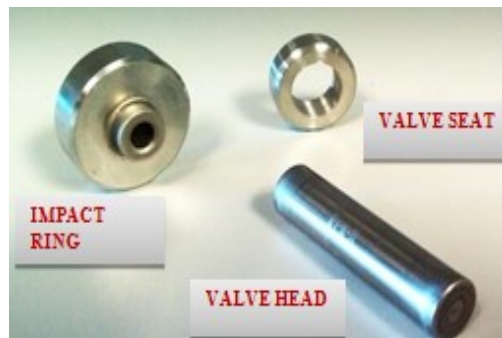
Figure 2 - 17: Homogenization valve parts
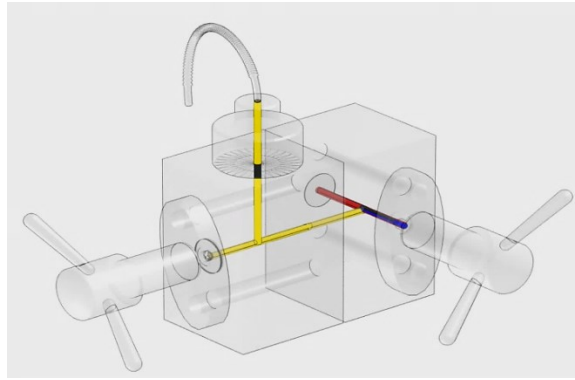
Figure 2 - 18: Schematic view of the flow channel during biomass homogenization
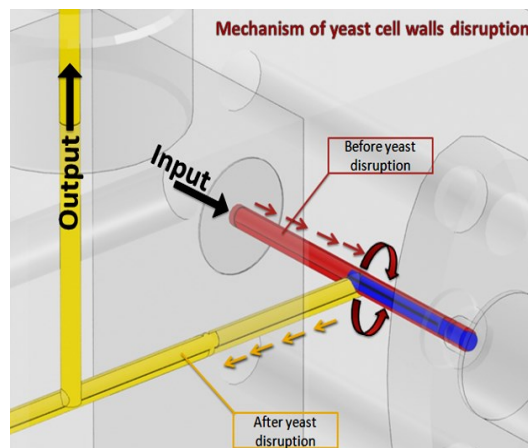
Figure 2 - 19: Schematic diagram showing input and output view of substrates before and after disruption

2.5.4.3 Valve Design and Homogenization Efficiency

Goulden and Phipps [160] have concluded that homogenization efficiency depends on the valve design since a valve with flat faces is considered inferior to one with corrugated faces; for example the liquid-whirl type valve. The different valves as seen in Figure 2-20 employed in the homogenization process, result in variation in the drop of pressure.
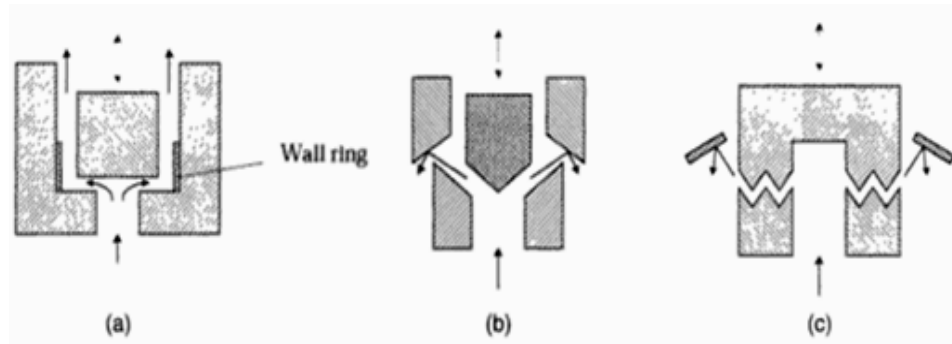
Figure 2 - 20: Pressure homogenization valves [162]

As shown in (Figure 2-20 (a)), the pressure homogenization valves consist of a plunger and the valve seat. Between the plunger and the valve seat, a ring gap is formed. As the compressed material enters the plug valve, it flows radially via the narrow ring gap and impacts on the surrounding wall ring. Slope seat valves (Figure 2-20 (b)) requires higher pressures, when compared to the flat-seated valves and the efficiency of the valve is increased if the flat-seated valve, has grooves on the surface (Figure 2-20 (c)) [161]. As a result of this, the droplets are compressed and expanded as they flow along the peaks of each groove.

The mechanism of homogenization which classifies it at been a low or high valve pressure homogenizer, is associated to specially designed experimental valves with an extended-orifice construction. The alteration of an experimental valve allows the possibility of studying factors related to homogenization. These factors include: (a) the time required for a particle to pass through the valve clearance; (b) the velocity through the valve clearance; (c) the entrance and exit conditions of the valve; and (d) the effect of two or more valves in series.

Variation in valve orifice length from 2.5 to 4.1 mm has no effect on either pressure drop or homogenization efficiency at a given velocity. However as the velocity through the valve of a fixed length increases, the pressure drop also increases which results in the improvement in homogenization efficiency. Therefore the use of a valve with a bevelled entrance results in decrease in both pressure drop and homogenization efficiency, as compared to a valve with a sharp entrance. The same valve with the bevel at the exit has no effect on pressure drop.

2.6 Parameters Affecting High Pressure Homogenization

Clarke *et al.* [139], Doulah *et al.* [38], Brookman *et al.* [39], Engler [79, 158], Fluory *et al.* [146, 148, 162], Diels *et al.* [156, 163], Harrison *et al.* [164], Siddiqi *et al.* [165] and Shirgaonkar [166] are some of the authors and researchers who have one way or the other contributed to cell wall disruption in HPH analyses. Their analyses have been based on critically analysing the parameters that affect high pressure homogenization during the disruption of the cell wall within the biomass substrates. Many of the suggestions about these mechanisms causing cell wall rupture are being made and are discussed herein. Substrates are also considered to be of different form and microstructure due to their contents and compositions. As a result of these factors, during homogenization, they work differently in the HPH in the release of their intracellular contents. The concern here is that HPH has a major role to play in the release of the contents, and as such the parameters that work against this process will be considered as some of the factors are thought to be environmental.

2.6.1 Temperature

Temperature effect on substrates during high-pressure homogenization cannot be underrated. Paquin [167] has classified the suspension temperature amongst others; the operating pressure, the number of passes through the valve along with the design of homogenizer valve as the major parameters determining the process efficiency. For example, from the work carried out by Feijoo *et al.* [168] on *Bacillus licheniformis* spores in ice cream mix using microfluidizer technology, it was evident that 68% of *Bacillus licheniformis* spores inoculated in milk was deactivated at 200 MPa only when the initial temperature of milk was 50 °C; this spore inactivation was attributed to the combined effects of HPH and the temperature reached during the process. During the HPH treatments, it was showcased that temperature increases even though the inoculation fluid before each HPH was 20 °C. The outlet sample temperature was 45 °C, and then cooled rapidly in ice afterwards. Diels *et al.* [169] therefore suggested that the heat

produced in HPH treatments contributes to cellular inactivation, in addition to the mechanical effects which are considered predominant at lower temperatures.

In their analysis, Roach and Harte [170] showed the effect of temperature on HPH and from the results presented temperature at the homogenizing increases as pressure increases due to frictional and shear forces during the homogenization process. This showed that homogenization temperature increased 17 °C per 100 MPa in a linear manner (where r^2 = 0.9669) (see Figure 2-21). This is in conformity with similar studies of an increase in temperature of approximately 12-18 °C/ 100 MPa as previously reported [170-173] and Thiebaud *et al.* [171] indicating that a second stage valve often used in the controlling of pressure drop in the first stage valve for the avoidance of low-pressure. This is thought to also have an effect on the operating temperature during homogenization.
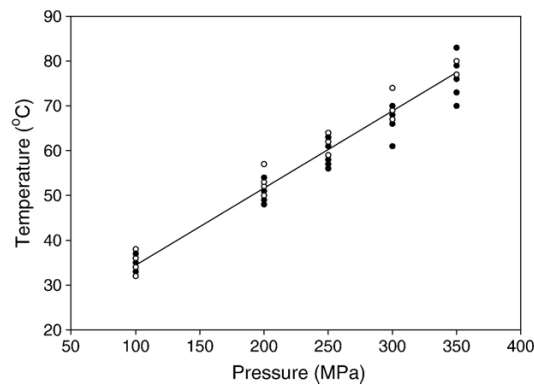
Figure 2 - 21: Temperature increases during high-pressure homogenization with data representing individual experiments showing linear regression for all points in plot [170]

2.6.2 High Pressure Gradient

Brookman and James [39] and Brookman [174] sought to explain the mechanism of cell rupture through their hypothesis in terms of the rapid release of pressure as cells pass through the HPH. Clarke *et al.* [139] studied and estimated the static pressure for a given streamline of flow through the use of computational fluid dynamics (CFD) showing pressure drop for the model used. Results from the model were obtained by estimating the static pressure at fixed points along the streamline of a single cell passing through the homogenizer. Based on this fact, it

is worthy of note to know that the zero pressure at the end of the streamline was artificially created by the pressure outlet boundary conditions in the CFD model. Figure 2-22 shows the pressure gradient of a liquid passing through the homogenizer valve.
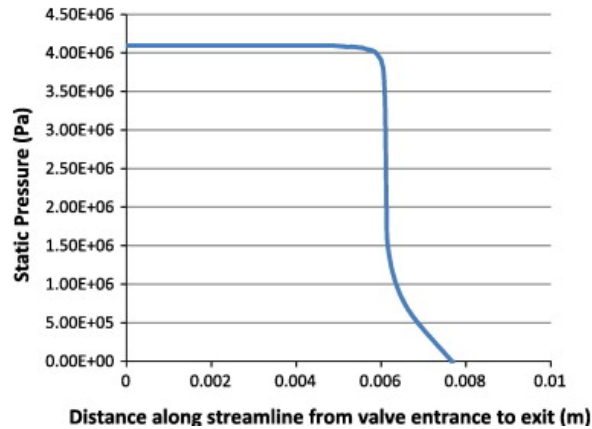
Figure 2 - 22: Pressure gradient of liquid passing through the homogenizer valve [139]

Previous work by Diels and Michiels [175] confirmed that the level of microbial inactivation caused by the application of high-pressure homogenization, to increase with the pressure level especially at high hydrostatic pressure (HHP). As pressure is applied, inactivation increases with the increasing pressure level and in some cases, results in the complete inactivation of the initial cell load. Figure 2-23 reveals, the micrograph structure showing the extent of the damage caused after *Saccharomyces cerevisiae* (*S. Cerevisiae*) has been subjected to 150 MPa under HPH at 2°C. Temperature, pressure, the number of passes, and the type of equipment are known to influence the effectiveness of microbial inactivation, and as such should be chosen well for the maximum degree of inactivation attainment. The elevation of process pressure results in an increase of microbial inactivation, and Brookman and James [39] measured the effect of pressure on the disintegration of *Saccharomyces cerevisiae* by the soluble protein. They found an exponentially increasing release of soluble protein with increasing pressure.
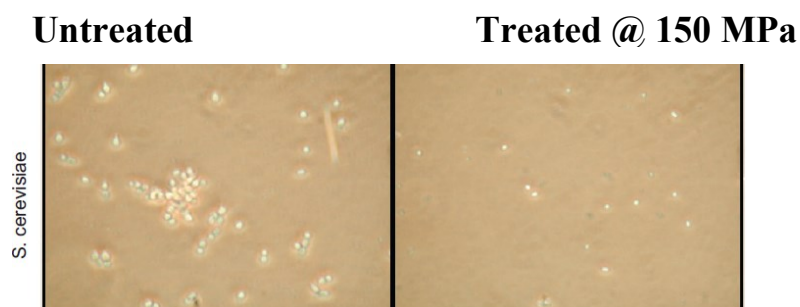
Figure 2 - 23: Micrograph of *Saccharomyces cerevisiae* (10 x magnifications) before and after HPH treatment at 150MPa with inlet temperature of 2°C. [176]

2.6.3 Number of Cycles (Passes)

The number of cycles (passes) is considered as a full cycle for complete homogenization of biomass substrate from the time of inlet and exiting at the outlet from the HPH. Under this condition, it is assumed to have covered a cycle (or pass) as other authors or researchers will call it. This parameter is thought to also contribute to the effect of using biomass substrates in HPH. As the cycle continues, more of the cell walls within the substrates are disrupted for the release of the intracellular contents. As the homogenizing cycle increases, this also reduces the particle size of the homogenized product.

In the study conducted by Sandra and Dalgleish [172], Reconstituted Skim Milk Powder (RSMP) was homogenized using UHPH at different pressures (41 − 186 MPa) with up to 6 passes as the number of cycles employed. The higher the pressure and the more the passes employed, the smaller was the average diameter of the casin micelles in the RSMP. Sandra and Dalgleish [172] confirmed higher pressure, increasing to 114 and 186 MPa to have caused a significant size reduction when compared with the control. Multiple passes did not seem to have further effect at 114 MPa, but further decrease of average micelle size at 186 MPa was observed with increasing numbers of passes. Furthermore, increasing pressure resulted in decreased average micelle size, and the extent of size reduction with the number of passes was more significant at higher pressure [172]. Previous results from the work of Hayes and Kelly [173] showed similarity and conformity with the work of Sandra and Dalgleish [172]. There was no reduction

in micelle size up to a pressure of 150 MPa but there were some decreases at 200 MPa.

2.6.4 Gap sizes

Juliane Floury and co-researchers have contributed greatly to the field through their various works and publications on gap sizes and its effect on HPH. They have emphatically worked in this field to present a clearer view on the operation as regards gap size effect on HPH. In the work of Floury *et al.* [148], measurements of the thickness of about 20 microscopic views of wax threads give us a mean value for the size of the narrow gap between valve and valve seat equal to 9.1 ± 0.71 μm at a homogenizing pressure of 10 MPa. As estimated by the equations of Nakayama and Phipps, the results obtained were equal to 7.6 and 7.75 μm, respectively, at the same operating pressure with water. Floury *et al*. [148] suggested that the difference in value above may be a result of the increase of the total pressure drop in the homogenizing valve when some wax grits that cross the narrow gap size. Innings and Trägårdh [177] studied flow in HPH and considered it very extreme with gaps of 10 – 100 μm and velocities of hundreds of m/s. This practically makes it impossible to measure the velocity fields. Contrarily, HPH has been found to be the most efficient means in the creation of sub-micron emulsions in low-viscous fluids, and for the realization of this particle size emulsion the HPH must be from a high-pressure piston pump with a narrow gap. Gap sizes are assumed to be a great determinant in the formation of different particle sizes in homogenized substrates. Innings and Trägårdh [177] explained that the pump creates a pressure of 10-500 MPa with the emulsion accelerated to velocities of up to hundreds of m/s in the gap. For the flow pattern and particle size distribution of substrate, an established relationship has been developed between the valve gap size and homogenizing pressure. The design of the gap size of the valve has been considered as another important aspect as part of the evaluation for the effectiveness on cell disruption in HPH [177]. Calligaris *et al.* [141] have hypothesized that both the valve design and the flow conditions in the homogenization valve gap allow different mechanical stresses to be suffered by the product. In conclusion, the operative pressure during homogenization is not the

sole critical factor that controls the overall effect of the process as the equipment engineering is inclusive to the efficient homogenization process.

2.6.5 pH

The pH value of the substrate in solution plays a role in the complete disruption of cell walls during the homogenization process of Baker's yeast and microalgae. Prepared buffer liquid was set to 5.3 pH value before mixing the biomass substrates in solution. Homogenized substrates were observed to have completely changed in terms of the pH value, and this indicates that HPH has changed the microstructure and content within the solution. Joscelyne and Trägårdh [178] examined pH as another parameter that is product dependent. They observed that membrane surface properties are pH dependent since membrane surfaces exhibit an iso-electric point at a given pH where the surface has no net charge. Iordache and Jelen [179] analysed heat treatment being the most measurable effect on whey protein functionality while others consider moderate heat treatment (60-70°C) to structurally unfold proteins, whereas at higher temperatures protein aggregation in various degrees may occur. This is dependent on important factor as pH.

Floury *et al.* [162] studied the effect of homogenizing pressure from (20 to 300 MPa) on model emulsions stabilized by whey proteins and part of the findings was that proteins are soluble on all ranges of pH and are also known as good emulsifiers at pH < 7. It was also found that the micro-particles sizes obtained from whey protein concentrate or isolate could be controlled by different conditions of pH, heat treatment, microfluidizer pressure, and the number of recirculations [167]. This therefore demonstrated that these micro-particles could be incorporated into food products (0.5% w/w protein) and when electronmicroscopy analysis was conducted [167].

2.6.6 Turbulence

In determining the true cause of cell wall breakage in a high pressure homogenizer, Kelly and Muske [180] considered this to take place at low

operating pressure in liquids of low viscosity. They argued that the mechanism of turbulence, pressure gradients and shear stresses could not be the cause of cell breakage as their analyses predicted that no breakage should occur under these conditions. According to Paquin [167], it is very difficult to rank cavitation, shear and turbulence in order of importance due to their force-induced phenomena in dynamic high pressure systems taking place simultaneously. Making some assumptions about the violence of the turbulence Siddiqi *et al.* [165] calculated that a tensile force of 540 μN could be generated along the cell wall of a 5 μm cell in a liquid with density and viscosity similar to water, and it has been proposed that to be sufficient to cause rupture in the cell wall breakage. On a similar note, Doulah *et al.* [38] have hypothesized turbulence has the greatest influence on cell wall disruption in HPH and in their prediction of the protein released, based on a mathematical model, was successful. The results obtained showed similarity with that from experimentation, and the turbulence produced as a result consists of random effects in total with no dominating frequency of oscillation. Further to this, Doulah *et al.* [38] stressed that where the energy of turbulence is high enough, this can exceed the minimum energy needed to break the cell wall, and through this disruption can occur. At that time Doulah *et al.* [38] have stated both the turbulence characteristics in the HPH along with the physical properties of the system, such as the cell wall breaking stress, to be unknown.

2.6.7 Cavitation

The cavitation effect on HPH has been analyzed and it is still under study. Gogate *et al.* [181] elucidated that the underlying mechanism for this spectacular effect of cavitation as the violent collapse of bubbles or cavities resulting in the generation of extremely high temperatures and pressures locally. This has been classified into four types; acoustic, hydrodynamic, optic and particle cavitation, depending on the mode of generation. Emphasis here will be on the hydrodynamic cavitation resulting from the disruption of Baker's yeast and microalgae biomass substrates in HPH. The collapse of cavities violently results in the formation of reactive hydrogen atoms and hydroxyl radicals, which combine invariably to form of hydrogen peroxide and to some extent, are considered responsible in the

promotion of oxidation reactions. Hydrodynamic cavitation can simply be generated by the passage of liquid through a constriction such as an orifice plate and when the liquid passes through the orifice, the kinetic energy or velocity of the liquid increases at the expense of the pressure [181]. As a result of this boundary layer separation occurs and substantial amount of energy will be lost in the form of a permanent pressure drop. Engineers have generally looked with caution at cavitation in hydraulic devices due to the problems of mechanical erosion. Balasundaram and Harrison [182] classified this bubble collapsing phenomenon as the conditions that are generated which would allow cell wall breakage to occur, and therefore, it could be termed a mechanism for cell wall rupture. This collapse can be studied more easily under the assumption that the bubble has become detached from the surface irregularity and that it is now flowing freely in the liquid before the external pressure is increased.

2.6.8 Wall Impact and Impingement

Wall impact and impingement are the two main causes of cell disruption in HPH according to Keshavarz-Moore *et al.* [183]. Based on the understanding of these words "impact" and "impingement", they have been explained in the following way, impact is the collision of two objects (for instance, a cell and the impact ring), whereas impingement is a special case of impact in which one object (for instance, the impact ring) is eroded gradually by large numbers of small impacts caused by numerous discrete solid objects (cells or solid impurities) flowing in the liquid at high velocity [183]. Engler and Robinson [184] suggested that shear, turbulence, or stress caused by impingement of a high velocity jet on a stationary surface may be responsible for disrupting cells when the flow pattern in a homogenizing valve is being considered. They eventually came to the conclusion that impingement of a high velocity jet of suspended cells on a stationary surface is necessary for effective disruption of cell walls by HPH, having realized that turbulence near the point of impact can enhance disruption. There have been several mutually interacting mechanisms proposed in the recent past regarding the cause of disruption, and these are still a matter of some debate, with different authors having different views on the actual causes of cell wall rupture.

Middelberg *et al.* [185] have indicated that high-pressure homogenization remains a poorly understood unit operation in spite of its apparent simplicity and widespread use for large scale disruption of microorganism and other particles. Based on these facts, Save *et al.* [186] have proposed that cavitation and the shock waves/pressure impulses produced as a result of cavity collapse are known to be responsible for cell disruption. Experiments on jet impingement from a circular orifice [183] showed that this pressure P_s is a function of the exit jet velocity from the orifice, the fluid density, orifice distance from the impingement wall, and the orifice diameter, but independent of fluid viscosity as shown in equation (2-1):

$$P_s = \frac{25\rho v^2 d^2}{X^2}$$

(2-1)

Where impingement pressure P_s at the point of impact is a function of exit jet velocity from the orifice v, the distance from the orifice to the impingement wall X, and the orifice diameter d. Keshavarez-Moore *et al.* [183] viewed and considered the dependence of yeast disruption on valve design and impact distance, and therefore identified impingement on the impact ring as a major cause of disruption for yeast. Engler and Robinson [184] constructed a special impingement device in the examination of the importance of impact as a mechanism of disruption. Based on the creation of the device, the associated stress within the fluid is considered as equivalent to the dynamic pressure of the fluid against the plate. This can be expressed as the maximum value of the dynamic pressure, and is in turn related to the impingement pressure *(P_s)* which is represented in equation (2-2)

$$P_s = \frac{1}{2}\rho v^2$$

(2-2)

Where ρ is the cell suspension density and v is the jet velocity.

2.6.9 Shear Stress

Many authors have considered and written about shear stress as a factor that affects high-pressure homogenization of biomass substrates during

homogenization. Most authors have assumed this to have arisen on the surfaces of cells in the operation of the homogenizer. Clarke *et al.* [139] highlighted that if these stresses were large enough, they could cause the rupture of the cell wall. There have been some controversies with this claim. These have denied the report that shear stress results in the cause of microbial breakage in low density suspension as that encountered with cells in water. Miller *et al.* [187] and Kelly and Muske [180] have concluded that at low viscosity, channel shear stress is unlikely to cause cell disruption. This was based on the gap size being in the range of 1-11 μm, the viscosity between 1-5 mPa s and the pressure within (0.138-0.965 MPa). On the contrary, channel shear stress will be considered the main cause of cell breakage only when viscosity is at higher value different from the data above. Clarke *et al.* [139] also concluded that breakage of the cellular component in the vicinity of the walls of the valve parts, either through shear or direct collision, as well as tearing by vortex shedding on weak points, could also be characterized under breakage by shear. Fluid shear stress has therefore been considered as the most influential cause of cell breakage, and can be accepted that there will be a lag of velocity in the gap region for the cells in comparison to the fluid. The phenomenon surrounding shear stress is dependent on the relative velocity between the solid as well as the surrounding liquid, and the same set of features is said to occur irrespective of whether the liquid is accelerating or decelerating.

2.6.10 Separation

Phipps demonstrated that separation and cavitation were likely to occur in the valve region at low pressures and were more susceptible to occur with square edged seats than rounded seats [188]. Kleinig and Middelberg [189] have related the pressure drop to separation. They have explained that pressure distributions could be predicted with good accuracy downstream of entry conditions, but flow near the inlet is considered to be dominated by separation and subsequent reattachment, making analytical solutions for the total pressure drop impractical. Some separation is predicted to occur in the square valve, but only at higher valve gaps (see Figure 2-24). Kleinig and Middelberg [189] used computational fluid dynamics in predicting valve region velocity and pressure fields, and based on the

simulation, predicted that no flow separation can occur in the cell-disruption seat over the range of valve gaps examined. This accordingly was show to be 24-7.6 μm, corresponding to pressure drops of 5-65 MPa). From the work on separation and cavitation conducted by Kleinig and Middelberg [189], this has been shown to be in agreement with the previous work of Phipps that flow in homogenizer valves will only separate and cavitate at low operating pressures, and that it is more likely to occur for a square-edged seat than for a seat with a rounded inlet. Further analysis showed that separation and cavitation do not influence flow in the valve region under normal homogenizer operating conditions where pressure is greater than 50 MPa.
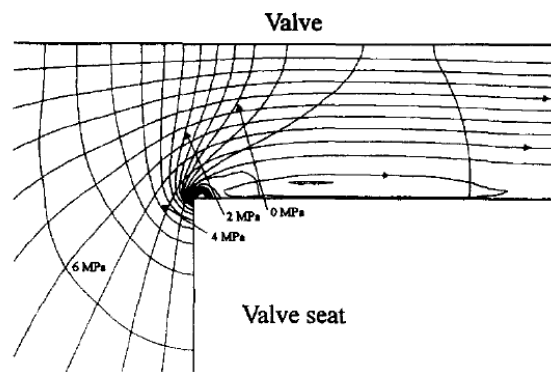
Figure 2 - 24: Results of numerical simulation for streamlines and pressure contours in the valve region of a square-edged inlet valve seat (30 μm valve gaps, 7 MPa total pressure drop) [189]

Physical disruption methods with process-scale application, are considered gentle, and result in large cell debris with advantage for separation of soluble proteins, enzymes, or other bio products. Middelberg [157] termed the process not advantageous due to the fact that the methods are limited in their applicability, which in most cases results in low efficiency.

2.7 Rheological Properties of Baker's Yeast and Microalgae

The considered biomass substrates; Baker's yeast (saccharomyces cerevisiae) and Microalgae (Chlorella vulgaris) show similarity in their rheological properties. Their viscosity and viscoelasticity are known to vary depending on the applied

external conditions, such as stress, strain, and temperature. Most commonly known properties of rheology are: viscosity, solubility, density and conductivity.

2.7.1 Viscosity

Viscosity plays a major role in the microbial inactivation of biomass substrates, as it is the measure of its resistance to gradual deformation by shear stress or tensile stress. It is the collapsible force that is involved in the disruption during homogenization. It is another form of bulk property with resistance to flow. Fluid temperature, on the other hand, is inversely related to fluid viscosity and fluid viscosity is known to affect bacterial inactivation by high-pressure homogenization. Diels *et al.* [169] demonstrated that the temperature effect on microbial inactivation could be explained by an indirect effect of fluid viscosity. The viscosity of fluid has an effect on some of the proposed mechanisms of cell disruption by high-pressure homogenization such as; turbulence [38], impact with solid surface [183], and extensional stress [190]. Furthermore, Harrison *et al.* [164], and Kleinig and Middelberg [189] explained the decrease in disruption with increased cell concentration by the increased viscosity of the homogenate. For example, *E. coli* based analysis as conducted by Diels *et al.* [163] demonstrated that the viscosity of cell suspensions containing 10^5-10^8 cfu/ml was not notably different, and neither was the efficiency of high-pressure homogenization inactivation on these suspensions. Low viscosity of diluted cell suspensions, as have been observed by Harrison *et al.* [164] and by Kleinig *et al.* [191] have used this guiding principles in proposing the increased levels of high-pressure homogenization inactivation upon *E.coli* cell suspension dilution. Therefore Diels *et al.* [163] then substantiated their points through demonstrating that bacterial inactivation by high-pressure homogenization was inversely related to the initial fluid viscosity. This has then led to Stevenson and Chen [192] predicting that viscosity influences the flow patterns in high-pressure homogenizing valves along with having effects on cavitation and fluid turbulence. The CFD model developed by Miller *et al.* [187] was eventually used in determining the effect of fluid viscosity on various fluid dynamic parameters thought to contribute to cell breakage in HPH.

2.7.2 Solubility

In comparison with clear distilled water most biomass substrates in solution are said to exhibits some negative effects; for example, heat treatment during homogenization decreases solubility. Temperature and homogenizing pressure are considered as factors in this process that show, great effects on the substrates during homogenization. As the pressure increases, so also the solubility of substrates increases. For example, homogenization of heat denatured whey proteins by a microfluidizer prior to spray drying causes an increment in the solubility upon reconstitution and as proven by some authors, the treatment employed could disintegrate the aggregate formed during heating. When compared to a control, treated samples were shown to have restored gelling properties upon heating. This was pH dependent. Floury *et al.* [193] showed 11S soy protein lost its solubility at pressure above 150 MPa due to protein denaturation and aggregation.

Similarly, Clarke *et al.* [139] have explained solubility on the basis of using Henry's law to support their claim, "*The law states that the solubility of a gas is proportional to the pressure in the liquid*". Solubility of the gas is said to decrease as the external pressure in a liquid decreases also. This apparently shows the release gas bubble noticeable in the liquid under reduced pressure, and the bubbles grow smaller when the external pressure increases. The gas gets trapped inside the bubble and eventually collapses as the bubble increases, but then slows down the collapse. This explanation also shows interaction between cavitation and solubility during homogenization.

2.7.3 Density

Density as a rheological property affects high-pressure homogenization (HPH) or the substrate in some form or another. This is in the form of energy density has a relationship with the machine parameters of pressure, rotational speed, and time, and it is considered the minimum droplet size achievable during homogenization. Energy density, or the volume specific energy input can simply be calculated from the power consumption, and the volume flow rate and the mean droplet diameter

may often be empirically related to the energy density as long as other parameters are kept constant. Similarly, emulsifier properties play a key role through the relationship between energy density and the volume fraction. The achievable mean droplet diameter as given depends strongly on the emulsifier. Clarke *et al.* [139] have identified density as a factor that affects the high-pressure homogenizer, and in their work the violent collapse of bubbles which explains the phenomenon of cavitation, have been shown to be very small. The forces that cause the collapse build up to such high values result in the density of the energy produced to be very large. Further to the work of Clarke *et al.* [139], it was deemed appropriate in modifying the computational fluid dynamics (CFD) to allow for special effects that occur once the external pressure fell below atmospheric pressure. This was as a result of the existence of large quantities of dissolved gases in cell suspensions in most of the studies of cell rupture. In this situation, where the pressure remains above atmospheric, the continuity equation can be simplified in predicting no changes in the fluid density, and in this cased the fluid becomes incompressible. When this is not the case, the pressure falls below atmospheric pressure and gas bubbles will develop in large numbers in the fluids with quantities of microbial cell suspensions. This will then result in a change in the average fluid density and eventually the fluid becomes compressible.

2.7.4 Conductivity

Cavitation is the dynamic process of gas cavity growth and the collapse in a liquid [175]. These cavities, in the presence of dissolved gases or vaporizable liquids, are formed when the pressure in a certain fluid volume is less than the saturation pressure of the gas or the vapour pressure of the liquid [175]. Conductivity is interrelated to cavitation and has been found to influence the degree of cavitation by affecting the heat dissipated from the collapsing bubble to the surrounding solution. This is found to have resulted through thermal conductivity of the dissolved gases. Exponential decrease in cavitation teds to increase the thermal conductivity of the dissolved gases. In addition to conductivity, fluid viscosity is considered to have also played an important role on the influence of cavitation. On the other hand, Shirgaonkar *et al.* [166] expressed cavitation through using the inception number. This is a dimensionless number generally used in the

characterization of the cavitation event, and can be represented with the equation 2-3 below:

$$\sigma = 2 \cdot \frac{P - P_v}{\rho v^2}$$

(2-3)

These are presented in the following way;

P = Local static pressure

P_v = Vapour pressure of the fluid

v = Local velocity

ρ = Fluid density

Knowing the predicted values of absolute pressure, as well as that of fluid velocity at the gap exit from numerical simulations, enables other unknown data to be worked out. There is the possibility of estimating the cavitation number in the downstream region of the homogenizing valve where cavitation is supposed to occur. Under ideal conditions cavitation occurs when $\sigma \leq 1.0$ Shirgaonkar *et al.* [166]. In reality, experiments have shown cavitation inception at values of $\sigma > 1.0$ [175].

2.8 Previous Research on Protein Yield from Homogenized Substrates – *(Saccharomyces cerevisiae/Chlorella vulgaris)*

Saccharomyces cerevisiae and *Chlorella vulgaris* has become a household name in research for renewable energy as biomass substrates. Their prominence as biomasses is as a result of their continued usefulness in the energy world through production of protein from their inner content. High-pressure homogenization as a mechanical technique for cell wall disruption of these biomasses is considered based on some of previous works done using the machine. In the work conducted by Spiden *et al.* [194], it was highlighted that *Saccharomyces cerevisiae* was chosen for their experimentation based on its representation as a model microorganisms with a well understood structure and similar dimensions to alternative industrial promising microorganisms such as oleaginous algae. High-

pressure homogenizer was selected as a technique for the disruption through considering the process parameters, such as pressure and number of passes. These were made to investigate cell counting, protein release, UV absorbance, turbidity, mass loss analysis, viscosity and particle sizing.

In a similar development, Shynkaryk *et al*. [195] investigated *Saccharomyces cerevisiae* in a combined electrically-assisted HPH technique for cell wall disruption in aqueous suspensions. Efficiency of HPH technique was thought to depend mainly on the homogenizing pressure and the number of passes but with breakage critically dependent upon the pressure above the threshold for protein yield. Yap *et al*. [196] evaluated microalgae cell for energy analysis through high-pressure homogenization. Such microalgae species as *Nannochloropsis* was considered and the analysis indicates that the energy load for HPH for algae considered could be minimized. This is when operated at higher pressure and fewer homogenization numbers of passes. Spiden *et al*. [197] compared *Saccharomyces cerevisiae* against microalga such as; *Chlorella sp., T. suecica* and *Nannochloropsis sp*. to evaluate their protein yield, cell count, UV absorbance and turbidity through HPH. Their findings indicated that these biomass substrates were all susceptible to rupture using the HPH with *T. suecica* considered has the most susceptible to rupture by HPH followed by *Saccharomyces cerevisiae* and *Chlorella sp.* while *Nannochloropsis sp.* showed more difficulty in terms of disruption using HPH.

In general, authors and researchers above, all have similar view on cell wall breakage of the biomasses considered in the release of protein concentration using the high-pressure homogenizer of one form or the other.

2.9   Summary

The review of literature has been conducted extensively covering all parts of the research work. Biomass as an energy source has been entirely covered with clear indications of the reasons for Baker's yeast and Chlorella vulgaris as choices of substrates in this study. Investigations by different researchers and authors have shown that protein content released are considered to be highly rated. Their

structures and inner contents are compatible when applicable buffer solutions are applied to their treatment before and after homogenization.

The mechanical disruption process through the use of a high-pressure homogenizer can result in higher protein yield as the disruption is rated to reduce the substrate particle size as low as 2 microns. HPH was therefore considered as the optimal choice for the disruption technique, and its use in the research conducted is in conformity with previous views [139, 156, 164, 166]. Different parameters are known to affect substrate during the homogenization process; these have all been researched with an emphasis on pressure, temperature, and number of cycles. Subsequent chapters will study these parameters to assess their effect on the substrates used in this research.

Chapter 3
Experimental and Analytical Procedures

3.1 Introduction

This chapter describes the materials, equipment and the methodologies used in this research. The results of each of the experiments are presented in the chapters to come with emphasis on the substrates and the dilution ratios of buffer against the substrates highlighted. These are also based on the methodologies and applicable equipment applied at the various steps taken in the course of the work. The following sub-sections are separated and elucidated accordingly for clarity to the reader.

Also, the software package selected for implementation of analysis in this research; *Design-Expert v.8* is discussed and generally overviewed in this Chapter. This was to create clarity and readability for a better understanding of the work presented with the applicable software. The software determined the ranges of each process parameter, along with the experimental layout presented for each biomass substrate. The section also will discuss the cost aspect in terms of energy and cost analysis as applied to the research.

3.2 Materials

Two different biomass materials were used as the main substrate in this work; yeast *(Saccharomyces cerevisiae)* and microalgae *(Chlorella vulgaris)*. The reasons for their selection have been fully explained in Chapter 2. Algae and yeast amongst others are microorganisms which utilizes inexpensive feedstock and waste as sources of carbon and energy for growth in the production of biomass, protein concentrate and amino acids. Most notably the reason for selecting these as biomass in this study is their superior nutritional quality, and potential to serve as a food and energy source due to their high photosynthetic efficiency. These were selected to be homogenized under the high-pressure using the High-pressure

homogenizer (HPH) with buffer solution as the co-digester (the buffer used for this research will be explained later in the chapter). These materials can also be considered as a sustainable source for bioenergy for reasons referred to above. The chosen materials for this study are yeast *(Saccharomyces cerevisiae)* and microalgae *(Chlorella vulgaris)*. Other materials used in this research apart from the biomass substrates will also be considered and discussed herein.

3.2.1 Baker's Yeast *(Saccharomyces cerevisiae)* Substrate

Sections 2.2.2, 2.2.4, 2.2.5, 2.2.8 and 2.2.10 have covered and explained more about yeast as a substrate for energy production and as a biological host. Various microorganisms such as yeast, algae, viruses and bacteria, as well as other biological products are disrupted to release the intracellular substances such as proteins, enzymes and vitamins which are found in high concentrations. The most ideal way, for efficient and effective cell rupture operations is the homogenization of these substrates using the high-pressure homogenizer. This can often maximize the yield from valuable sources of this material and at the same time keep the product quality at a very high level. Yeast as an effective biomass for the production of energy has been proven by many authors, including Weiland [91], who have highlighted that all types of biomass can be used as substrates for biogas production as long as they contain carbohydrates, proteins, fats, cellulose and hemicelluloses as the main components. Biogas composition and methane yield is dependent on the type of feedstock, the digestion system as well as the retention time according to [198]. In the work carried out by Hammerschmidt *et al.* [199], Baker's yeast (Saccharomyces cerevisiae) was used as feed for the production of liquid biofuels in a continuous one-step process under hydrothermal conditions in the presence of excess hydrogen and K_2CO_3. Furthermore from the same work done by Hammerschmidt *et al.* [199], wherein yeast conversion experiments were performed in an up-flow reactor under near-critical water conditions, and with temperature 330 - 450 °C and pressure 20-32 MPa. This revealed the approximated chemical composition of yeast and the analysis of the dry matter of feed as shown in Tables 3-1 and 3-2. Yeast was used as a feed for the study because of its almost constant chemical composition. This has already been used

for the production of proteins and amino acids in a closed batch reactor at temperatures from 100 - 250 °C and pressures of 101.35 kPa - 3.97 MPa [200]. The choice of yeast choice in this research is not limited to just its homogenization for the release of intracellular matter for energy conversion or for food products manufacture, but also to the fact that its particle size can be reduced to as small as 0.02 μm for use in research.

3.2.1.1 Protein Extraction from Homogenized Baker's Yeast

Fernandez *et al.* [201] have experimented through evaluating the rheological behaviour and stability of oil-in-water emulsions prepared with aqueous dispersions obtained from homogenized Baker's yeast *(Saccharomyces cerevisiae)*, refined sunflower oil, and hydrocolloids that are widely used in low-in-fat mayonnaises formulation. Preparation of yeast aqueous dispersions by high-pressure homogenization was conducted by the rupturing of yeast whole cells in an alkaline medium through HPH. The reduction of nucleic acid content (RNA) was performed first by heat treating the sample at alkaline pH before the cell rupture. Particle size distribution of the aqueous dispersion was determined by laser diffraction using a Malvern Mastersizer 2000E analyser. From the results, it was seen that higher yield in the formulation of yeast dressing with yeast aqueous dispersion were obtained as compared to others such as water, refined sunflower oil and hydrocolloids. This study also indicated, that the high pressure homogenization (1500 bar, 3 passes) in alkaline medium ensured a good degree of protein dispersibility (>50%) in aqueous dispersions. Yeasts possess advantages over other microorganisms because of their larger size which makes it easier to harvest. Other distinguishing factors that are advantageous to yeasts are; the lower nucleic add content, high lysine content and ability to grow under acidic pH.

3.2.1.2 Baker's Yeast form and Storage

Baker's yeast *(Saccharomyces cerevisiae)* fresh and in block form during the experimental research was provided by Dublin Food Sales, Ireland. This product was refrigerated between 0 – 6 °C for freshness on the day of its collection so as to

keep it clean and remain fresh before use, as well as to keep it from contaminants from other sources. For handling, it was recommended that yeast be kept cool as it deteriorates rapidly when the yeast goes up to 8 °C [202], and the storage air temperature should be maintained between 0 and 6 °C, otherwise the yeast would generate heat and start gassing in a confined space. For this reason there should be air gaps within the storage compartment [202]. As Baker's yeast is composed of living cells of aerobically grown *Saccharomyces cerevisiae* and majority of the proteins in the cells are known to be glycolytic enzymes. Thus the high protein content correlates with high gassing power [203]. Baker's yeast qualities include its rate of gas production, along with the long term stability during storage before being used. Figures 3-1(A) and (B) show a typical example of yeast (*Saccharomyces cerevisiae)* substrates in block and homogenized forms where Table 3-1 describes its chemical composition and Table 3-2 identifies its dry matter elemental composition .
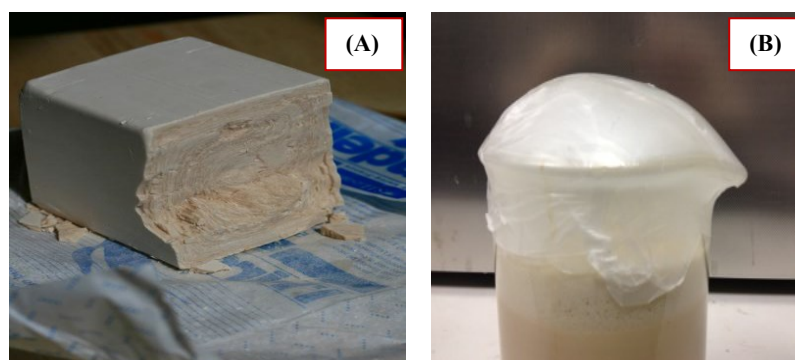
Figure 3 - 1: Sample of Baker's yeast; (A) in Block form and (B) in homogenized state

Table 3 - 1: Approximate chemical composition of yeast [200]

Parameter	Unit	Chemical composition of 1Kg yeast (s.cerevisiae)
Protein	(g/kg)	167
Fatty acids	(g/kg)	12
Carbohydrates	(g/kg)	11
Dietary fibre	(g/kg)	69
Minerals	(g/kg)	21
Moisture	(g/kg)	720
Heating value	kJ/kg	3470

Table 3 - 2: Analysis of the dry matter of Baker's yeast feed [107]

Parameter	Unit	Analysis of yeast dry matter
Carbon	(%)	45.0
Hydrogen	(%)	6.70
Nitrogen	(%)	7.02
Oxygen	(%)	33.4
Ash	(%)	7.92
Sulphur	(g/kg)	3.27
Phosphorus	(g/kg)	9.36
Sodium	(g/kg)	0.55
Potassium	(g/kg)	1.4-45.7
Magnesium	(g/kg)	1.10
Calcium	(g/kg)	0.63
Iron	(g/kg)	0.06

3.2.2 Microalgae *(Chlorella vulgaris)* Substrate

Chlorella vulgaris has been discussed extensively in Section 2.2.6 and its suitability as a biomass substrate is beyond question due to the fact that proteins and lipids content within their cell is high enough to yield biogas as compared to other biomass materials [85]. Their use has gone lately from human consumption to the production of energy [85]. They can grow autotrophically and heterotrophically with a wide range of tolerance to different temperatures, salinity, pH and nutrient availabilities. *Chlorella vulgaris* along with *Chlorella Protothecoides* are two widely available microalgae strains in the commercial applications for food and nutritional purposes. Heredia-Arroyo *et al.* [204] have indicated that they can show great potential as future industrial bioenergy producers due to their robustness, high growth rate, and high oil content. They can be cultured under the same conditions; autotrophic and heterotrophic. Accordingly, Heredia-Arroyo *et al.* [204] revealed in their results that *Chlorella vulgaris* could grow on autotrophic, mixotrophic and heterotrophic modes; and the mixotrophic cultivation especially could produce more cell biomass than the autotrophic or heterotrophic cultures, individually or combined [204].

3.2.2.1 Previous Work on Chlorella Vulgaris

The work carried out by Abreu *et al.* [205] in determining the growth parameters and biochemical compositions of the green microalga *Chlorella vulgaris* cultivated under different mixotrophic conditions showed similar results. It was highlighted that using the main dairy industry by-product could be considered as a feasible alternative in reducing the costs of microalgal biomass production. This is based on the fact that the addition of expensive carbohydrates to the culture medium would not be necessary. From the findings, the results indicate that the highest specific growth rates were 0.43 and 0.47 g/day when the substrates were cultivated under mixotrophic conditions using cheese whey (CW) powder solution, along with mixtures of glucose and galactose as organic carbon sources, respectively. This result is in agreement with the result from Heredia-Arroyo *et al.* experimental work carried out using *Chlorella vulgaris* as a substrate, [204] which

also indicated that the values obtained were almost 3.5 times higher than those produced under the photoautotrophic mode of nutrition. This again also agreed with the findings from Kong *et al.* [206] which reported that mixotrophic *Chlorella vulgaris* growth in glucose yielded higher biomass contents and productivity than cells grown under photoautotrophic conditions. This yield, and the biomass accumulation of *Chlorella vulgaris* during the cultivation, has been promoted through the role played by the organic substrate. It therefore has come to be realized that microalgae grew faster which thus provides high productivities of biomass, lipids, starch, and proteins: hence, the particular reason for *Chlorella vulgaris* choice as a biomass substrate in this research.

3.2.2.2 *Chlorella Vulgaris* Sample and Storage

Table 2-5 of Section 2.2.10 in Chapter 2 shows the general composition of different human food sources and algae (% of dry matter). It shows *Chlorella vulgaris* to be higher in terms of the protein content. This reflects the reason for one of its consideration as a biomass substrate amongst others in this research.

A sample of the substrate is shown in Figure 3-2. This was supplied by a Culture Collection of Algae and Protozoa (CCAP) of the Scottish Marine Institute, United Kingdom. This determination of the strain, was through the identification of CCAP 211/11B from the original author Beijerinck 1890, where freshwater in Delft, Holland was used [207].

The culture conditions as demanded by the CCAP required the temperature to be 15 °C ± 2 °C, and for faster growth, it should be grown at 20 – 25 °C in cool white fluorescent tubes about 10 cm from the culture, with an intensity of 30-40 $\mu mol/m^2s$, and 12 hours light and 12 hours of darkness (for faster growth, use continuous light). Refer to Appendix A for further information on the strain data.
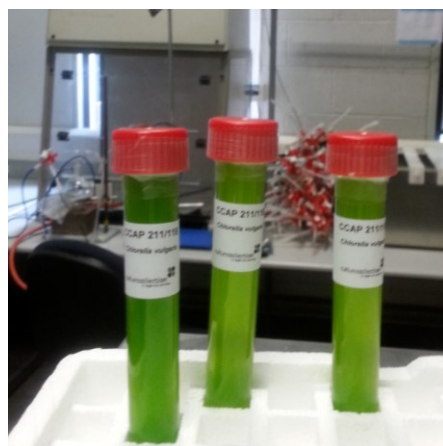
Figure 3 - 2: Chlorella vulgaris with strain number CCAP 211/11B [207]

3.2.3 Deionised Water

This was required at all times in the preparation of the pH controlled buffer solution before embarking on the experiments. Deionizing systems use a mixture of cation and anion exchange resins which are usually in a mixed bed. These resins exchange cations and anions in the source water for H^+ and OH^-, which, when combined, form H_2O leaving only the residual H^+ and OH^- produced by auto dissociation (see equation 3-1).

$$H^+ + OH^- \leftrightarrow H_2O \tag{3-1}$$

With the pH of deionised water close to 7, the equilibrium constant of this reaction is considered to be 1×10^{-14} at 25°C. The resistivity and conductivity ranges are thought to be (10^{-18} MΩ. cm) and ($0.1 - 0.0555$ μS/cm) respectively [208].

It is water that has the ions removed and is usually deionized by ion exchange process. This has become necessary so as not have interference during any chemistry experimental work as the presence of ions could switch places and alter the experimental results. Above all, conductivity may occur as water with ions have higher conductivity than the water without ions. This should not be confused with distilled water which is water known to have many impurities as salts, colloidal particles, and are removed through one or more processes of distillation.

3.2.4 Buffer Solution Used in this Research

The buffer solution for controlled pH was prepared using the chemical compounds supplied from Sigma-Aldrich. The solutions denoted as A, B and C will be explained therein.

Solution A

(0.1M KH_2PO_4 + 0.15M NaCl)   (3-2)

This is equivalent of 1litre

13.6g of KH_2PO_4 weighed into beaker and dissolved using the deionised water, also; 8.8g of NaCl weighed into a beaker and dissolved using the deionised water; both are mixed together and filled to the 1 litre mark. This was repeated thrice for 3 litres of solution to be obtained.

Solution B

(0.1M K_2HPO4 + 0.15M NaCl)   (3-3)
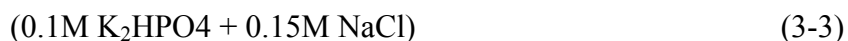
4.6g of K_2HPO_4 was weighed into a beaker and dissolved using the deionised water, also; 1.8g of NaCl weighed into a beaker and dissolved using the deionised water. Again both were mixed together and filled to the 200 ml mark in a flat-bottom volumetric flask.

Solution C

Put pH probe in solution A and gradually add Solution B into Solution A. Continue stirring while the 3000 ml beaker is sitting on the magnetic stirrer until the pH scale of attained 5.3 is obtained. The solution so obtained is known as solution C.

3.2.5 Protein Reagent

This is a reagent for detecting protein in a solution. The key objective of this work is to determine the protein concentration in the homogenized biomass substrates using the reagent. Protein reagent is a blue solution through which a Bovine

Serum Albumin (BSA) standard curve is produced. A high-quality, calibrated BSA solution (2 mg/mL) is serially diluted to create the protein assay standard curves. This is required in the measurement of protein concentration by means of a spectrophotometer. The procedure involved firstly preparing dilutions using 0.1 M phosphate buffer, pH 7.0, of each protein to 0.5, 5, 2, 4, and 5 mg/mL, then a series of dilutions were prepared starting at 100 mg/ based on the product, T1949 Total Protein Reagent [209]. These bovine serum albumin (BSA) solutions are considered as protein concentration reference standards for use in bicinchoninic acid assay (BCA), Bradford and other protein assay protocols. It is a universally accepted reference protein for total protein quantitation with the albumin standard precisely formulated at 2 mg/mL in an ultrapure 0.9% sodium chloride solution [210].

3.3 Equipment

The main machine used in this research was the GYB40-10S /GYB60-6S 2-Stage homogenizing valve HPH and has been described extensively in Chapter 2. Other pieces of equipment used in this research work are as listed in Table 3-3 which includes characterisation and electrical equipment. Others not listed can be referred to in Appendix E

Table 3 - 3: Characterisation and Electrical Equipment

Centrifuge
Scanning Electron Microscope (SEM)
Spectrophotometer
Energy Meter
Laboratory Oven
High-Speed Stirrer
Weighing Scale
Hotplate (Balance) Magnetic Stirrer
pH Meter
Delsa Nano C (Particle Size Analyser)

3.4 Experimental Procedures

Two-way experimental procedures have been applicable to this research. These are almost similar but with slight difference in the measurement and quantification. The reason for this has been as a result of the substrates state; yeasts being in solid form and microalgae in liquid form as supplied by the institute; CCAP (see Figure 3-2) [207]. These will be discussed herein in the sub-sections that follow.

3.4.1 Experimental Procedure for Baker's Yeast *(Saccharomyces cerevisiae)*

In addition to the two-way experimental procedures as previously explained, two approaches have been employed in the experimental work in this study. The RSM approach was used in conducting the optimization of all experimental work. The

experimental procedure based on the RSM technique will unfold in the next Chapter.

The One-Variable-At-a-Time (OVAT) approach was also employed for the experiments; this was aimed at investigating the effect of the higher pressure homogenizer device (GYB40-10S 2-stage homogenizing valves HPH) as a cell disruption machine on protein yield from the biomass materials considered which have been homogenized using the buffer solution, and to determine range of dataset for the parameters considered in the study.

3.4.1.1 Homogenization

For the experimental work on the use of the HPH, start by cleaning machine by running clean water through it and while the machine is on for about half an hour, it clears and cleans up the debris and particle that would probably cause error in the process. While the cleaning up is in place, break down the solid Baker's yeast and weigh out 950 g into the beaker. Measure 725 ml of Phosphate buffer (solution C) and then pour into the broken yeast. Mix using the electric laboratory mixer. For further cleaning, pass 2 litres of deionised water through the homogenizer and when the deionised water is almost completely empty in the HPH that is when the poured deionised water is almost at the inlet conical section, pass through the sample of yeast suspension (approx. 1625 ml) almost immediately down the feeder's tank of the HPH.

By turning the first and second hand wheel to increase pressure build up and balancing of pressure respectively, the desired pressure is attained (see Figure 2-16 of Section 2.5.3 in Chapter 2). As the connected pipe for yeast collection at the homogenizer outlet becomes cloudy during the substrate homogenization, this flows through to the exit, then start collecting the suspension in a graduated cylinder. It is important at this point to ensure that the temperature remain constant. After collecting one litre of the cloudy suspension (yeast suspension mixed with deionised water). This was thrown away as it would have mixed with deionised water used for the cleaning of HPH at the start of the experiment. For each new homogenized sample, pressure was recorded for data purposes. For

cycle more than 1, the collected homogenized yeast at the HPH exit was poured in again into the feeder's tank. Temperature was checked regularly with a thermometer to achieve the desired temperature before pre-treating in the HPH.

The homogenized yeast collected, was considered as homogenized undiluted yeast while the untreated yeast is regarded as the mixed soluble yeast that never passed through high pressure homogenizer (HPH); i.e. unhomogenized. The homogenized undiluted yeast was then separated into 4 tubes measuring 10 ml, 20 ml, 30 ml and 100 ml each. Phosphate buffer (solution C) with pH 5.3 in the ratio of 90 ml, 80 ml and 70 ml was added to the 10, 20 and 30 ml tubes respectively, to achieve 100 ml of sample, thus yielding ratios of 10:90, 20:80, 30:70 and 100% or 0.100.

3.4.1.2 Centrifugation

Each of the samples was emptied into the centrifuge tubes, and then centrifuged at 13,000 rpm over an hour as detailed in the operation manual. In order to separate the supernatant from the pellets, the appropriate procedures were followed. The supernatant was filtered using the syringe and syringe filter. 200 µl of the filtered sample and 900 µl (×2) of the Buffer (solution C) was taken into a test tube, that is; 2000 µl in total. Also, 2000 µl of homogenized undiluted yeast was taken. This process was repeated 6 times.

500 µl of each of the replicate tubes were taken into a cuvette and then diluted with 2000 µl of total protein reagent. The results for each of the six replicate cuvettes for each sample in the dataset were averaged to form a single reading for that sample, using the spectrophotometer and the results so achieved are read of on the protein curve. The spectrophotometer was set at the wavelength of 550 nm. This was left to stay for 30 minutes before determining the protein concentration.

3.4.1.3. Spectrophotometer

Technically, what the spectrophotometer is measuring is not how much light is absorbed, but how much is transmitted. The percentage transmitted can be easily converted to absorbance by using this formula (see equation 3-4);

$$\text{absorbance} = \log\left(\frac{1}{\%\ \text{transmittance}}\right)$$

(3-4)

There are two ways of determining protein concentration; the first way is through the use of the Beers-Lambert law.

From the equation, the absorbance equals the concentration of the molecule of interest (c), times the length of the path the light takes through the cuvette (b; always 1 cm for our spectrophotometers), times the extinction coefficient (ε) as shown in (equation 3-5);

$$\text{Abs} = \varepsilon bc$$

(3-5)

The extinction coefficient is the part that is specific for each compound and must be determined experimentally. It can be determined from the standard curve through solving for ε, because the absorbance and concentration are known, and it can also measure the width of the cuvette. Once ε is known it can then be used for other solutions of the same molecule.

The other way is by determining the concentration from the standard curve (a graph of absorbance against concentration for standard solutions whose concentrations are known). This is then compared with the absorbance of an unknown solution of the same molecule to that curve. Using the linear graph equation (equation of a straight line) equation 3-6;

$$y = mx + C$$

(3-6)

Where, m = slope or gradient, and C = Intercept at Y-axis

Therefore, the protein concentration at the X-axis can then be solved since the absorbance value on the Y-axis is known from the standard (protein) curve. Based on the prepared standard protein curve (see Appendix F), the protein concentration yield was determined through UV absorbance rate of the solution reading from the Spectrophotometer as the light passes across the liquid (liquid diluted with the total protein reagent). Section 3.5 below explains in detail protein curve preparation and spectrophotometer.

3.4.2 Experimental Procedure for Microalgae *(Chlorella vulgaris)*

The experimental procedure for microalgae was basically similar to the procedure described above for Baker's yeast; the difference is the measurement and quantification of the substrate against the phosphate buffer (solution C) pH 5.3.

10 ml of *Chlorella vulgaris* is mixed into 1000 ml of buffer solution C (phosphate buffer) at any time before pre-treating in the homogenization stage. The microalgae were not cultured and were pre-treated the same way supplied (by the Institute; CCAP). After the pre-treatment using the HPH, the other steps taken were same for the Baker's yeast. For further reference on the strain supplied, refer to Appendix A of this thesis.

3.5 Protein curve preparation and spectrophotometer

A standard protein curve preparation is needed for determination of the protein concentration. One absolute way for determining the concentration of any given protein in a solution having an unknown protein concentration is to compare the unknown solution with a set of protein solutions of known concentrations. This works by having the curve calibrated and in the process enable to determine the exact protein concentration measure in a solution under investigation. Therefore the absorbance associated with a set of protein solutions of known concentrations is otherwise known as the protein standard curve. Before setting up the assay, the protein to be used as a standard is decided upon and the range which it is likely to be sensitive is determined. As sensitivity varies from one reagent batch to another, immunoglobulin G (IgG) is frequently used as a standard in Bradford assay in the

same way as BSA (bovine serum albumin). With the BSA solutions, 0.1 M phosphate buffer, pH 7.0 of each protein to 0.5, 1, 2, 4 and 5 mg/ml were prepared to dilutions. Starting at 100 mg/ml and prepared serial dilutions were made using Total Protein Reagent and with the UV procedure a Standard Curve for BSA was prepared omitting 0.25 mg/ml dilution. The absorbance of the resulting solution is measured using the spectrophotometer (Figure 3-10) and the measured absorbance of the protein versus the known concentration of BSA is plotted. The resulting graph will then be the protein standard curve for determining the unknown protein concentration (see Appendix F).

3.6 Energy Cost Analysis

The cost analysis of the high-pressure homogenizer (HPH) was necessary in the experimental set up, to determine how much energy was consumed in the disruption of the biomasses, (Baker's yeast and Chlorella vulgaris in the liberation of the inner contents (protein) through their cell wall breakage). In doing this, an energy meter by Efergy was employed, which measures electrical energy consumption on any appliance. The tabulated and recorded cost for both biomasses were then translated and entered into the design expert along with the homogenization parameter to efficiently analyse the cost effectiveness of the process.

3.7 *Design of Experiment* (DOE)

3.7.1 Introduction

The Section discusses the general view on *design of experiment (DOE)* in relation to the considered design; Box Behnken design (BBD), analysis of the design as well as the desirability approach function.

3.7.2 Design of Experiment (DOE) Overview

This technique enables designers in determining simultaneously the individual and interactive effects of many factors that could affect the output results in any design. This was developed by Sir Ronald Fisher in the early 1920s at Rothamsted Agricultural Field Research Station in Harpenden London and in his experiment;

he used DOE that could differentiate the effect of fertilizer and the effect of other factors. This has been used since in wide range of disciplines. It can be used in finding answers in situations such as; "What is the relationship between factors and responses?", "What are the best combinations of factors value so as to maximize or minimise multi responses?", "What is the main contributing factor to a system?" and so on.

Taguchi and 2-level factorial design methods are the commonest designs amongst the many design of DOE. These are characterized by the lowest number of runs when studying a process with multiple factors and multiple responses. However, based on this fact, the quadratic effect of each factor cannot be determined using a 2-level factorial design, while also the interactions between the factors affecting the process cannot be determined through the use of the Taguchi method. This is as a result of the alias structures and this determines which factors are confounded with each other [211]. For these two reasons, the Taguchi and 2-level factorial designs are mainly used as screening designs in the identification of the main effects within a system. Realistically, Response Surface Methodology (RSM) on t one hand is able to fully determine all the factor's effects and their interactions. RSM is therefore considered as the chosen experimental methodology in this research through specifically using the Box-Behnken Design (BBD) in the implementation. RSM as a statistical technique is specially designed in optimizing the system's output, where the maximal and minimal goals are considered. Equation 3.5 shows the function identifying the response surface and consists of three capital-sigma summations. The operative and study regions are coincident in this particular design and signified each factor being investigated over its whole range. This is considered the competitive advantage for BBD over the central composite design (CCD), which is another example of the RSM approach [212]

3.7.3 Response Surface Methodology (RSM)

Box and Wilson [213] introduced the response surface methodology (RSM) concept in the 1950s having considered it as the best known type of DOE design. It has been adopted for the experiments of this research and will be elucidated in

the chapters to come. This also follows the Box-Behnken Design (BBD) whose variables are shown respectively in the appropriate chapters. RSM is a collection of statistical and mathematical techniques that can be used in the improvement, development, and in the optimizing processes, products, and systems. The goal is to find the model of the proposed system, by performing data fitting and regression analysis and the methodology is applied to the measured yields using the statistical software, *Design-Expert v 8.0*. Based on this, RSM also specifies the relationships among one or more of the measured responses and the essential controllable input factors [214]. Therefore all variables being measurable, and be repeated with negligible error, the response surface can be expressed by function y, where k is considered the number of independent variables:

$$y = f(x_1, x_2, \ldots x_k) \tag{3-7}$$

RSM is a mathematical and statistical technique set useful for modelling, interpreting and predicting the outputs of interest to several input variables χ (from level i to j) with the aim of optimizing a single or multiple responses y_s [211, 213]. To optimize the responses y_s, it is necessary to find an appropriate approximation for the true functional relationship between the independent variables and the response surface. A second order polynomial (Equation 3-8) is usually used in RSM [211, 215], where the values of the model coefficients b_0, b_i, b_{ij} and b_{ii} can be estimated using regression analysis.

$$y = b_o + \sum b_i \chi_i + \sum b_{ij} \chi_i \chi_j + \sum b_{ii} \chi_{ii}^2 + \varepsilon \tag{3-8}$$

The first summation term represents the main factor effects, the second term reflects the quadratic effects, and the third stands for the two-factor interaction. As stated above, the independent variables in this research will be described in chapters to come. The second order polynomial model, given by equation 3-8 was applied on one or two responses given as cost (Euro/hour) and protein yields (mg/mL). The same statistical software was used in the generation of the analysis of variance (ANOVA) and the response plots.

3.7.4 Box Behnken Design (BBD)

BBD is one of the most popular response surface methodology design (RSM) alongside central composite design (CCD). BBD is based on three levels of each input factor and are usually coded as -1, 0, +1 representing (minimum, central and maximum). This design was developed by Box and Behnken in 1960 [215]. This is constructed by first combining two-level factorial designs with incomplete block designs and thereon a specified number of central points are added. A schematic diagram for a BBD of three factors is presented in Figure 3-3.
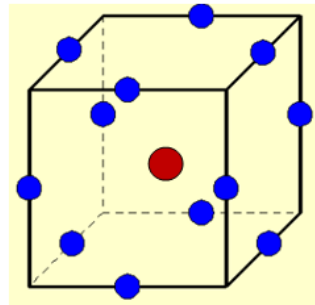
Figure 3 - 3: Schematic diagram for BBD of three factors [216]

Each dot in Figure 3-3 represents an experimental run and the full design of experiment in the case of BBD with 3 factors and 3 levels requires 17 runs indicating 12 border runs (the dots in blue colour at the midpoints of the cube's vertices) and 5 replications of the central point (in red), which is where the ideal solution is predicted to lay, based on the investigator's experience. Particularly, BBD has the following related characteristics that distinguish and place it in a better competitive advantage as when compared to CCD. The main features are:

➢ BBD design has 3 levels for each factor.
➢ The design should be sufficient to fit a quadratic model; meaning it is created for quadratic model estimation.
➢ Each factor is placed at one of the three equally spaced values, usually coded as -1, 0, +1.
➢ It provides strong coefficient estimates near the centre of the design space, but weaker at the corners of the cube as a result of non-existence design points at these locations.
➢ Sensitive design to missing data points and failed runs. It requires at least a double replication of runs to achieve an accurate model.

> Has user-defined specific and equidistant positioning of design points. The estimation variance should more or less depend only on the distance from the centre (this achievable exactly for the designs with 4 and 7 factors), and should not vary too much inside the smallest cube containing the experimental points.

3.7.5 Advantages of (BBD) over Central Composite Design (CCD)

BBD have some advantages over the Central Composite Design (CCD). These will be elucidated below:

> BBD requires that factors be varied over 3 levels as this makes experimentation less costly if actual prototypes are being constructed in the experimentation.

> They are all spherical designs that can rotate with some provision of orthogonal blocking.

> Separation of runs into blocks for the Box-Behnken design allows blocks to be used in such a way that the estimation of the regression parameters for the factor effects is not affected by the blocks.

> Another advantage of these designs is that there are no runs where all factors are either at the +1 or -1 levels.

> The main advantage of BBD is in addressing the issue of where the experimental boundaries should be, and in particular avoidance of treatment combinations that are extreme.

> BBD offers the advantage of requiring fewer numbers of runs, but this disappears when a factor of 4 or more is used.

3.7.6 Design Analysis

Determining the squares of the model requires the use of some mathematical equations. These mathematical equations (3-9 – 3-16) are detailed completely in Appendix G1.

3.7.7 Response Surface Methodology (RSM) Required Steps

The Response Surface Methodology approach is considered as a set of sequential steps, studied with the purpose of optimizing the final protein yield and cost effectiveness, which are regarded as the outcomes of the system under investigation. The following steps were performed so as to develop a mathematical model for the proposed protein production system:

1. Determining the essential process input factors.
2. Determining the limits for each factor considered.
3. The development of a design matrix.
4. Performing the experiment.
5. Measuring the responses.
6. Development of the mathematical model
7. Estimation of the coefficient in the model.
8. Testing the adequacy of the developed models.
9. Model reduction.
10. Development of the final reduced model.
11. Post analysis.

3.7.7.1 Determining the essential process input factors

The essential input factors that affect the output of the system can be identified through conducted research and a literature review as applicable to this study or by conducting a preliminary study. From the study, it emerged that particle size reduction was an important variable on responses such as protein concentration yield, and possibly production cost in euro/hour. The number of cycles (passes) and temperature were considered as factors.

3.7.7.2 Finding the limits of each factor

In other to determine the limit of each factor, trial homogenization of biomass substrate materials were performed, for ranges of pressure, temperature, and number of cycles.

As different HPH's have different working pressures, it was critical not to operate above the working pressure specified by the manufacturer. For the current HPH; GYB40-10S high pressure homogenizer, it had a maximum working pressure not exceeding 90 MPa and as a result the range 30-90 MPa was considered after several trials and from a literature study. The number of cycles, were set at 1-5, and temperature ranges were set as $15 - 25$ °C for the first set of experiments, and $30 - 50$ °C for the second set of experiments. *Design-Expert v.8* software was used to code the data, develop the design matrix, and analyse the case; the limits for each were coded via the following relationship;

$$X_1 = \frac{2(2X-(Xmax+Xmin)}{(Xmax-Xmin)} \qquad (3\text{-}17)$$

Where;

X_1 is the required coded value,

X is any value of the factor which wanted to be coded, and

X_{max}, X_{min} are the upper and lower limits of the factor being coded respectively [208].

3.7.7.3 The development of the design matrix

The design matrix reported shows the response's mean values for both biomasses; *Saccharomyces cerevisiae* and *Chlorella vulgaris,* along with the different ratios (10:90, 20:80 and 30:70) considered. For yeast (*Saccharomyces cerevisiae)* two temperature ranges were applied (15-25°C) and (30-50°C) and for Microalgae *(Chlorella vulgaris)* only one temperature range of (30-50°C) was applied. Substrate to buffer ratios of (10:90, 20:80 and 30:70) were applicable to all conducted experimental work and for the three factors, the total number of runs is 17. These experimental runs are enough to estimate the coefficients in Equation 3-8.

3.7.7.4 Performing the experiment

The cell disruption and homogenization experiments were accomplished accordingly in relation to the design matrix and in a random order so as to avoid any systematic error occurrence in the experimental work.

3.7.7.5 Measuring the responses

All responses, mentioned previously in chapter one, were measured and recorded for responses in all experiments and then used in the development of the model.

3.7.7.6 Development of the mathematical model

The functional relationship, as an example for three factors representing any response of interest can be expressed as y = f (A, B, C) and Equation 3-8 can be transformed into:

$$Y = b_0 + b_1A + b_2B + b_3C + B_{11}A^2 + b_{22}B^2 + b_{33}C^2 + b_{12}AB$$
$$+ b_{13}AC + b_{23}BC + b_{33}C^2 + b_{12}AB + b_{13}AC + b_{23}BC \qquad (3\text{-}18)$$

3.7.7.7 Estimation of the coefficient in the model

Regression analysis was applied in order to estimate the values of the coefficients in Equation 3-18.

3.7.7.8 Testing the adequacy of the developed models

The analysis of variance (ANOVA) was used to test the adequacy of the models developed. The statistical significance of the models developed and of each term was examined using the sequential F-test, lack-of-fit test, and other adequacy measures (i.e. R^2, Adj- R^2, Pred. R^2 and Adequate Precision) using the same software to obtain the best fit. The Prob >F (is sometimes called the *p-value*) of the model and of each term in the model can be computed by means of ANOVA. If the Prob >F of the model and of each term in the model does not exceed the

level of significance (i.e. $\alpha = 0.05$), then the model may be considered adequate within the confidence interval of $(1- \alpha)$; thus in this example 95% will be reliable. For the lack-of-fit test, the lack of fit could be considered insignificant if the Prob >F of the lack of fit exceeds the level of significance. Table 3-4 below is a summary of the ANOVA table [211, 214]. The term SS_i represents the sum of squares of the terms in the model, while MS_R and (F_{cal} − value) represent, respectively, the mean square of the residuals and a comparison of the term variance with residual (error) variance. The follow up equations representing each and every one of these; R^2, Adj- R^2, Pred. R^2 and Adequate Precision can be seen at Appendix G2

Table 3 - 4: *ANOVA* Table for full model [211]

Source	SS	df	MS	$F_{cal.}$- Value	p-value or Prob > F
Model	SS_M	p			
A	SS_a	1			
B	SS_b	1			
C	SS_c	1			From table or software library
AB	SS_{ab}	1			
AC	SS_{ac}	1	Each SS divided by its df	Each MS divided by MS_R	
BC	SS_{bc}	1			
A^2	SS_{aa}	1			
B^2	SS_{bb}	1			
C^2	SS_{cc}	1			
Residual	SS_R	N-p-1			-
Lack of Fit	SS_{lof}	$N - p - n_0$			From table
Pure Error	SS_E	$n_{0 - 1}$			-
Cor Total	SS_T	N - 1	-	-	-

Where;

P: Number of coefficients in the model.
N: Total number of runs.
n_0: Number of centre points.
df: Degree of freedom.
MS: Mean square.
MS_R: Mean square of the residuals

3.7.7.9 Model reduction

The complete mathematical model as shown in Equation 3-18 would normally contain some terms that are not significant and as such, are eliminated , i.e. terms with *p-value* being greater than α. This elimination can be done manually or automatically by choosing one of the selection procedure provided by the software.

3.7.7.10 Development of the final reduced model

The final reduced model is determined by applying the above steps, and can be built upon at this stage, by the software. The significant terms are only contained in the final reduced model at this stage, but a further reduced quadratic ANOVA Table can be produced if the need be.

3.7.7.11 Post analysis

Once the final model has been obtained, the factors and factors-interaction effects will be interpreted via contours and perturbation plots provided by the software. These plots can also be presented in the form of 3D graphs where they represent the factors that contribute in the response.

Finally, by using the developed model, it is easy to optimise cell disruption and homogenization conditions in the biomass substrates to improve the process and lead to the desired protein concentration yield, as well as economic feasibility (cost) of the conducted research.

3.7.8 Optimization

3.7.8.1 Optimization through Desirability Approach Function

The desirability approach is a method that allows for the optimization of a model through constraining the allowed variability of certain factors. This is recommended due to its advantages such as simplicity, availability in *Design Expert*, and thus provides flexibility in weighting and giving user-defined importance for input variables and responses. Solving such multiple response

optimization problems using this technique consists of using an approach that combines multiple responses into a dimensionless measure performance known as the overall desirability function (D). The desirability approach consists of transforming each estimated response, Y_i, into a unit-less bounded by $0 < d_i < 1$, where a higher d_i value indicates that Y_i is more desirable. If $d_i = 0$, Y_i is totally undesirable, or vice versa when $d_i = 1$ [217].

In this study, the individual desirability for each response d_i is calculated using equations 3-24 – 3-27 (see Appendix G3). The shape of the desirability function can be changed by the weighted field wt_i. Weights are used to give emphases which are added to the upper/lower bounds or to emphasize the target value. Weights could be ranged between 0.1 and 10; weights greater than one gives more emphasis to the goal (D), while weights less than one give less emphasis. In the desirability objective function (D), each response can be assigned an important (r), relative to the other responses. Importance varies from the least important of 1(+), to the most important, a value of 5 (+++++). If the varying degrees of importance are assigned to the different responses, the overall objective function is shown below in equation 3-28 (see Appendix G3), where n denotes the number of responses in the system and T_i is the target value of the ith response [212].

3.7.8.2 Numerical and Graphical Optimization

Optimizing using the Design-Expert software identifies a combination of factor levels that is simultaneously satisfying certain requirements which are usually referred to as the *"optimization criteria"* at every one of the responses and input variables, i.e. multiple-response optimization. Carrying optimization using the graphical and numerical methods is by choosing the desired targets for each factor and response. The numerical optimization features in the software so as to maximize the objective function and provides the associated solution points in the variable domain. This process that involves optimization combines the goals and maximizes the overall desirability function (D)

The software defines regions where requirements simultaneously meet the proposed criteria in the graphical optimization. This is done through

superimposing or overlaying critical response contours on a contour plot. The best compromise can then be performed through visual search and when it involves cases of many responses, it is best recommended to perform the numerical test first; otherwise it will not be possible to cover the feasible region. The graphical optimization displays the area of feasible response values in the factor space. Regions that do not fit the optimization criteria are shaded [212]. Chapter 4 provides examples of numerical optimization with the desirability function (D) selected.

3.8   Summary

The chapter have covered the materials and experimental procedures as applicable to the research. Most importantly, the equipment characterisations have also been highlighted. These were used in the different processes of the experimental work. A protein curve was prepared to determine the protein content in the substrate after homogenization through the use of a spectrophotometer. As the substrates considered in the research were two, two different experimental procedures have been presented with measurement and quantification showcased for both substrates. Design of Experiment software has been highly studied and was required to predict and optimise the homogenizing process after treating the yeast and the micro algae via Response Surface Methodology (RSM) so as to develop mathematical models that relate the process input parameters to their output responses. The next chapter will study the three most important input parameters of homogenization process; the number of cycle (passes), temperature, and pressure. These will be thoroughly investigated to determine their effects on the homogenized substrates along with the output features; protein concentration yield, and cost for the energy consumption.

Chapter 4
Results and Discussion

4.1 Introduction

This Results and Discussion chapter has been divided into three categories. This starts off by determining the set range by one-variable-at-a-time (OVAT) approach for the operational parameter; (15 - 25°C) for temperature, (30 - 90 MPa) for pressure and number of cycles as (1 - 5). These were determined through experimentation with the substrates used in this study, Baker's yeast *(Saccharomyces cerevisiae)* and Microalgae *(Chlorella vulgaris),* to determine the effect of temperature on yeast. Another range of temperature (30 – 50°C) was also considered for Baker's yeast *(Saccharomyces cerevisiae)* to compare these results. As the results showed no appreciable difference between the two sets of experiments conducted, the temperature range of 30 – 50 °C was not applied to Microalgae *(Chlorella vulgaris)*.

Particle size analysis was performed on the substrates using Delsa Nano C; a software package for determining the distribution of particle sizes on substrates in suspension, with sample size ranging between 0.6 nm to 7 μm. Scanning Electron Microscope (SEM) analysis was also conducted on yeast biomass. Characterisation analyses were conducted using the both processes to determine the effect of HPH on the biomass substrates after homogenization.

For clarity and readability, the presented work in this section has been divided into two parts: Baker's yeast *(Saccharomyces cerevisiae)* and Microalgae *(Chlorella vulgaris)*, with the former further split into Baker's yeast homogenized at temperature range (15-25 °C) and Baker's yeast homogenized at temperature range of 30 to 50 °C, while the latter (Microalgae) is split into Microalgae homogenized at a temperature range of 15 to 25 °C. The results obtained were achieved through the application of *Response Surface Methodology (RSM)* in developing mathematical models for the substrates above via the *Design Expert V.8*. These were required in predicting the process. In further analysis the substrates were also investigated considering the analysis of variance (ANOVA),

analysis for each response; their validation along with the effects of process parameter of the substrates on each response. These are all discussed and showcased in the Section.

Finally, numerical and graphical optimization was applied to the responses to determine the energy cost and feasibility of the process.

4.2 Baker's Yeast Analysis

In determining the protein concentration yields from treated and untreated Baker's yeast and to also determine the set range of the parameters for further experimental work, different level experiments were conducted.

4.2.1 Baker's Yeast Control Sample

Control samples were prepared, to compare them with the treated samples. This was required in determining the set range of the parameters; pressure, temperature and number of cycles (passes), applicable to this research before the commencement of the experiments using the HPH. The control samples are those samples that never passed through the homogenizer, i.e. are unhomogenized, but have been treated with solution C (Refer to Chapter 3). The control samples did not undergo any pressure and number of cycles, since they never passed through HPH. It was however possible to determine the temperature, which was close to that of the room temperature and could be quantified into ratios since it was treated with solution C. The UV absorbance rate as shown in Table 4-1 is the amount of protein content that has been absorbed under UV light in the Spectrophotometer after being treated with the total protein reagent. For further details, see Appendix F for the conversion process to protein concentration (mg/mL).

Again as seen in the results presented in Table 4-1, it is seen that the untreated Baker's yeast can be considered as the control sample. The samples were separated into ratios in solution with solution C at the rate of 10:90, 20:80 and

30:70. The results obtained indicate that protein concentration increased with the increased ratio of dilution of Baker's yeast against the solution (Solution C).

Untreated Baker's yeast, at 10% to solution C at 90%, yielded 0.002 mg/mL, While 20% to 80% of solution C and 30% to 70% of solution C resulted in 0.005 mg/mL and 0.008 mg/mL respectively.

Table 4 - 1: Control Samples – Untreated Baker's Yeast at Different Ratios

Ratios	UV Absorbance Rate	Protein Conc. (mg/mL)
10:90	0.0901	0.002
20:80	0.0903	0.005
30:70	0.0905	0.008

4.2.2 Comparison Analysis Based on Pressure, Number of Cycle and Ratios with Treated Baker's Yeast

Tables 4-2 to 4-4 along with the graphs presented in Figures 4-1 to 4-3 represent the comparison analyses based pressure, number of cycles, and ratio with the control experiment sample at the different ratios depicted in Table 4-1. This showcases the effect of the parameters on the yielded protein concentration. From the conducted experiment, Table 4-2 shows the result obtained when the analysis is based on pressure. Protein yields increased as the pressure applied during the homogenization increased. With the dilution ratio, the number of cycles and temperature constant, the protein yield rises with the pressure applied. This supported the view of Brookman and James [39] that exponentially increasing release of soluble protein being found with increasing pressure.

Figure 4-1 has also shows this graphically in the variation of the proteins yields in the treated samples compared with the untreated Baker's yeast. The treated samples homogenized at 30, 60 and 90 MPa, against the untreated sample show results of protein yields as; 0.020, 0.190 and 0.860 mg/mL respectively.

Protein yield was found to be minimal in the untreated sample as low as 0.002 mg/mL and only 0.020 mg/mL for the sample homogenized at 30 MPa pressure. This therefore shows an increase of 11 times the original.

Table 4 - 2: Comparison analysis based on pressure for Baker's yeast

Pressure (MPa)	No of Cycle	Temp. (°C)	Ratio	UV Abs.	Protein Conc. (mg/mL)
30	1	20	10:90	0.0912	0.020
60	1	20	10:90	0.1017	0.190
90	1	20	10:90	0.1433	0.860
Untreated	-	20	10:90	0.0901	0.002
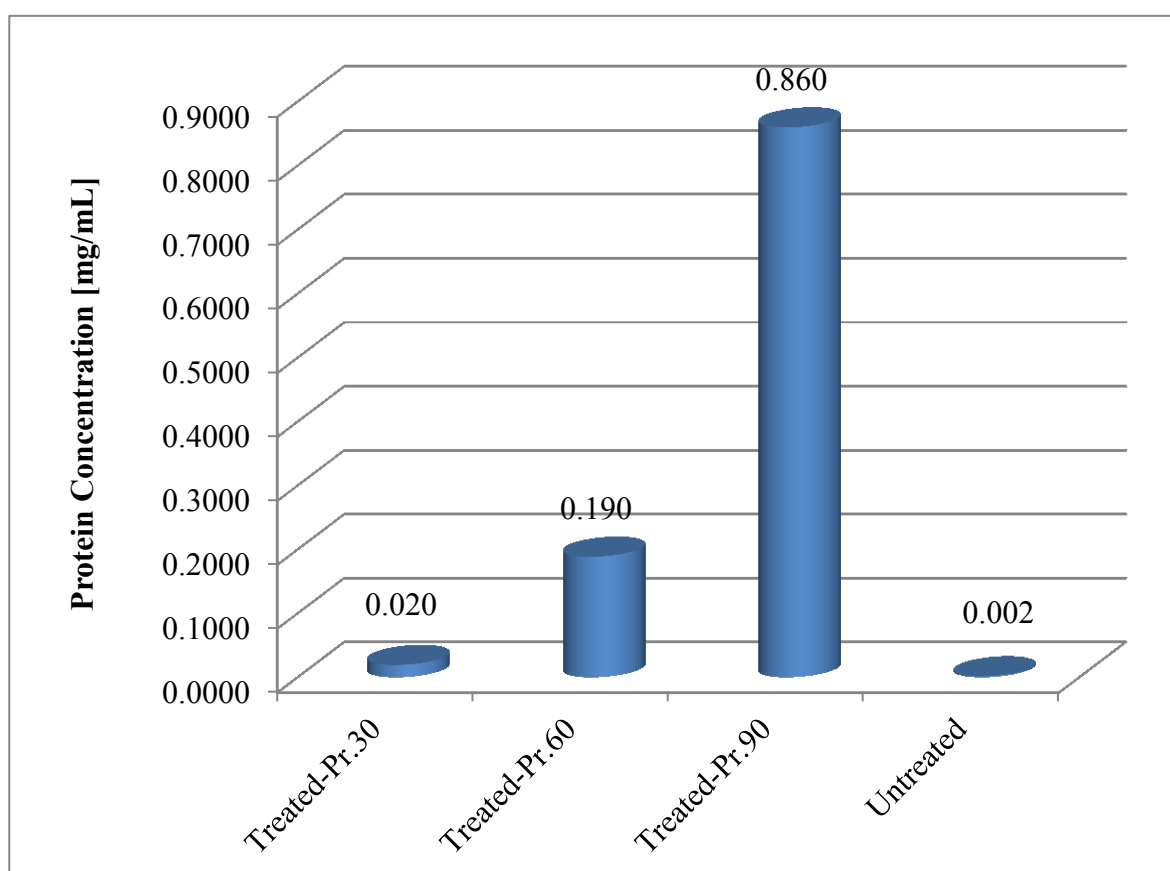
Figure 4 - 1: Protein yields comparison from treated and untreated samples of Baker's yeast via pressure analysis

Table 4-3 compares the protein yield based on the number of cycles. The yield increases as the number of cycle (passes) increases. This shows protein yields of 0.020, 0.050 and 0.1290 mg/mL for the 1, 3, and 5 cycles respectively, wherein the pressure and the dilution ratio remain constant. This supports the view of Baldwin and Robinson [218], that inactivation increased with an increasing number of passes. Their conclusion has yet to be proven that the increase in the

fraction disruption was rather small when the number of passes exceeded three, these they obtained when *Candida albicans* was used as the microorganism. Their results were compared to those obtained in Table 4-3. There were variations found in the comparisons which was an indication that high-pressure homogenizer did affect the biomass substrates, when the untreated sample was compared with the treated at the pressures considered (see Table 4-1).

Contrarily, Geciova *et al.* [54] have attributed the higher number of cycles (say, 3 to 5 at a moderate pressure level (<150 MPa)) being preferred to a single pass at a higher pressure. This is to avoid excessive temperature that will result in damage to the biological constituents of the substrate.

Table 4 - 3: Comparison of each analysis based on the number of cycles

Pressure (MPa)	No of Cycle	Temp. (°C)	Ratio	UV Abs.	Protein Conc. (mg/mL)
30	1	20	10:90	0.0912	0.020
30	3	20	10:90	0.093	0.050
30	5	20	10:90	0.098	0.129
Untreated	-	20	10:90	0.0901	0.002
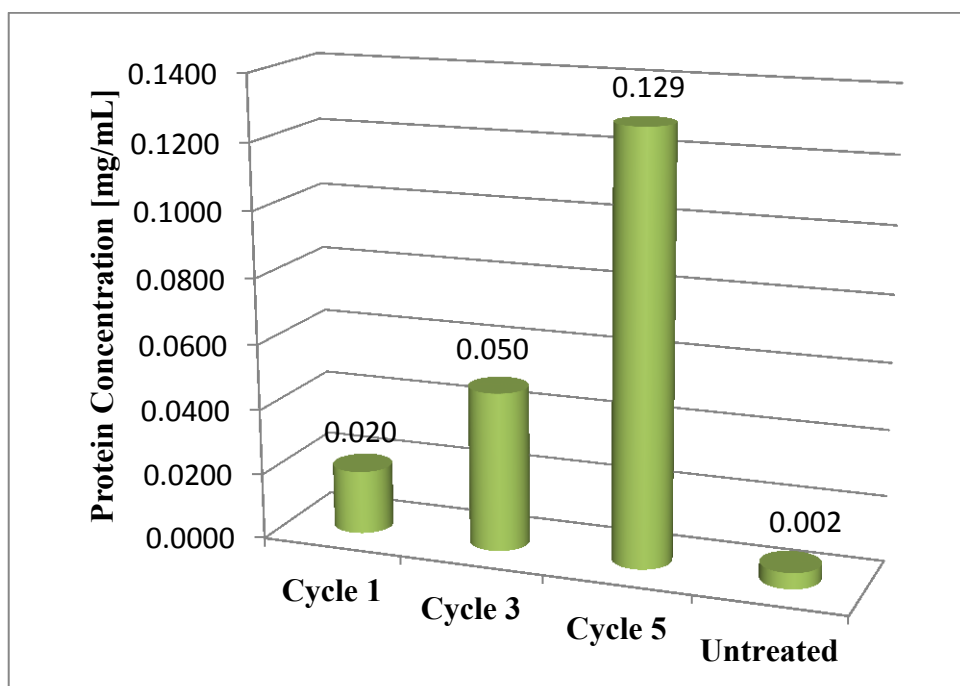
Figure 4 - 2: Protein yields from treated and untreated samples of Baker's yeast with number of cycles as basis for consideration

Table 4-4 depicts the protein yield results, based on ratio, from treated and untreated Baker's yeast. This shows that protein yield increases with the ratio of substrate dilution with the solution C. At the various dilution ratios, the protein yield increases steadily, with the highest protein concentration (0.084 mL) obtained at the 30:70 dilution ratios. While the lowest yield was obtained from 10:90 ratios with the value 0.020 mL increasing by 66.5% from 10:90 ratio to 20:80 and increased further by 159.8% from 20:80 to 30:70 ratio. These results on protein concentration yield are supported by the research of Thiebaud *et al.* [171]. The result has also proven that the protein yields from untreated Baker's yeast occur at a very minimal level and that these require treatment to enable more cell wall break down for the liberation of protein contents within the inner layer of Baker's yeast.

Table 4 - 4: Comparison analysis based on ratios 10:90, 20:80, and 30:70 with the untreated Baker's yeast

Pressure (MPa)	No of Cycle	Temp. (°C)	Ratio	UV Abs.	Protein Conc. (mg/mL)
30	1	20	10:90	0.0912	0.02
30	1	20	20:80	0.092	0.032
30	1	20	30:70	0.0952	0.084
Untreated	-	20	30:70	0.0839	0.008

In the same way that protein increased with the number of cycles, this is also true for increases in ratios from 10:90 to 30:70 of treated yeast to dilution with solution C.

The OVAT approach has indicated that treated samples yield more protein concentration compared to the untreated samples within the parameters of the experimental work.

In general, in term of the considered parameters of pressure, temperature and number of cycles, it is observed that during homogenization through HPH for Baker's yeast resulted in higher protein yield when there were increases in the value of these parameters. Thiebaud *et al*. [171] highlighted in their paper that the

pressure build-up in the intensifier and in the pipe section located before the HPH valve result in the increasing temperature due to the substrate compression. They further stressed that with increasing passes, repeat homogenization of the same fluid two or more times is assumed both the mean diameters and the width of size distribution of the fat globules [171].
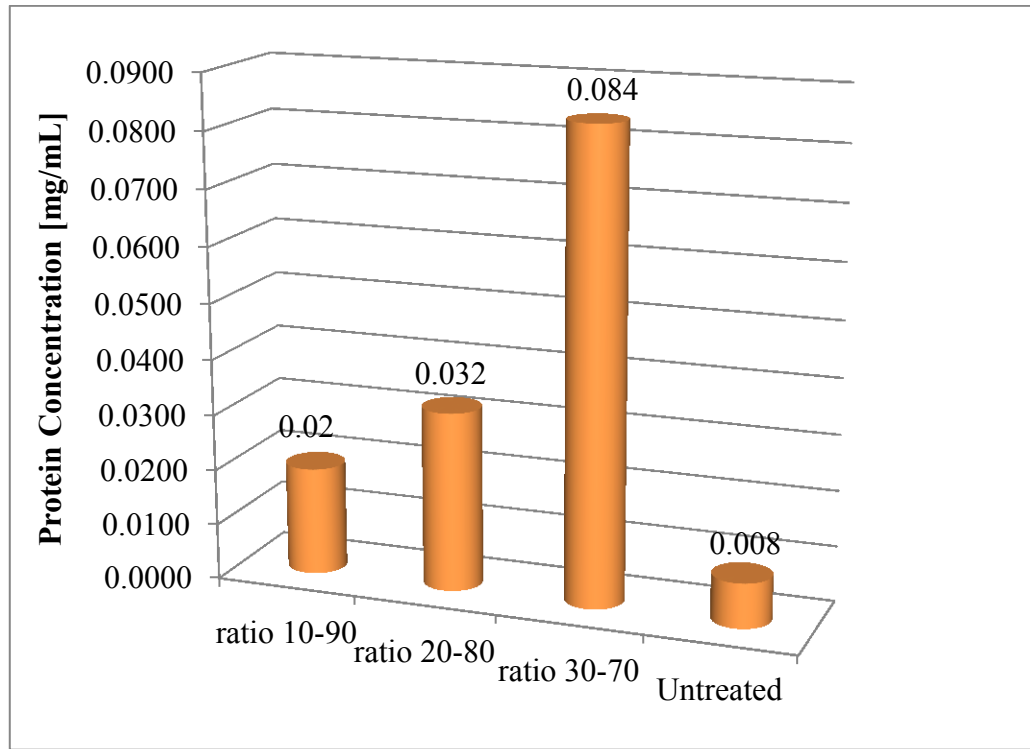
Figure 4 - 3: protein yields from treated and untreated samples with ratios 10:90, 20:80, and 30:70 for Baker's yeast as centre for basis

4.3 Microalgae Analysis

As conducted with Baker's yeast, trial experiments were also conducted using Microalgae *(Chlorella vulgaris)*. This was needed to determine the protein concentration yields from treated and untreated sample of Microalgae. Doing this also enabled the set range of the parameters for further experimental work to be established through the One-Variable-At-a-Time approach (OVAT).

4.3.1 Microalgae Control Sample

The results presented in Table 4-5 show untreated Microalgae being considered as the control samples. The samples were separated into ratios in solution with solution C at the rate of 10:90, 20:80 and 30:70 respectively. The results so obtained indicate that protein concentration increased with an increase ratio of dilution of Microalgae against the solution (solution C). The UV absorbance rate with the corresponding protein concentration yields are as shown in Table 4-5.

Table 4 - 5: Control samples – Untreated Microalgae at different ratios

Ratios	UV Absorbance Rate	Protein Conc. (mg/mL)
10:90	0.091	0.02
20:80	0.092	0.032
30:70	0.093	0.05

4.3.2 Comparison Analysis Based on Pressure, Number of Cycle and Ratios with Treated Microalgae (Chlorella vulgaris)

Tables 4-6 to 4-8, along with the graphs in Figures 4-4 to 4-6, represent a comparative analysis based on pressure, the number of cycles, and the ratios, with the control experiment sample (Table 4-5). This demonstrates the effect of the parameters on the yielded protein concentration. Table 4-6 shows the result obtained when the analysis is based on pressure. Protein concentration increased with the pressure applied during the homogenization, whereas the dilution ratio and number of cycles remained constant. This is supported by the findings of Brookman and James [39] which found that an exponentially increasing release of soluble protein can be achieved with increasing pressure. Protein yield was found to be minimal in the untreated sample, as low as 0.02 mg/mL and with 0.10 mg/mL when homogenized at 30 MPa pressure. This therefore shows an increase of 501.2% in the protein yielded.

Figure 4-4 shows graphically the variation of the proteins yield in the treated samples against the untreated Microalgae. Based on the results obtained, it is

evident that Baker's yeast yielded higher protein concentration at 60 and 90 MPa of 0.190 and 0.860 mg/mL respectively (Table 4-2). The protein yield at 30 MPa for Microalgae shows higher yield as compared to that of Baker's yeast with result as 0.020 mg/mL (Table 4-2).

Table 4 - 6: Comparison analysis based on pressure for Microalgae

Pressure (MPa)	No of Cycle	Temp. (°C)	Ratio	UV Abs.	Protein Conc. (mg/mL)
30	1	20	10:90	0.096	0.10
60	1	20	10:90	0.099	0.15
90	1	20	10:90	0.106	0.26
Untreated	-	20	10:90	0.091	0.02
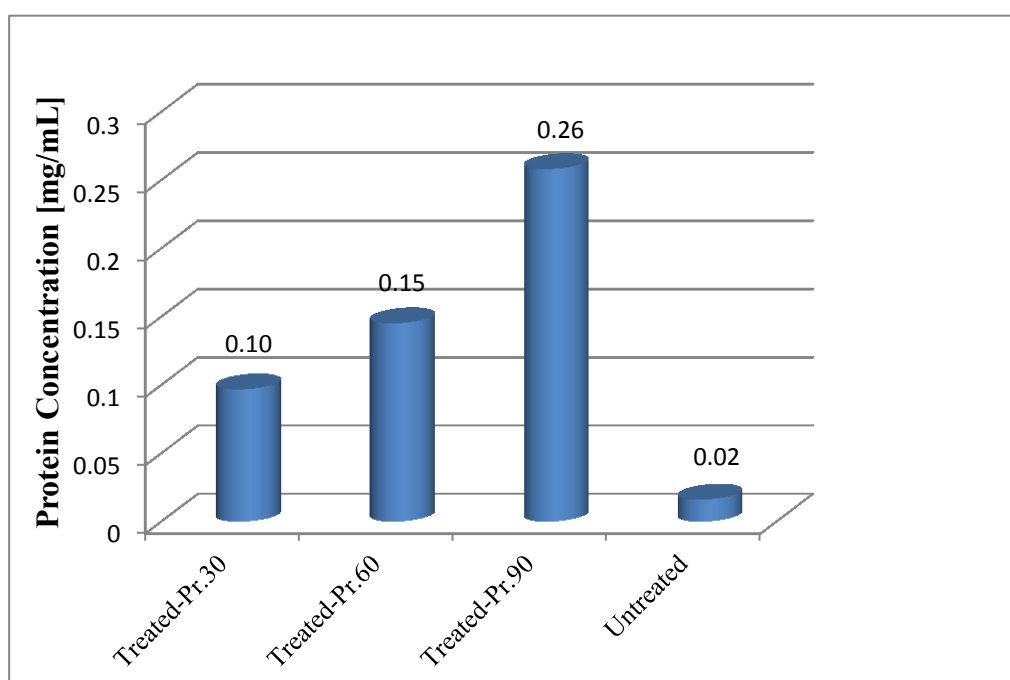
Figure 4 - 4: Comparison of protein yields from treated and untreated samples of Microalgae at various pressures 30, 60 and 90 MPa

Also Table 4-7 compares the protein yield based on the number of cycles. The protein yield increased as the number of cycle (passes) increased [169, 171, 174-176], while pressure and dilution ratio remained constant. The number of cycles was increased from 5 to 6 in the trial experiment for Microalgae, to confirm any

appreciable difference in the protein concentration yield. This supported the view of Baldwin and Robinson [218], who found that inactivation, occurred with increasing number of passes. Their conclusion suggested that the fraction disrupted was rather small when the number of passes exceeded three, a result they obtained when *Candida albicans* was used as the microorganism substrate. Their result was not supported in this research which shows a factor of 1.5 increases from 3 cycles to 5, compared to a factor of 1.33 from 1 cycle to 3 cycles. This was an indication that the high-pressure homogenizer did positively affect the biomass substrates and comparing the untreated sample with the treated at different pressure showed considerable difference. The untreated sample of Microalgae showed minimal protein yield, since it was not homogenized and as such, the cell walls were not ruptured. When compared to the protein obtained for cycle 1, it indicated that there was an improvement of protein yield by 199.7%. The untreated sample considered here was the 10:90 dilution ratios (see Table 4-5). The protein yield showed some improvement even after 5 cycles where 5 and 6 cycles yielded 0.190 and 0.230 mg/mL respectively. This however does not complement the work of Vachon *et al.* [219] which proved that after five passes at 200 MPa, an 8.3-log reduction was obtained for *E. coli* O157:H7, while a reduction of about 5.8 log CFU/ml was obtained for *L. monocytogenes* exposed to 300 MPa after five passes. This probably was based on the substrate considered or on the homogenization pressure. Contrary to this, Geciova *et al.* [40] have attributed higher number of cycles (3 to 5), at a moderate pressure level (<150 MPa) being preferred to a single pass at a higher pressure, to avoid excessive temperatures and the resulting damage to biological constituents of the substrate.

Table 4 - 7: Comparison analysis of UV absorption and protein concentration at various numbers of cycles and constant pressure and temperature

Pressure (MPa)	No of Cycle	Temp. (°C)	Ratio	UV Abs.	Protein Conc. (mg/mL)
30	1	20	10:90	0.096	0.100
30	3	20	10:90	0.098	0.130
30	5	20	10:90	0.102	0.194
30	6	20	10:90	0.104	0.226
Untreated	-	20	10:90	0.091	0.002
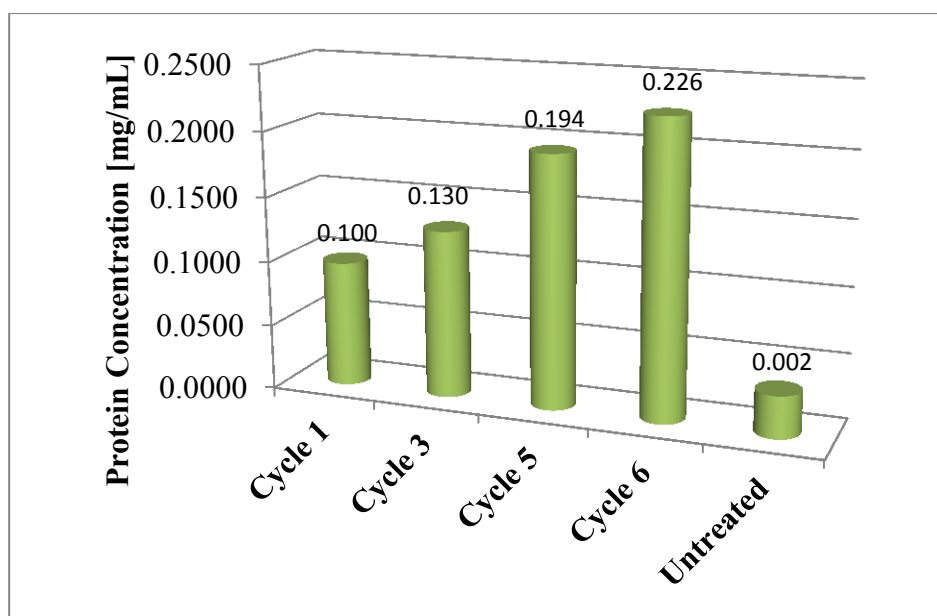
Figure 4 - 5: Comparison of protein yields from treated and untreated samples of Microalgae with the number of cycles as the basis for consideration

Tables 4-8 gives the analyses of the protein concentration yield from treated and untreated Microalgae at various ratios of 10:90, 20:80 and 30:70. This shows that the protein concentration yield increased with ratio of substrate dilution with the solution C. At the various dilution ratios, the protein yielded increases steadily with the highest protein concentration rate obtained at the 30:70 dilution ratios to the value of 0.10 mL. While lowest yield was obtained from 10:90 ratio increasing by 16.63% from 10:90 ratio to 20:80 and increased again by 14.26% from 20:80 to 30:70 ratio. The results presented in terms of protein concentration yield supports the findings of Thiebaud *et al.* [171], where protein concentration yield increased with the increase of dilution ratio. The result has also proven that there are protein yields, although minimal from untreated Microalgae. This shows that required treatment enables more cell wall breakdown for the liberation of protein contents within the inner layer of the substrates.

Table 4 - 8: Comparison analysis based on ratios 10:90, 20:80, and 30:70 with the untreated Chlorella vulgaris

Pressure (MPa)	No of Cycle	Temp. (°C)	Ratio	UV Abs.	Protein Conc. (mg/mL)
30	1	20	10:90	0.096	0.100
30	1	20	20:80	0.097	0.113
30	1	20	30:70	0.098	0.130
Untreated	-	20	30:70	0.093	0.050

When Microalgae sample was compared with Baker's yeast (Figure 4-1), untreated Microalgae show higher yield of protein concentration with increasing dilution ratio. Both had the highest yield at a ratio 30:70 dilution rate. Microalgae resulted in a 34.96 % increment in the protein concentration yield at 30:70 dilution ratios with solution C when compared to Baker's yeast at the same ratio of dilution.

The OVAT approach to the substrate has indicated that treated samples yielded more protein concentration when compared to the untreated samples within parameters of the experimental work.
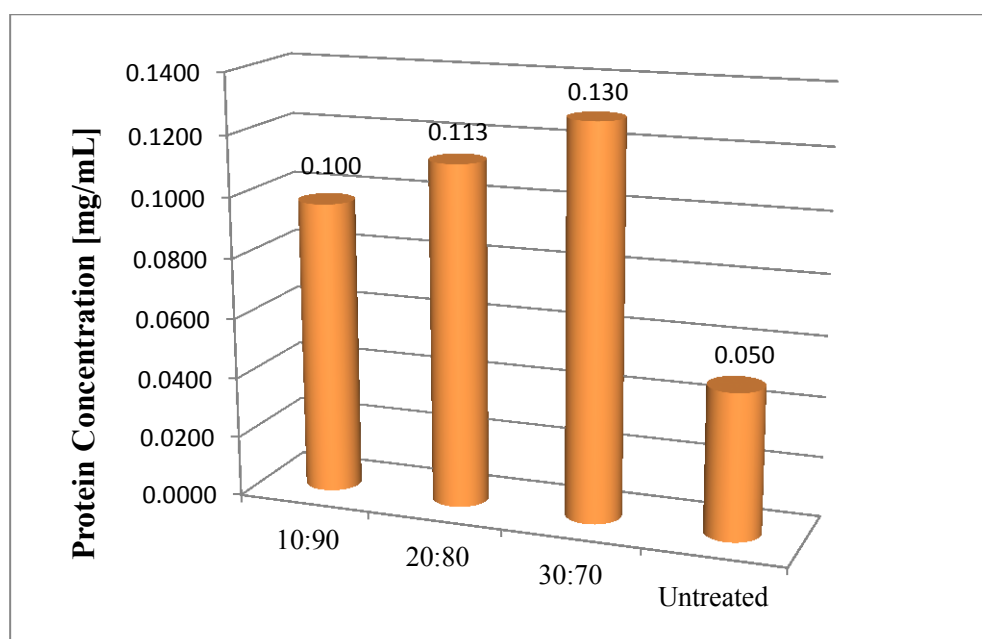
Figure 4 - 6: Protein yields from treated and untreated samples of Microalgae at varying ratios of 10:90, 20:80 and 30:70

4.4 Structural Deformation of Baker's Yeast and Analyses through Scanning Electron Microscope (SEM)

This Section analyses and discusses structural deformation as effected by HPH during yeast homogenization. This analysis was carried out using the Scanning Electron Microscope (SEM). The SEM has been discussed previously in Chapter 3, and its use, enabled particle size analysis to be conducted on biomass substrates such as Baker's yeast. Studies carried out showed that SEM is not suitable for liquid biomass substrates, and for this purpose it was unable to be used in analysing Microalgae *(Chlorella vulgaris)* since it was delivered in liquid form. Further attempt to dry it in the oven for possible analysis, left no traces of it to be examined. Delsa Nano C was therefore considered as an alternative as use in determining the particle size distribution of Microalgae *(Chlorella vulgaris)*. Analyses based on SEM have been sectioned into 2 parts; the 15 – 25 °C temperature range, and the 30 – 50 °C temperature range. Untreated Baker's yeast with the treated (Homogenized) Baker's yeast at different ratios; 10:90, 20:80, and 30:70 images were compared through accessing their deformation under SEM. The operating parameters pressure, temperature, and the number of cycles for homogenizing each samples were also considered. All SEM images provided herein are at the same magnification of 100 microns

4.4.1 SEM for Baker's yeast homogenized between 15 – 25 °C temperature ranges

Untreated Baker's yeast and the dilutions at the different ratios:

Figure 4-7 depicts SEM images that have not been treated through the HPH, and in particular image (a) in the Figure is not in any ratio which means that it has not been diluted with solution C in any form. Images b, c and d show the Baker's yeast structure untreated with the three ratios of dilution with solution C, 10:90, 20:80, and 30:70. From the image shown in Figure 4-7 (a), no deformations in the images observed under the SEM, similarly ratios 10:90, 20:80, and 30:70 also showed no structural damage because the samples had not passed through the HPH. Figure 4-7 (a-d) compares them with other images in this research which were treated and passed through the HPH. The magnification applied to the

images was the same throughout the study and because these are untreated, pressure, temperature and the number of cycles has not been considered.

Treated (homogenized) Baker's yeast at 30 MPa and at 25°C, along with the dilutions at the different ratios:

Figure 4-8 depict images (e, f and g) corresponding to Baker's yeast homogenized at dilution ratios with solution C of 10:90, 20:80 and 30:70, respectively. These have been homogenized at the first considered level of the cycle (1 Cycle) at a temperature of 25 °C and at 30 MPa pressure. With the homogenized pressure at 30 MPa and cycle number at 1, the structural deformation on the images showed some damage visible to the eye. The shaft-like state in image (e), spore-like state in (f), and coated-like state in (g) are all due to the dilution and quantification rate before dryness at 105°C. The original slurry state of the homogenized yeast at 1 cycle, 30 MPa and at 25 °C show some difference between before and after homogenization. This is clearly seen when compared to the untreated samples in Figure 4-7 (a, b, c, and d).

Treated (homogenized) Baker's yeast at 30 MPa and at 20°C, along with the dilutions at the different ratios:

Figure 4-9 depict images (h, i, and j) and these indicate the next level of cycle (3 Cycles), with the 3 different rates of dilution also shown to determine the extent of structural deformation of the substrates after treatment. The Baker's yeast has been homogenized at a temperature of 20 °C and 30 MPa pressure. Homogenizing at 3 cycles is seen to create some distortion and deformation on the SEM images being considered. Liu *et al.* [220] revealed that efficient breakage of the cell wall is as a result of a strength-providing component which is necessary in the effective removal of intracellular compounds. SEM use in the research has been necessitated so as to observe any alteration undergone by the yeast cells after the disruption process in every cycle. Disruption at every cycle during homogenization is said to break open and releases the inner contents within the cell walls. Another method of observing the alteration within the yeast cells after

disruption is the Transmission electron microscopy (TEM), but this has not been considered in this research due to non-availability.

Treated (homogenized) Baker's yeast at 30 MPa and 25°C, along with the dilutions at the different ratios:

Figures 4-10 depict images (k, l, and m) and it is the third level of the cycle where the substrates have been homogenized over 5 cycles in the treatment under the high-pressure homogenizer. The pressure and temperature considered are same as above; 30 MPa and 25 °C respectively. Running the homogenizer over 5 cycles on the substrates elongates and stretches out the inner components that have not been broken in the previous cycles. This as a result make the end product to be greatly slurried, and the generated heat through cavitation then allows the homogenized soluble Baker's yeast to be very viscous due to the high pressure that have been applied during the homogenization.

From a comparison of the images in Figures 4-8 to 4-10, with those in Figure 4-7, it is clear and evident that there are changes in the microstructure and inner content of Baker's yeast after the homogenization processes. Physical changes were observed during the homogenization process in the form of size of cell debris, viscosity and the surface area of the homogenized yeast. These physical changes are as a result of homogenizing at the considered parameters such as, higher pressure, temperature, and the number of cycles. Baker's yeast cell wall disruption by mechanical means liberates the inner contents which are known to contain protein. Accordingly, during the disruption process, the loss of cell wall mannoproteins in the yeast will alter the wall porosity, and this is said to facilitate the release of intracellular macromolecules with no effect on the wall integrity. The release of these intracellular molecules is determined by the functionality of the plasma membrane and the porosity of the yeast cell wall.

As a result of this, Shirgaonkar *et al.* [166] have highlighted alot of controversy existing in the literature as regards the exact cause of the cell disruption in the high-pressure homogenization (HPH). As discussed previously in Chapters 2, many authors have therefore postulated their different views on this issue; Save *et al.* [186] have proposed that cavitation and the shockwaves/pressure impulses

produced as a result of cavity collapse are responsible for cell disruption, while Keshavaraj Moore *et al.* [183] proposed the impingement and impact as the main causes for the cell disruption. Middelberg [157] has also reviewed the proposed physical processes responsible for the disruption of fat globules and microorganisms during homogenization.
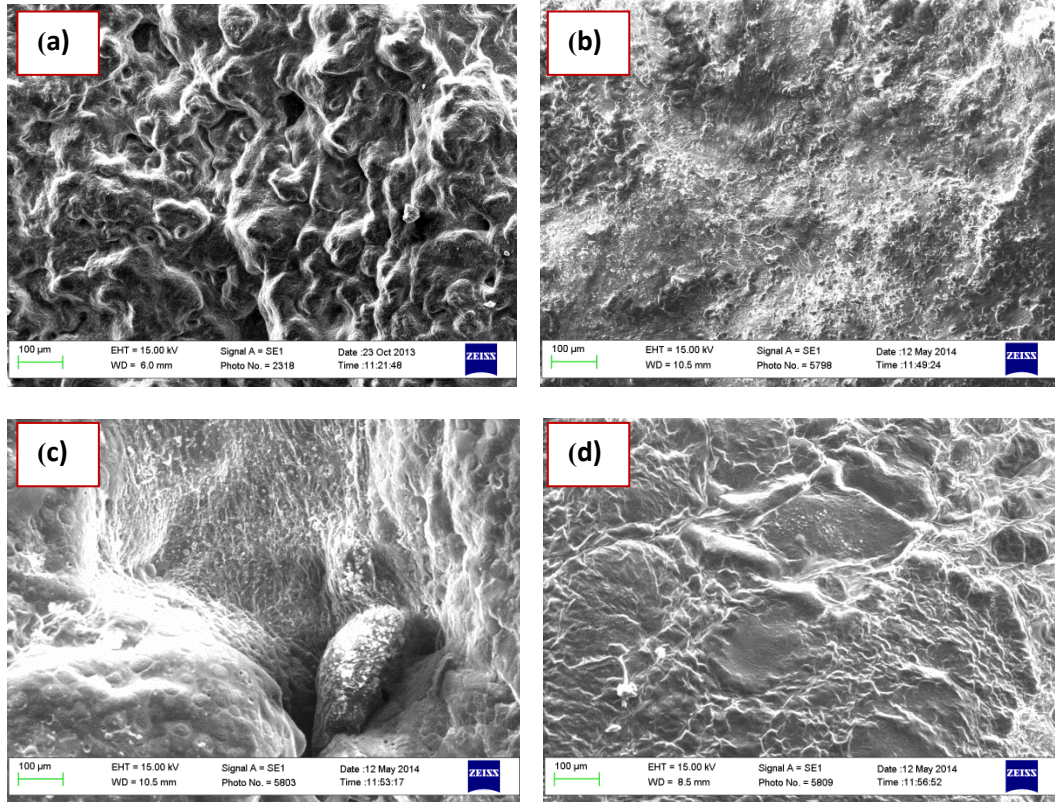
(a) Untreated yeast with no ratio; (b) Untreated yeast at 10:90 ratio of solution C; (c) Untreated yeast at 20:80 ratio of solution C; (d) Untreated yeast at 30:70 ratio of solution C

Figure 4 - 7: Untreated Baker's yeast at no ratio and ratios at 10:90, 20:80 and 30:70 of solution

The overall aim of disruption of biomass substrates is to reduce the particle size which leads to an increase in the surface area. As the cell walls of the substrates are broken down, this will in the process releases the inner most contents of the cell wall; the released protein then increases the fermentation rate of the substrates. The presented images are for the 15 – 25 °C temperature range.
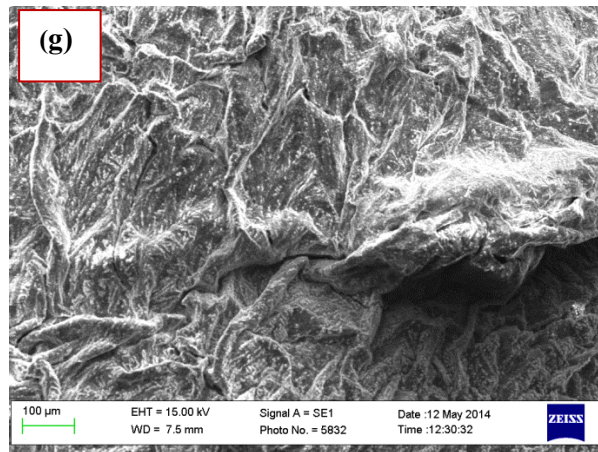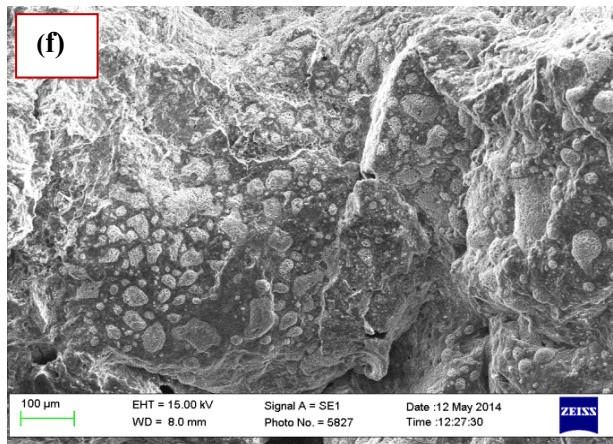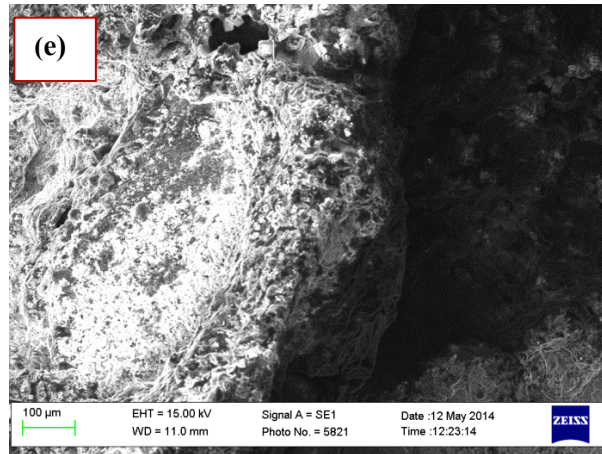
(e) At 1 cycle with ratio 10:90 of solution C; (f) At 1 cycle with ratio 20:80 of solution C and (g) At 1 cycle with ratio 30:70 of solution C

Figure 4 - 8: Homogenized Baker's yeast at 1 Cycle with dilution ratio of 10:90, 20:80 and 30:70 of solution C
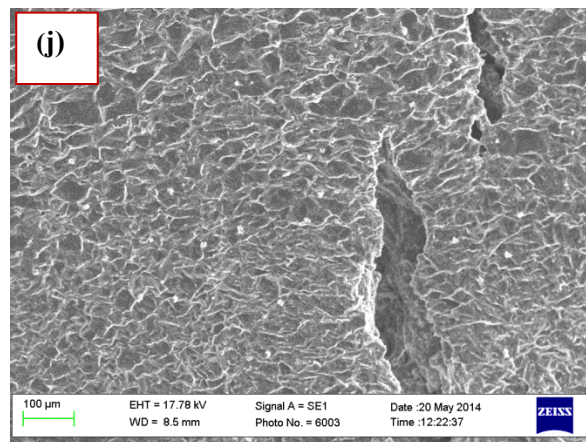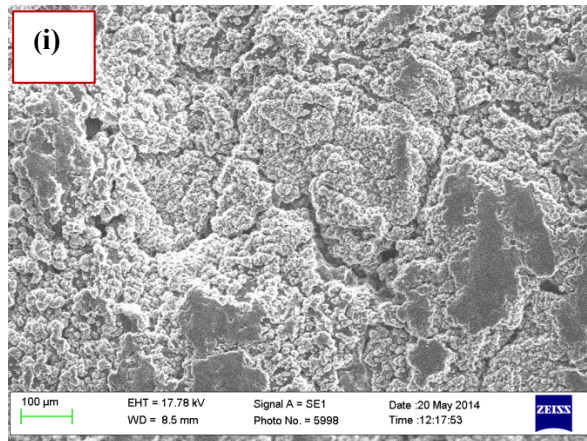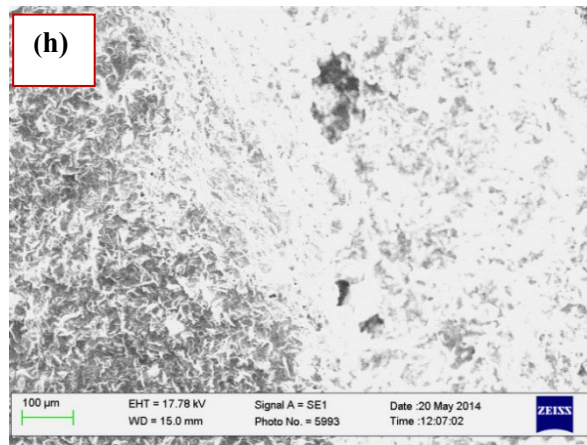
(h) At 3 cycles with dilution ratio 10:90 of solution C; (i) At 3 cycles with dilution ratio 20:80 of solution C; (j) At 3 cycles with dilution ratio 30:70 of solution C

Figure 4 - 9: Homogenized Baker's yeast at 3 Cycles with dilution ratio of 10:90, 20:80 and 30:70 of solution C
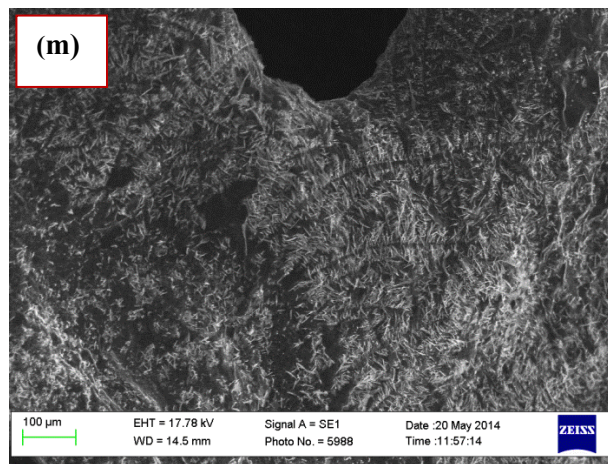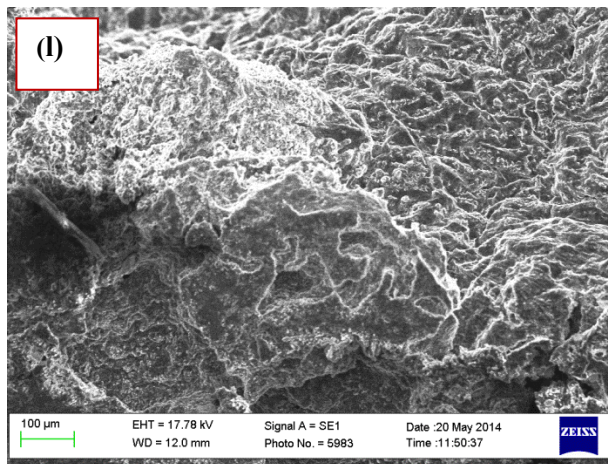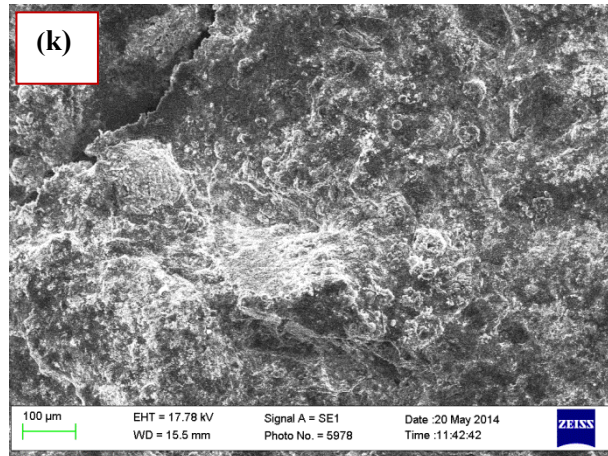
(k) At 5 cycles with dilution ratio 10:90 of solution C; (l) At 5 cycles with dilution ratio 20:80 of solution C; (m) At 5 cycles with dilution ratio 30:70 of solution C

Figure 4 - 10: Homogenized Baker's yeast at 5 Cycles with dilution ratio of 10:90, 20:80 and 30:70 of solution C

4.4.2 SEM for Baker's yeast homogenized between 30 – 50 °C temperature ranges

This Section analyses and discusses SEM images obtained from the homogenization of Baker's yeast between 30 - 50°C. Section 4.4.1 had previously discussed that between 15 - 25°C. Figure 4-7 depicted SEM images that had not been treated through the HPH and particularly, image (a when there is not in any ratio. Images b, c, and d show the Baker's yeast structure untreated with the three ratios of dilution; 10:90, 20:80 and 30:70 with solution C.

Basically, Sections 4.4.1 and 4.4.2 are no different except for the fact that pressures and temperatures in both sections are different. The control samples which are otherwise considered as the images (a, b, c and d) depicted in Figure 4-7 will serve as the basis for the comparison in terms of structural deformation of the homogenized samples. From the images shown, there are no deformations in the images viewed under the SEM other than the increment in the dilution rate of Baker's yeast which has increased by 10% at every level of the dilution. The magnification applied to the images is same throughout the study and because these are untreated; pressure, temperature and number of cycles have not been considered as the soluble yeast had not passed through the HPH. The main reason for this control sample is to determine the extent of damage that had been caused in the treated samples of homogenized Baker's yeast.

Treated (homogenized) Baker's yeast at 60 MPa and 50°C, along with the dilutions at the different ratios:

Images in (n, p, and q) of Figure 4-11 correspond to Baker's yeast homogenized at dilution of 10:90, 20:80 and 30:70, respectively. These had been homogenized at the first considered level of cycle (1 Cycle) at a temperature of 50 °C and 60 MPa pressure. With the homogenized pressure at 60 MPa and the cycle number at 1, the structural deformation on the images showed some damage which is visible clearly to the naked eye, even without the SEM equipment. When the Baker's yeast was fully homogenized at 1 cycle with a high pressure of 60 MPa, and at 50°C, the resultant effects of damages caused at ratios of 10:90, 20:80 and 30:70 of solution C dilution, reflect fracture, cracks and caving in on the dried samples

of homogenized yeast. These effects are due to a combination of parameters taking place within the soluble yeast such as temperature, shear stress, surface area reactant of the mixture. As seen in the 20:80 dilution ratio of solution C Baker's yeast, the visible stretches and cracks are as a result of the tensional forces not being able to hold yeast together again after being stretched out during homogenization at 50 °C.

Treated (homogenized) Baker's yeast with 3 cycles at 60 MPa and 40°C, along with the dilutions at the different ratios:

From the image illustration as shown in (r, s, and t) of Figure 4-12, the number of cycles have increased to 3 and sample was homogenized at 60 MPa and 40°C. The resultant effect of deformation is very pronounced on the (s and t) images of the Figure where there are larger cracks and gulley resulting from the effect of 3 cycles on the homogenized yeast. The number of cycle and pressure has shown greater effects on the deformation of these images because homogenizing at this pressure with 3 cycles means that the yeast has been stretched beyond the extensional limit during homogenization, and then becomes visible when examined using the SEM equipment.

Treated (homogenized) Baker's yeast with 5 cycles at 60 MPa and 50°C, along with the dilutions at the different ratios:

Homogenization at 5 cycles in this research was considered the highest level of the cycle. This was achievable through conducting experimental work at 60 MPa and 50°C. it is assumed that disruption cannot be achieved with a single homogenizer pass and as such, multiple passes are often considered. Based on the fact that the mechanism of disruption is still not clear, its performance is optimised through maintaining small valve gaps; hence, high-velocity jets with short impact-ring diameters are considered [157]. Homogenizing at 5 cycles, as seen from the (image w) in Figure 4-13 wherein there are thread-like structures on top of the image. These are some of the microstructures that have been totally deformed within the sample.
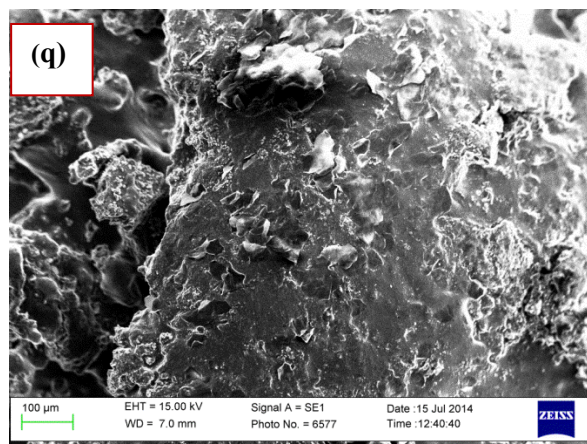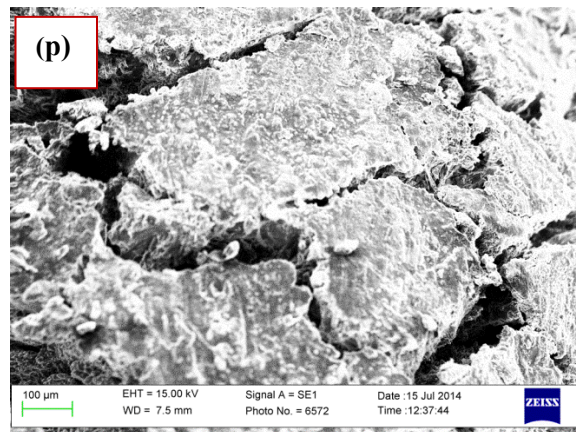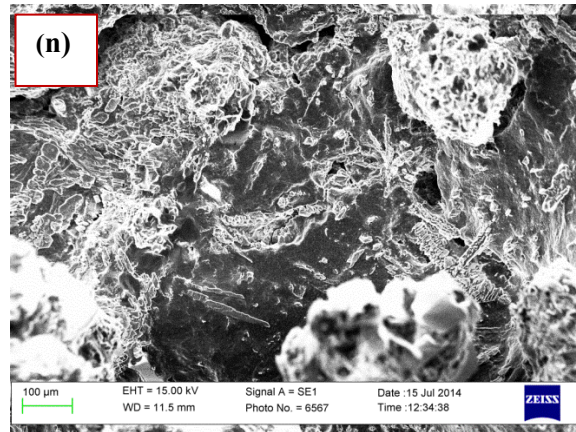
(n) At 1 cycle with dilution ratio 10:90 of solution C; (p) At 1 cycle with dilution ratio 20:80 of solution C;(q) At 1 cycle with dilution ratio 30 - 70 of solution C

Figure 4 - 11: Homogenized Baker's yeast at 1 Cycle with dilution ratios of 10:90, 20:80 and 30:70 of solution C
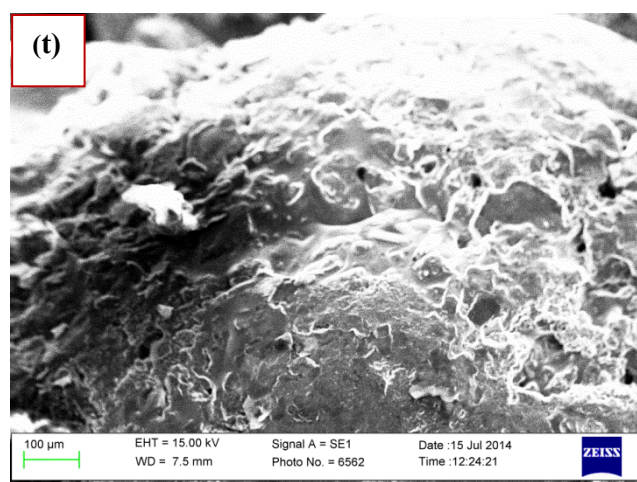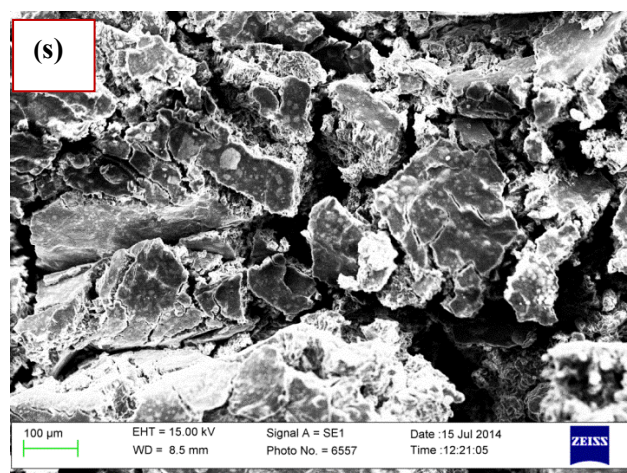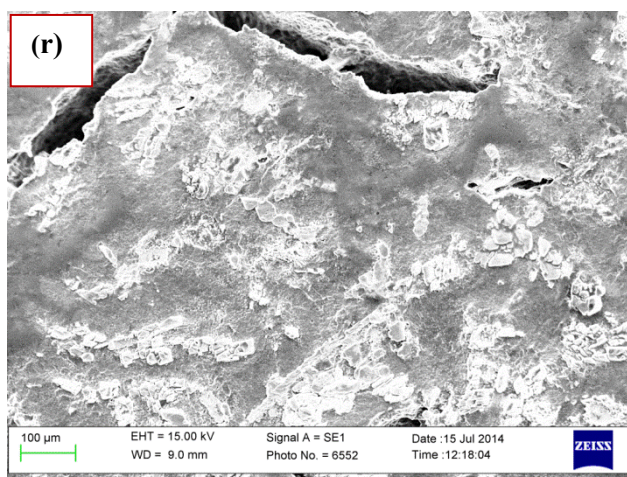
(r) At 3 cycles with dilution ratio 10:90 of solution C; (s) At 3 cycles with dilution ratio 20:80 of solution C; (t) At 3 cycles with dilution ratio 30:70 of solution C

Figure 4 - 12: Homogenized Baker's yeast at 3 Cycles with dilution ratios of 10:90, 20:80 and 30:70 of solution C
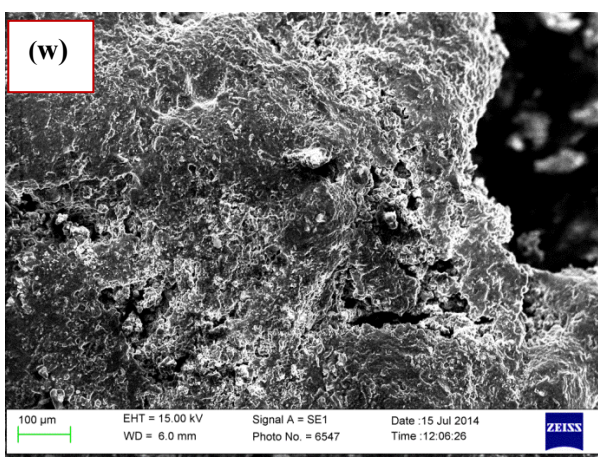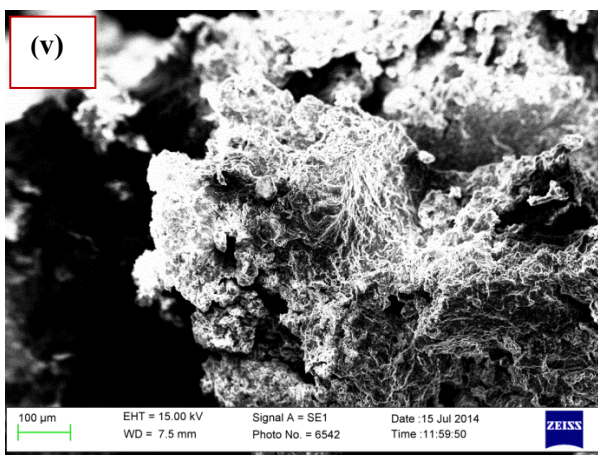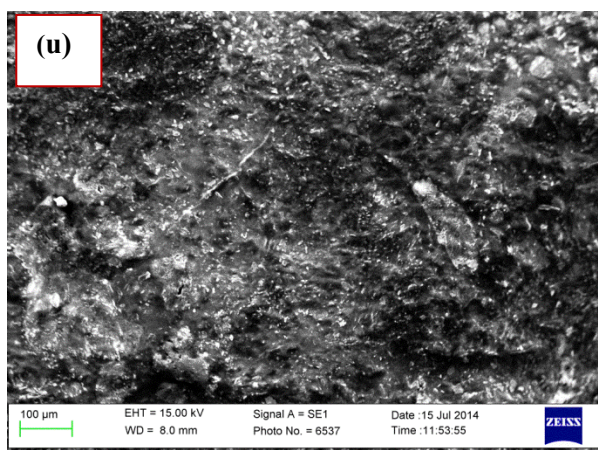
(u) At 5 cycles with dilution ratio 10:90 of solution C; (v) At 5 cycles with dilution ratio 20:80 of solution C; (w) At 5 cycles with dilution ratio 30:70 of solution C

Figure 4 - 13: Homogenized Baker's yeast at 5 Cycles with dilution ratios of 10:90, 20:80 and 30:70 of solution C

On a general note, the different forms of deformation in the homogenized Baker's yeast have revealed some facts. It is evident that homogenization did in fact affect changes in the microstructure of the Baker's yeast substrates based on the SEM analyses. The images shown in this study have invariably caused reductions of particle sizes and resulted in the increment of the surface area (Figure 4-8 to 4-13) when compared with image that have not undergone any treatment and at no ratio of dilution as seen at Figure 4-7(a). The deformations, as shown, have great disparity in the samples for temperature ranges (30 - 50°C) to those of (15 - 25°C). There are several factors to consider in relation to these effects. Increased pressure from 30 MPa to 60 MPa applied during the homogenization is one to consider. This means that at this pressure, the gap size within the HPH would have reduced as compared to the size during 30 MPa pressure. This will result in the homogenized yeast being forced through the small opening gap size of about 1 – 11 μm according to Kelly and Muske [180].

Another factor to consider is the temperature effect which was increased from 20 and 25 °C to 40 and 50 °C, respectively. High temperature changed the viscosity of the substrate but it was not proven to be the exact cause of changes in the inner structure of the substrates. Based on this study, it is very apparent that high temperature has effected changes in the deformation of the microstructure (see Figures 4-11 to 4-13).

The biomass slurry state enabled its passage through HPH exit; this results in the breaking down of yeast cell wall contents due to the effect of increasing the cycle from 1 to 5. The deformation results further due to the increased cycle with the gap size also constricted for the homogenized yeast to flow out at the exit. Based on the need of this equipment (SEM) in this study, its usefulness cannot be underestimated due to its requirement in analysing the microstructural features of solid bodies' surfaces as in the yeast cells.

4.5 Particle Size Analyses

4.5.1 Particle size analysis of Baker's yeast using the Delsa Nano C – Dynamic Light Scattering (DLS) Instrument

The particle size measurements were analysed, using the Delsa Nano C for Baker's yeast of untreated and treated samples, at different pressures and number of cycles. Table 4-9 shows values of the treated against the untreated samples to determine the extent of deformation carried out during the homogenization process.

Table 4 - 9: Samples of Baker's yeast during the particle size analysis showing number distribution

Samples	Baker's Yeast	Number Distribution (Concentration)
1	Untreated	14744.1 ± 92.7
2	30 MPa, 1 Cycle	11203.9 ± 75.8
3	30 MPa, 3 Cycles	8817.3 ± 59.7
4	30 MPa, 5 Cycles	7487.8 ± 50.2
5	60 MPa, 1 Cycles	6379.6 ± 42.7
6	60 MPa, 3 Cycles	4521.6 ± 39.9
7	60 MPa, 5 Cycles	4084.2 ± 35.9
8	90 MPa, 1 Cycles	3402.0 ± 30.3
9	90 MPa, 3 Cycles	3125.7 ± 17.1
10	90 MPa, 5 Cycles	2771.2 ± 10.9

The Table shows that the number distribution decrease as the Baker's yeast samples parameters intensify. This indicates that as the applied pressure and number of cycles increase during homogenization, more cell walls within the substrates are broken down. It implies eventually that the software is effective in determining the particle sizes of the substrate. The number distribution is the concentration of particles dispersed in a fluid and it is measured as percentage. DLS is a known technique for determining the size distribution of small particle in suspension. Studies have shown that larger particles in suspension affect size measurement compared to smaller particles, therefore larger particle can be over

represented in terms of their measurement of size. The obtained results can be presented as intensities, number and volume concentrations of the particles [221].

As shown in Figure 4-14, the combined effect of the first seven samples are plotted in terms of the number distribution (in percentage) and the size of the particle in (nm) after disruption in the HPH. The diameter of the samples can be determined from the horizontal axis. The labels represent: 1 as the untreated, while 7 represents 60 MPa, 5 Cycles. (Table 4-9).
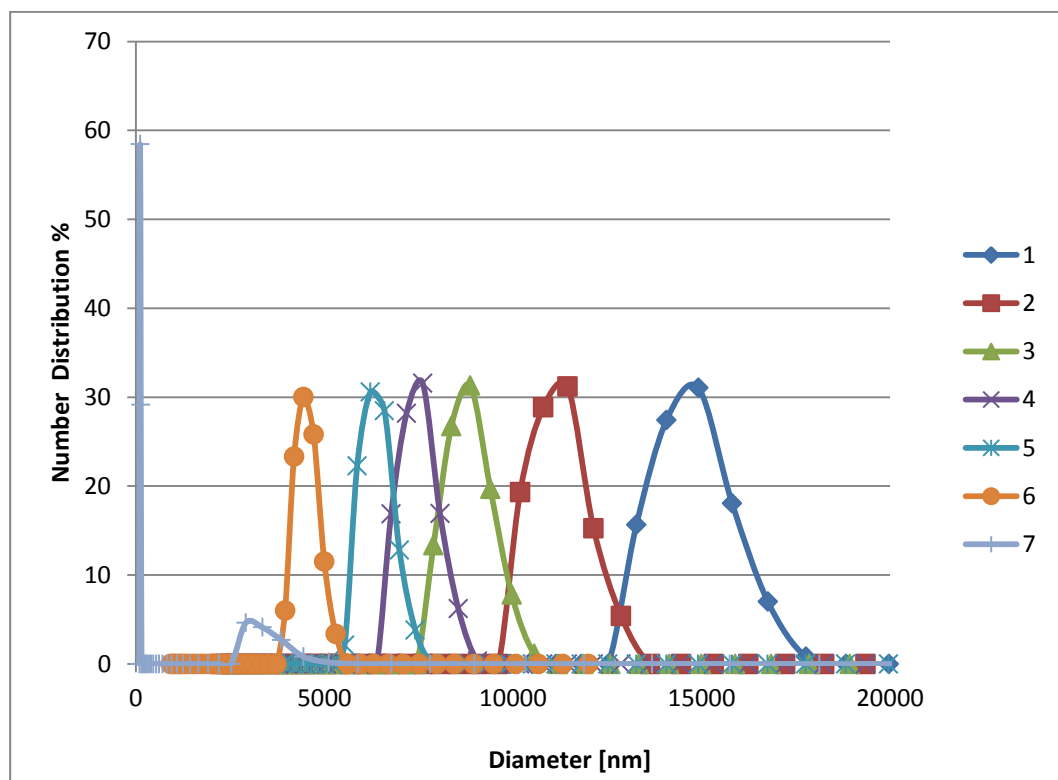
Figure 4 - 14: Combined graph showing Baker's yeast number distribution as % of concentration of particle dispersed versus diameter measured

The measurement conditions, as required by the machine set up, are refractive index, intensity, viscosity, and the cumulants are the diameter (measured in nanometers), as well as the poly dispersity index (PDI). This is an indication of variance in the sample; a low PDI (usually less than 0.2) indicates that the sample is monodispersed. The Delsa Nano C also provides much other information regarding the size of the particles in suspension: the cumulant result, the intensity,

volume, and number distributions along with a record of the autocorrelation function.
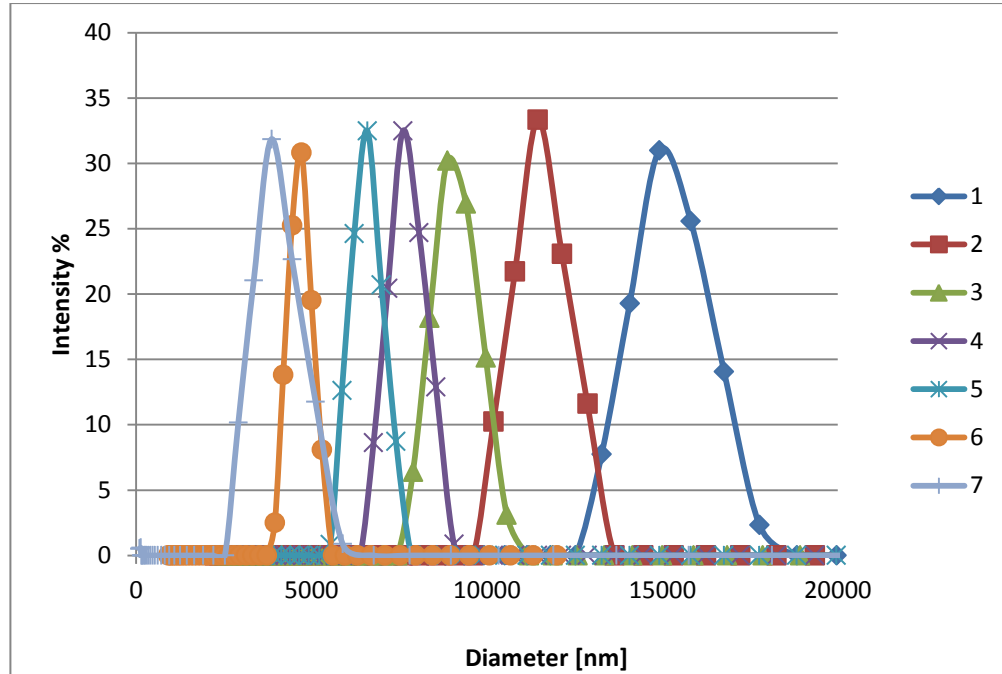
Figure 4 - 15: The combined intensity frequencies versus diameter of Baker's yeast in suspension

The intensity graph shows also the effect of particle size on the substrate wherein 1 is the untreated sample, and 7the homogenized sample at 60 MPa and 5 cycles. The measure of the intensity frequency reduces gradually by shifting to the left on the graph, which is an indication that homogenization in the HPH did have an effect on the particle size distribution, as shown in Figure 4-15. The idea of using the Delsa Nano C is to obtain a reduction in the size of the particles in the homogenized substrates. As the pressure and number of cycles increase during cell disruption in the HPH, the particles size of the substrates is reduce. In principles as the gap size of the HPH closes, the homogenized Baker's yeast as a result is compressed through the small opening (2-5 μm) [139]. As a result, the homogenized substrate becomes slurry with totally reduced particle sizes [146, 148, 193, 222]. As seen in the Figures (4-14 and 4-15), the difference between them is that Figures 4-14 is the concentration of the particle dispersed in a fluid

and it is measured in numbers as percentage and which in essence, is showing the number distribution of the dispersed particle in that fluid. Whereas Figure 4-15 shows the intensity frequencies of the particle and is considered as the scattering strength of the particle dispersed in the fluid. Both graphs are plotted against the diameter as size of the particle dispersed measured in (nm) [223].

4.5.2 Particle size analysis of Microalgae using Delsa Nano C

The supplied culture of Microalgae was unable to be viewed under the Scanning Electron Microscope (SEM) due to the nature of the substrate since, after drying in the oven to remove moisture and the water contents, there was no visible specimen remaining in the crucible for further examination. For this purpose Delsa nano C was a better choice.

Table 4 - 10: Samples of Microalgae taken during the particle size analysis showing frequency of number distribution (Concentration)

Samples	Microalgae	Number Distribution (Concentration)
1	Untreated	16278.6 ± 93.6
2	30 MPa, 1 Cycle	15420.2 ± 90.5
3	30 MPa, 3 Cycles	14422.8 ± 82.2
4	30 MPa, 5 Cycles	13021.6 ± 75.8
5	30 MPa, 6 Cycles	11129.7 ± 70.5
6	60 MPa, 1 Cycle	10429.3 ± 62.5
7	60 MPa, 3 Cycles	9956.1 ± 58.1
8	60 MPa, 5 Cycles	9357.2 ± 56.8
9	60 MPa, 6 Cycles	8834.8 ± 56.0
10	90 MPa, 1 Cycle	6959.7 ± 54.5
11	90 MPa, 3 Cycles	5980.9 ± 52.6
12	90 MPa, 5 Cycles	4507.0 ± 46.2
13	90 MPa, 6 Cycles	3063.1 ± 41. 7

The Delsa nano C was used in the particle size analysis of Baker's yeast and as such, it was applied to Microalgae for same purpose. As in the case of Baker's yeast, Microalgae in solution as a substrate required particle sizing through dynamic light scattering (DLS). Determining the particle sizing was performed after high-pressure homogenization of the substrates at different pressures, number of cycles, and temperature being the main parameters in this study.

Table 4-10 shows values of the treated against the untreated to determine the extent of deformation during the homogenization process, to determine particle sizing.

The substrates were homogenized at varying pressure and number of cycles. Each sample was taken using the glass cuvette to analyse it in the particle size analyser (Delsa Nano C). The aim of this work was to determine and to compare the treated samples with the untreated (sample 1), which is considered as the control sample in the conducted work. There were standard deviation error bars for each result recorded; these are indications that the sample contained some level of impurities which invariably will lead to some errors in value in the samples (from untreated sample to sample 13). Results obtained for tests from untreated to sample 13 are indication, and the presence of different particle sizes within the conducted experiments. Unlike Baker's yeast, there was more consistency in the generated result as compared to the results for the Microalgae.

4.6 *Design of Experiment* and Analyses of Results

These onward sections will analyse experimental results based on three categories of set of experiments and data acquisition. These are; Baker's yeast homogenized at temperature 15 - 25°C, Baker's yeast homogenized at temperature 30 - 50°C, as well as Microalgae homogenized at 15 - 25°C, with the dilution of substrate with solution C considered as most important analytically in this study.

4.7 Baker's yeast homogenized at a temperature of 15 – 25 °C

The experiment was designed based on a three level Box Behnken design (BBD) which includes one full replication for this substrate. Trial samples of Baker's yeast were performed by varying one of the process variables in determining the working range of each variable. With the maximum pressure of the high-pressure homogenizer considered as 100 MPa from the manufacturer, it was recommended never to go beyond 90 MPa as the operating working pressure. Also with a pressure lower than 30 MPa considered as infinitesimal, and with whose application in the HPH, never showed appreciable effect. Hence the working pressure was set between 30 and 90 MPa. These were the criteria for choosing the working ranges. Temperature ranges were chosen as the homogenization process needed to be within ± 5 °C of room temperature since room temperature is around 20 °C [224]. The number of cycles used was chosen for an improved homogenization process. Table 4-11 shows homogenizer input variables along with the design levels used for this substrate and, the experiment was carried out according to the design matrix shown in Table 4-12 in a random order to avoid any systematic error using the HPH alongside with the two measured responses. Ratios as a variable factor were used categorically and as identified by the design expert software. This was required to determine the effect of the dilution concentration of yeast and the solution C on other parameters. For this substrate, two responses were identified; protein concentration and cost. The energy monitor connected to the HPH was required to calculate and work out this cost. Other costs were negligible as the same trends will be applicable to the overall cost at the end. Mathematical models were developed successfully to predict the responses as explained above. The procedures described earlier in Chapter 3 were followed to determine and record these responses. Particularly, the averages of at least six measurements for protein concentration are presented. The full experimental measured data of protein concentration can be seen in Table 4-12. These were obtained from the measured UV absorbance results using the spectrophotometer to get the protein concentration from the homogenized yeast. The protein curve for working out the protein concentration and the applied calculation is provided in Appendix F.

Table 4 - 11: Process variables and experimental design levels used

Variables	Code	Unit	Limits Coded/actual		
			-1	0	+1
Pressure	A	MPa	30	60	90
Number of Cycles	B	-	1	3	5
Temperature	C	°C	15	20	25
Ratio	D	-	10:90	20:80	30:70

Table 4 - 12: Design matrix with actual values and calculated/experimentally measured responses for homogenized Baker's yeast

Exp. No.	Run Order	Factor 1 A: Pressure (MPa)	Factor 2 B: No. of cycles -	Factor 3 C: Temp (°C)	Factor 4 D: Ratio -	Response 1 Protein Conc. (mg/mL)	Response 2 Cost (Euro/h)
1	45	30	1	20	10:90	0.0016	0.1
2	28	90	1	20	10:90	0.5935	0.13
3	47	30	5	20	10:90	0.0161	0.48
4	38	90	5	20	10:90	0.8597	0.39
5	24	30	3	15	10:90	0.0097	0.27
6	5	90	3	15	10:90	0.0806	0.43
7	41	30	3	25	10:90	0.0048	0.4
8	11	90	3	25	10:90	0.0968	0.45
9	1	60	1	15	10:90	0.1887	0.11
10	25	60	5	15	10:90	0.3468	0.33
11	37	60	1	25	10:90	0.2129	0.12
12	6	60	5	25	10:90	0.3226	0.46
13	43	60	3	20	10:90	0.1823	0.41
14	32	60	3	20	10:90	0.1613	0.41
15	16	60	3	20	10:90	0.4597	0.41
16	7	60	3	20	10:90	0.4274	0.41
17	14	60	3	20	10:90	0.2129	0.41
18	8	30	1	20	20:80	0.0484	0.1
19	20	90	1	20	20:80	1.1242	0.13
20	48	30	5	20	20:80	0.0968	0.48
21	23	90	5	20	20:80	1.3387	0.39
22	17	30	3	15	20:80	0.0323	0.27
23	26	90	3	15	20:80	0.0968	0.43

24	50	30	3	25	20:80	0.0323	0.4
25	21	90	3	25	20:80	0.1613	0.45
26	35	60	1	15	20:80	0.2306	0.11
27	22	60	5	15	20:80	0.6161	0.33
28	34	60	1	25	20:80	0.4081	0.12
29	33	60	5	25	20:80	0.6452	0.46
30	49	60	3	20	20:80	0.3339	0.41
31	9	60	3	20	20:80	0.4065	0.41
32	3	60	3	20	20:80	0.4952	0.41
33	51	60	3	20	20:80	0.5645	0.41
34	29	60	3	20	20:80	0.5081	0.41
35	30	30	1	20	30:70	0.0839	0.1
36	36	90	1	20	30:70	1.5494	0.13
37	2	30	5	20	30:70	0.1613	0.48
38	19	90	5	20	30:70	1.7694	0.39
39	40	30	3	15	30:70	0.0484	0.27
40	13	90	3	15	30:70	1.2032	0.43
41	4	30	3	25	30:70	0.0484	0.4
42	42	90	3	25	30:70	0.8065	0.45
43	10	60	1	15	30:70	0.2935	0.11
44	15	60	5	15	30:70	0.8823	0.33
45	39	60	1	25	30:70	0.6097	0.12
46	31	60	5	25	30:70	0.9742	0.46
47	46	60	3	20	30:70	0.4984	0.41
48	44	60	3	20	30:70	0.6597	0.41
49	12	60	3	20	30:70	0.5613	0.41
50	18	60	3	20	30:70	0.6871	0.41
51	27	60	3	20	30:70	0.7839	0.41

4.7.1 Development of mathematical model for Baker's yeast cell wall disruption with temperature range of 15 - 25°C

Table 4 - 13: ANOVA table for Protein Concentration reduced quadratic model (15 - 25°C) range

Source	Sum of Squares	DF	Mean Square	F Value	p-value Prob > F	
Model	7.223	9	0.803	21.511	< 0.0001	Significant
A-Pressure	3.447	1	3.447	92.400	< 0.0001	
B-No. of cycles	0.300	1	0.300	8.048	0.0070	
C-Temperature	0.004	1	0.004	0.096	0.7579	
D-Ratio	1.652	2	0.826	22.138	< 0.0001	
AD	0.768	2	0.384	10.296	0.0002	
B^2	0.582	1	0.582	15.604	0.0003	
C^2	0.528	1	0.528	14.143	0.0005	
Residual	1.530	41	0.037			
Lack of Fit	1.365	29	0.047	3.433	0.0139	Not Significant
Pure Error	0.165	12	0.014			
Cor Total	8.753	50				
$R^2 = 0.825$			Pred. $R^2 = 0.695$			
Adj. $R^2 = 0.787$			Adeq. Precision = 21.086			

Validation of the model:
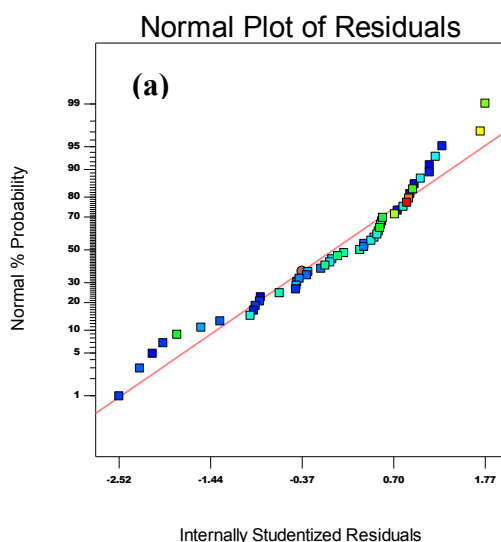
The normal plot of residuals above shows the normal probability plot indicating whether the residuals follow a normal distribution, in which case the points will

follow a straight line or as close to the diagonal. One can expect some moderate scatter points even with a normal distribution. This was generated by the *Design Expert* software for the model, given in Figure 4-16 (a). In other words, the linearity of the residuals indicates that they are normally distributed and so, ANOVA analysis can be performed. While the predicted versus actual plot (Figure 4-16 (b)) is a scattered plot, once the trend is linear i.e. close to the diagonal, it means it is normally distributed.
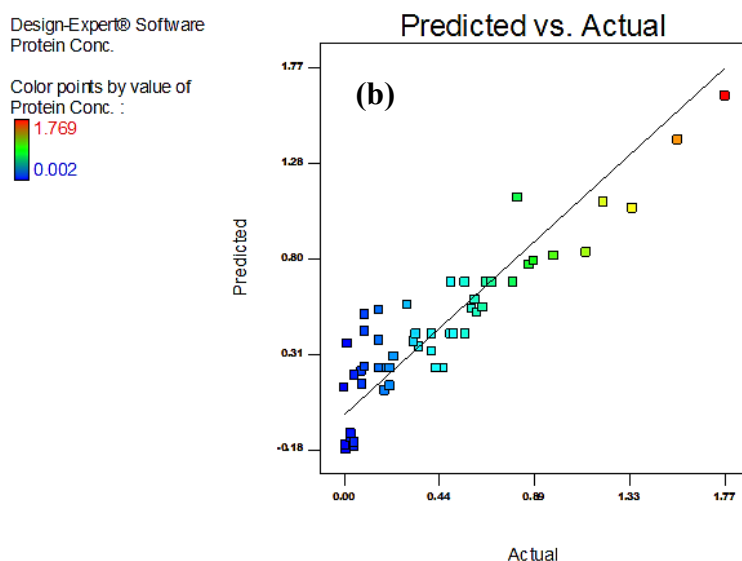
Figure 4 - 16: Scatter diagrams of normal plot of residuals (a) and protein concentration yields (b)

The fit summary output indicates that, for the responses, the reduced quadratic models (protein Concentration) and (Cost) are statistically recommended for further analyses as they have the maximum predicted and adjusted R^2 [225, 226]. Through selecting the step-wise regression method, the insignificant model terms can automatically be eliminated. The resulting ANOVA Tables (as shown in Tables 4-13 and 4-14 for the reduced quadratic models outline the analysis of variance for the responses (Protein Concentration and Cost), and illustrate the significant model terms. These also show the other adequacy measures R^2, adjusted R^2, and predicted R^2 as 0.825, 0.787 and 0.695, respectively for Table 4-13, and 0.966, 0.960 and 0.943 respectively for Table 4-14. The entire adequacy measures are close to 1, which are in reasonable agreement and therefore indicate

adequate models because the statistical analysis as considered by the *Design Expert*, it indicates that any value equal to or greater than 0.5 is considered as close to 1 when determining the adequacy measures R^2, adjusted R^2, and predicted R^2. The adequate precision being equal to 21.086 for protein concentration yield and 35.186 for cost indicates an adequate model, as the adequacy value was >> 4 and an indication of good model discrimination [225, 226]. The adequate precision compares the range of the predicted value at the design points to the average prediction error.

Figure 4-16 (a and b) and 4-19 (a and b) are the replica plots of the predicted against the actual response, and the residual of the normal plot of protein concentration response and that of predicted versus actual response, and the residual of the normal plot of cost response respectively. The analysis of variance indicates that the number of cycles, pressure as well as temperature, and their interactions are the most significant factors affecting the protein concentration yields. The predicted vs. Actual plots are shown in Figure 4-16b and Figure 4-19b. This figure indicates that the developed models are adequate because the residuals are minimal, since these tend to be close to the diagonal line. The normal plot of residuals in Figure 4-16a and 4-19a indicates that the assumptions of normal distribution of the data are respected; therefore the ANOVA can be applied to study the dataset.

An adequate model means that the reduced model has successfully passed all the required statistical tests and can be used to predict the responses, or to optimize the process, and so on. The final mathematical models linked to the responses with regard to the coded factors and actual factors as determined by the software are respectively in Equations (4-1) to (4-4) and (4-5) to (4-6) with equations 4-2 to 4-4 in the dilution ratio form; 10:90, 20:80 and 30:70, and Equation 4-6 representing that for cost respectively.

Based on the ANOVA Table 4-13, the point prediction technique and an appropriate model was based on the fact that, Adjusted R^2 minus Predicted R^2 must be < 0.2 and in this case, it was 0.092.

As R^2 equalled 0.825, it implied that 82.5% of the variability in the data has been explained by the model and a F-Value model of 21.51 implied that the model was significant since it is only 0.01% chance that the F-Value model was disrupted by scatter/ noise.

Based on the final equation in terms of coded factors and those in terms of the actual factors for ratios, 10:90, 20:80, and 30:70, protein concentration yield can be worked out using the associated equation for any set of the ratios to determine this yield. In the final equation in terms of coded factors, as given below, the square brackets indicated, represents the ratios of categorical factor in coded terms. This can be used to predict the protein concentration yield when homogenized under HPH. For example in the ratios considered in this research; 10:90, 20:80, and 30:70, their representation in coded factors were [1, 0], [-1, -1] and [0, 1] respectively and when solved into the equation of the coded factors gives the result as shown in the final equation in terms of coded factors (see Equation 4-1).

Final Equation in Terms of Coded Factors:

*Protein Concentration = 0.44489468 + 0.379003898 * A + 0.111854839 * B*
$\qquad$ *+ 0.012232258 * C - 0.204003099 * D [1] - 0.029809551 * D[2]*
$\qquad$ *- 0.179205511*AD[1] - 0.065092608 * AD [2] + 0.214389389*
$\qquad$ *B^2 - 0.204106579 * C^2* $\qquad\qquad$ (4-1)

Final Equation in Terms of Actual Factors:

Ratio 10:90;

*Protein Concentration = -3.158745622 + 0.006659946 * Pressure - 0.265656664*
$\qquad$ *No. of cycles + 0.329016978 * Temperature +0.053597347*
$\qquad$ *No. of cycles^2 - 0.008164263 * Temperature^2*

$\qquad\qquad\qquad\qquad\qquad\qquad\qquad\qquad\qquad\qquad$ (4-2)

Ratio 20:80;

*Protein Concentration = -3.21277788 + 0.01046371 * Pressure - 0.265656664*
$\qquad$ *No. of cycles + 0.329016978 * Temperature + 0.053597347*
$\qquad$ *No. of cycles^2 - 0.008164263 * Temperature^2*

$\qquad\qquad\qquad\qquad\qquad\qquad\qquad\qquad\qquad\qquad$ (4-3)

Ratio 30:70;

Protein Concentration = -3.56793713 + 0.020776734 * Pressure - 0.265656664

$\qquad$ ** No. of cycles + 0.329016978* Temperature + 0.053597347*

$\qquad$ ** No. of cycles^2 - 0.008164263 * Temperature^2*

$$(4\text{-}4)$$

Effect of process parameters on the responses - Protein Concentration

The perturbation plot for the protein concentration yield from the 15 – 25 °C temperature range is illustrated in Figure 4-17 as (a), (b), and (c). The perturbation plot helped in comparing the effect of all the factors at a particular point in the design space. The lines represent the behaviours of each factor while holding the others constant at the centre point. This type of display can be used to determine the factors that most affect the response. From the illustrations, pressure and the number of cycles affect the protein concentration yield. This was in agreement with these authors and researchers [162-164, 171, 194, 197, 227-229] wherein pressure showed a very significant effect in the production of protein. As highlighted, an increase in pressure, A; resulted in high protein concentration yield; while the number of cycle, B showed minimal rise in the effect to the yield of protein, and the temperature factor was shown not to have an effect on the yield.

Considering the categorical factor of ratio designated as D in this study, protein concentration yield has been seen to give the highest yield at the ratio 30:70 when compared to other ratios of 10:90 and 20:80. Invariably, this shows that as the ratio increased, the yield in protein concentration also increased at the same rate as the pressure rises seen at Figure 4-17(c).

From the three scenarios (Figure 4-17), it is evident that pressure (A) and number of cycle (B) both have a strong effect on the protein concentration yield as both have an upward trend from minimum to maximum factor. This is different from that of the temperature (C) which showed a downward trend in its behaviour. The behaviour of the three parameters are pronounced in the 30:70 ratio of the perturbation plot where protein concentration yield was considered the highest yield compared to other two ratios (10:90 and 20:80).
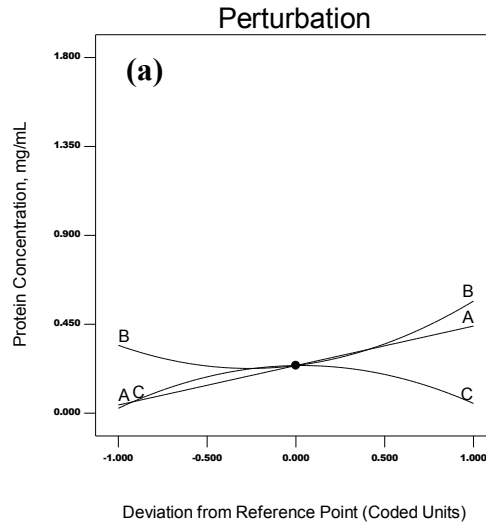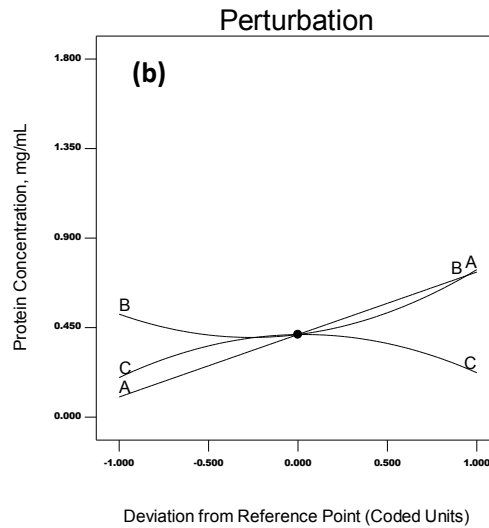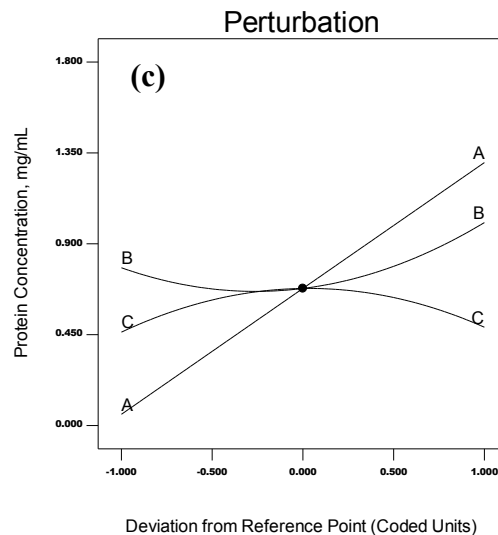
Figure 4 - 17: Perturbation plots (a), (b), and (c) showing the effect of process parameters on protein concentration yield, with ratio as the categorical factor on the response

Effect of process parameters on the responses – Cost

Figure 4-18 shows the interaction plot of the effect of pressure (A) and ratio (D) on protein yield concentration. Pressure has been shown to be the most important parameter in the homogenization of biomass substrate using HPH. Comparing the ratios (categorical factor) in Figure 4-18, it showed a wider disparity at a ratio 30:70 in protein concentration yield compared to the 10:90 and 20:80 ratios. The pressure interaction was also considered, as it was a significant parameter in terms of protein yield concentration. During the homogenization process, high-pressure is intended to lower or reduce the gap size on the valves slit within the HPH, to enable the soluble Baker's yeast to be constricted through the small opening. As a result, the cell walls of the yeast are broken down to release the intracellular content of protein.
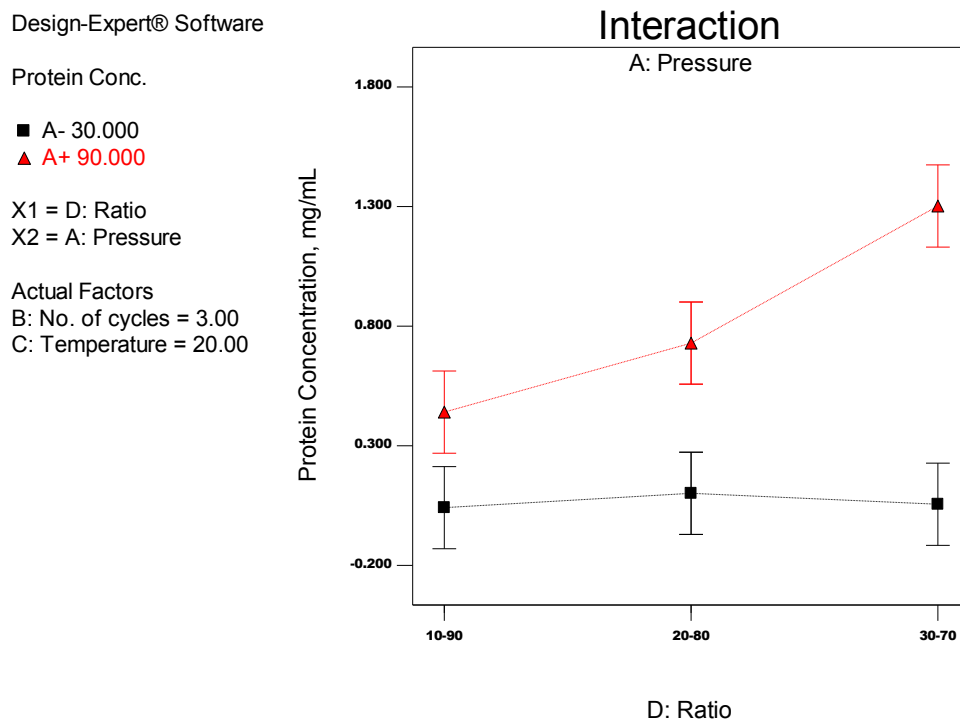
Figure 4 - 18: Interaction plot showing the effect of Pressure (A) and Ratio (D) on protein concentration yield

Table 4 - 14: ANOVA Table for cost reduced – Baker's yeast (15 - 25°C) Temperature Range

Source	Sum of Squares	DF	Mean Square	F Value	Prob > F	
Model	0.848	8	0.106	149.417	< 0.0001	Significant
A-Pressure	0.008	1	0.008	11.894	0.0013	
B-No. of cycles	0.540	1	0.540	761.208	< 0.0001	
C-Temperature	0.032	1	0.032	44.457	< 0.0001	
AB	0.011	1	0.011	15.224	0.0003	
AC	0.009	1	0.009	12.793	0.0009	
BC	0.011	1	0.011	15.224	0.0003	
B^2	0.227	1	0.227	319.733	< 0.0001	
C^2	0.006	1	0.006	8.113	0.0068	
Residual	0.030	42	0.001			
Lack of Fit	0.030	30	0.001			
Pure Error	0.000	12	0.000			
Cor Total	0.878	50				
$R^2 = 0.966$			Pred $R^2 = 0.943$			
Adj $R^2 = 0.960$			Adeq Precision = 35.186			

Validation of the models developed

Table 4-14 above, shows the ANOVA table for cost reduced as a quadratic model, for Baker's yeast over a 15 – 25 °C temperature range. The point prediction technique and the appropriateness of a model is based on the fact that; Adj R^2 minus Pred. R^2 must be less than 0.2 and in this case, it was at 0.017.

R^2 equalled 0.966 which implied that 96.6% of the variability in the data has been explained by the model and F-Value model equalled 149.42 implying that the model was significant since there was only a 0.01% chance that the F-Value model occurred due to noise. The "Prob > F" was the same as the P-value, implying that this must be greater than the F-value model and with a value of < 0.0001, was then considered significant (see Section 3.6.7 of Chapter 3 for reference)

The normal plot of residuals follow a diagonal straight line as shown in Figure 4-19 (a), indicating a normal distribution. In order to determine the normality of the data Figure 4-19 (b) was used. The linearity of the residuals indicated that they were normally distributed and thus the ANOVA could be performed. While the Predicted versus Actual plot (Figure 4-19 (b)) was a scattered diagram and the trend was almost linear, i.e. close to the diagonal, therefore normally distributed.
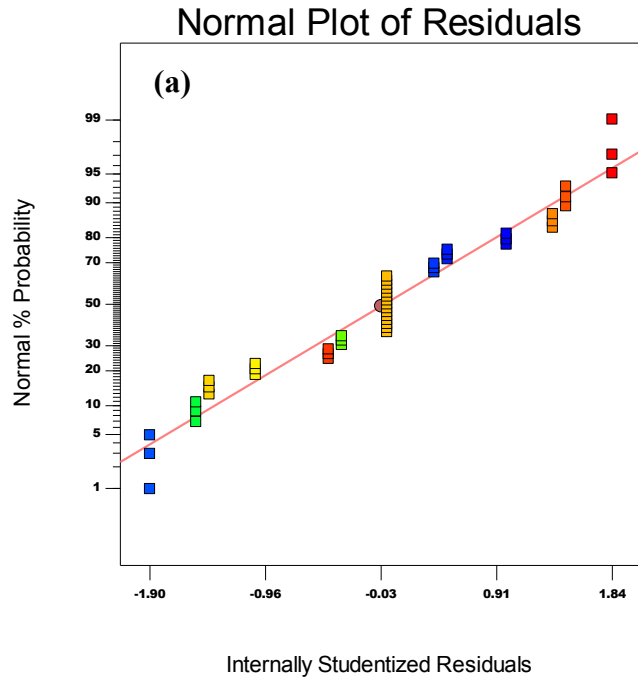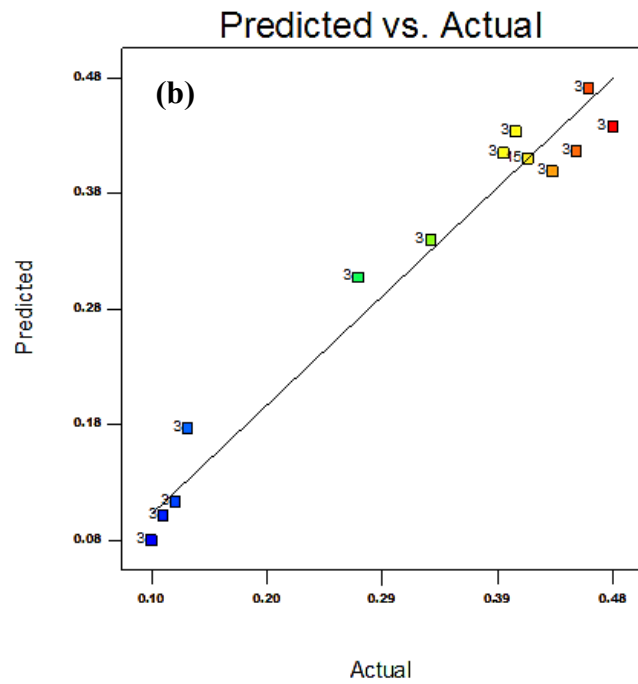
Figure 4 - 19: Scatter diagrams of normal plot of residuals (a) and cost (b)

Final Equation in Terms of Coded Factors:

$$Cost = 0.409 + 0.019 * A + 0.150 * B + 0.036 * C - 0.030 * A * B - 0.028 * A * C$$

$$+0.030 * B * C - 0.134 * B\wedge2 - 0.021 * C\wedge2 \qquad (4\text{-}5)$$

Final Equation in Terms of Actual Factors:

Cost = – 0.770 + 0.006 * Pressure + 0.246* No. of cycles + 0.043

– 0.001*Pressure * No. of cycles + 0.000 * Pressure * Temperature

+ 0.003 * No. of cycles*Temperature – 0.033 * No. of cycles^2

– 0.001 * Temperature^2 (4-6)

Figures 4-16 (a-b) and 4-19 (a-b) present the relationship between the measured and predicted values of protein concentration yield and cost. These scatter diagrams indicate that the above mathematical models exhibit a good agreement between the measured and estimated values of the above measured responses. These Figures indicate that the developed models are adequate owing to the residuals in the prediction of each response being small, as the residuals tend to be close to the diagonal lines.
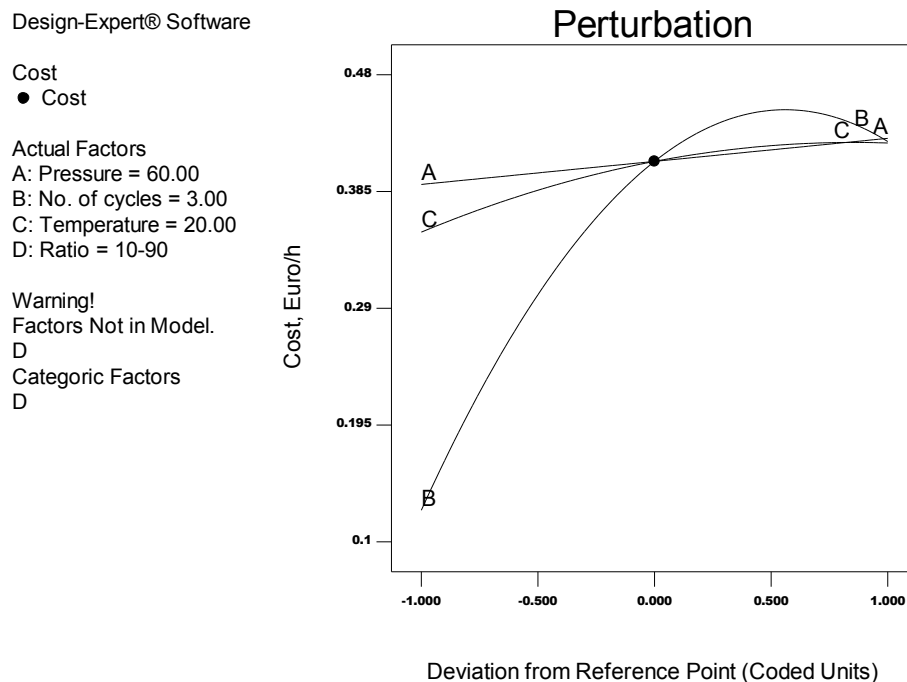
Figure 4 - 20: Perturbation plot showing the effect of process parameters on cost with ratios as the categorical factor on the response

The perturbation plot in Figure 4-20 shows the effect of process parameters on cost. The associated cost, in terms of protein concentration yield, has been shown to be effective where pressure and temperature were considered. While pressure and temperature were considered as factors for cost effectiveness, they both have shown to be of slightly positive effects on cost. The number of cycle's effect was considered mostly positive in terms of cost. This rose to about €0.40/hour before a downward trend was observed. A categorical factor of 10:90 ratios shows better cost effectiveness for protein concentration yield. A sharp decrease after the midpoint was a clear indication that number of cycles did not result in an effective cost for the protein concentration yield.

In Figures 4-21 and 4-22, a relationship was established between the number of cycles and, pressure and temperature, to weaken the cell walls, in order to increase protein yield. Previous studies by Siddiqi *et al.* [165], Diels *et al.* [169], and Ekpeni *et al.* [227] revealed that after two to three passes, the entire cell wall had completely broken down releasing the protein in the biomass substrates, due to the application of shear stress by the HPH, therefore the Number of cycle does improves the homogenization process [169, 227].

Figure 4-21, shows the interaction between pressure and the number of cycles in terms of cost; again, both have proven to be the effective parameters for cost determination when the categorical factor is considered at 10:90. An interaction took place around cycle 4, which will be considered as the cycle for better protein yield, whereas no notable interaction results between temperature and number of cycles. Homogenizing at a higher number of cycles is considered best for complete disruption of the biomass substrate, in order to effectively release its inner contents for higher protein yield.

The perturbation plot in Figure 4-20, shows that the horizontal axis indicated a deviation from its reference point (Coded Units); -1, 0, and +1, with -0.5 and +0.5 in between the three level of design. At a coded units of -1, the actual value of the parameters was 30 MPa for pressure, 1 for number of cycles, 15 °C for temperature and 10:90 for ratio. For coded units 0, the actual value of the parameters was 60 MPa for pressure, 3 for number of cycles, 20 °C for

temperature and 20:80 for ratio. For coded units +1, this related to 90 MPa for pressure, 5 for number of cycles, 25 °C for temperature and 30:70 for ratio (see Table 4-11 for reference), for the coded/actual limits of the variable parameters.
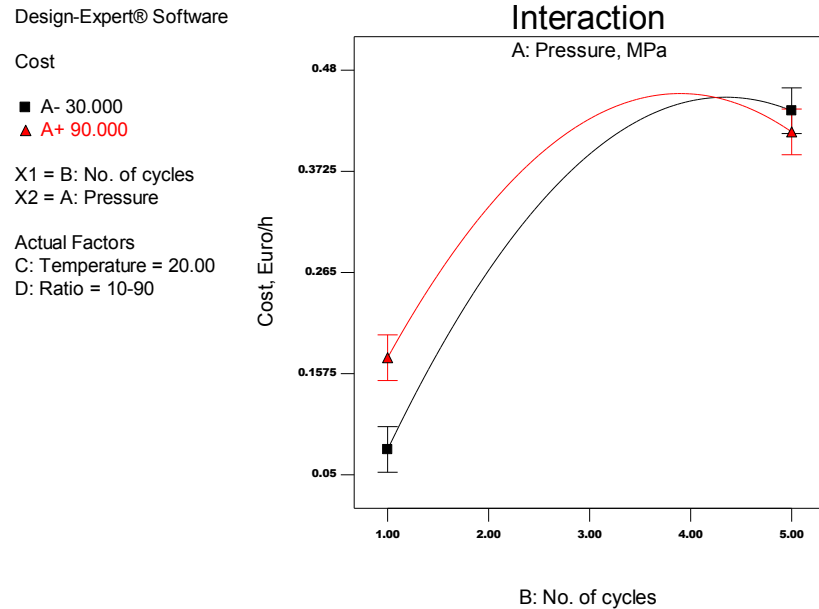
Figure 4 - 21: Interaction plot showing the effect of Pressure (A) and number of cycles (B) on cost
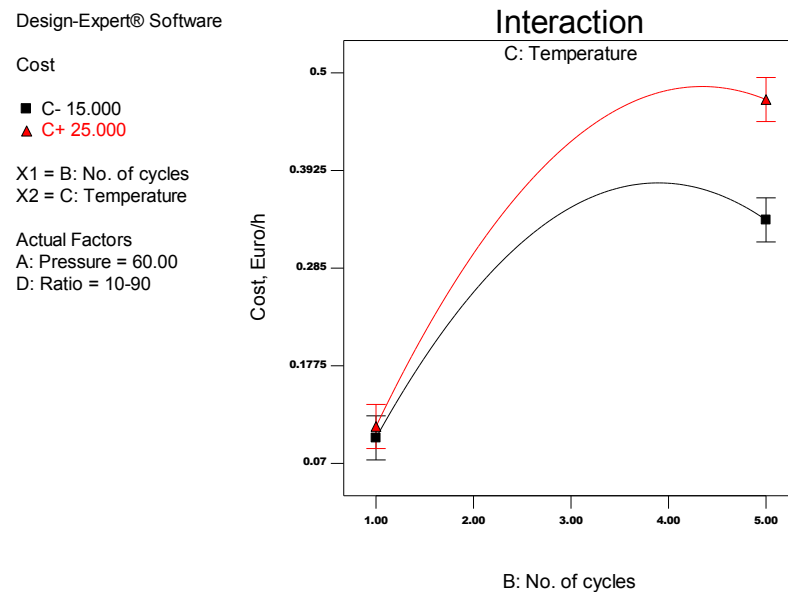
Figure 4 - 22: Interaction plot showing the effect of number of cycle (B) and temperature (C) on cost

Design-Expert® Software

Cost
0.48
0.1
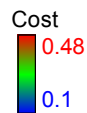
X1 = B: No. of cycles
X2 = C: Temperature

Actual Factors
A: Pressure = 60.00
D: Ratio = 10-90
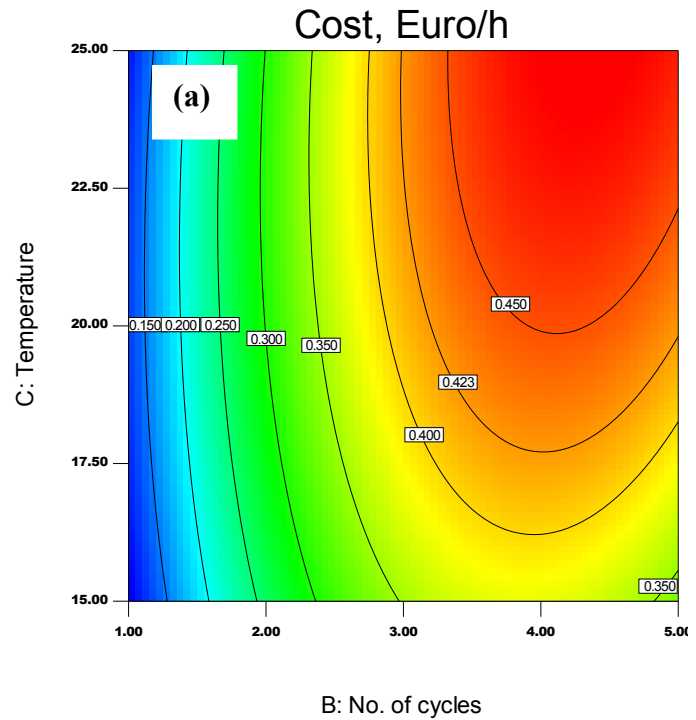
Design-Expert® Software

Cost
0.48
0.1

X1 = A: Pressure
X2 = B: No. of cycles

Actual Factors
C: Temperature = 20.00
D: Ratio = 10-90
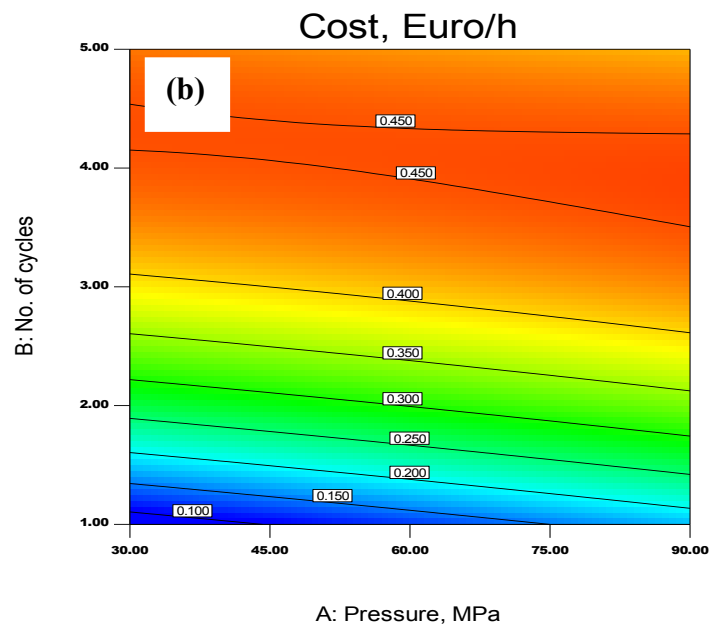
Figure 4 - 23: Contour plots (a) and (b) showing the effect of number of cycles, temperature and pressure on the response – cost (this shows zone with highest software-estimated cost)

Figure 4-23 (a and b) show contour graphs for the effects of temperature and the number of cycles. Emphasis has been placed on the Euro per hour (€/hour) rather than the Euro per milligram (€/mg) of protein yield. This is because the former

determines the energy cost based on the usage of HPH for homogenizing the Baker's yeast to release protein. Whereas Euro per milligram of protein yield can only be determined after it has been homogenized. Though it is of importance, it was not considered necessary in this research. The idea here was to determine the energy cost of the machine (HPH) in breaking down the cell walls within the Baker's yeast to liberate the protein content.

The red and orange colours zones in the Figures 4-23 (a) and (b) respectively represent high cost.

Figure 4 - 24: Response surface plot of cost in Euro/h (with actual factors pressure considered at 60 MPa and ratio of 10:90)

Figure 4-24 is a response surface (RS) plot showing the effect of two parameters (temperature and number of cycles) against cost. It is seen that lower number of cycles over any temperature yielded lower cost.

4.8 Baker's yeast homogenized at temperature 30 – 50 °C

Table 4 - 15: Process variables and experimental design levels used

Variables	Code	Unit	Limits Coded/actual		
			-1	0	+1
Pressure	A	MPa	30	60	90
Number of Cycles	B	-	1	3	5
Temperature	C	°C	30	40	50
Ratio	D	-	10:90	20:80	30:70

This information presented in Table 4-15 was used to determine the effect temperature range had on the homogenized Baker's yeast. The variables with their coded and actual value in the experimental design used here for the 30-50 °C temperature range was similar to the previous one used in the 15 – 25 °C temperature range, except that the temperature range increased from 15 – 25 °C to 30 - 50 °C.

Table 4 - 16: Design matrix with actual values and calculated/experimentally measured responses

Exp. No.	Run Order	Factor 1 A: Pressure MPa	Factor 2 B: No. of cycles -	Factor 3 C: Temp (°C)	Factor 4 D: Ratio	Response 1 Protein Conc. [mg/mL]	Response 2 Cost [Euro/h]
1	13	30	1	40	10:90	0.0161	0.11
2	18	90	1	40	10:90	0.6290	0.15
3	23	30	5	40	10:90	0.0968	0.47
4	10	90	5	40	10:90	0.9145	0.4
5	5	30	3	30	10:90	0.0484	0.29
6	48	90	3	30	10:90	0.1290	0.43
7	45	30	3	50	10:90	0.0645	0.41
8	36	90	3	50	10:90	0.2258	0.47
9	11	60	1	30	10:90	0.2661	0.12
10	42	60	5	30	10:90	0.3581	0.35
11	49	60	1	50	10:90	0.3177	0.13
12	12	60	5	50	10:90	0.2903	0.47
13	9	60	3	40	10:90	0.4597	0.42
14	25	60	3	40	10:90	0.5194	0.42
15	47	60	3	40	10:90	0.4726	0.42

16	37	60	3	40	10:90	0.6726	0.42
17	27	60	3	40	10:90	0.6258	0.42
18	6	30	1	40	20:80	0.0645	0.11
19	32	90	1	40	20:80	1.1306	0.15
20	21	30	5	40	20:80	0.1097	0.47
21	28	90	5	40	20:80	1.1210	0.4
22	8	30	3	30	20:80	0.0806	0.29
23	29	90	3	30	20:80	0.1855	0.43
24	43	30	3	50	20:80	0.1742	0.41
25	16	90	3	50	20:80	0.2710	0.47
26	51	60	1	30	20:80	0.2871	0.12
27	24	60	5	30	20:80	0.6403	0.35
28	1	60	1	50	20:80	0.4145	0.13
29	2	60	5	50	20:80	0.7871	0.47
30	20	60	3	40	20:80	0.5968	0.42
31	31	60	3	40	20:80	0.5758	0.42
32	34	60	3	40	20:80	0.5565	0.42
33	30	60	3	40	20:80	0.8677	0.42
34	44	60	3	40	20:80	0.7935	0.42
35	4	30	1	40	30:70	0.0919	0.11
36	35	90	1	40	30:70	0.9500	0.15
37	40	30	5	40	30:70	0.1452	0.47
38	3	90	5	40	30:70	1.3387	0.4
39	38	30	3	30	30:70	0.1129	0.29
40	22	90	3	30	30:70	0.2371	0.43
41	15	30	3	50	30:70	0.1968	0.41
42	19	90	3	50	30:70	0.3226	0.47
43	41	60	1	30	30:70	0.3097	0.12
44	26	60	5	30	30:70	0.9435	0.35
45	7	60	1	50	30:70	0.5855	0.13
46	39	60	5	50	30:70	0.9919	0.47
47	14	60	3	40	30:70	0.6371	0.42
48	46	60	3	40	30:70	0.6097	0.42
49	33	60	3	40	30:70	0.7306	0.42
50	50	60	3	40	30:70	0.9629	0.42
51	17	60	3	40	30:70	0.9016	0.42

The design matrix with actual values and calculated/experimentally measured responses are as shown in Table 4-16. Given that the data was generated by *Design Expert,* the experiments were carried out to measure the responses of protein concentration in (mg/mL) and Cost in (Euro/hour). These were conducted randomly for simplicity in terms of saving time, resources and to remove bias.

Thus the DOE indicated a run order for the experimentation and the "Exp. Number" was used to identify the sample.

Table 4 - 17: ANOVA Table for Protein Concentration Reduced Quadratic Model (30 – 50 °C)

Source	Sum of Squares	DF	Mean Square	F Value	Prob > F	
Model	4.184	8	0.523	13.435	< 0.0001	Significant
A-Pressure	1.629	1	1.629	41.855	< 0.0001	
B-No. of cycles	0.298	1	0.298	7.655	0.0084	
C-Temperature	0.045	1	0.045	1.166	0.2865	
D-Ratio	0.474	2	0.237	6.091	0.0048	
A^2	0.669	1	0.669	17.174	0.0002	
B^2	0.168	1	0.168	4.309	0.0441	
C^2	0.885	1	0.885	22.741	< 0.0001	
Residual	1.635	42	0.039			
Lack of Fit	1.418	30	0.047	2.621	0.0400	Not Significant
Pure Error	0.216	12	0.018			
Cor Total	5.819	50				
$R^2 = 0.719$			Pred $R^2 = 0.567$			
Adj $R^2 = 0.666$			Adeq Precision = 15.552			

4.8.1 Development of mathematical models for Baker's yeast with temperature range (30 - 50°C)

The DOE method was used in the analysis of the measured responses. The fit summary provided outputs for the responses in the reduced quadratic models (protein concentration) and (cost) which were statistically recommended for further analyses, due to the maximum predicted and adjusted R^2. The test of significance of the regression models, the test for significance on individual coefficients, and the 'Lack of Fit' test were performed using the same statistical package. Through selecting the step-wise regression method, the insignificant model terms could automatically be eliminated. The resulting ANOVA Tables, as shown in Tables 4-17 and 4-18 for the reduced quadratic models outline the analysis of variance for the responses (protein concentration and cost) and illustrate the significant model terms. These also show the other adequacy measures R^2, adjusted R^2 and predicted R^2 as 0.719, 0.666 and 0.567, respectively for Table 4-17, and 0.975, 0.971 and 0.959 respectively for Table 4-18. The entire

adequacy measurement are close to 1, which are in reasonable agreement because the statistical analysis as recognised by the *Design Expert*, indicates that any value equal to or greater than 0.5 is considered as close to 1 when determining the adequacy measures R^2, adjusted R^2, and predicted R^2. The adequate precision being equal to 15.552 for protein concentration yield, and 41.65 for cost, indicating an adequate model [225, 226], see Tables 4-17 and 4-18. The adequate precision compared the range of the predicted values at the design points to the average prediction error.

These values are $\gg$ 4; therefore an adequate model is implied [225]. Figures 4-25 (a and b) and 4-29 (a and b) were a replica plot of the Predicted versus the Actual response, the residual of the normal plot of protein concentration response, as well as the residual of the normal plot of cost response were found to be normally distributed. The analysis of variance indicated that the number of cycles, pressure as well as temperature and their interactions were the most significant factors affecting the protein concentration yield. The predicted versus the actual plots are shown in Figures 4-25(b) and 4-29(b) for protein yield and cost respectively, indicating adequate models. The normal plot of residuals in Figure 4-25(a) and 4-29(a) indicate that the assumptions of normal data distribution were respected; therefore the ANOVA could be applied to the study.

The final mathematical models linked to the responses with regards to the coded factors and actual factors as determined by the software, are given respectively in Equations (4-7) to (4-10) and (4-11) to (4-12) with Equations (4-8) to (4-10), including the dilution ratios; 10:90, 20:80 and 30:70 and Equation (4-12) representing that of cost.
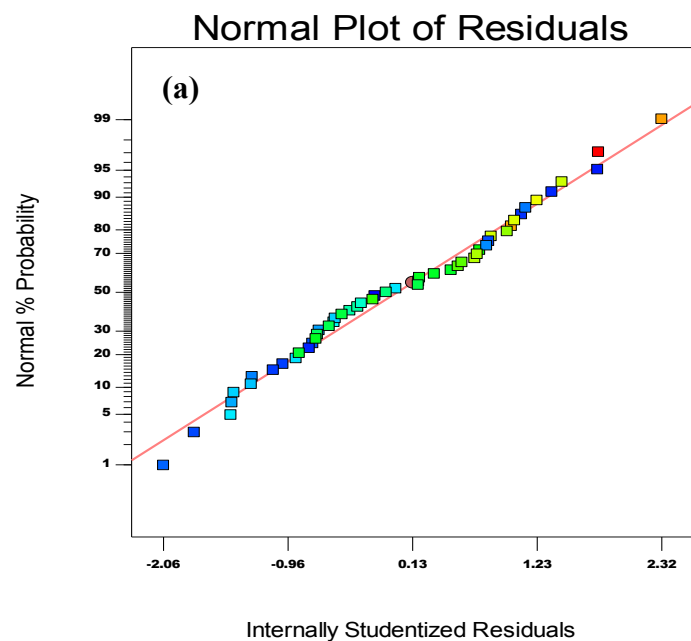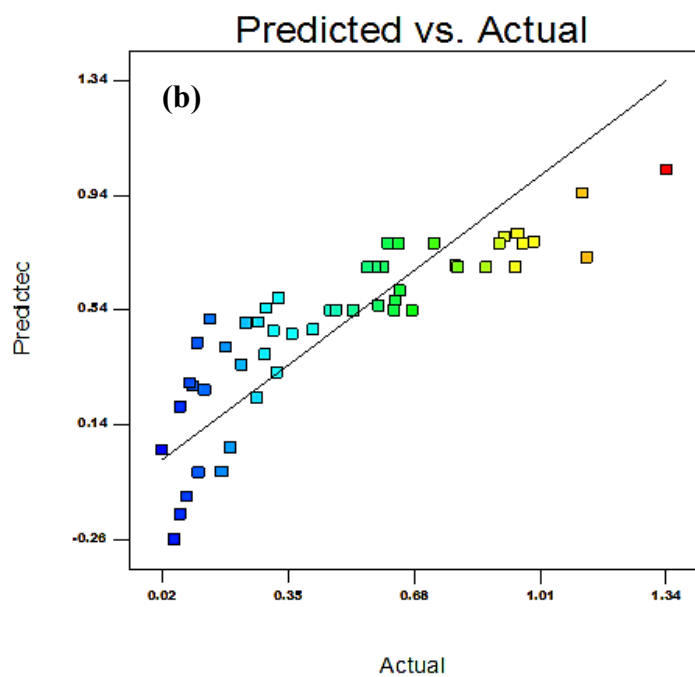
Figure 4 - 25: Scatter diagrams of normal plot of residuals (a) and cost (b) for 30 -50 °C

146

Validation of the models developed:

Final Equation in Terms of Coded Factors:

Protein Concentration = 0.665483871 + 0.260551075 * A + 0.111424731 * B

+ 0.043481183 * C - 0.127672359 * D[1] + 0.022327641 * D[2]

- 0.230053763 * A^2 + 0.115241935 * B^2 - 0.264731183 * C^2

$$(4\text{-}7)$$

Final Equation in Terms of Actual Factors:

Ratio 10:90;

Protein Concentration = -5.22097209 + 0.0039358871 * Pressure – 0.117150538

* No. of cycles + 0.216133065 * Temperature - 0.000255615

Pressure^2 + 0.028810484 No. of cycles^2 – 0.002647312 *

Temperature^2   (4-8)

Ratio 20:80;

Protein Concentration = -5.07097209 + 0.0039358871 * Pressure - 0.117150538

* No. of cycles + 0.216133065 * Temperature - 0.000255615

Pressure^2 +0.028810484 No. of cycles^2 – 0.002647312 *

Temperature^2   (4-9)

Ratio 30:70;

Protein Concentration = -4.987955013 + 0.0039358871 * Pressure -0.117150538

* No. of cycles + 0.216133065 * Temperature - 0.000255615

Pressure^2+0.028810484 No. of cycles^2 – 0.002647312 *

Temperature^2   (4-10)

The final equations in terms of coded factors and that of the actual factors for the ratios, 10:90, 20:80, and 30:70 as generated by the *Design Expert software* were also used to determine the protein concentration yield.

Effect of process parameters on the responses - Protein Concentration

The perturbation plot for the protein concentration yield from the 30 - 50 degrees temperature range is illustrated in Figure 4-26 as (a), (b), and (c). The perturbation plot helped to compare the effect of all the factors at a particular point in the design space. This has previously been discussed under the 15 - 25 °C temperature ranges. Perturbation plots under this section have indeed shown great differences as compared to that under the 15 - 25 °C temperature range. Temperature is shown to be major contributing factor in protein concentration yield. Counter to the results in the previous section, due to the temperature of the biomass substrate before being homogenized. The pressure and temperature were effects on the yield of protein concentration. The plot demonstrated that increasing both parameters improved protein concentration yield up to the centre value and then started to drop as both tended to increase above the centre limit. One of the reasons for this, was because the substrate has been treated under heat to raise the temperature, passing it through the HPH over number of cycles, say 3, would have entirely broken down the cell wall of the yeast substrate.

Categorical factors of ratios in this study, was to determine the highest yield of protein at any ratios. This has no implied order which means the settings of a categorical factor were discrete and had no intrinsic order [230]. Protein concentration yield is highest at the categorical factor of 30:70 ratios when compared to the other ratios of 10:90 and 20:80. Invariably, it therefore means that as the ratio increases, the yield in protein concentration also increases at the same rate as the pressure rises. However, in this case here, only the number of cycles has taken the incremental rate in the protein concentration yield. This can be seen in Figure 4-26 (c). Both pressure and temperature effects had an opposite effect to the number of cycles in terms of protein yield of as indicated in Figures 4-26 (a, b, and c).

Perturbation, 30-50 deg C

(a)

Perturbation, 30-50 deg C

(b)

Perturbation, 30-50 deg C

(c)

Figure 4 - 26: Perturbation plots (a), (b), and (c) showing the effects of process parameters on protein concentration yield with ratios as the categorical factor on the response

149

Figure 4 - 27: Contours plots (a), (b), and (c) showing the effect of the number of cycles, temperature, and pressure on the response – protein concentration yield

Figure 4-27 shows the contour graphs for the effect of temperature, pressure and number of cycle on protein yield. This is presented in the categorical factors (D) as a, b, and c, representing 10:90, 20:80, and 30:70, respectively. This plot provide a 2-dimensional view where all points that have the same response are connected to produce contour lines of constant responses, and thus, illustrate the optimum level of each variable on protein concentration yield. From the values provided, the blue areas contained 0.016129 of protein yields while the red zone contains the highest software-estimated protein concentration yield. With the number of cycles and pressure considered as parameters, more protein yield tends to be produced from the ratio of 30:70. The yellow area in Figure 4-27 (c) yield of protein is more pronounced. This is shown with the value of the contour plots as 0.935 while that of ratios 10:90, and 20:80 are considered as, 0.702 and 0.852 respectively. As the same actual factors of temperature of (40°C) given for the 3 ratios, 10:90, 20:80, and 30:70, protein yield was estimated highest in the ratio of 30:70 dilution.
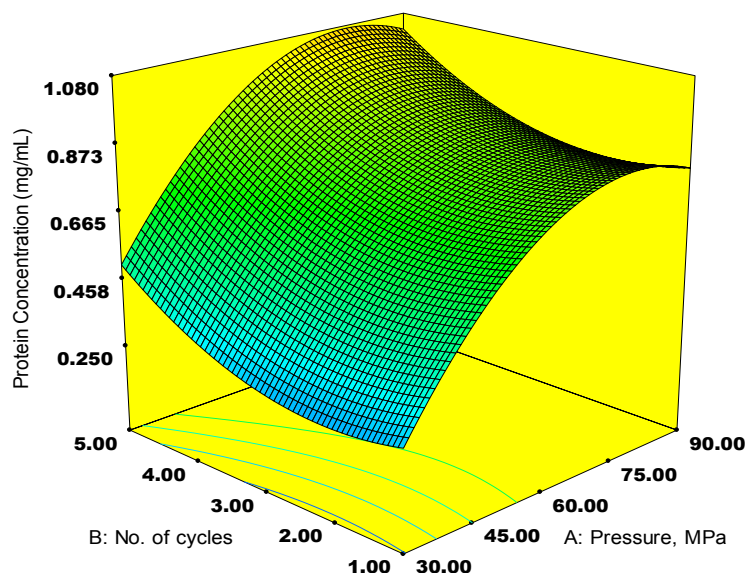
Figure 4 - 28: Response surface plot of protein concentration yield in (mg/mL) (with actual factors temperature considered at 40 °C and the ratio at 30:70)

151

Figure 4-28 is the response surface plot of protein concentration yield in (mg/mL) (with actual factors temperature at 40°C, and the ratio, at 30:70). This shows the effect of pressure and number of cycles on the yield. In the plot, the red zone shows areas of higher concentration of protein yield, while the blue zones are zone with the lowest concentration of protein yield. It is evident from the Figure 4-28 that as the pressure increases the protein yield also increases, while the relationship between the number of cycles and the operating pressure is opposite.

Table 4 - 18: ANOVA Table for Cost Reduced Quadratic Model for (30 - 50°C) Temperature Range

Source	Sum of Squares	DF	Mean Square	F Value	Prob > F	
Model	0.8268	8	0.1034	208.1489	< 0.0001	Significant
A-Pressure	0.0108	1	0.0108	21.8268	< 0.0001	
B-No. of cycles	0.5222	1	0.5222	1051.6139	< 0.0001	
C-Temperature	0.0315	1	0.0315	63.5168	< 0.0001	
AB	0.0091	1	0.0091	18.2771	0.0001	
AC	0.0048	1	0.0048	9.6672	0.0034	
BC	0.0091	1	0.0091	18.2771	0.0001	
B^2	0.2313	1	0.2313	465.8403	< 0.0001	
C^2	0.0039	1	0.0039	7.9306	0.0074	
Residual	0.0209	42	0.0005			
Lack of Fit	0.0209	30	0.0007			
Pure Error	0.0000	12	0.0000			
Cor Total	0.8477	50				
$R^2 = 0.9754$			Pred $R^2 = 0.9587$			
Adj $R^2 = 0.9707$			Adeq Precision = 41.65			

Validation of the Model:

Table 4-18 above, shows the ANOVA Table for cost reduced as a quadratic model, for Baker's yeast over the 30 – 50 °C temperature range. The point prediction technique and the appropriateness of a model is based on the fact that; Adj R^2 minus Pred. R^2 must be less than 0.2 and in this case, it was at 0.012. R^2 equalled 0.9754 which implied that 97.5% of the variability in the data has been explained by the model and F-Value model equalled 208.15 implying that the

model was significant. The "Prob > F" was the same as the P-value, and it implied that this must be greater than the F-value model, in the table and as it was < 0.0001, it therefore meant that there was 0.01% chance that the F-Value model occurred and was then considered significant (see Section 3.6.7 of Chapter 3 for reference) and have also been explained previously in this Chapter.
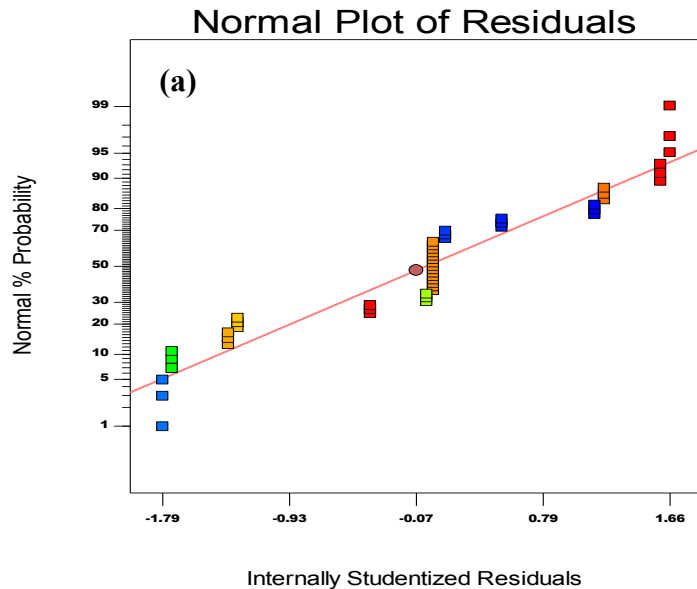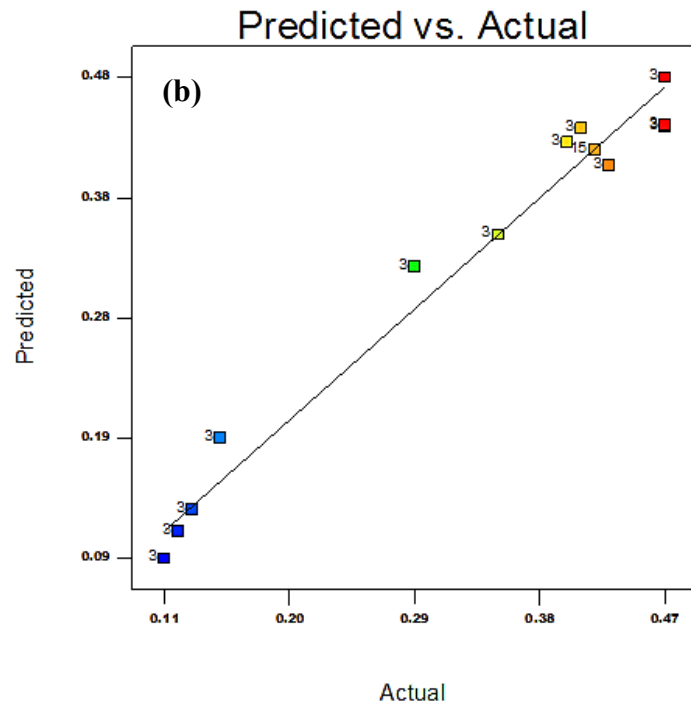
Figure 4 - 29: Scatter diagrams of normal plot of residuals (a) and cost (b) (30 - 50 °C) Temperature Range

Final Equation in Terms of Coded Factors:

$Cost = 0.4189 + 0.0213 * A + 0.1475 * B + 0.0363 * C - 0.0275 * A * B$

$- 0.0200 * A * C + 0.0275 * B * C - 0.1351 * B^2 - 0.0176 * C^2$

(4-11)

Final Equation in Terms of Actual Factors:

$Cost = - 0.6535 + 0.0048 * Pressure + 0.2489 * No. of cycles + 0.0176$

$*Temperature - 0.0005 *Pressure * No. of cycles - 0.0001 * Pressure *$

$Temperature + 0.0014 * No. of cycles * Temperature - 0.0338 * No. of$

$cycles^2 - 0.0002 * Temperature^2$

(4-12)

Effect of process parameters on the responses – Cost

The perturbation plot shown in Figure 4-30 illustrates the cost effectiveness, Euro/hour, resulting from the effect of the parameters on protein concentration yields. Pressure and temperature were shown to be very cost effective for the improvement of yield in protein concentration. On the other hand, the parameter "number of cycles", showed different trends in the attainment of this goal. This means that the biomass sample was treated under heat, to increase the temperature before homogenization. While cycle time seems to be effective in targeting improved protein yield at least to the 4th cycle, beyond this point it had a downward trend which invariably resulted in further protein yield. From the perturbation plot, it is evident that as the homogenizing pressure for rupturing the substrate increase temperature increased up to the 4th cycle. Beyond that point the protein yield continue to drop while the other variables increased. The reason for this trend was assumed to be due to substrate heating before homogenization based on the categorical factor of 10:90 ratio. This was the reverse for the 15 - 25 °C temperature range (Baker's yeast) where indeed cycle had a major role to play in the disruption process and which in effect showed to be more cost effective in the process.

Perturbation, 30-50 deg C
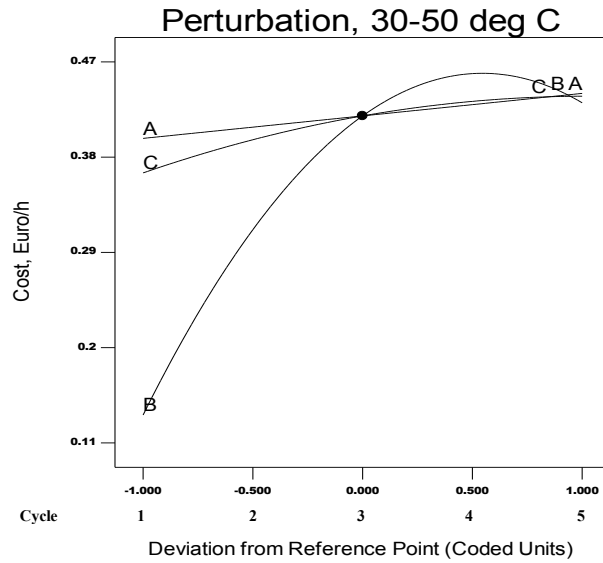
Figure 4 - 30: Perturbation plot showing the effect of process parameters on cost with ratios as the categorical factor in the response

There are no actual levels, of interaction between temperature and pressure in determining the cost effectiveness when considering these parameters for the 30 - 50 degree temperature range of homogenization. There tends to be a wider disparity between the parameters at a pressure of 30 MPa as compared to the 90 MPa pressure. For ratio 10:90, and as shown, it has been proven that there was no noticeable interaction within the considered parameters; this may be different for others levels of ratios.
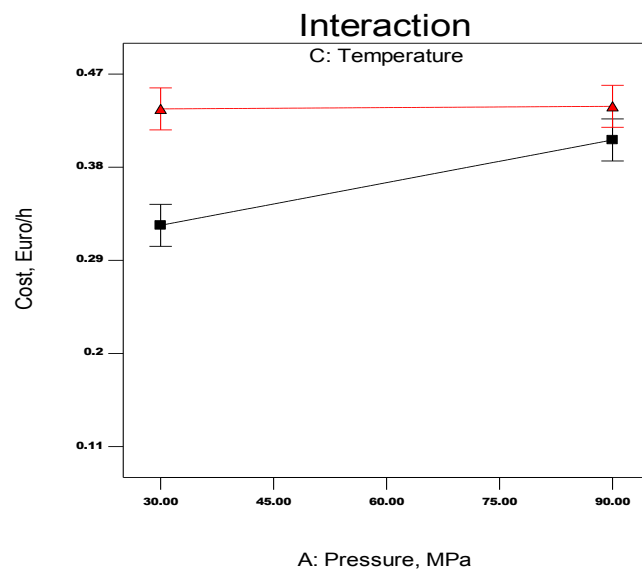
Interaction

Figure 4 - 31: Interaction plot showing the effect of Pressure (A) and number of cycles (B) on cost

155

Figure 4-32 shows the contour graph of the effect of temperature and the number of cycles on cost. The ratio resulting in this yield is the 30:70 which was also, considered as the categorical factors.
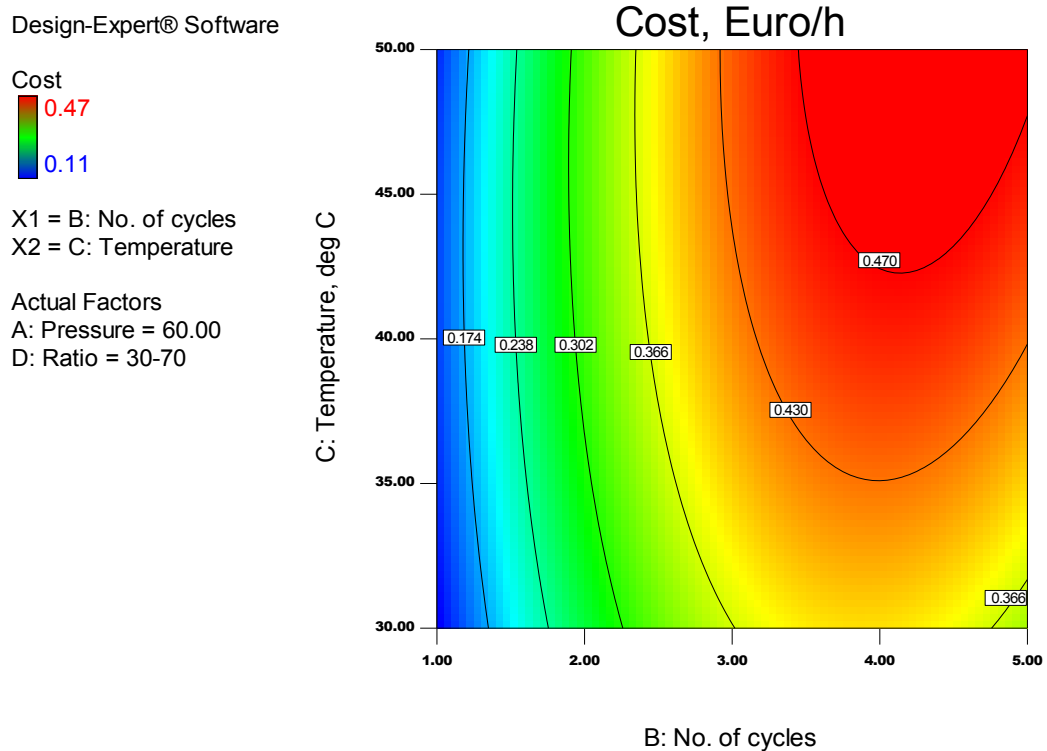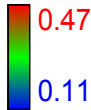
Figure 4 - 32: Contours plot showing the effect of number of cycles and temperature on the response – cost (this shows zone with highest software-estimated cost)

The response surface plot showing the effect of two parameters (temperature and number of cycles) over the response (cost in euro/hour) is shown in Figure 4-33. This graph is presented in 3-dimensions, with the actual factors; 60 MPa in pressure, and 20:80 as categorical ratios. The red zone highlights the zone with highest cost of €0.47/hour and the blue zone; the zone with least cost; €0.11/hour. These are shown in Figure 4-33. It was also evident that as the number of cycles increased, the cost in Euro/hour also increased. The temperature and the euro/hour cost were in reverse and therefore had an impact on the cost effectiveness of the protein concentration yield. From Figures 4-30 and 4-32, it was very clear that if all the process factors increased, the cost in Euro/hour decreased as well. This could be related to the following facts. Firstly, as the homogenizing pressure

increased the temperature of the soluble Baker's yeast increased resulting in more slurry soluble material which led to a higher protein yield, [169]. Secondly, the gap size reduced through increased pressure, due to the opening become constricted and during homogenization, the soluble material tended to flow through the small slit thereby **breaking** down more of the cell walls to release higher protein content within the substrate. These are the underlying factors to consider in the release of protein and are in agreement with [139, 165 227].
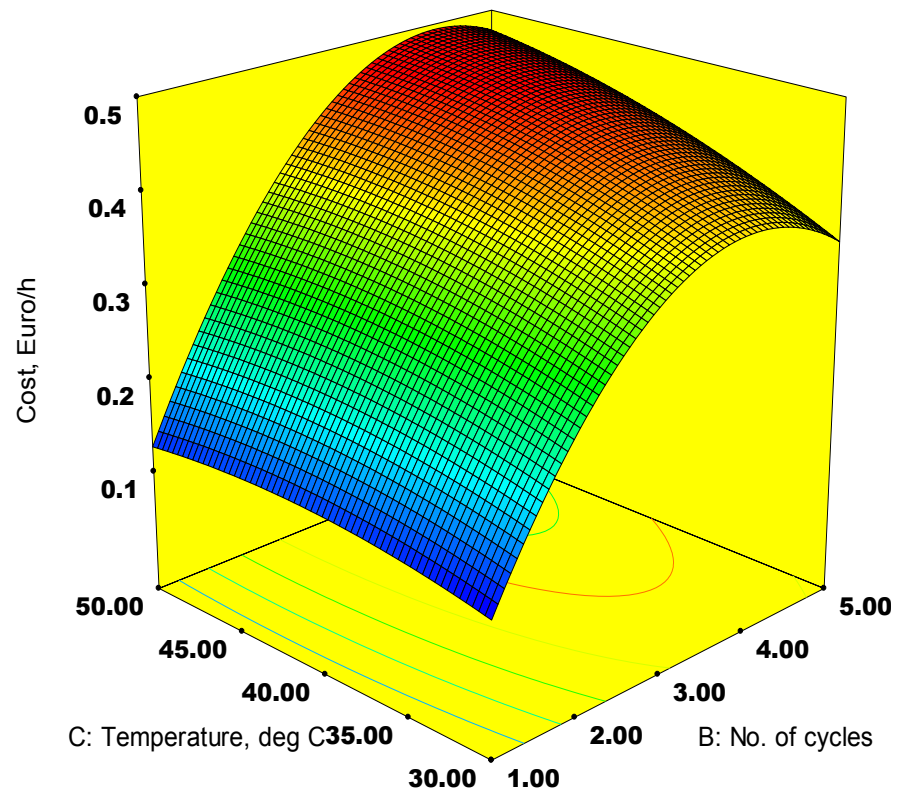
Figure 4 - 33: Response surface plot of cost in Euro/h (with actual factors pressure considered at 60 MPa and ratio at 20:80)

4.9 Microalgae homogenized at temperature 15 – 25 °C

The same process variables and experimental design levels used in the 15 – 25 °C temperature for Baker's yeast were also applied for homogenized Microalgae (*Chlorella vulgaris*) at the same temperature and other variables. *Chlorella vulgaris* species of the strain identification, CCAP 211/11B as classified by the institute in Scotland UK were applicable here (see Appendix A).

The process variables and experimental design level applied was the same that used before in the 15 - 25 °C temperature range of Baker's yeast (see Table 4-11). The design matrix with actual values and calculated/experimentally measured responses are shown in Table 4-19

Table 4 - 19: Design matrix with actual values and calculated/experimentally measured responses

Exp. No.	Run Order	Factor 1 A:Pressure	Factor 2 B:No. of cycles	Factor 3 C: Temp	Factor 4 D:Ratio	Response 1 Protein Conc.	Response 2 Cost
		MPa	-	(°C)	-	[mg/mL]	[Euro/h]
1	51	30	1	20	10:90	0.0914	0.1
2	25	90	1	20	10:90	0.2070	0.18
3	32	30	5	20	10:90	0.1559	0.39
4	3	90	5	20	10:90	0.2823	0.41
5	8	30	3	15	10:90	0.1532	0.28
6	7	90	3	15	10:90	0.2930	0.32
7	46	30	3	25	10:90	0.2823	0.31
8	30	90	3	25	10:90	0.2769	0.33
9	20	60	1	15	10:90	0.2150	0.12
10	9	60	5	15	10:90	0.2312	0.4
11	24	60	1	25	10:90	0.3602	0.14
12	40	60	5	25	10:90	0.3844	0.37
13	22	60	3	20	10:90	0.2688	0.34
14	13	60	3	20	10:90	0.2043	0.34
15	38	60	3	20	10:90	0.2258	0.34
16	42	60	3	20	10:90	0.2661	0.34
17	15	60	3	20	10:90	0.1909	0.34
18	4	30	1	20	20:80	0.1452	0.1
19	2	90	1	20	20:80	0.2194	0.18
20	43	30	5	20	20:80	0.2177	0.39

21	5	90	5	20	20:80	0.2930	0.41
22	50	30	3	15	20:80	0.2769	0.28
23	6	90	3	15	20:80	0.3172	0.32
24	29	30	3	25	20:80	0.3817	0.31
25	31	90	3	25	20:80	0.3306	0.33
26	18	60	1	15	20:80	0.2634	0.12
27	11	60	5	15	20:80	0.2312	0.4
28	47	60	1	25	20:80	0.3710	0.14
29	16	60	5	25	20:80	0.4113	0.37
30	17	60	3	20	20:80	0.2688	0.34
31	26	60	3	20	20:80	0.2903	0.34
32	12	60	3	20	20:80	0.2769	0.34
33	49	60	3	20	20:80	0.3038	0.34
34	37	60	3	20	20:80	0.2984	0.34
35	10	30	1	20	30:70	0.1694	0.1
36	33	90	1	20	30:70	0.2742	0.18
37	28	30	5	20	30:70	0.2581	0.39
38	27	90	5	20	30:70	0.4220	0.41
39	45	30	3	15	30:70	0.2823	0.28
40	48	90	3	15	30:70	0.3629	0.32
41	36	30	3	25	30:70	0.3011	0.31
42	41	90	3	25	30:70	0.4462	0.33
43	21	60	1	15	30:70	0.3091	0.12
44	39	60	5	15	30:70	0.2688	0.4
45	44	60	1	25	30:70	0.3790	0.14
46	23	60	5	25	30:70	0.4624	0.37
47	1	60	3	20	30:70	0.3091	0.34
48	19	60	3	20	30:70	0.3118	0.34
49	34	60	3	20	30:70	0.3172	0.34
50	35	60	3	20	30:70	0.3199	0.34
51	14	60	3	20	30:70	0.3065	0.34

Table 4 - 20: ANOVA for Protein Concentration reduced quadratic model (15-25°C)

Source	Sum of Squares	DF	Mean Square	F Value	Prob > F	
Model	0.2520	11	0.0229	18.7647	< 0.0001	Significant
A-Pressure	0.0425	1	0.0425	34.7949	< 0.0001	
B-No. of cycles	0.0157	1	0.0157	12.8673	0.0009	
C-Temperature	0.0583	1	0.0583	47.7505	< 0.0001	
D-Ratio	0.0590	2	0.0295	24.1627	< 0.0001	
AD	0.0082	2	0.0041	3.3643	0.0449	
BC	0.0035	1	0.0035	2.8493	0.0994	
A^2	0.0131	1	0.0131	10.7653	0.0022	
B^2	0.0037	1	0.0037	2.9998	0.0912	
C^2	0.0513	1	0.0513	41.9980	< 0.0001	
Residual	0.0476	39	0.0012			
Lack of Fit	0.0416	27	0.0015	3.0870	0.0220	Not Significant
Pure Error	0.0060	12	0.0005			
Cor Total	0.2996	50				
$R^2 = 0.8411$			Pred $R^2 = 0.7008$			
Adj $R^2 = 0.7963$			Adeq Precision = 20.503			

Validation of the Model:

The Figures 4-34 (a) and (b) showed linearity and therefore were normally distributed. From the ANOVA Table 4-20, the point prediction technique and an appropriate model indicated that, Adj R^2 minus Pred. R^2 was 0.096 that is < 0.2. The same trends as in previous sections for the normality of plots and validation of data were also applicable here. This was necessary to determine good model discrimination based on the analysis of the ANOVA Table [215-217, 225-227]. As R^2 equalled 0.8411 it implied that 84.1% of the variability in the data has been explained by the model. The F-Value model equalled 18.76, implying that the model was significant since it only led to 0.01% chance that the F-Value model occurred as a result of noise.

Based on the final equation in terms of coded factors and those in terms of the actual factors for ratios, 10:90, 20:80, and 30:70 (Equations 4-13 – 4-16), protein concentration yield can be worked out using the associated equation for any of the ratios.
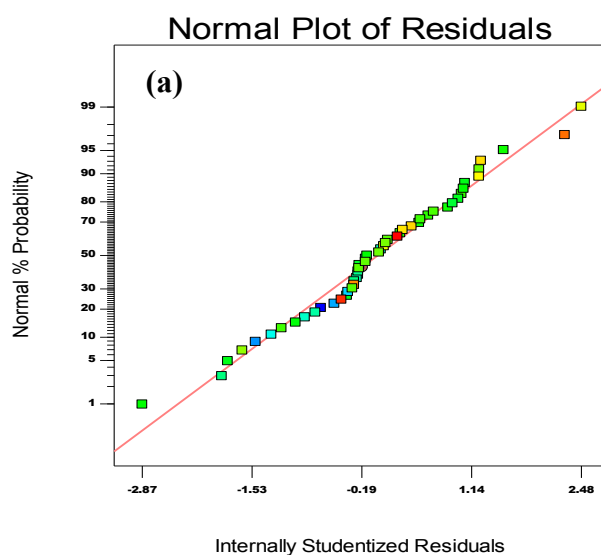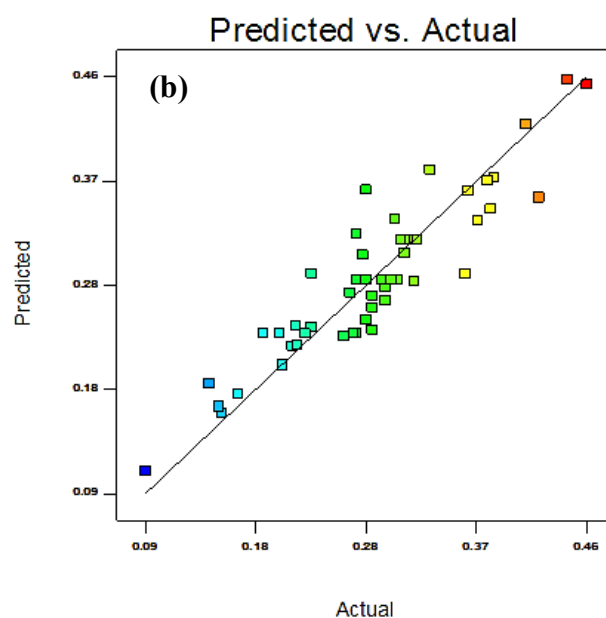
Figure 4 - 34: Scatter diagrams of normal plot of residuals (a) and of protein concentration yields (b)

Final Equation in Terms of Coded Factors:

Protein Concentration = 0.2772 + 0.0421 * A + 0.0256 * B + 0.0493 * C – 0.0435 *D[1]+ 0.0040 * D[2] + 0.0050 * AD[1] – 0.0247* AD[2]+ 0.0170* BC – 0.0323 * A^2 – 0.0170 * B^2 + 0.0637 * C^2   (4-13)

Final Equation in Terms of Actual Factors:

Ratio 10:90;

*Protein Concentration = 0.8583 + 0.0059 * Pressure + 0.0043 * No. of cycles –*

> *0.0972* Temperature + 0.0017 * No. of cycles*Temperature +*

> *0.0000*Pressure^2 – 0.0043* No. of cycle^2 + 0.0025*

> *Temperature*   (4-14)

Ratio 20:80;

*Protein Concentration = 0.9652 + 0.0049 * Pressure + 0.0043 * No. of cycles –*

> *0.0972* Temperature + 0.0017 * No. of cycles*Temperature +*

> *0.0000*Pressure^2 – 0.0043* No. of cycle^2 + 0.0025*

> *Temperature*   (4-15)

Ratio 30:70;

*Protein Concentration = 0.9117 + 0.0064 * Pressure + 0.0043 * No. of cycles –*

> *0.0972* Temperature + 0.0017 * No. of cycles*Temperature +*

> *0.0000*Pressure^2 – 0.0043* No. of cycle^2 + 0.0025*

> *Temperature*   (4-16)

4.9.1 Development of mathematical models for Microalgae (*Chlorella vulgaris*)

The same software was used to analyse the measured response. The test for significance of the regression models, tests for significance on each model coefficient, and lack of fit test were carried out. The step-wise regression method; which eliminates the insignificant model terms automatically, was applied. Two ANOVA Tables for the reduced quadratics models have been obtained (see Table 4-20 and 4-21). These Tables summarised the analysis of each response and showed the significant model terms, and others, such as; Adequacy measure R^2, Adjusted R^2 and Predicted R^2. From the Tables, the adequacy models are close to

1. The developed quadratic mathematical models, in terms of coded factors and actual values, are represented in Equations 4-13 to 4-16 for protein concentration yield (mg/mL) and 4-17 to 4-18 for cost in (Euro/hour). Wherein, these equations, (Equations 4-13 and 4-17) represent the coded form.

Effect of process parameters on the responses - Protein Concentration

The perturbation plot for the protein concentration yield from the 15 - 25 °C temperature range for Microalgae (*Chlorella vulgaris*) is illustrated in Figure 4-35 as (a), (b), and (c). These aided in comparing the effect of all the factors at a particular point in the design space. Perturbation plots under this Section showed great difference as compared to that of the previous two; that of 15 - 25 °C and that of 30 – 50 °C temperature ranges for Baker's yeast. Temperature was shown to be effective in protein concentration yield in the three plots. The reason for this change has been attributed to the temperature effect of the biomass substrate before homogenization. The substrate state would have changed completely and the internal contents affected, due to heat effect before the treatment under HPH. The substrate temperature was raised to within the room temperature before the homogenization was conducted, (15, 20, and 25°C) that is, before the substrate was passed through the high-pressure homogenizer. This process, affected the change in behaviour of the substrate. Other parameters and their effects were also of importance up till the midpoint, and then subsequently resulted in the behaviour pattern by the shifting downward of the parameters A, and B, i.e. Pressure and Number of cycles. Temperature influenced the higher yield of protein in 4-35 (a, b, and c), considered highest in the ratio of 30:70 perturbation plots, the cell walls would have been broken down completely to release the protein contents internally [163, 169].

As the highest protein concentration yield has resulted from the homogenization process, as seen in the plot (c), that was; at the ratio 30:70 with the yield of 0.3 mg/mL of protein concentration, and when compared to the previous two; 15 - 25 °C and 30 - 50 °C temperature ranges of Baker's yeast, the results were 0.65 and 0.7 mg/mL respectively (see Figures 4-17 (c) and 4-26 (c)). This meant that as the

ratio increased, the yield in protein concentration also increased at the same rate as pressure rose.

From the analysis, ratio played a very important role in the conversion of input into responses (protein concentration yields and cost). A higher dilution ratio resulted in higher protein concentration yield.
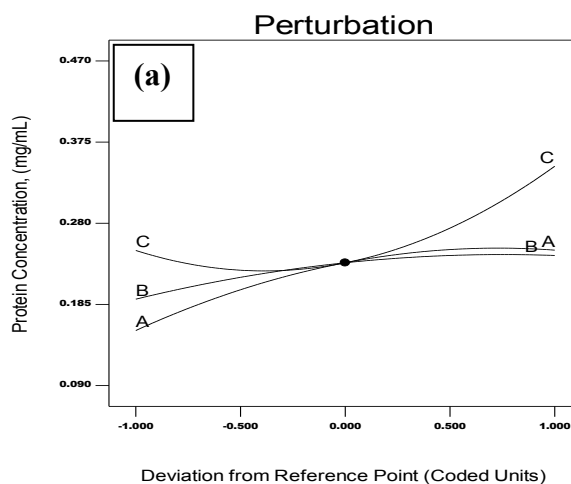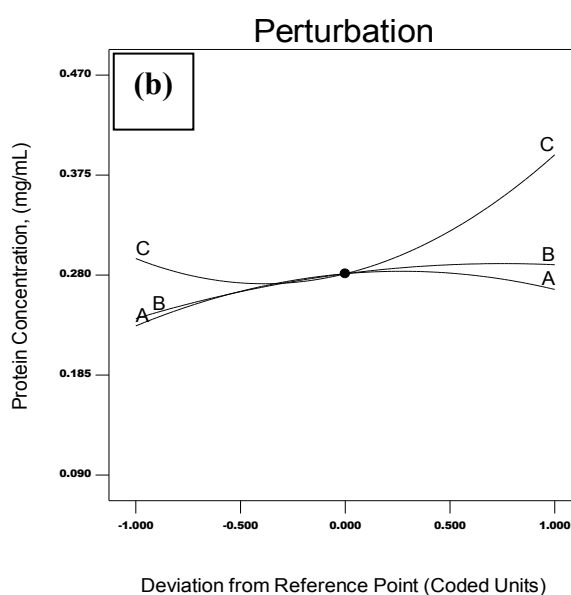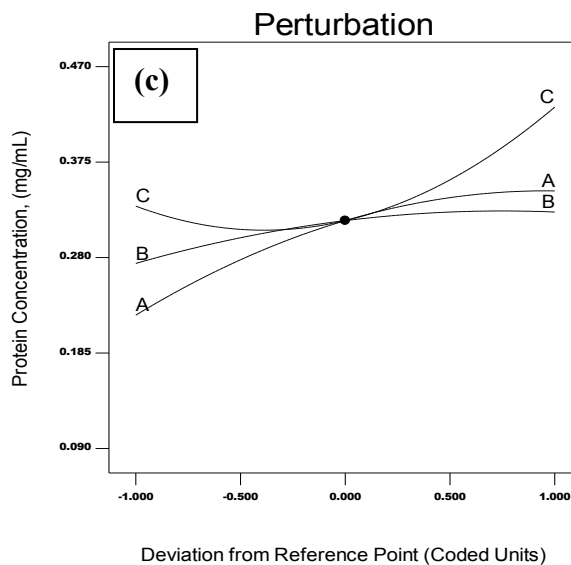
Figure 4 - 35: Perturbation plots (a), (b), and (c) showing the effect of process parameters on protein concentration yield with ratio as the categorical factor on the response

165

The interaction plots showing the three categorical factors of ratio in Figure 4-36 indicate some level of interaction within the ratios. At the pressure of 30 MPa, there was an interaction between 20:80 and 30:70 and at pressure 90 MPa; also there was interaction between 10:90 and 20:80. To maximize protein concentration yield, it therefore required some level of interaction within the categorical factors. Hence the two levels of interaction of pressure, (A), and ratio, (D) are considered as the most significant model terms associated with protein concentration yield. Though actual factors of "number of cycles" and "temperature" are considered at 3 °C and 20 °C respectively in the interaction plot, but have not being of consideration in the protein concentration yield.
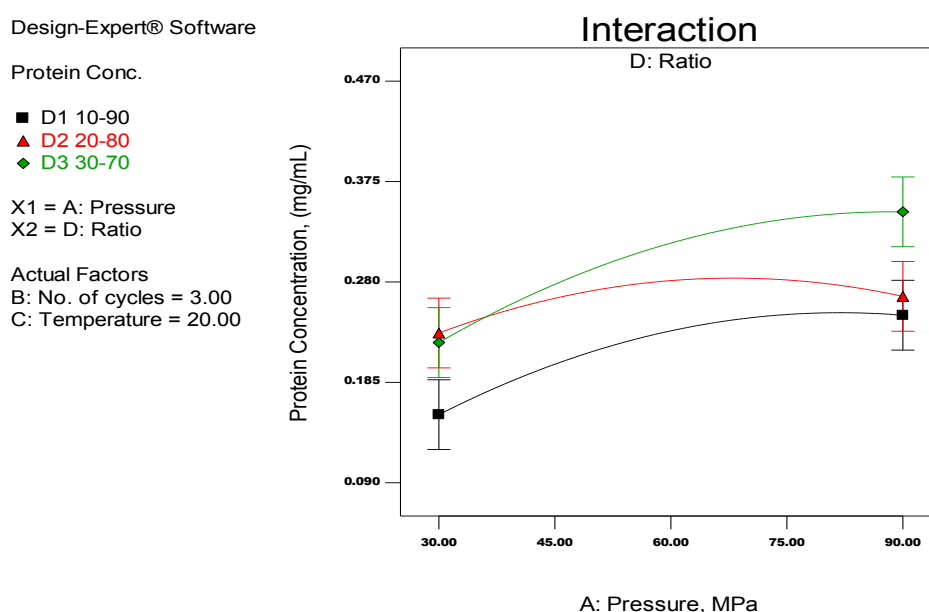
Figure 4 - 36: Interaction plot showing the effect of Pressure (A) and Ratio (D) on protein concentration yield

In another development, Figure 4-37 showed the interaction plot of the effect of "temperature" and "number of cycles" on protein concentration. From the plot, there seems to be no interaction at the considered level of categorical factor (D) of 10:90. The yield of protein concentration as shown in the plot seems to be close at "cycle 1" but with wider disparity at cycle 5. This was as a result of the temperature effect which had resulted over time during homogenization. At the start of cycle 1 heat generated as a result of Microalgae homogenization would be

infinitesimal, but as the cycle increased, the homogenized substrate tends to generate more heat that would create the opening at cycle 5 (see Figure 4-37).
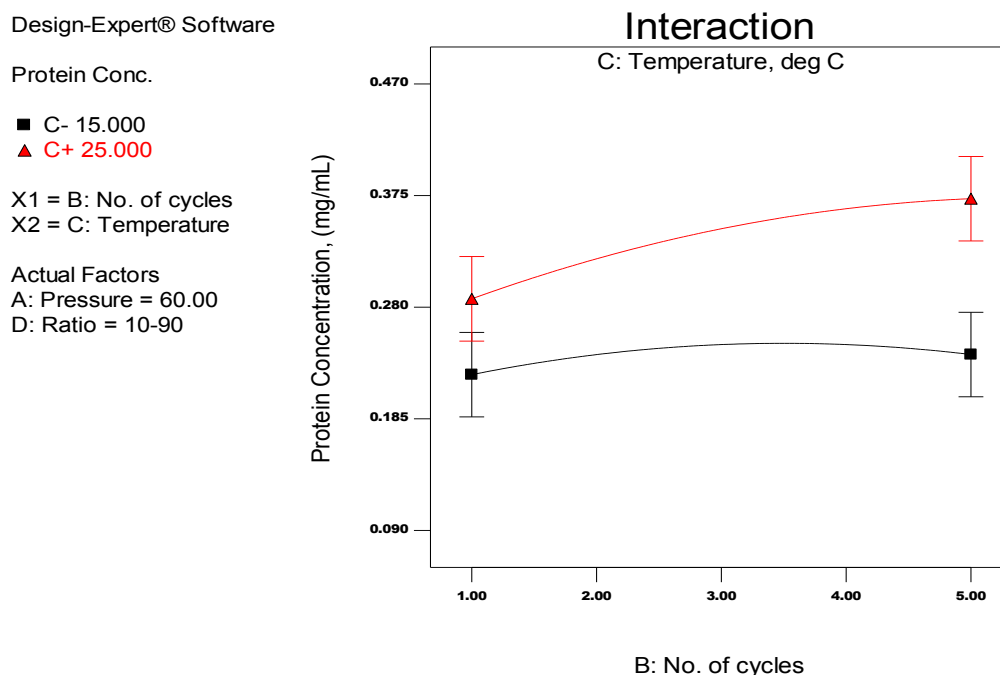
Figure 4 - 37: Interaction plot showing the effect of Temperature (C) and Number of cycle (C) on protein concentration yield with categorical factor considered at 10:90

Figure 4-38 reveals the result of the contour plots showing the effect of number of cycles and temperature on the response (protein concentration yield). As analysed from the previous section with Figure 4-27, heat generated from homogenized substrate in HPH becomes noticeable, for example from the third cycle, and by the fifth cycle, this would have completely heated up to cause total disruption of the substrate. Hence at 5 cycles, and 25°C, heat would have submerged at the top right hand corner when homogenized at a pressure of 60 MPa resulting in the protein concentration yield of 0.462371 as shown in the plot with the (Red zone showing the heat affected zone of higher concentration yield of protein). Whereas at the bottom left hand corner, below 15°C, the zone was considered green and is seen as lower concentrations yield of protein. For Microalgae, the temperature effect has aided the higher yield of protein concentration over number of cycles during homogenization. Parameters of cycles and temperature considered in the ratio of 30-70 homogenization of substrate played an important role in the yield of protein

concentration. Illustrated in the plots are the red colour zone and this as estimated by the software, was the zone with the highest protein concentration yield.
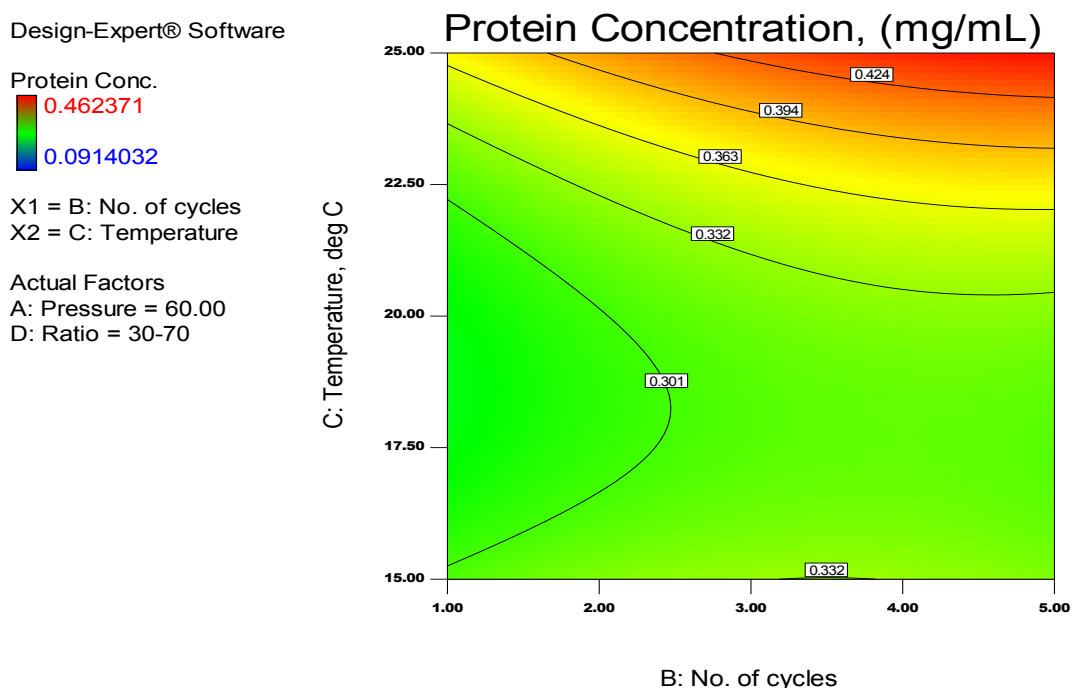
Figure 4 - 38: Contours plots showing effect of the number of cycles and temperature on the response – protein concentration yield (this shows zone with highest software-estimated protein concentration yield)

Figure 4-39 shows the response surface plot of the effect of the effect of the "number of cycle" and "temperature" on the response, protein concentration. The model was displayed in 3D with actual factors of pressure considered at 60 MPa and the "ratio" at 30:70 over the "number of cycles" between 1 and 5 and "temperature" between 15 °C and 25 °C. The protein concentration was given between maximum and minimum yields of 0.46 mg/mL and 0.09 mg/mL respectively. The combined effects of the parameters as applicable to this study, tended to yield the optimum result of responses. Protein generated from the biomasses considered have shown to give the highest yield at high temperature and number of cycles due to their prominent role played in the Microalgae biomass disruption process. It was therefore evident that as number of cycles increased protein concentration increased also. It invariably implied that temperature and protein concentration yield was in reverse and as a result had impact on protein concentration yield.

Design-Expert® Software

Protein Conc.

0.462371

0.0914032

X1 = B: No. of cycles
X2 = C: Temperature

Actual Factors
A: Pressure = 60.00
D: Ratio = 30-70
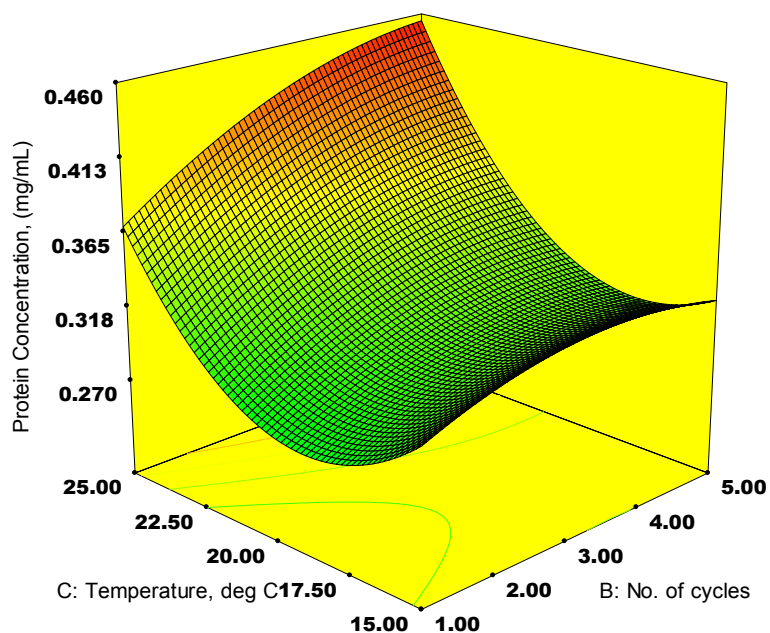
Figure 4 - 39: Response surface plot of protein concentration (with actual factors of pressure considered at 60 MPa and ratio at 30:70)

Table 4 - 21: ANOVA table for cost reduced quadratic model – Microalgae (15 – 25 °C) range

Source	Sum of Squares	DF	Mean Square	F Value	Prob > F	
Model	0.4699	9	0.0522	1359.0996	< 0.0001	Significant
A-Pressure	0.0096	1	0.0096	249.9048	< 0.0001	
B-No. of cycles	0.3978	1	0.3978	10356.4048	< 0.0001	
C-Temperature	0.0003	1	0.0003	8.7857	0.0050	
AB	0.0027	1	0.0027	70.2857	< 0.0001	
AC	0.0003	1	0.0003	7.8095	0.0079	
BC	0.0019	1	0.0019	48.8095	< 0.0001	
A^2	0.0010	1	0.0010	25.1754	< 0.0001	
B^2	0.0474	1	0.0474	1233.5965	< 0.0001	
C^2	0.0057	1	0.0057	148.4837	< 0.0001	
Residual	0.0016	41	0.0000			
Lack of Fit	0.0016	29	0.0001			
Pure Error	0.0000	12	0.0000			
Cor Total	0.4715	50				
R^2 = 0.9967			Pred R^2 = 0.9941			
Adj R^2 = 0.9959			Adeq Precision = 108.40			

Validation for the Model:

Table 4-21 above, shows the ANOVA Table for cost reduced as a quadratic model, for Microalgae over a 15 – 25 °C temperature range. The point prediction technique and the appropriateness of the model is based on the fact that; Adj R^2 minus Pred. R^2 was 0.002.

R^2 equalled 0.9967 and F-Value model equalled 1359.1, the "Prob > F" was same as the P-value, therefore the model was considered significant.
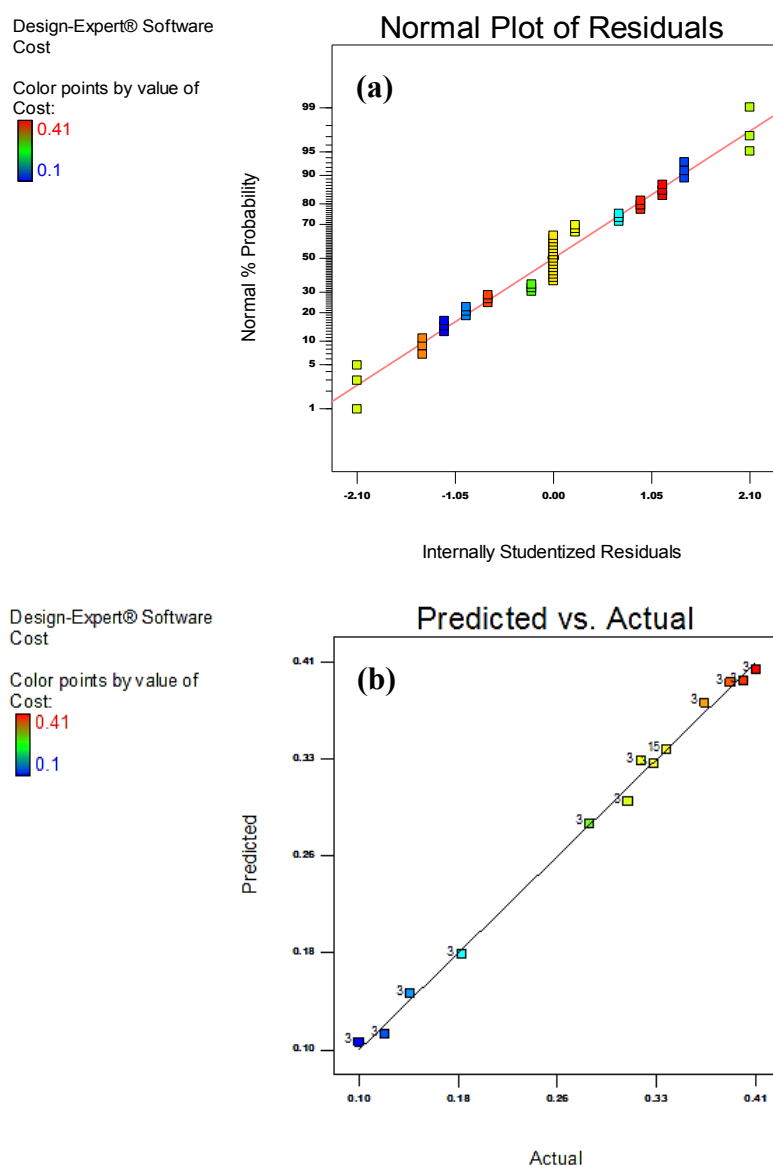
Figure 4 - 40: Scatter diagrams of normal plot of the residuals (a) and the cost (b) (15 - 25 °C) Temperature Range for Microalgae

Final Equation in Terms of Coded Factors:

$$Cost = 0.34 + 0.02 * A + 0.12875 * B + 0.00375 * C - 0.015 * A * B - 0.005 * A * C - 0.0125 * B * C - 0.00875 * A^2 - 0.06125 * B^2 - 0.02125 * C^2 \tag{4-17}$$

Final Equation in Terms of Actual Factors:

$$Cost = -0.58094 + 0.00325 * Pressure + 0.19625 * No. \ of \ cycles + 0.0405 * Temperature - 0.00025 * Pressure * No. \ of \ cycles - 3.3E\text{-}05 * Pressure * Temperature - 0.00125 * No. \ of \ cycles * Temperature - 9.7E\text{-}06 * Pressure^2 - 0.01531 * No. \ of \ cycles^2 - 0.00085 * Temperature^2 \tag{4-18}$$

The contour graph is one of the plots that can be developed by *Design Expert*. In the same way as the contour improves the yield of protein concentration, it also creates a higher yield for protein concentration through maximization of the yield at a cost that is effective. Temperature has been proven to be very cost effective in the 15 - 25 °C temperature range for Microalgae *(Chlorella vulgaris),* as compared to the other two scenarios for Baker's yeast above. This has been substantiated by Harrison *et al.* [164] and Diels *et al.* [169]. Harrison *et al.* [164] have reported a 1.6 fold increase of the protein release of *Alcaligenes eutrophus* when the process temperature increased from 12 °C to 26 °C and the research conducted by Diels *et al.* [169], it resulted in a gradual increase in the inactivation of *E.coli, Y. Enterocolitica* and *S.aureus* when the process temperature was increased. Also, in the work carried out by Thiebaud *et al.* [171], both high homogenization pressures and higher inlet temperature for the substrate subsequently increased the microbial inactivation. These were increased from 200 MPa and 4 °C to 300 MPa and 14 °C or 24 °C to an improved yield of the sample. In the other work carried out by Yap *et al.* [196], they analysed the energy load for HPH of a given Microalgae and therefore concluded that this must be minimized by operation at higher pressure for fewer passes for an appreciable yield of protein concentration. These therefore

support the current research being presented and invariably proven that the chosen parameters of pressure, temperature, number of cycle and indeed ratio as a categorical factor did all have an effect on the protein concentration yield and the associated energy cost.
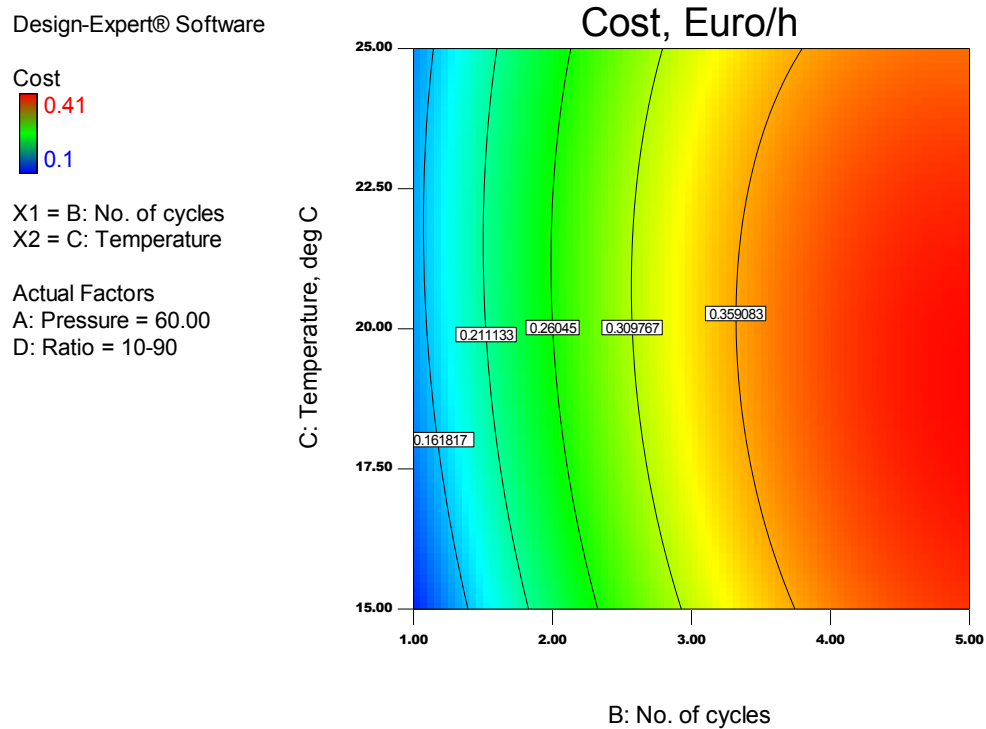
Figure 4 - 41: Contours plots showing the effect of number of cycles and temperature on the response – cost (this shows zone with highest software-estimated cost)

The perturbation plot (Figure 4-42) shows the operating parameters; pressure, temperature, and number of cycles affect the response (cost) up to the midpoint until the temperature starts drop. The pressure and the number of cycles continue the trend, with number of cycles showing steadier results. This has taken place based on the categorical factor of 10:90; and the scenarios may be different when other categorical factors are considered (see Figure 4-42). The three parameters did have an effect on the energy cost (in Euro/hour) of the usage of the HPH to homogenize the substrate of Microalgae *(Chlorella vulgaris)*. The number of cycles had an effect up to the 5th cycle and afterwards had a negative effect on the cost, as the yield was reversed. Pressure and temperature also had an effect on the cost, with pressure having a larger effect than temperature despite (temperature yielding a good result up to the midpoint of 20 °C).

Cost
● Cost

Actual Factors
A: Pressure = 60.00
B: No. of cycles = 3.00
C: Temperature = 20.00
D: Ratio = 10-90

Warning!
Factors Not in Model.
D
Categoric Factors
D
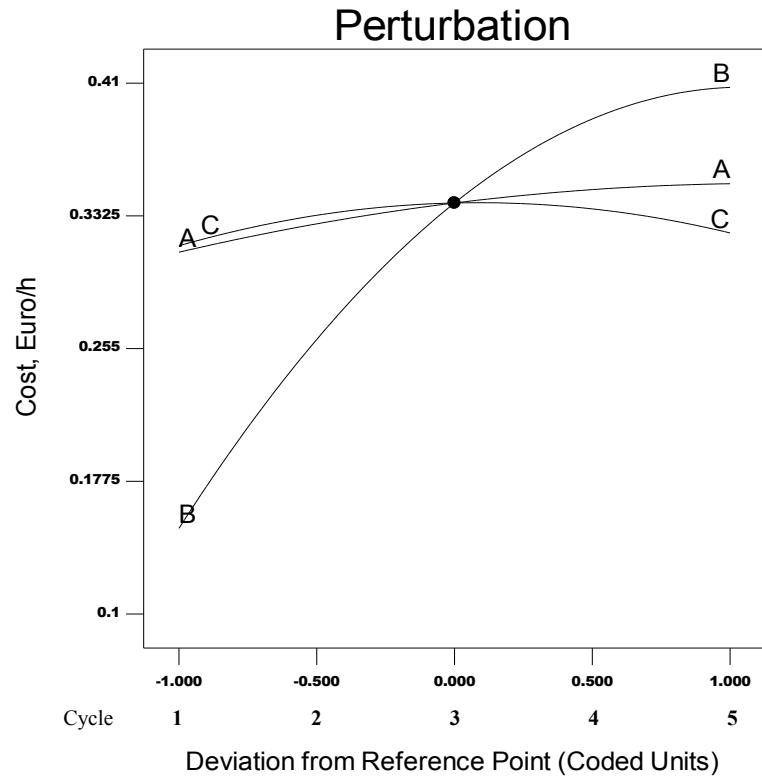
Figure 4 - 42: The perturbation plot showing the effect of process parameters on cost with ratio as categorical factor

The response surface plot (RS), as in Figure 4-43, shows the effect of pressure and the number of cycles on the cost of energy in the homogenization of Microalgae to yield protein concentration. Based on the substrate *(Chlorella vulgaris)*, the actual factors are considered to be 20 °C and the categorical ratio 10:90. The combined effect of pressure and the number of cycle yielded optimum results for cost as effectiveness towards higher yield in protein concentration. The RS plot showed maximum of €0.41/hour and minimum of €0.1/hour in terms cost of energy towards protein concentration production. The scenarios presented are different from that previously discussed under the substrate; Baker's yeast when homogenized at 15 – 25 °C and 30 – 50 °C.
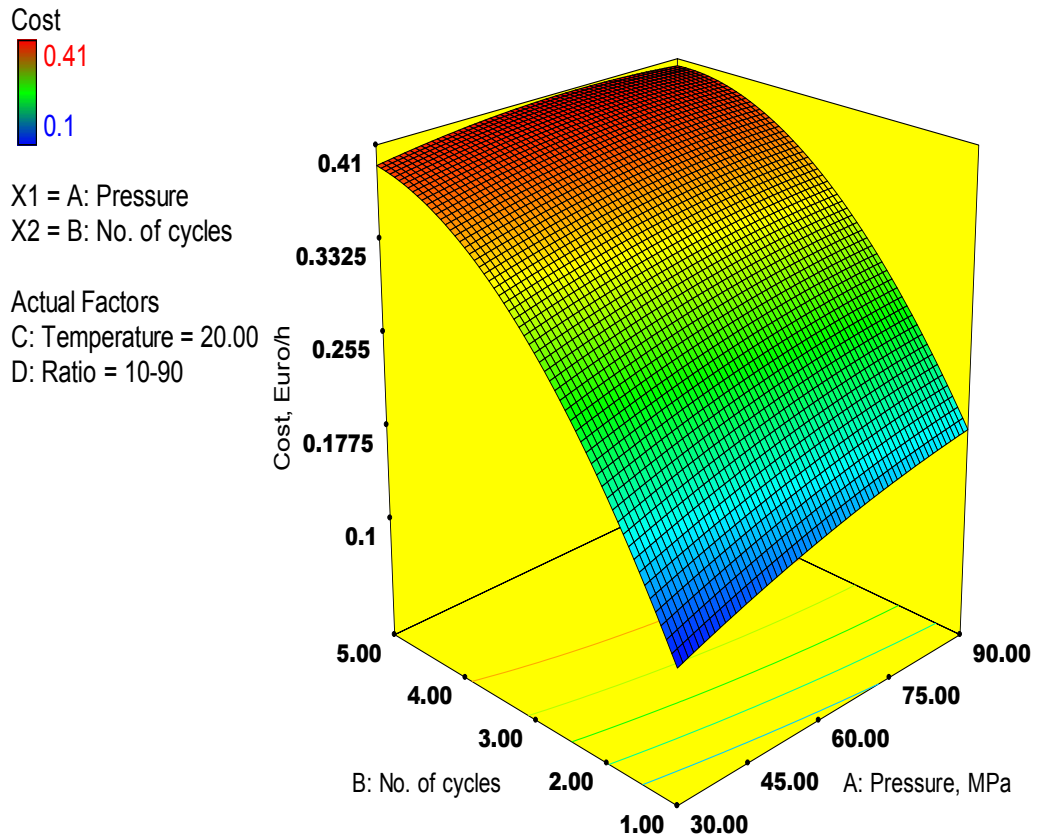
Figure 4 - 43: The Response surface plot of cost in Euro/h (with actual factors temperature considered at 20 °C and the categorical factor ratio at 10:90)

4.10 Optimization of homogenization process and parameters

It was necessary to optimize the homogenizing process for the substrates for optimal yield of protein concentration and cost effectiveness of energy. The research through *Design Expert software* application centres on obtaining results with maximum yield at minimum expense. The desirability function is one of the most widely used methods in industry for the optimization of multiple response processes. This was based on the quality of a product or process which has multiple characteristics, and such a process is unacceptable if outside some of the desired limits. The method therefore found operating conditions that would provide the most desirable value for the response.

In this section, optimization will be considered in two ways; numerical and graphical and in each of the cases; the 15 - 25 °C temperature range, 30 - 50 °C temperature range both for Baker's yeast homogenization and the 15 - 25 °C temperature range for Microalgae homogenization, the optimization conditions will be applied just as has been discussed in the previous chapters.

4.10.1 Baker's yeast (Homogenized at temperature range 15 - 25°C)

4.10.1.1 Numerical Optimization (Over the 15 – 25 °C Temperature Range)

Four criteria have been implemented in the numerical optimization of this substrate. The criteria were based on quality and cost where quality was referred to as higher yield of protein concentration, and cost, as the most effective energy cost in attaining the highest yield of protein concentration. Two criteria were considered for quality (restricted and not restricted) while cost was also based on two criteria (restricted and not restricted). The target was to minimise cost and maximize protein concentration yield. The condition has been set out with one as restricted (with constraints), and the other, without restriction.

Table 4-22 comparison of the quality (Protein concentration yield) in both restricted and not restricted scenarios. The target was to maximize protein concentration yield. For every factor and response, each goal was given a level of importance rated between 1 and 5, where 1 was considered as the lowest rating and 5 as the highest rating. As shown in Table 4-22, Protein concentration yield was the target, therefore it was rated 5 and every other condition must be fulfilled to achieve this goal by maximizing pressure, number of cycles, temperature, and minimizing ratio at the minimum cost to achieve optimal protein concentration yield, through numerical optimization.

Table 4 - 22: Quality (Restricted and Not Restricted) for Protein Concentration Yield

Factor or Response	Restricted		Not restricted	
	Goal	Importance	Goal	Importance
Pressure	Maximize	3	In range	3
No. of cycles	Maximize	3	In range	3
Temperature	Maximize	3	In range	3
Ratio	In range	3	In range	3
Protein Conc.	Maximize	5	Maximize	5
Cost	In range	3	In range	3

Table 4-23 shows the optimal solution as obtained by *Design Expert* showing the desirability to be 0.93 with the cost of €0.43, and the dilution ratio of baker yeast to solution C as 30:70. The temperature, number of cycles and pressure are given as 25 °C, 5 and 90 MPa. This was considered and analysed based on 2 categorical factors of ratios, between 20:80, and 30:70. The selection by the Design Expert was based on the cost effective of optimum quality of protein concentration yield. Hence the first 10 yields were considered. Based on the 'Not Restricted' quality of protein concentration yield depicted in Table 4-22, it can be deduced in Table 4-24 that all parameters were in the range except protein concentration which needed to be maximized. This showed that there was no restriction attached; meaning that there were no constraints and again, desirability was given by the *Design Expert* at 0.92 when the first 10 generated results by *Design Expert* were considered. The first 10 results are considered so as to determine and find the optimal conditions for the quality in terms of protein yield. Based on the analysis of Table 4-22, the desirability selected by the software were considered the best and optimal solutions for the highest yield of protein considering other factors of applied parameters (see Tables 4-23 and 4-24). It was therefore evident from the results analysed in both tables (Tables 4-23 and 4-24), that yield of protein concentration tended to be higher with no restriction based on the desirability selections. This was 11.7% in favour of the 'Not Restricted' with a 2.4% saving in energy cost for homogenizing in the release of protein concentration.

Table 4 - 23: The Optimal Solution as Obtained by *Design Expert* for Quality – Restricted (Constrained)

Number	Pressure	No. of cycles	Temp.	Ratio	Protein Conc.	Cost	Desirability	
1	90.00	5.00	25.00	30-70	1.44	0.43	0.93	Selected
2	90.00	5.00	24.00	30-70	1.49	0.43	0.93	
3	90.00	5.00	23.00	30-70	1.58	0.43	0.91	
4	89.40	5.00	22.00	30-70	1.60	0.43	0.88	
5	75.00	5.00	25.00	30-70	1.12	0.45	0.80	
6	90.00	4.00	25.00	30-70	1.18	0.45	0.79	
7	90.00	5.00	24.00	20-80	0.94	0.43	0.78	
8	90.00	5.00	25.00	20-80	0.88	0.43	0.78	
9	90.00	5.00	23.00	20-80	1.01	0.43	0.77	
10	86.00	5.00	23.00	20-80	0.92	0.44	0.75	

Table 4 - 24: The Optimal Solution as Obtained by *Design Expert* for Quality – (Not Restricted)

Number	Pressure	No. of cycles	Temp	Ratio	Protein Conc.	Cost	Desirability	
1	90.00	5.00	20.00	30-70	1.63	0.42	0.92	Selected
2	90.00	5.00	19.00	30-70	1.62	0.41	0.92	
3	89.98	5.00	22.00	30-70	1.58	0.43	0.89	
4	87.41	5.00	20.00	30-70	1.57	0.42	0.89	
5	90.00	5.00	16.00	30-70	1.53	0.38	0.87	
6	90.00	5.00	24.00	30-70	1.51	0.43	0.86	
7	90.00	5.00	19.00	30-70	1.51	0.43	0.85	
8	90.00	1.00	20.00	30-70	1.40	0.17	0.79	
9	90.00	1.00	20.00	30-70	1.40	0.18	0.79	
10	90.00	1.00	21.00	30-70	1.40	0.17	0.79	

Table 4 - 25: Cost for Protein Concentration Yield

Factor or Response	Restricted		Not restricted	
	Goal	**Importance**	**Goal**	**Importance**
Pressure	Maximize	3	In range	3
No. of cycles	Maximize	3	In range	3
Temperature	Maximize	3	In range	3
Ratio	In range	3	In range	3
Protein Conc.	In range	5	Maximize	2
Cost	Minimise	3	In range	5

Considering the analysis based on cost, some restrictions in form of constraints were put in place as obtained from the *Design Expert*. This was to minimise cost for optimal yield of protein concentration. When this is compared to the not restricted condition, it yielded lower protein concentration, based on the desirability selected. As €0.10 yielded 0.13 mg/mL of protein in terms of cost (see Table 4-27), it was also seen that €0.28 yielded 1.12 mg/mL of protein concentration in in terms of cost for the restricted (see Table 4-26). This invariably illustrated, that cost effectiveness could be achieved on a larger scale. In comparison, this resulted in 64.3% yield when constrained and was therefore favoured as opposed to the 'Not Restricted'.

In essence, 'Energy cost' for operating the high-pressure homogenizer to breakdown the cell wall within the substrate has resulted at a minimal cost of €0.28/hour yielding 1.12 mg/mL of protein concentration. In terms of protein yield, this has favourable the 'Restricted' at 88.4% when compared to the value of protein concentration yield at Table 4-27, wherein the yield of 0.13 mg/mL of protein concentration resulted from the energy cost of homogenizing the substrate at €0.10/hour.

**Table 4 - 26: Optimal Solution as Obtained by Design Expert for Cost –
Restricted (Constrained)**

Number	Pressure	No. of cycles	Temp	Ratio	Protein Conc.	Cost	Desirability	
1	90.00	2.00	25.00	30-70	1.12	0.28	0.57	Selected
2	90.00	2.00	25.00	10-90	0.26	0.28	0.57	
3	90.00	2.00	25.00	20-80	0.55	0.28	0.57	
4	90.00	2.00	25.00	30-70	1.14	0.24	0.56	
5	84.00	2.00	25.00	30-70	1.01	0.26	0.56	
6	84.00	2.00	25.00	20-80	0.50	0.25	0.55	
7	85.00	2.00	25.00	10-90	0.24	0.25	0.55	
8	77.00	2.00	25.00	20-80	0.42	0.27	0.54	
9	89.00	5.00	25.00	30-70	1.42	0.43	0.47	
10	90.00	5.00	23.00	30-70	1.56	0.43	0.46	

**Table 4 - 27: Optimal Solution as Obtained by Design Expert for Cost – (Not
Restricted)**

Number	Pressure	No. of cycles	Temp	Ratio	Protein Conc.	Cost	Desirability	
1	39.00	1.00	25.00	20-80	0.13	0.10	1.00	Selected
2	44.00	1.00	19.00	20-80	0.34	0.10	1.00	
3	39.00	1.00	16.00	30-70	0.17	0.06	1.00	
4	39.00	1.00	16.00	10-90	0.03	0.06	1.00	
5	46.00	1.00	18.00	20-80	0.31	0.09	1.00	
6	30.00	1.00	20.00	20-80	0.20	0.08	1.00	
7	59.00	1.00	15.00	10-90	0.12	0.10	1.00	
8	54.00	1.00	16.00	30-70	0.54	0.10	1.00	
9	60.00	1.00	15.00	20-80	0.30	0.10	1.00	
10	30.00	1.00	20.00	10-90	0.14	0.08	1.00	

4.10.1.2 Graphical Optimization (over the 15 – 25 °C Temperature Range)

For the graphical optimization, the optimal range of each response has to be
considered by bringing it from the numerical optimization results in order to have
them present graphically. The graphical optimization therefore allows visual
selection of the optimal process conditions according to certain criteria that have
been considered in the numerical optimization process. Graphical optimization

results in plots, called an overlay plot and the green /shaded areas on the overlay plots are the region which are considered to have met the proposed criteria.

Graphical Optimization Based on Pressure and Number of Cycle for the 15 – 25 °C Temperature range of Baker's Yeast Homogenization

The result from the overlay plot shows a protein yield of 0.23 mg/mL and cost effectiveness required in its homogenization between €0.24 and €0.43. The protein concentration yield was considered to be homogenized with 2 or 3 number of cycles which corresponded to the costs at €0.24 and €0.43. At the categorical factor of 10:90 ratios, the green shaded area shows the region of higher protein yield along with the associated costs (see Figure 4-44). As in the case of graphical optimization where multiple responses are considered, the software defines regions where requirements simultaneously meet the proposed criteria. Superimposing or overlaying critical response contours on a contour plot. As the visual search for the best compromise becomes possible, graphical optimization then displays the area of feasible response values in the factor space [231].

Figures 4-45 and 4-46 show the overlay plots of graphical optimization based on pressure and number of cycle for the 15 – 25 °C temperature ranges of Baker's yeast homogenization. This reflected the categorical factors of ratios, 20:80 and 30:70. The higher protein yields are depicted by the green region within the plots. The protein concentration yield was similar to that obtained in the 10:90 ratios, achieved at 2 or 3 cycles. This was produced at pressures over 50 and with wider disparity of pressure during the homogenization. In regards to the 30:70 ratios, it was achieved even at lower pressure at over 40 MPa, and with the widest disparity of pressure, compared with the other two categorical factors of ratios (10:90, and 20:80). The results were achieved at 2 and 3 Number of cycles at a cost of €0.24 and €0.43 respectively. From the three scenarios (Figures 4-44 to 4-46), it was evident that the number of cycles and pressure had most of the influence, and the other factors remain the same for the three scenarios.
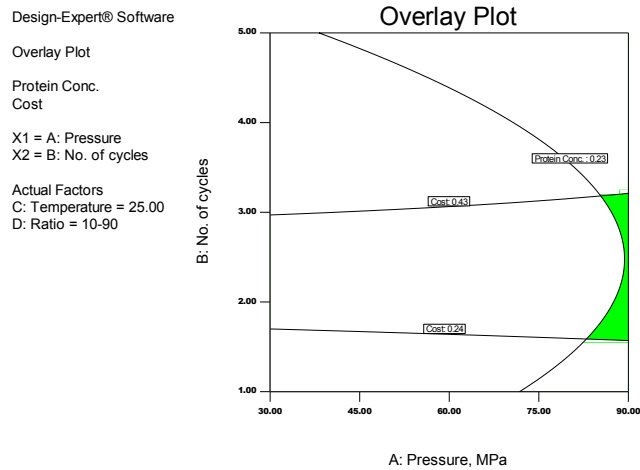
Figure 4 - 44: Overlay plot showing the optimal region of higher protein yield with associated cost for 10:90 ratios - (Quality)
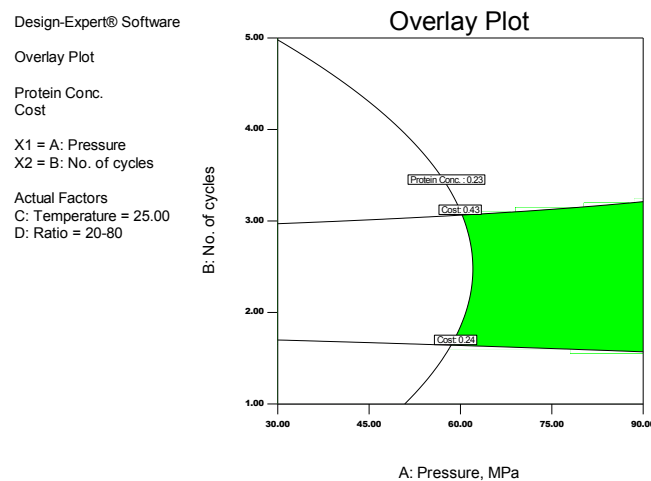
Figure 4 - 45: The optimal region of higher protein yield with associated cost for 20:80 ratios - (Quality)
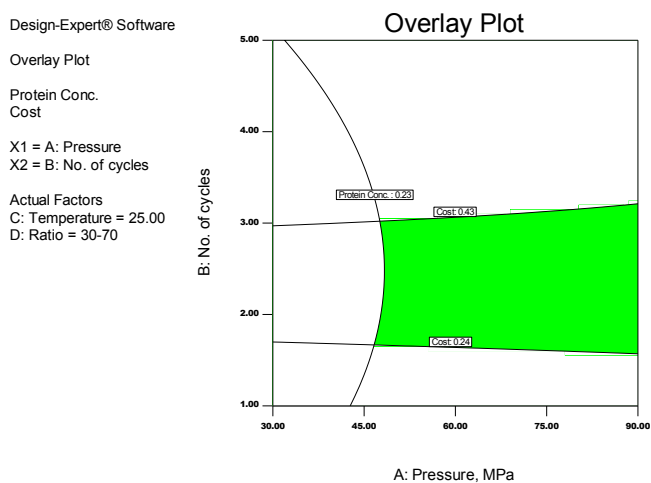
Figure 4 - 46: The optimal region of higher protein yield with associated cost for 30:70 ratios - (Quality)

Graphical Optimization Based on Pressure and Temperature for the 15 – 25 °C Temperature range of Baker's Yeast Homogenization – (Cost)

In Figures 4-47 to 4-49, the categorical factors of ratios 10:90, 20:80, and 30:70 were applied to determine the protein concentration yield and their associated cost in achieving the target. Homogenizing pressure and temperature effects were seen to influence the protein concentration yields, and the cost for achieving this goal of maximizing protein yield and minimizing cost.

In Figure 4-47, this produced a protein concentration of 0.12 mg/mL at minimal cost of €0.10 when homogenized at 60 MPa pressure, and temperature between 18 °C and 22 °C. Other actual factors were considered at 1 cycle and at categorical factors of 10:90 ratios. While at pressures between 40 and 60 MPa, a wider temperature range 17 °C to 23 °C resulted in a protein concentration yield of 0.12 mg/mL and a cost of €0.05, which was at a lower value of the temperature at 17 °C or at €0.10, yielding 0.34 mg/mL when homogenized at 20 °C and a pressure of 60 MPa in Figure 4-48.

Whereas in Figure 4-49, the pressure ranges of 40 MPa to 50 MPa yielded protein concentrations of 0.34, and 0.12 mg/mL at different temperature ranges from 18 °C to 22 °C at cost range of €0.10 to €0.34. Other actual factors, like number of cycles, and categorical factor of ratios, were considered at 1 and 30:70 respectively. It was therefore evident that the categorical factor of 30:70 ratios (Figure 4-49) tended to be most favourable. Protein concentration yield and energy cost showed to be economically feasible when compared to other two figures (Figures 4-47 and 4-48).
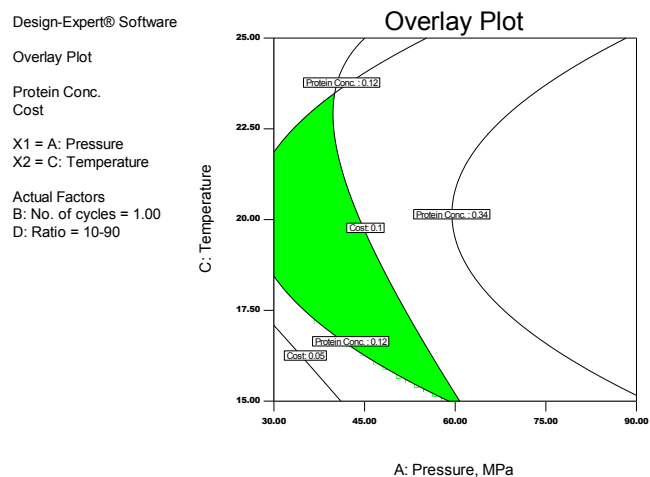
Figure 4 - 47: The optimal region of higher protein yield with associated Cost for 10:90 ratios
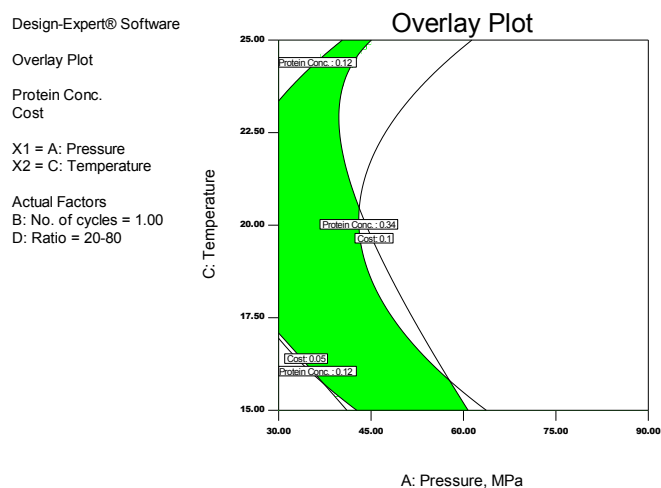
Figure 4 - 48: The optimal region of higher protein yield with associated Cost for 20:80 ratios
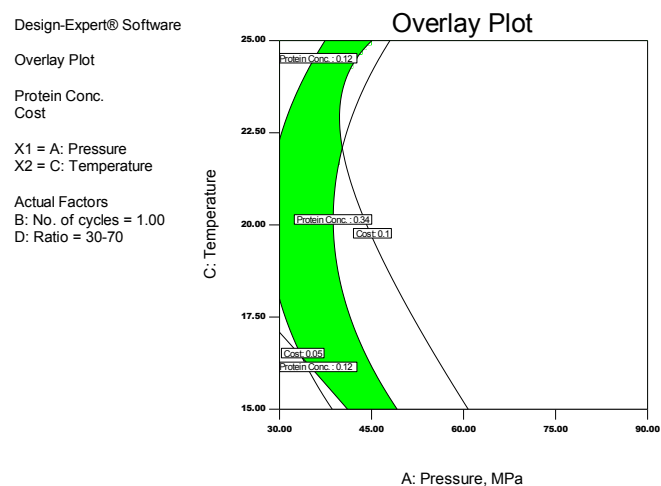
Figure 4 - 49: The optimal region of higher protein yield with associated Cost for 30:70 ratios

4.10.2 Baker's yeast (Homogenized at temperature range 30 - 50°C)

4.10.2.1 Numerical Optimization (Over the 30 – 50 °C Temperature Range)

Table 4 - 28: Quality for Protein Concentration yield - Restricted

Name	Goal	Lower Limit	Upper Limit	Lower Weight	Upper Weight	Importance
Pressure	maximize	30.00	90.00	1.00	1.00	3.00
No. of cycles	maximize	1.00	5.00	1.00	1.00	3.00
Temperature	maximize	30.00	50.00	1.00	1.00	3.00
Ratio	is in range	10:90	30:70	1.00	1.00	3.00
Protein Conc.	maximize	0.02	1.34	1.00	1.00	5.00
Cost	is in range	0.11	0.47	1.00	1.00	3.00

From Table 4-28 above, the numerical optimization for quality in the yield of protein concentration was analysed for homogenizing Baker's yeast over a temperature range of 30 – 50 °C. Quality was used here to describe the economic effectiveness of protein concentration in terms of higher yield. The emphasis was to maximize protein concentration yield at minimal cost.

Table 4 - 29: The Optimal solution for 3 combinations of categorical factor levels – Quality (Restricted)

No.	Pressure	No. of cycles	Temp	Ratio	Protein Conc.	Cost	Desirability	
1	90.00	5.00	47.00	30:70	0.93	0.45	0.85	Selected
2	86.00	5.00	47.20	30:70	0.95	0.45	0.84	
3	90.00	5.00	46.60	20:80	0.86	0.45	0.82	
4	90.00	5.00	45.50	20:80	0.88	0.45	0.81	
5	90.00	5.00	45.90	10:90	0.73	0.44	0.76	
6	81.00	5.00	45.10	10:90	0.79	0.45	0.75	
7	75.00	5.00	45.40	10:90	0.78	0.45	0.73	
8	90.00	4.00	45.80	30:70	0.77	0.47	0.71	
9	85.00	4.00	46.90	30:70	0.77	0.47	0.70	
10	87.00	4.00	42.20	30:70	0.87	0.47	0.70	

Table 4-29 shows the optimal desired solution. A desirability of 0.85 was achieved, when homogenized at 90 MPa, over 5 cycles, at 47 °C temperature and a categorical factor of 30:70 ratio yielding 0.93 mg/mL at a cost of €0.45.

Whereas in the real sense of it, the second on the list at Table 4-29 showed a better result in terms of the protein concentration yield when homogenized at even lower pressure of 86 MPa and a slightly higher temperature of 47.2 °C resulted in 0.95 mg/mL of protein concentration. This was an increment of 2.2% of the yield when compared to the desired one rated by the *Design Expert* as 85. One reason to consider here, for the desirability selection would probably be as a result of the lower operating temperature that was applicable.

Table 4 - 30: Quality for Protein Concentration yield – Not Restricted (Over the 30 – 50 °C Temperature Range)

Name	Goal	Lower Limit	Upper Limit	Lower Weight	Upper Weight	Importance
Pressure	is in range	30.00	90.00	1	1.00	3.00
No. of cycles	is in range	1.00	5.00	1	1.00	3.00
Temperature	is in range	30.00	50.00	1	1.00	3.00
Ratio	is in range	10:90	30:70	1	1.00	3.00
Protein Conc.	maximize	0.02	1.34	1	1.00	5.00
Cost	is in range	0.11	0.47	1	1.00	3.00

Table 4-30 shows the quality for protein concentration yield for no restrictions attached. A desirability of 0.80 was achieved at a 30:70 ratio as the categorical factor's choice yielding 1.07 mg/mL of protein concentration and at a cost of €0.43, through the homogenization at 77 MPa, 5 cycles and at a temperature of 40.8 °C. Based on the criteria above, the 'Not Restricted' scenario was favourable compared to the 'Restricted'. It resulted in higher protein concentration yield, and at a lower energy cost in the desirability selections (see Tables 4-29 and 4-31). From the scenario above, the 'Not Restricted' has been favoured as against the 'Restricted' resulting in 13.1% increment in protein concentration yield and a 4.7% of energy saving in terms of the cost. (see the desirability selections of Tables 4-29 and 4-31 of both 'Restricted' and 'Not Restricted' to compare results).

Table 4 - 31: The Optimal solution for 3 Combinations of Categorical Factor Level – Quality (Not Restricted)

No.	Pressure	No. of cycles	Temp.	Ratio	Protein Conc.	Cost	Desirability	
1	77.00	5.00	40.80	30:70	1.07	0.43	0.80	Selected
2	80.00	5.00	40.90	30:70	1.07	0.43	0.80	
3	77.00	5.00	42.00	30:70	1.07	0.44	0.80	
4	77.00	5.00	41.00	20:80	0.99	0.43	0.74	
5	76.00	5.00	42.00	20:80	0.99	0.44	0.73	
6	77.00	1.00	41.00	30:70	0.85	0.16	0.63	
7	77.00	5.00	41.00	10:90	0.84	0.43	0.62	
8	81.00	5.00	41.00	10:90	0.84	0.43	0.62	
9	82.00	5.00	38.00	10:90	0.82	0.42	0.60	
10	77.00	1.00	41.00	20:80	0.77	0.16	0.57	

4.10.2.2 Graphical Optimization (Over the 30 – 50 °C Temperature Range)

The green shaded areas in the overlay Quality plots, Figures 4-50 to 4-53, are the regions that met the best criteria. These depicted the categorical factors of 10:90, 20:80, and 30:70 ratios as seen in Figures 4-50 to 4-52 respectively while Figure 4-53 was another form of the Figure 4-52, over 30 to 50 °C temperature range.

Figure 4-50 tended to produce a higher yield protein of 0.72 mg/mL, however at higher pressure and temperature, homogenized in 5 cycles, realistically it would not be cost effective. The same trend was applicable to the categorical factors of 20:80 ratios; resulting in higher energy cost for the process (see Figure 4-51). At the 30:70 categorical factor ratio, a protein concentration yield of 0.95 mg/mL was achieved when homogenized at 5 cycles at an energy cost of €0.47 (Figure 4-52). Also Figure 4-53 produced an optimal result at a reduced temperature of 40.81 °C which was in contrast with the temperature applied in Figure 4-52 (46.96 °C). At 2 and 4 cycles a 0.76 mg/mL yield of protein concentration was achieved for €0.16 and €0.44 when homogenized at pressures of 58 and 9 MPa respectively. Figures 4-52 and 4-53 compared favourably when others (Figures 4-50 and 4-51) were considered.
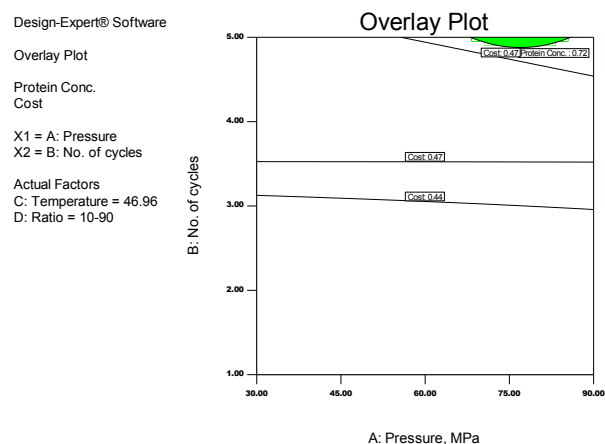
Figure 4 - 50: The optimal region of higher protein yield with associated Quality for 10:90 ratios (Number of cycles vs. Pressure plot)
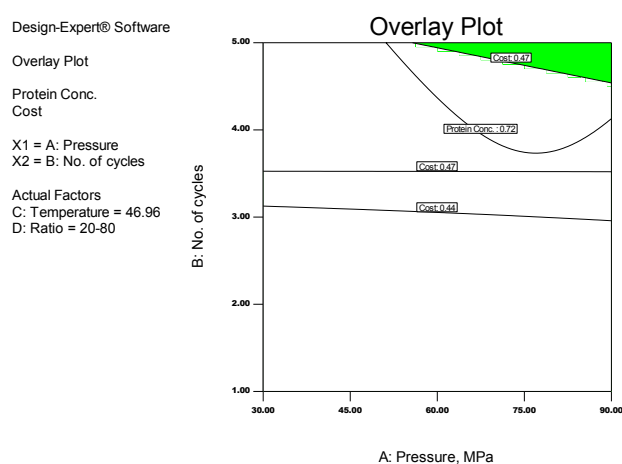
Figure 4 - 51: The optimal region of higher protein yield with associated Quality for 20:80 ratios (Number of cycles vs. Pressure plot)
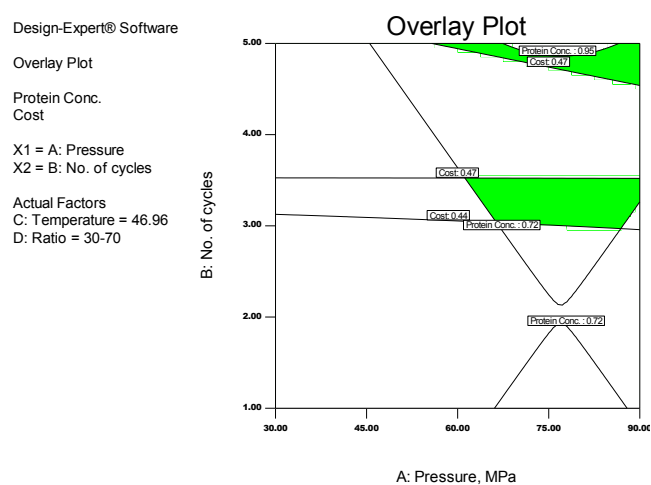
Figure 4 - 52: The optimal region of higher protein yield with associated Quality for 30:70 ratios (Number of cycles vs. Pressure plot)
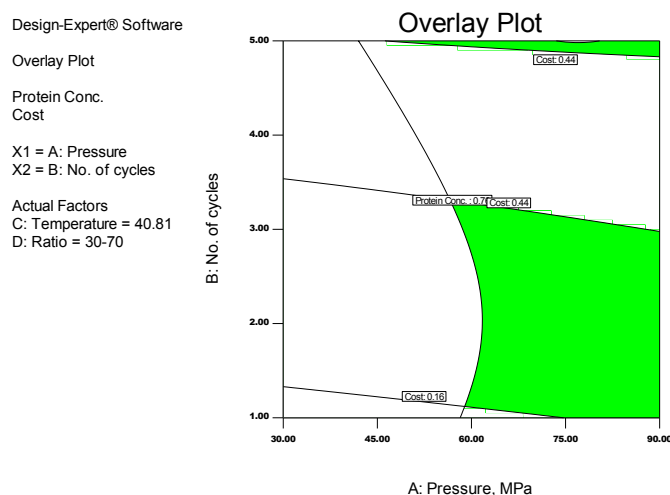
Figure 4 - 53: The optimal region of higher protein yield with associated Quality for 30:70 ratios (at a temperature of 40.81°C)

Graphical Optimal Solution for Cost with Restriction (Over the 30 − 50 °C Temperature Range)

The costs overlay plots for optimal solutions with restrictions, for the categorical factors ratios of; 10:90, 20:80, and 30:70 overlay plots are shown in Figures 4-54 to 4-56. The overlay plots showed pressure plotted against number of cycles with the actual factors of ratios and temperature. This varied in the determinant of an optimal yield of protein and their associated cost. For the 10:90 ratios, €0.27 resulted in the yield of 0.32 mg/mL when homogenized at 2 cycles, 90 MPa and at 36.65 °C while the same yield of protein concentration could also be achieved at 4 cycles, 90 MPa at a cost €0.41. The same was applicable to both the 20:80 and 30:70 categorical ratios at the same cost as well as another at the 30:70 categorical ratios resulting in 0.98 mg/mL of protein when homogenized at 5 cycles.
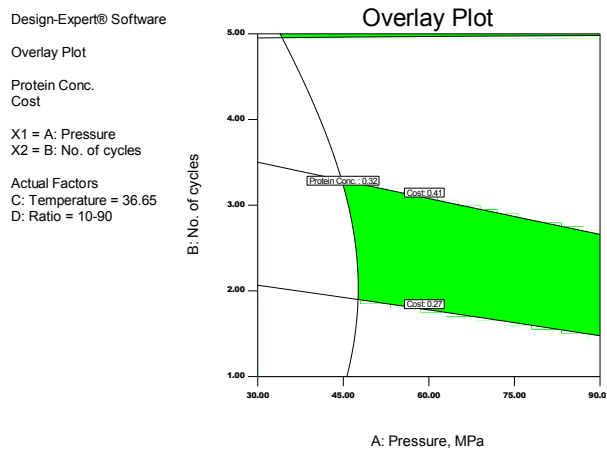
Figure 4 - 54: The optimal region of higher protein yield with associated Cost for 10:90 ratios (Number of cycle vs. Pressure plot)
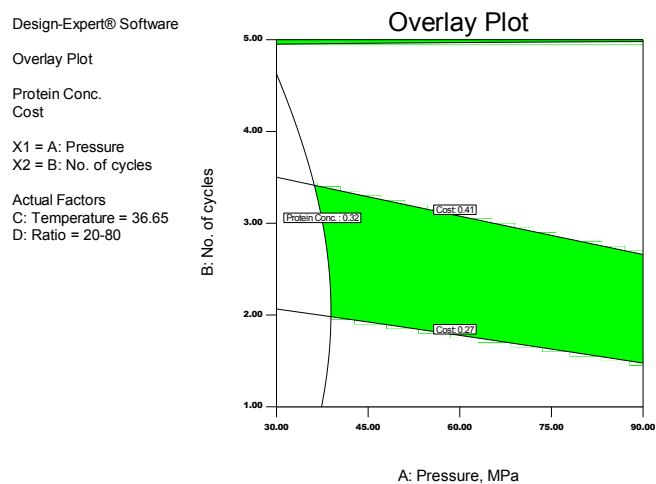
Figure 4 - 55: The optimal region of higher protein yield with associated Cost for 20:80 ratios (Number of cycle vs. Pressure plot)
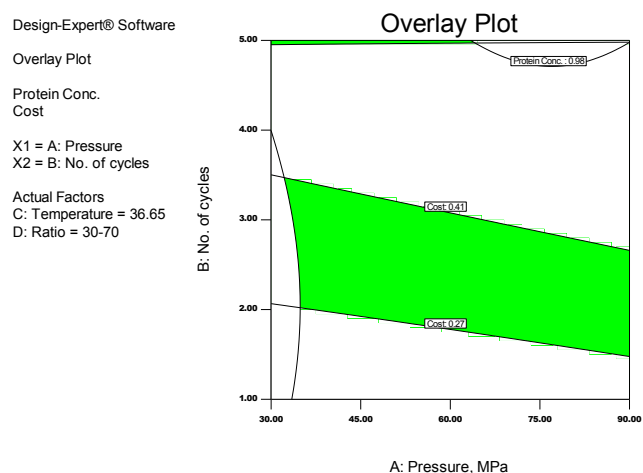
Figure 4 - 56: The optimal region of higher protein yield with associated Cost for 30:70 ratios (Number of cycle vs. Pressure plot)

Figures 4-57 and 4-58 analysed the two categorical factors of 10:90 and 20:80 when Baker's yeast substrates were homogenized over the temperature range of 30 - 50 °C. In particular, three green shaded areas in the Figure 4-58, revealed that the overlay plot satisfied some criteria in terms of energy cost required for homogenizing the substrate, and therefore indicated that the process parameters of homogenizer indeed were economically feasible in terms of maximizing protein at minimal cost. Both Figures 4-57 and 4-58 showed a protein concentration yield of 0.76 mg/mL was achieved at 5 cycles and 90 MPa, as and at a cost of €0.44. This (0.76 mg/mL of protein concentration) was also attained for a cost of €0.16 and €0.44 when homogenized at 75 MPa pressure using 2 and 4 cycles respectively.

This seems realistic based on the data on the overlay plot and with the working parameters considered; as protein concentration yield can be more cost-effective over a categorical factor of 20:80 ratio. This was based on the fact that as the number of cycles for homogenizing the substrates increases, more cell walls will be broken down to further release the intracellular protein at a higher operating pressure.
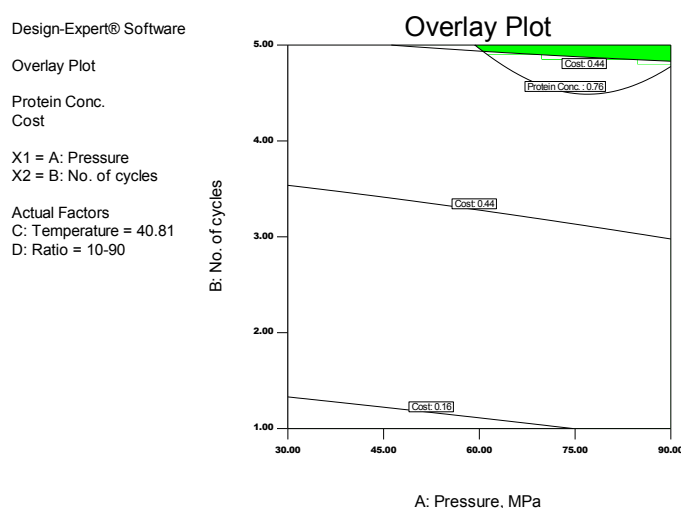
Figure 4 - 57: shows the optimal region of higher protein yield with associated Cost for 10:90 ratios (Number of cycle vs. Pressure plot)
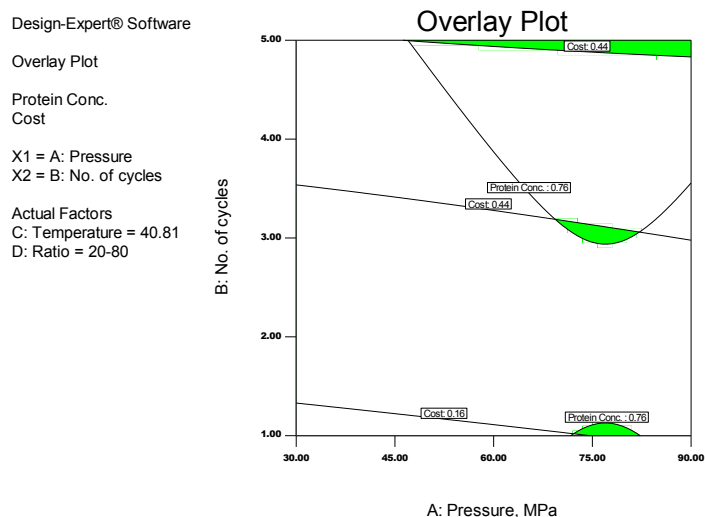
Figure 4 - 58: The optimal region of higher protein yield with associated Cost for 20:80 ratios (Number of cycle vs. Pressure plot)

Optimal Solution for Cost (Not Restricted) – Over the 30 – 50 °C Temperature Range

This section describes the cost associated with 'No Restriction' as an optimal solution for Baker's yeast homogenized over the 30 – 50 °C temperature range. These are considered in the Figures 4-59 to 4-61 detailed below. 'Cost with no restrictions' meant that every parameters both as factors and responses are in range except the protein concentration which was been determined and as such, was required to be maximized. These also included cost and categorical factors of ratios and were varied to determine the cost effectiveness of the protein concentration through homogenization of the substrate.

From the Figures 4-59 to 4-61 depict the categorical factors of 10:90, 20:80, and 30:70 ratios respectively and all had similar trends but with some differences in their yields. Two cases were visible in Figure 4-59 wherein 0.06 mg/mL protein yield was achieved when homogenized at 38 and 52 MPa pressures, 1 cycle and at a temperature of 32.95 °C at a cost of €0.08 to €0.11 respectively. Similarly energy costs of €0.08 and €0.11 in Figure 4-60 yielded 0.52 mg/mL protein concentration when homogenized at 32 and 54 MPa. The same yield also resulted from homogenizing at 40 and 50 MPa pressure, at 1 cycle for the plot (see Figure

4-61), resulting in a similar cost. So despite the ratio, if one chose 1 cycle and an average pressure of around 40 MPa, a maximum yield would be achieved but to the greatest effect of using 20:80 or 30:70 ratios. That is, an increased dilution ratio resulting in a higher protein concentration yield and this is in agreement with work carried out by Diels & Michiels [175] and Save *et al*. [188].
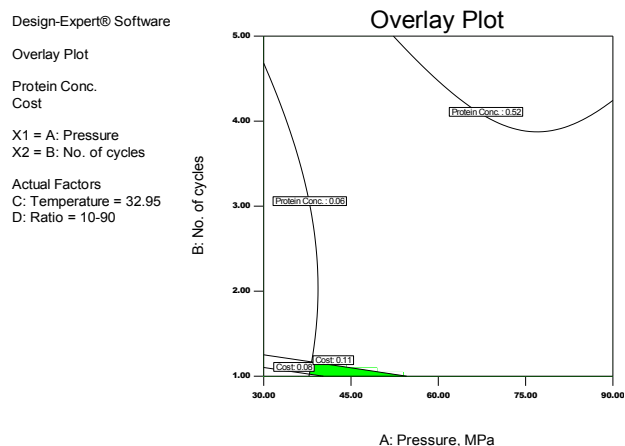
Figure 4 - 59: The optimal region of higher protein yield with associated Cost for 10:90 ratios (Number of cycle vs. Pressure plot)
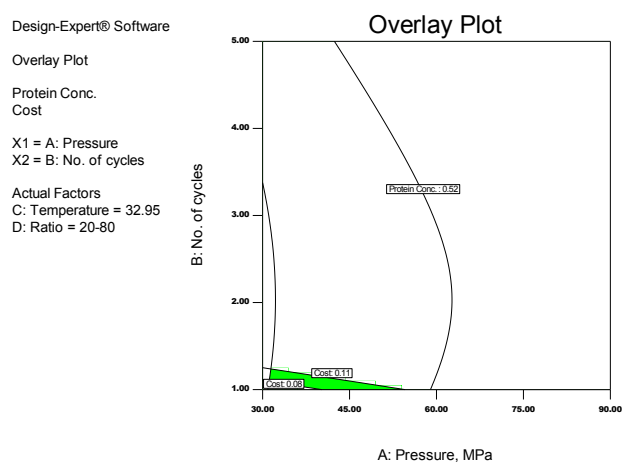
Figure 4 - 60: The optimal region of higher protein yield with associated Cost for 20:80 ratios (Number of cycle vs. Pressure plot)
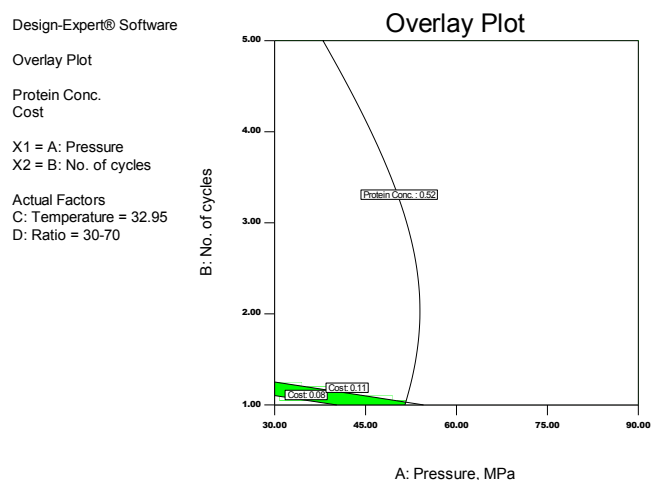
Figure 4 - 61: The optimal region of higher protein yield with associated Cost for 30:70 ratios (Number of cycle vs. Pressure plot)

4.10.3 Microalgae (Homogenized at 15-25 °C Temperature Range)

4.10.3.1 Numerical Optimization (Over the 15 – 25 °C Temperature Range)

Table 4-32 shows the restrictions and parameters used to determine the quality of protein concentration yield against over the 15 – 25 °C temperature range. In maximizing protein concentration yield, the lower and upper limits were set based on the yield that resulted, at 0.10 and 0.46 mg/mL respectively. The aim was to attain 0.46 mg/mL, considering the cost which was within the range. This cost should be as low as ever for the purpose of cost effectiveness.

Table 4 - 32: Quality for Protein Concentration Yield - Restricted

Name	Goal	Lower Limit	Upper Limit	Lower Weight	Upper Weight	Importance
Pressure	maximize	30	90.00	1	1.00	3.00
No. of cycles	maximize	1	5.00	1	1.00	3.00
Temperature	maximize	15	25.00	1	1.00	3.00
Ratio	is in range	10-90	30-70	1	1.00	3.00
Protein Conc.	maximize	0.10	0.46	1	1.00	5.00
Cost	is in range	0.1	0.41	1	1.00	3.00

Table 4-33 depicts the desirability/optimized results for the categorical factors of 10:90, 20:80, and 30:70 ratios, and within the parameters and limited availability of resources required for homogenization. *Design Expert Software* identified the optimal solution at a pressure, number of cycles, temperature, ratio and cost at 90 MPa, 5, 25°C, 30:70 and €0.37 respectively, to yield the maximum 0.48 mg/mL of protein concentration.

Table 4 - 33: Optimal Solutions for 3 Combinations of Categorical Factor Level for Quality

No.	Pressure	No. of cycles	Temp	Ratio	Protein Conc.	Cost	Desirability	
1	90.00	5	25.00	30:70	0.48	0.37	1.00	Selected
2	90.00	5	24.00	30:70	0.46	0.38	0.98	
3	90.00	5	25.00	30:70	0.48	0.37	0.98	
4	79.00	5	25.00	30:70	0.48	0.37	0.96	
5	90.00	4	25.00	30:70	0.48	0.37	0.95	
6	90.00	5	25.00	20:80	0.40	0.37	0.94	
7	90.00	5	25.00	20:80	0.40	0.37	0.93	
8	90.00	5	25.00	10:90	0.39	0.37	0.92	
9	90.00	4	25.00	30:70	0.46	0.36	0.92	
10	86.00	5	25.00	10:90	0.39	0.37	0.91	

Tables 4-34 and 4-35 examines and analyses the 'Not-restricted' quality for protein concentration yield and the optimal solutions for 3 combination of categorical factor of 10:90, 20:80, and 30:70 ratios. This was similar to the scenarios of Table 4-33 (the difference was in the 'Restricted' and 'Not-restricted').

The optimal yield for the protein concentration was 0.47 mg/mL, based on the desirability. Tables 4-33 and 4-35 compared the 'Restricted' and 'Not Restricted' of protein concentration yield, and the energy cost associated for the yield. Based on the criteria for desirability selections, the 'Not Restricted' has been favoured in comparison to the 'Restricted'. This was proven to have yielded an increment of 2.1% in the protein concentration and an energy saving cost of 2.8%

Table 4 - 34: Quality for Protein Concentration Yield - Not Restricted

Name	Goal	Lower Limit	Upper Limit	Lower Weight	Upper Weight	Importance
Pressure	is in range	30	90	1	1	3
No. of cycles	is in range	1	5	1	1	3
Temperature	is in range	15	25	1	1	3
Ratio	is in range	10:90	30:70	1	1	3
Protein Conc.	maximize	0.1	0.46	1	1	5
Cost	is in range	0.1	0.41	1	1	3

Table 4 - 35: Optimal Solutions for 3 Combinations of Categorical Factor Levels for Quality

No.	Pressure	No. of cycles	Temp	Ratio	Protein Conc.	Cost	Desirability	
1	85.00	4	25.00	30:70	0.47	0.36	1	Selected
2	87.00	3	25.00	30:70	0.47	0.35	1	
3	72.00	5	25.00	30:70	0.47	0.38	1	
4	87.00	4	25.00	30:70	0.47	0.38	1	
5	74.00	5	25.00	30:70	0.46	0.38	1	
6	68.00	5	25.00	30:70	0.47	0.38	1	
7	77.00	4	25.00	30:70	0.46	0.38	1	
8	81.00	4	25.00	30:70	0.47	0.38	1	
9	76.00	4	25.00	30:70	0.46	0.37	1	
10	80.00	5	25.00	30:70	0.48	0.37	1	

Tables 4-36 and 4-37 again looked at the cost in realizing protein concentration yield and with the restricted condition attached to the parameters. The main input parameters (Pressure, temperature, and number of cycles) were maximized, while the categorical factors of ratios and protein concentration were in range. This would enable *Design Expert* to determine the cost at a minimal level for higher protein yield. Table 4-37 found an optimal solution of only 0.36 mg/mL but at cost of €0.27/hour, at a pressure of 90 MPa, 2 cycles, 25 °C and ratio of 20:80.

Table 4 - 36: Cost for Protein Concentration Yield - Restricted

Name	Goal	Lower Limit	Upper Limit	Lower Weight	Upper Weight	Importance
Pressure	maximize	30	90	1	1	3
No. of cycles	maximize	1	5	1	1	3
Temperature	maximize	15	25	1	1	3
Ratio	is in range	10:90	30:70	1	1	3
Protein Conc.	is in range	0.1	0.46	1	1	2
Cost	minimize	0.1	0.41	1	1	5

Table 4 - 37: Optimal Solutions for 3 Combinations of Categorical Factor Levels for Cost

No	Pressure	No. of cycles	Temp	Ratio	Protein Conc.	Cost	Desirability	
1	90.00	2.00	25.00	20:80	0.36	0.27	0.57	Selected
2	90.00	2.00	25.00	10:90	0.34	0.27	0.57	
3	90.00	2.00	25.00	30:70	0.44	0.27	0.57	
4	88.00	2.00	25.00	10:90	0.33	0.25	0.56	
5	85.00	2.00	25.00	10:90	0.34	0.26	0.56	
6	90.00	3.00	25.00	30:70	0.45	0.31	0.55	
7	80.00	2.00	25.00	30:70	0.43	0.26	0.55	
8	90.00	2.00	24.00	10:90	0.30	0.27	0.55	
9	78.00	2.00	25.00	20:80	0.38	0.28	0.55	
10	69.00	2.00	25.00	30:70	0.42	0.24	0.53	

Tables 4-38 and 4-39 show the cost for protein concentration (not restricted) along with optimal solutions for the three combinations of categorical factor levels. The 'Not Restricted' (Table 4-38) was used to determine the cost of yielding the protein concentration and this showed all parameters to be in range, except protein was maximized, and cost, minimized. The order of importance for protein concentration and cost for homogenizing the substrate were rated as 2 and 5 respectively, as for previous temperature ranges/optimization. Table 4-39 shows the optimal parameters that achieved a cost of €0.11 yielding 0.30 mg/mL of protein concentration at a categorical factor of 30:70 ratios at 1 cycle at a pressure of 55 MPa and a temperature of 15 °C.

In comparison, the 'Not Restricted' was considered more favourable in terms of cost for protein concentration yield based on optimal selection, over the combinations of categorical factor, with 30:70 ratio for the 'Not Restricted' showing the best result with lower pressure, temperature and number of cycles.

Table 4 - 38: Cost for Protein Concentration Yield – Not Restricted

Name	Goal	Lower Limit	Upper Limit	Lower Weight	Upper Weight	Importance
Pressure	is in range	30	90.00	1	1.00	3.00
No. of cycles	is in range	1	5.00	1	1.00	3.00
Temperature	is in range	15	25.00	1	1.00	3.00
Ratio	is in range	10:90	30:70	1	1.00	3.00
Protein Conc.	maximize	0.1	0.46	1	1.00	2.00
Cost	minimise	0.1	0.41	1	1.00	5.00

Table 4 - 39: Optimal Solutions for 3 Combinations of Categorical Factor Levels for Cost – (Not Restricted)

No	Pressure	No. of cycles	Temp	Ratio	Protein Conc.	Cost	Desirability	
1	55.00	1	15.00	30:70	0.30	0.11	0.83	Selected
2	63.00	1	15.00	30:70	0.31	0.12	0.83	
3	59.00	1	15.00	30:70	0.30	0.11	0.83	
4	51.00	1	25.00	30:70	0.35	0.14	0.83	
5	45.00	1	25.00	30:70	0.33	0.13	0.83	
6	60.00	1	25.00	30:70	0.37	0.15	0.82	
7	42.00	1	25.00	30:70	0.32	0.12	0.82	
8	64.00	1	25.00	30:70	0.38	0.15	0.82	
9	37.00	1	25.00	30:70	0.30	0.12	0.82	
10	32.00	1	25.00	20:80	0.29	0.11	0.82	

4.10.3.2 Graphical Optimization (Over the 15 – 25 °C Temperature Range)

Quality for Homogenization of Protein Concentration Yield - Restricted (Over the 15 – 25 °C Temperature Range)

Figures 4-62 to 4-64 details the restricted constraints graphical representation of the categorical factor levels of 10:90, 20:80, and 30:70 ratios of the quality of protein concentration yield from high-pressure homogenization of Microalgae (*Chlorella vulgaris)*.

Figure 4-62 4-64, reveals protein concentration yield of 0.37 mg/mL at a cost of €0.36 and €0.37 homogenized at 65 MPa (Figure 4-62), 30 - 90 MPa (Figure 4-63) and 60 – 90 MPa (Figure 4-64) respectively and 25 °C, and at 4 - 5 cycles along

with at a categorical factor of 10:90 ratios, 20:80 ratios, and 30:70 ratios respectively.
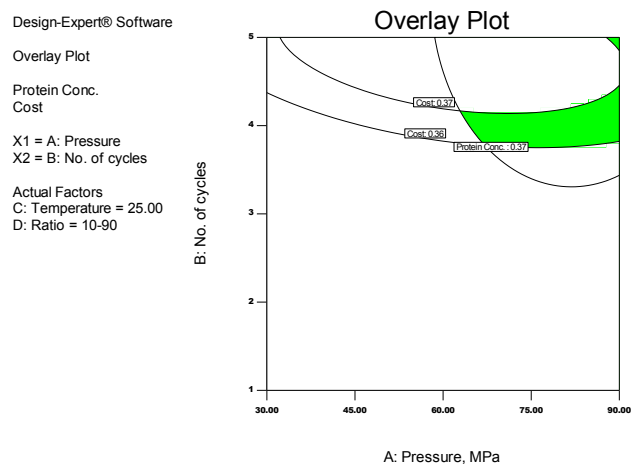
Figure 4 - 62: The optimal region of higher protein yield with associated Quality for 10:90 ratios – (Restricted)
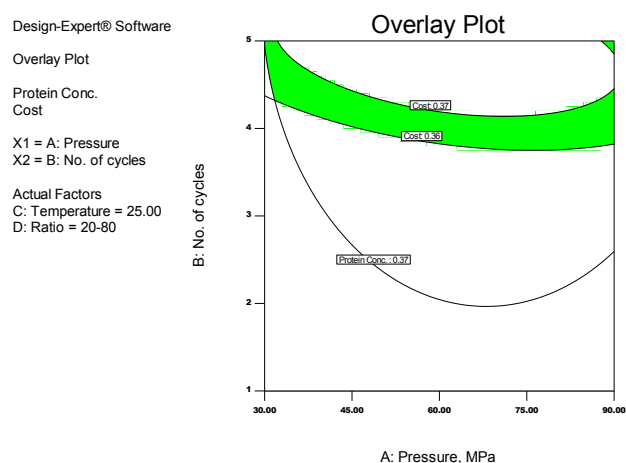
Figure 4 - 63: The optimal region of higher protein yield with associated Quality for 20:80 ratios – (Restricted)
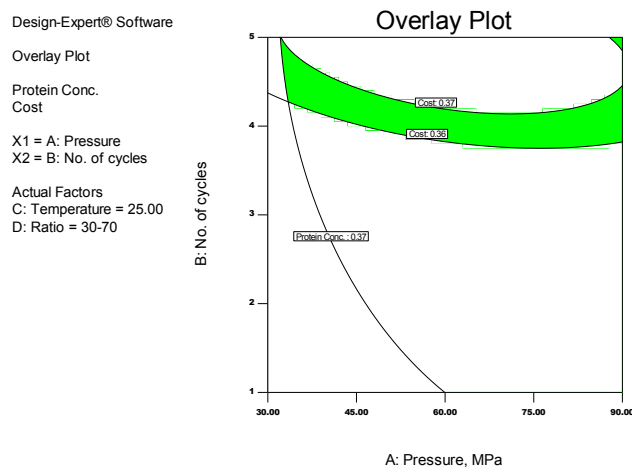
Figure 4 - 64: The optimal region of higher protein yield with associated Quality for 30:70 ratios – (Restricted)

Cost for protein concentration yield – Restricted

Figures 4-65 to 4-67, shows the cost for the protein concentration yield with some restrictions. The main parameters were maximized; temperature, pressure and the number of cycles. Cost was minimized, while protein concentration and ratio were in range when one observes the results in Figures 4-65 to 4-67, a maximum protein concentration yield of 0.95 mg/mL, was achieved at a homogenized pressure of 65 – 85 MPa, at 3 - 4 cycles, and were achieved at costs of €0.44 and €0.47 respectively, for a categorical factor of 30:70 ratio (Figure 4-67).
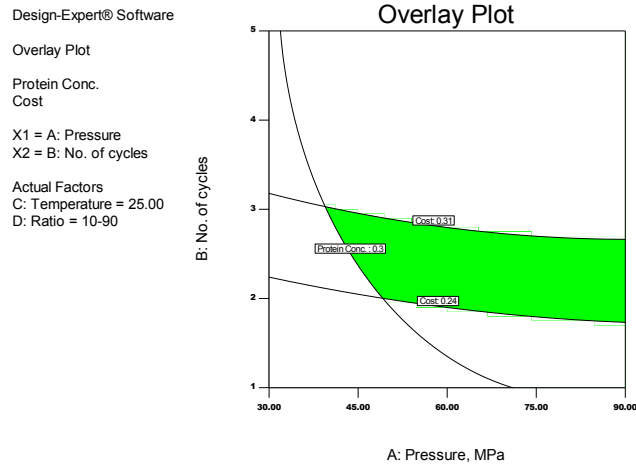
Figure 4 - 65: The optimal region of higher protein yield with associated Cost for 10:90 ratios – (Restricted)
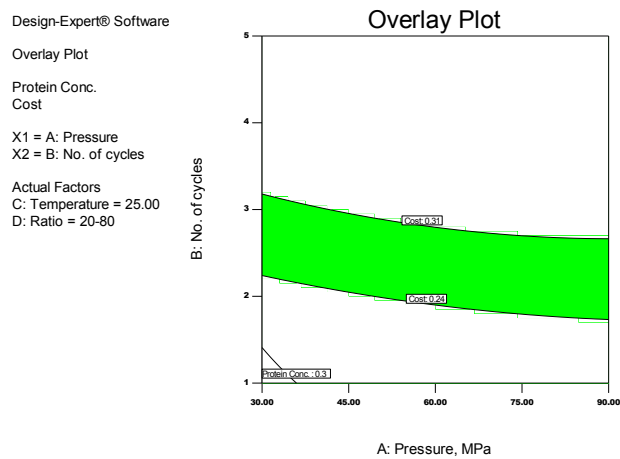
Figure 4 - 66: The optimal region of higher protein yield with associated Cost for 20:80 ratios – (Restricted)
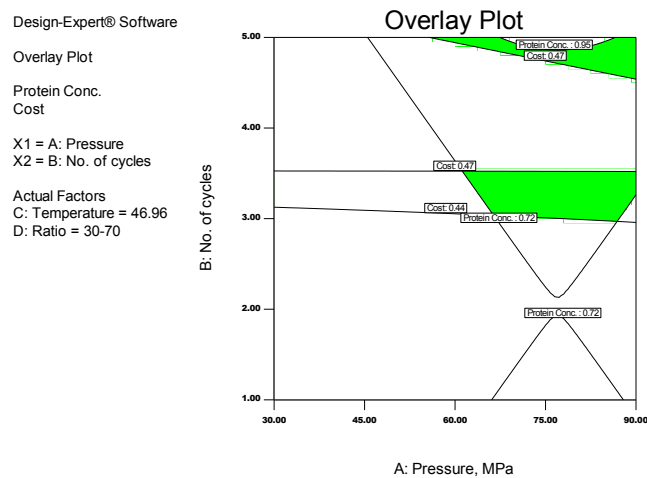
Figure 4 - 67: The optimal region of higher protein yield with associated Cost for 30:70 ratios – (Restricted)

202

4.11 Summary

Economic feasibility of the process as presented using the *Design Expert* software, showed results and optimization on protein concentration yield and energy cost with a consideration most feasible when the substrate to buffer solution ratio is increased. The entire results presented have provided some clarification of the behaviours of the biomass substrates. The design of experiment through the response surface methodology (RSM) have critically analysed the process of maximizing protein yield and minimizing energy cost associated with the homogenization. These have been presented in three scenarios of homogenizing the substrates in the form of Baker's yeast at 15 – 25 °C, and 30 – 50 °C temperature ranges, and Microalgae at 15 – 25 °C temperature range. Further analyses in the optimization section showcased the different parameters and their effects on the yield of protein concentration and the cost to that effect. Numerical optimization of the process showed the 'Restricted' and the 'Not Restricted' of the quality of the protein concentration yield along with the energy cost in producing the protein concentration. The 30 – 50 °C temperature range of Baker's yeast showed the best of result in all when the three scenarios were compared in attaining the target of highest protein concentration yield at minimal cost. This as compared, showed the desirability selection of 0.93 mg/mL of protein concentration yield attainable at a cost of €0.45 (Restricted) and 1.07 mg/mL of protein concentration yielded at a cost of €0.43 for the 'Not Restricted' (see Tables 4-29 and 4-31) respectively. This showed a 13.1% increment of protein concentration yield and an energy saving cost of 4.7%. Whereas, in consideration of other two substrates, homogenized at both 15 – 25 °C for Baker's yeast (Tables 4-23 and 4-24) and microalgae (Tables 4-33 and 4-35). The results presented were in favour of the 'Not Restricted' yielding increments of 11.7% and 2.1% of protein concentration and energy saving costs of 2.4% and 2.8% for both Baker's yeast and microalgae respectively. Pressure and Number of cycles have proven to be very effective in the attainment of protein concentration and energy cost for homogenizing the substrates. Temperature was mostly effective in the 30 - 50 °C temperature range of Baker's yeast, as described in the optimization section.

Overall, the 'Not restricted' compared favourably well when the 'Restricted' was considered in achieving protein concentration and the energy cost for the process.

Chapter 5
Conclusion and Future Work

5.1 Conclusion

In this study, Baker's yeast (*Saccharomyces cerevisiae*) and Microalgae (*Chlorella vulgaris*) have been thoroughly investigated as biomass substrates through their use in a high-pressure homogenizer (HPH). A mechanical (cell disruption) pre-treatment machine was utilized to shear the biomass in the liberation of the inner contents, particularly protein, whose use has become prominent all over the world as a feedstock for biogas production. Cell rupture enhanced the recovery of the biological products, located inside cells; therefore, HPH is one method capable of rupturing the cells, assuming the ideal optimized conditions are used to extract the maximum protein concentrations. However the selection of ideal parameters has to be weighed against cost, as to propose a biomass generation system. The cost of production should be as low as possible to ensure an overall optimized system. Thus this study investigated the production of stable emulsions from these products, using HPH for each of these substrates, and assessed, the protein concentration yield and its relative cost.

Based on the conducted research, the following conclusions were drawn from the results obtained in the work and as such, should only be applicable to the substrates considered:

- A high-pressure homogenizer was found to enhance protein concentration yield of both biomass substrates through the cell rupturing of the cell walls to release the intracellular components of protein concentration within.

- Adequate measurements showed that there was good model discrimination for all statistical investigations conducted hence, model significance was achievable.

- For both One-Variable-At-a-Time and *Design of Experiments* (OVAT and DOE) analysis, within the categorical factors of 10:90, 20:80, and 30:70

ratios, 30:70 ratios showed highest yields of protein concentration, and thus, considered the best ratio for protein concentration output.

- The influencing process parameters for high protein yield production (if cost was not a factor) were the homogenizing pressure and the Number of cycles. These tend to completely breakdown and disrupt the cell walls of the substrates to release the entire protein content.

- The optimal homogenizing conditions for Baker's yeast were identified at a pressure of 90MPa, 5 cycles, and a temperature of 20°C along with categorical factors of 30:70 ratios yielding a maximum protein concentration of 1.7694 mg/mL, and a minimum total operating cost of €0.39/hour for a 15 to 25 ^{o}C temperature range of Baker's yeast (*Saccharomyces cerevisiae*) as biomass. This indicates that an increase in dilution ratio of the substrate led to an increase in protein concentration yield when homogenized.

- Optimization analyses of the economic feasibility of the process through the associated energy cost in maximizing protein concentration yield were observed. This showed that optimizing the process, did improve the maximization of the protein yield at minimal energy cost, (when homogenized at 90 MPa, 2 cycles, 25 ^{o}C and at a categorical factor of 30:70 ratios. This yielded 1.12 mg/mL of protein concentration at a cost of €0.28/hour). This therefore resulted in protein concentration yield enhancement of 58% and an energy cost saving of 39.3%.

- Results obtained from *Chlorella vulgaris* compared consistently well with that from *Saccharomyces cerevisiae* – an indication that the applied equipment and software were in good agreement on.

5.2   Thesis Contribution

➢ The technique and method developed is applicable to a whole range of applications. This work can act as a template that helps future researchers in this related field.

➢ In the conduct of experiments through OVAT and DOE, an approach of specifying precise ranges proved beneficial. This technique can help future researchers to build on the developed analysis.

➢ Implementing DOE techniques to optimise the results found after HPH treatment.

➢ Identifying the most suitable variables as input parameters (Pressure, Temperature, Number of Cycle and Ratio) along with protein concentration (mg/mL) and cost (Euro/hr) as output (Responses) through experimentation.

➢ Identifying the best parameters for optimum yields of intracellular protein release as an output (response).

➢ Establish the ratios of dilution (substrate against solution C) during experimental work which as a result, led to the categorical factors being determined as; 10:90, 20:80 and 30:70 and which was required to identify and optimize the highest yields from the results. This could be found more accurately for higher protein concentration yield if the ratio was to be increased.

➢ Cost determinants as a function and guide towards optimum economic yield of results of protein concentration.

5.3 Recommendation for Future Work

The following has been recommended as part of future work in addition to this research;

- Other biomass substrates like some species of microalga and energy producing substrates should be considered to verify the use and results of *Saccharomyces cerevisiae/Chlorella vulgaris* from HPH.

- Other kinds of yeasts such as Brewer's yeast and genetically engineered types could be considered also to verify the results from the Baker's yeast (*Saccharomyces cerevisiae*).

- Comparison of ultrasonic or autoclaves results to that of the current HPH result, to determine any difference when set under the same conditions.

- Alternative temperature ranges (50 ^{o}C and over) and pressure ranges (90 MPa and over) to determine protein concentration yield and associated energy cost so as to compare these with the current results.

- For future particle size reduction, analysis could be performed by increasing the range in number of cycles from 1-5 to different number of cycles (e.g. 1 - 9). This will indicate if there are further deformations or reduction in size of particles after the 5th cycle of homogenization.

- Particle size distribution using the "Delsa Nano C" (particle size analyser) may be more accurately found if other techniques such as the Mastersizer 3000 were available.

- Consideration of a different categorical factor of ratio, possibly 40:60 or 50:50 as against the current categorical factors of ratios used in this research; 10:90, 20:80, and 30:70.

- Other parameters such as Density, Viscosity and Cell turbidity could be considered as well, to further determine the yield in protein concentration.

References

[1]   Omer, A. M., (2008). Energy, environment and sustainable development. *Renewable and Sustainable Energy Reviews*, *12*, 2265-2300.

[2]   Nzila, C., Dewulf, J., Spanjers, H., Kiriamiti, H and Van Langenhove, H., (2010). Biowaste energy potential in Kenya, *Renewable Energy 35, 2698 – 2704.*

[3]   Oseni, M. O. (2011). An analysis of the power sector performance in Nigeria. *Renewable and Sustainable Energy Reviews 15(9),* 4765-4774.

[4]   Nelson, V. (2011). Introduction to renewable energy. CRC Press.

[5]   Orr, L. (2006). Changing the world's energy systems. Available at: <http://www.energyandcapital.com/articles/trickle-down-enernomics/1488> (Accessed August, 2015)

[6]   United Nation (2013). World Rising Population to Reach 9.6 Billion. Available at: <https://www.un.org/en/development/desa/news/population/un-report-world-population-projected-to-reach-9-6-billion-by-2050.html>   (Accessed August, 2015)

[7]   World   Bank   (2012)   Available   at: <http://siteresources.worldbank.org/INTURBANDEVELOPMENT/Resources/336387-1334852610766/Chap3.pdf > (Accessed August, 2015)

[8]   Environmental   protection   agency   EPA   (2010).   Available   at: <http://www.epa.ie/pubs/reports/indicators/epa_factsheet_waste_v2.pdf> (Accessed August 2015)

[9]   Commission of the European Communities, (2005). Green Paper on Energy Efficiency. Doing More with Less.com 265 final, Brussels.

[10]   EC, (2009). Directive 2009/28/EC of 23 April 2009 on the promotion of the use of energy from renewable sources. European Commission (EC), Brussels. Available   at: <http://eur-lex.europa.eu/LexUriServ/LexUriServ.do?uri=OJ:L:2009:140:0016:0062:EN:PDF> (Accessed August, 2015)

[11]   Boerrigter H., Rauch R., (2006). Review of applications of gases from biomass gasification, ECN Biomass, Coal & Environmental research, Petten, Netherlands.

[12]   Pueraria, F., Bosio, B., & Heyenb, G. (2014). Energy Efficiency Optimisation in Different Plant Solutions for Methanol Production from Biomass Gasification. *Chemical Engineering*, *37*, 301-306 DOI: 10.3303/CET1437051

[13]   United Nation Environmental Programme. (2012). Available at: <http://www.unep.org/gpwm/FocalAreas/WasteAgriculturalBiomass/tabid/56456/Default.aspx > (Accessed August, 2015)

[14]   Claassen, P. A. M., Van Lier, J. B., Contreras, A. L., Van Niel, E. W. J., Sijtsma, L., Stams, A. J. M., ... & Weusthuis, R. A. (1999). Utilisation of biomass for the supply of energy carriers. *Applied microbiology and biotechnology*, *52*(6), 741-755.

[15]   Field, C. B., Campbell, J. E., & Lobell, D. B. (2008). Biomass energy: the scale of the potential resource. *Trends in ecology & evolution*, *23*(2), 65-72.

[16]   Faaij, A. (2006). Modern biomass conversion technologies. *Mitigation and adaptation strategies for global change*, *11*(2), 335-367.

[17]   Mosier, N., Wyman, C., Dale, B., Elander, R., Lee, Y. Y., Holtzapple, M., & Ladisch, M. (2005). Features of promising technologies for pretreatment of lignocellulosic biomass. *Bioresource technology*, *96*(6), 673-686.

[18]   Divya, D., Gopinath, L. R., & Christy, P.M.(2015). A review on current aspects and diverse prospects for enhancing biogas production in sustainable means. *Renewable and Sustainable Energy Reviews*, *42*, 690-699.

[19]   Ward, A. J., Hobbs, P. J., Holliman, P. J., & Jones, D. L. (2008). Optimisation of the anaerobic digestion of agricultural resources. *Bioresource technology*, *99*(17), 7928-7940.

[20]   Demirbas, A. (2000). Biomass resources for energy and chemical industry. *Energy Edu. Sci. Technol*, *5*(1), 21-45.

[21]   Duku, M. H., Gu, S., & Hagan, E. B. (2011). A comprehensive review of biomass resources and biofuels potential in Ghana. *Renewable and Sustainable Energy Reviews*, *15*(1), 404-415.

[22]   Bioenergy, I. E. A. (2009). Bioenergy–a sustainable and reliable energy source. *International Energy Agency Bioenergy, Paris, France*.

[23]   Kaygusuz, K., & Keleş, S. (2012). Sustainable bioenergy policies in Turkey. *Journal of Engineering Research and Applied Science*, *1*(1), 34-43.

[24]   Lee, J. (1997). Biological conversion of lignocellulosic biomass to ethanol. *Journal of biotechnology*, *56*(1), 1-24.

[25] Fengel, D., Wegener, G., (1984). Wood: Chemistry, Ultrastructure, Reactions. De Gruyter, Berlin

[26] McKendry, P. (2002). Energy production from biomass (part 2): conversion technologies. *Bioresource technology*, *83*(1), 47-54.

[27] Hayes, D. J., Fitzpatrick, S., Hayes, M. H., & Ross, J. R. (2006). The Biofine Process: Production of levulinic acid. furfural and formic acid from lignocellulosic feedstocks. *Biorefineries–Industrial Processes and Product*, *1*, 139-164.

[28] Balat, M., Balat, H., & Öz, C. (2008). Progress in bioethanol processing. *Progress in energy and combustion science*, *34*(5), 551-573.

[29] Hendriks, A. T. W. M., & Zeeman, G. (2009). Pretreatments to enhance the digestibility of lignocellulosic biomass. *Bioresource technology*, *100*(1), 10-18.

[30] Puri, V. P. (1984). Effect of crystallinity and degree of polymerization of cellulose on enzymatic saccharification. *Biotechnology and Bioengineering*, *26*(10), 1219-1222.

[31] Taherzadeh, M. J., & Karimi, K. (2008). Pretreatment of lignocellulosic wastes to improve ethanol and biogas production: a review. *International journal of molecular sciences*, *9*(9), 1621-1651.

[32] Ariunbaatar, J., Panico, A., Esposito, G., Pirozzi, F., & Lens, P. N. (2014). Pretreatment methods to enhance anaerobic digestion of organic solid waste. *Applied Energy*, *123*, 143-156.

[33] Carrère, H., Dumas, C., Battimelli, A., Batstone, D. J., Delgenès, J. P., Steyer, J. P., & Ferrer, I. (2010). Pretreatment methods to improve sludge anaerobic degradability: a review. *Journal of hazardous materials*, *183*(1), 1-15.

[34] Mata-Alvarez J, Mace S, Llabres P. (2000)Anaerobic digestion of organic solid wastes. An overview of research achievements and perspectives. Bioresour Technol; 74:3–16

[35] Engelhart M, Kruger M, Kopp J, Dichtl N. (2000).Effects of disintegration on anaerobic degradation of sewage excess sludge in down-flow stationary fixed film digesters. Water Sci Technol 41:171–9.

[36] Chisti, Y., & Moo-Young, M. (1986). Disruption of microbial cells for intracellular products. *Enzyme and Microbial Technology*, *8*(4), 194-204.

[37] Follows, M., Hetherington, P. J., Dunnill, P., & Lilly, M. D. (1971). Release of enzymes from bakers' yeast by disruption in an industrial homogenizer. *Biotechnology and bioengineering*, *13*(4), 549-560.

[38] Doulah, M. S., Hammond, T. H., & Brookman, J. S. G. (1975). A hydrodynamic mechanism for the disintegration of Saccharomyces cerevisiae in an industrial homogenizer. *Biotechnology and Bioengineering*, *17*(6), 845-858.

[39] Brookman, G., & James, S. (1974). Mechanism of cell disintegration in a high pressure homogenizer. *Biotechnology and Bioengineering*, *16*(3), 371-383.

[40] Geciova, J., Bury, D., & Jelen, P. (2002). Methods for disruption of microbial cells for potential use in the dairy industry—a review. *International Dairy Journal*, *12*(6), 541-553.

[41] Peternel, Š. (2013). Bacterial cell disruption: a crucial step in protein production. *New biotechnology*, *30*(2), 250-254.

[42] Asif, M., & Muneer, T. (2007). Energy supply, its demand and security issues for developed and emerging economies. *Renewable and Sustainable Energy Reviews*, *11*(7), 1388-1413.

[43] Hall, C., Tharakan, P., Hallock, J., Cleveland, C., & Jefferson, M. (2003). Hydrocarbons and the evolution of human culture. *Nature*, *426*(6964), 318-322.

[44] Tainter, J. (1990). *The collapse of complex societies*. Cambridge University Press.

[45] Wilkinson, P., Smith, K. R., Joffe, M., & Haines, A. (2007). A global perspective on energy: health effects and injustices. *The Lancet*, *370*(9591), 965-978.

[46] Yergin, D. (2006). Ensuring energy security. *Foreign affairs*, 69-82.

[47] Bang, G. (2010). Energy security and climate change concerns: Triggers for energy policy change in the United States?. *Energy Policy*, *38*(4), 1645-1653.

[48] Bielecki, J. (2002). Energy security: is the wolf at the door?. *The quarterly review of economics and finance*, *42*(2), 235-250.

[49] Von Hippel, D., Suzuki, T., Williams, J. H., Savage, T., & Hayes, P. (2011). Energy security and sustainability in Northeast Asia. *Energy Policy*, *39*(11), 6719-6730.

[50] Grubler, A., & Cleveland, C. J. (2008). Energy transitions. *Encyclopedia of Earth*.

[51] Fouquet, R., (2009). A brief history of energy. In: Evans, J., Hunt, L.C. (Eds.), International Handbook of the Economics of Energy. Edward Elgar Publications, Cheltenham, UK, and Northampton, MA, USA.

[52] Saxena, R. C., Adhikari, D. K., & Goyal, H. B. (2009). Biomass-based energy fuel through biochemical routes: A review. *Renewable and Sustainable Energy Reviews*, *13*(1), 167-178.

[53] Bridgwater, A. V., Meier, D., & Radlein, D. (1999). An overview of fast pyrolysis of biomass. *Organic Geochemistry*, *30*(12), 1479-1493.

[54] Bridgwater, A. V. (1999). Principles and practice of biomass fast pyrolysis processes for liquids. *Journal of analytical and applied pyrolysis*, *51*(1), 3-22.

[55] Balat, M. (2005). Use of biomass sources for energy in Turkey and a view to biomass potential. *Biomass and Bioenergy*, *29*(1), 32-41.

[56] Özbay, N., Pütün, A. E., Uzun, B. B., & Pütün, E. (2001). Biocrude from biomass: pyrolysis of cottonseed cake. *Renewable Energy*, *24*(3), 615-625.

[57] Demirbaş, A. (2001). Biomass resource facilities and biomass conversion processing for fuels and chemicals. *Energy conversion and Management*, *42*(11), 1357-1378.

[58] Sheth, P. N., & Babu, B. V. (2009). Experimental studies on producer gas generation from wood waste in a downdraft biomass gasifier. *Bioresource Technology*, *100*(12), 3127-3133.

[59] Balat, M. (2006). Biomass energy and biochemical conversion processing for fuels and chemicals. *Energy Sources, Part A*, *28*(6), 517-525.

[60] Wolin, M. J., Miller, T. L., & Stewart, C. S. (1997). Microbe-microbe interactions. In *The rumen microbial ecosystem* (pp. 467-491). Springer Netherlands.

[61] Cauvain, S. P., & Young, L. S. (2007). *Technology of breadmaking*. Springer.

[62] Dziezak, J. D. (1987). Yeasts and yeast derivatives: definitions, characteristics, and processing. *Food technology (USA)*.

[63] Halász, A., & Lásztity, R. (1990). *Use of yeast biomass in food production*. CRC Press.

[64] Alais, C., & Linden, G. (1991). *Food biochemistry*. Ellis Horwood Ltd.

[65] Reed, G., & Nagodawithana, T. W. (1991). Yeast technology. 2nd ed. New York: Van Nostrand Reinhold; pp. 416.

[66] Russell, I., Jones, R., & Stewart, G. G. (1987). Yeast--the primary industrial microorganism. *Biological research on industrial yeasts/editors, Graham G. Stewart,* Russell I, Klein RD and Hiebsch RR, CRC Press, Boca Raton, FL, pp 2-20

[67] Evangelista J. (1989). Tecnologia de Alimentos, 2nd edn, Livraria Atheneu Editora, Rio de Janeiro

[68] Fukuda, H., Kondo, A., & Tamalampudi, S. (2009). Bioenergy: Sustainable fuels from biomass by yeast and fungal whole-cell biocatalysts. *Biochemical Engineering Journal*, *44*(1), 2-12.

[69] Beudeker, R. F., Van Dam, H. W., Van der Plaat, J. B., & Vellenga, K. (1990). Developments in baker's yeast production. *Yeast biotechnology and biocatalysis*, 103-146.

[70] Phaff, H. J., & Macmillan, J. D. (1978). Yeasts: Description of various genera and species of special interest. *CRC Handbook of Microbiology*, 295.

[71] Reed, G., & Peppler, H. J. (1973). *Yeast technology*.

[72] Clackmannanshire, S. (1979). S. Burrows. *Microbial biomass*, *4*, 31.

[73] Northcote, D. H., & Horne, R. W. (1952). The chemical composition and structure of the yeast cell wall. *Biochemical Journal*, *51*(2), 232.

[74] Zechmeister, L., & Tóth, G. (1936). Einwirkung von flüssigem Ammoniak auf Octaacetyl-cellobiose. *Justus Liebigs Annalen der Chemie*, *525*(1), 14-24.

[75] Haworth, W. N., & Hirst, E. L. (1937). F. A. Isherwood. *J. Chem. Soc*, *784*.

[76] Ling, A R., Nanji, R. D. & Panton, F. J. (1925). J. Inst. Brew. 31, 316.

[77] Yeast cell wall structure. Available online at: <http://bilingualbiology10.blogspot.ie/2010/11/kingdom-fungi.html> (Accessed August, 2015)

[78] Lancashing, W. E. (1986). Modern genetics and brewing technology. *B rew2 er*, *72*, 345.

[79] Engler, C. R. (1985). Disruption of microbial cells in comprehensive biotechnology. In M. Moo-Young, & C.L. Cooney (Eds.), Vol. 2 (pp. 305–324). UK: Pergamon.

[80] Yeast internal structure. Available online at: <http://www.allaboutfeed.net/Special-focus/Yeast-Special/Application-of-yeast-cell-wall-in-swine/> (Accessed August, 2015)

[81] Dunahay, T., Benemann, J., & Roessler, P. (1998). *A look back at the US Department of Energy's aquatic species program: biodiesel from algae* (Vol. 328). Golden: National Renewable Energy Laboratory.

[82] Oswald, W. J., & Golueke, C. G. (1960). Biological transformation of solar energy. *Advances in applied microbiology*, *2*, 223-262.

[83] Benemann, J. R., Weissman, J. C., Koopman, B. L., & Oswald, W. J. (1977). Energy production by microbial photosynthesis. *Nature*, *268* (5615), 19-23.

[84] Pittman, J. K., Dean, A. P., & Osundeko, O. (2011). The potential of sustainable algal biofuel production using wastewater resources. *Bioresource Technology*, *102*(1), 17-25.

[85] Brennan, L., & Owende, P. (2010). Biofuels from Microalgae—a review of technologies for production, processing, and extractions of biofuels and co-products. *Renewable and sustainable energy reviews*, *14*(2), 557-577.

[86] Brune, D. E., Lundquist, T. J., & Benemann, J. R. (2009). Microalgal biomass for greenhouse gas reductions: potential for replacement of fossil fuels and animal feeds. *Journal of Environmental Engineering*, *135*(11), 1136-1144.

[87] Pulz, O., Scheibenbogen, K., & Groß, W. (2008). Biotechnology with cyanobacteria and Microalgae. *Biotechnology Set, Second Edition*, 105-136.

[88] Jørgensen, P. J. (2009). *Biogas-Green Energy: Process, Design, Energy Supply, Environment*. Researcher for a Day.

[89] Balsari, P., Bonfanti, P., Bozza, E., & Sangiorgi, F. 14–20 August 1983. Evaluation of the influence of animal feeding on the performances of a biogas installation (mathematical model). In *Third International Symposium on Anaerobic Digestion. Boston, MA, USA, A* (Vol. 20, p. 7).

[90] Amon, T., Kryvoruchko, V., Amon, B., Moitzi, G., Lyson, D., Hackl, E., ... & Pötsch, E. (2003). Optimierung der Biogaserzeugung aus den Energiepflanzen Mais und Kleegras. *Endbericht Juli*.

[91] Weiland, P. (2010). Biogas production: current state and perspectives. *Applied microbiology and biotechnology*, *85*(4), 849-860.

[92] Amon, T., Amon, B., Kryvoruchko, V., Zollitsch, W., Mayer, K., & Gruber, L. (2007). Biogas production from maize and dairy cattle manure—influence of biomass composition on the methane yield. *Agriculture, Ecosystems & Environment*, *118*(1), 173-182.

[93] Pöschl, M., Ward, S., & Owende, P. (2010). Evaluation of energy efficiency of various biogas production and utilization pathways. *Applied Energy*, *87*(11), 3305-3321.

[94] Sialve, B., Bernet, N., & Bernard, O. (2009). Anaerobic digestion of Microalgae as a necessary step to make microalgal biodiesel sustainable. *Biotechnology advances*, *27*(4), 409-416.

[95] Oslaj, M., Mursec, B., & Vindis, P. (2010). Biogas production from maize hybrids. *Biomass and bioenergy*, *34*(11), 1538-1545.

[96] Amon, T., Kryvoruchko, V., Amon, B., Buga, S., Amin, A., Zollitsch, W., Mayer, K., Pötsch, E., 2004a. Biogaserträge aus landwirtschaftlichen Gärgütern. In: BAL Gumpenstein, BMLFUW (Ed.) BAL-Bericht über das 10. Alpenländische Expertenforum zum Thema Biogasproduktion— Alternative Biomassenutzung und Energiegewinnung in der Landwirtschaft am 18–19 März 2004. ISBN 3-901980-72-5, pp. 21–26. <http://www.nas.boku.ac.at/4536.html> (Accessed August, 2015)

[97] Chandra, R., Takeuchi, H., & Hasegawa, T. (2012). Methane production from lignocellulosic agricultural crop wastes: A review in context to second generation of biofuel production. *Renewable and Sustainable Energy Reviews*, *16*(3), 1462-1476.

[98] Nasseri, A. T., Rasoul-Amini, S., Morowvat, M. H., & Ghasemi, Y. (2011). Single cell protein: production and process. *American Journal of food technology*, *6*(2), 103-116.

[99] Heredia-Arroyo, T., Wei, W., & Hu, B. (2010). Oil accumulation via heterotrophic/mixotrophic Chlorella protothecoides. *Applied biochemistry and biotechnology*, *162*(7), 1978-1995.

[100] Rasoul-Amini, S., Ghasemi, Y., Morowvat, M. H., & Mohagheghzadeh, A. (2009). PCR amplification of 18S rRNA, single cell protein production and fatty acid evaluation of some naturally isolated Microalgae. *Food Chemistry*, *116*(1), 129-136.

[101] Kim, J. K., Tak, K. T., & Moon, J. H. (1998). A continuous fermentation of Kluyveromyces fragilis for the production of a highly nutritious protein diet. *Aquacultural engineering*, *18*(1), 41-49.

[102] Coutteau, P., Lavens, P., & Sorgeloos, P. (1990). Baker's yeast as a potential substitute for live algae in aquaculture diets: Artemia as a case study. *Journal of the World Aquaculture Society*, *21*(1), 1-9.

[103] Cizik (2014). Utilization and properties of biogas/ Renewable alternative. <http://www.renewable-alternative.com/2014/03/utilization-and-properties-of-biogas.html > (Accessed August, 2015).

[104] Biogas Basics (2014). Available at: <https://energypedia.info/wiki/Biogas_Basics> (Accessed August, 2015)

[105] Schaffner, G., & Matile, P. (1981). Structure and composition of baker's yeast lipid globules. *Biochemie Und Physiologie Der Pflanzen*, *176*(7), 659-666.

[106] Zweytick, D., Athenstaedt, K., & Daum, G. (2000). Intracellular lipid particles of eukaryotic cells. *Biochimica et Biophysica Acta (BBA)-Reviews on Biomembranes*, *1469*(2), 101-120.

[107] Leber, R., Zinser, E., Paltauf, F., Daum, G., & Zellnig, G. (1994). Characterization of lipid particles of the yeast, Saccharomyces cerevisiae. *Yeast*, *10*(11), 1421-1428.

[108] Brown, M. R., Jeffrey, S. W., Volkman, J. K., & Dunstan, G. A. (1997). Nutritional properties of Microalgae for mariculture. *Aquaculture*, *151*(1), 315-331.

[109] Becker, W. (2004). 18 Microalgae in Human and Animal Nutrition. *Handbook of microalgal culture: biotechnology and applied phycology*, 312.

[110] Becker, E. W. (1988). Micro-algae for human and animal consumption.

[111] Soletto, D., Binaghi, L., Lodi, A., Carvalho, J. C. M., & Converti, A. (2005). Batch and fed-batch cultivations of Spirulina platensis using ammonium sulphate and urea as nitrogen sources. *Aquaculture*, *243*(1), 217-224.

[112] Hatti-Kaul, R., & Mattiasson, B. (2003). Release of protein from biological host. *Isolation and purification of proteins. CRC Press, Boca Raton*, 1-28.

[113] Porro, D., Sauer, M., Branduardi, P., & Mattanovich, D. (2005). Recombinant protein production in yeasts. *Molecular biotechnology*, *31*(3), 245-259.

[114] Klinke, H. B., Thomsen, A. B., & Ahring, B. K. (2004). Inhibition of ethanol-producing yeast and bacteria by degradation products produced during pre-treatment of biomass. *Applied microbiology and biotechnology*, *66*(1), 10-26.

[115] Laureano-Perez, L., Teymouri, F., Alizadeh, H., & Dale, B. E. (2005). Understanding factors that limit enzymatic hydrolysis of biomass. *Applied Biochemistry and Biotechnology*, *124*(1-3), 1081-1099.

[116] Agbor, V. B., Cicek, N., Sparling, R., Berlin, A., & Levin, D. B. (2011). Biomass pretreatment: fundamentals toward application. *Biotechnology advances*, *29*(6), 675-685.

[117] Arduengo, P.M. (2010) Sloppy technicians and the progress of science. *Promega Connections* http://promega.wordpress.com/2010/03/15/sloppy-technicians (Accessed August, 2015)

[118] Kumar, P., Barrett, D. M., Delwiche, M. J., & Stroeve, P. (2009). Methods for pretreatment of lignocellulosic biomass for efficient hydrolysis and biofuel production. *Industrial & Engineering Chemistry Research*, *48*(8), 3713-3729

[119] Palmowski, L., & Miller, J. (2000). Influence of the size reduction of organic waste on their anaerobic digestion. *Water science and technology*, *41*(3), 155-162.

[120] Sun, Y., & Cheng, J. (2002). Hydrolysis of lignocellulosic materials for ethanol production: a review. *Bioresource technology*, *83*(1), 1-11.

[121] Ball milling. Available at: <http://www.understandingnano.com/nanomaterial-synthesis-ball-milling.html> (Accessed August, 2015)

[122] Alvira, P., Tomás-Pejó, E., Ballesteros, M., & Negro, M. J. (2010). Pretreatment technologies for an efficient bioethanol production process based on enzymatic hydrolysis: a review. *Bioresource technology*, *101*(13), 4851-4861.

[123] Novarino, D., & Zanetti, M. C. (2012). Anaerobic digestion of extruded OFMSW. *Bioresource technology*, *104*: 44-50.

[124] Tyagi, V. K., & Lo, S. L. (2011). Application of physico-chemical pretreatment methods to enhance the sludge disintegration and subsequent anaerobic digestion: an up to date review. *Reviews in Environmental Science and Bio/Technology*, *10*(3), 215-242.

[125] Wang, F., Wang, Y., & Ji, M. (2005). Mechanisms and kinetics models for ultrasonic waste activated sludge disintegration. *Journal of Hazardous Materials*, *123*(1), 145-150.

[126] Benabdallah El-Hadj, T., Dosta, J., Marquez-Serrano, R., & Mata-Alvarez, J. (2007). Effect of ultrasound pretreatment in mesophilic and thermophilic

anaerobic digestion with emphasis on naphthalene and pyrene removal. *Water research*, *41*(1), 87-94.

[127] Tiehm, A., Nickel, K., Zellhorn, M., & Neis, U. (2001). Ultrasonic waste activated sludge disintegration for improving anaerobic stabilization. *Water Research*, *35*(8), 2003-2009.

[128] Xie, X., Mikkelsen, T. S., Gnirke, A., Lindblad-Toh, K., Kellis, M., & Lander, E. S. (2007). Systematic discovery of regulatory motifs in conserved regions of the human genome, including thousands of CTCF insulator sites. *Proceedings of the National Academy of Sciences*, *104*(17), 7145-7150.

[129] Nieves-Soto, M., Hernández-Calderón, O. M., Guerrero-Fajardo, C. A., Sánchez-Castillo, M. A., Viveros-García, T., & Contreras-Andrade, I. (2012). Biodiesel Current Technology: Ultrasonic Process a Realistic Industrial Application.

[130] Lysis-centrifuge. Available at: <http://www.stowa-selectedtechnologies.nl/Sheets/Sheets/Baker.Process..Lysate.Thickening.Centrifuge.html#centrifuge > (Accessed August, 2015)

[131] Dohányos, M., Zábranská, J., & Jenícek, P. (1997). Enhancement of sludge anaerobic digestion by using of a special thickening centrifuge. *Water Science and Technology*, *36*(11), 145-153.

[132] Zabranska, J., Dohanyos, M., Jenicek, P., Kutil, J., & Cejka, J. (2006, May). Mechanical and rapid thermal disintegration methods of enhancement of biogas production—full-scale applications. In *Proceedings of the IWA specialized conference on sustainable sludge management: state-of-the-art, challenges and perspectives, Moscow, Russia, May* (pp. 29-31)

[133] Nah, I. W., Kang, Y. W., Hwang, K. Y., & Song, W. K. (2000). Mechanical pretreatment of waste activated sludge for anaerobic digestion process. *Water research*, *34*(8), 2362-2368.

[134] Elliott, A., & Mahmood, T. (2007). Pretreatment technologies for advancing anaerobic digestion of pulp and paper biotreatment residues. *Water research*, *41*(19), 4273-4286.

[135] Hollander beater machine. Available online at: < www.thefiberwire.com > (Accessed August, 2015)

[136] Barbir, F. (2009). Transition to renewable energy systems with hydrogen as an energy carrier. Energy 34 308-12.

[137] De Boer, K., Moheimani, N. R., Borowitzka M.A. & Bahri. P.A. (2012). Extraction and conversion pathways for Microalgae to biodiesel: a review focused on energy consumption. *J. Appl Phycol*

[138] Ahmad-Raus, R., Mel, M., Mohd-Abdullah, S.N & Yusoff, K. (2010). Cell rupture of recombinant Escherichia coli using high pressure homogenizer. *Journal of Applied Sciences 10 (21) 2717-20*

[139] Clarke, A., Prescott, T., Khan, A & Olabi, A.G. (2010). Causes of breakage and disruption in a homogeniser. *Applied Energy, 87: 3680-90*

[140] Hopkins, T.R. (1991). Physical and chemical cell disruption for the recovery of intercellular proteins. *Bioprocess. Technol. 12 57-83*

[141] Calligaris, S., Foschia, M., Bartolomeoli, I., Maifreni, M & Manzocco, L. (2012). Study on the applicability of high-pressure homogenization for the production of banana juices. *Food Science and Technology 45: 117-21*

[142] Donsi, F., Annunziata, M. & Ferrari, G. (2013). Microbial inactivation by high pressure homogenization: Effect of the disruption valve geometry. *Journal of Food Engineering 115: 362-70*

[143] High-pressure homogenizer. Available at: <http://www.pharmainfo.net/pharma-student-magazine/nanoemulsions-0 > (Accessed August, 2015)

[144] High pressure homogenizer types. Available at: <http://www.beei.com/High-Pressure-Homogenizer-Products> (Accessed August, 2015)

[145] Qian, C., & McClements, D. J. (2011). Formation of nanoemulsions stabilized by model food-grade emulsifiers using high-pressure homogenization: factors affecting particle size. *Food Hydrocolloids*, *25*(5), 1000-1008.

[146] Floury, J., Legrand, J., & Desrumaux, A. (2004). Analysis of a new type of high pressure homogeniser. Part B. Study of droplet break-up and recoalescence phenomena. *Chemical Engineering Science*, *59*(6), 1285-1294.

[147] Kleinig, A. R., & Middelberg, A. P. (1997). Numerical and experimental study of a homogenizer impinging jet. *AIChE journal*, *43*(4), 1100-1107.

[148] Floury, J., Bellettre, J., Legrand, J., & Desrumaux, A. (2004). Analysis of a new type of high pressure homogeniser. A study of the flow pattern. *Chemical Engineering Science*, *59*(4), 843-853.

[149] GYB40-10S/GYB60-6S High pressure homogenizers Users' Instruction. Available at: <www.donghuamachine.com> (Accessed August, 2015)

[150] Ciron, C. I. E., Gee, V. L., Kelly, A. L., & Auty, M. A. E. (2010). Comparison of the effects of high-pressure microfluidization and conventional homogenization of milk on particle size, water retention and texture of non-fat and low-fat yoghurts. *International Dairy Journal, 20*(5), 314-320.

[151] Briñez, W.J., Roig-Sagues, A.X., Hernández-Herrero, M. M., & Guamis-Lopez, B., (2006a). Inactivation of Listeria innocua inoculated into milk and orange juice using ultrahigh-pressure homogenization. *Journal of Food Protection 69, 86–92.*

[152] Kheadr, E.E., Vachon, J.F., Paquin, P., Fliss, I., (2002). Effect of dynamic high pressure onmicrobiological, rheological and microstructural quality of Cheddar cheese. *International Dairy Journal 12, 435–446.*

[153] Sodini, I., Remeuf, F., Haddad, S., & Corrieu, G. (2004). The relative effect of milk base, starter, and process on yogurt texture: a review. *Critical reviews in food science and nutrition, 44*(2), 113-137.

[154] Lanciotti, R., Sinigaglia, M., Angelini, P., & Guerzoni, M.E., (1994). Effects of homogenization pressure on the survival and growth of some food spoilage and pathogenic microorganisms. *Letters in Applied Microbiology 18, 319–322.*

[155] Guerzoni, M.E., Vannini, L., Lanciotti, R., & Gardini, F., (2002). Optimisation of the formulation and of the technological process of egg-based products for the prevention of Salmonella enteritidis survival and growth. *International Journal of Food Microbiology 73, 367–374.*

[156] Diels, A.M.J., Wuytack, E.Y., & Michiels, C.W., (2003). Modelling inactivation of Staphylococcus aureus and Yersinia enterocolitica by high-pressure homogenisation at different temperatures. *International Journal of Food Microbiology 87, 55–62.*

[157] Middelberg, A.P.J. (1995). Process–scale disruption of microorganisms. *Biotechnol. Adv. 13:491–551.*

[158] Engler, C.R. (1990). Cell disruption by homogenizer. In J.A. Asenjo (ed.), *Separation processes in biotechnology.* Marcel Dekker, New York, *95–105.*

[159] Popper, L., and Knorr, D. 1990. Applications of high-pressure homogenization for food preservation. *Food Technol. 44:84–89.*

[160] Goulden, J. D. S., & Phipps, L. W. (1962). The effect of homogenization pressure on the mean diameter of the fat globules in homogenized milk. In *International Congress of Food Science & Technology* (Vol. 1, pp. 765-768).

[161] Kessler, H.G. (1981). Food engineering and dairy technology. Freising, Germany: A. Kessler Verlag.

[162] Floury, J., Desrumaux, A., & Lardieres, J. (2000). Effect of high pressure homogenization on droplet size distributions and rheological properties of model oil-in-water emulsions. Innovative *Food Science and Emerging Technologies, 1, 127–134.*

[163] Diels, A. M. J., Callewaert, L., Wuytack, E. Y., Masschalk, B., & Michiels, W. (2005). Inactivation of Escherichia coli by high-pressure homogenisation is influenced by fluid viscosity but no by water activity and product composition. *International Journal of Food Microbiology, 101, 281–291.*

[164] Harrison, S.T.L., Chase, H.A., and Dennis, J.S. (1991). The disruption of *Alcaligenes eutrophus* by high pressure homogenization:key factors involved in the process. *Bioseparation 2:155–166.*

[165] Siddiqi, S.F., Titchener-Hooker, N.J., and Shamlou, P.A. (1997). High-pressure disruption of yeast cells: The use of scale down operations for the prediction of protein release and cell debris size distribution. *Biotechnol. Bioeng. 55:642–649.*

[166] Shirgaonkar, I.Z.S., Lothe, R.R., and Pandit, A.B. (1998). Comments on the mechanism of microbial cell disruption in high-pressure and high-speed devices. *Biotechnol. Prog. 14:657–660.*

[167] Paquin, P. (1999). Technological properties of high-pressure homogenizers: The effect of fat globules, milk proteins and polysaccharides. *Int. Dairy J. 9:329–335.*

[168] Feijoo, S. C., Hayes, W. W., Watson, C. E., & Martin, J. H. (1997). Effects of Microfluidizer Technology on Bacillus licheniformis Spores in Ice Cream Mix. *Journal of dairy science, 80(9), 2184-2187.*

[169] Diels, A. M., Callewaert, L., Wuytack, E. Y., Masschalck, B., & Michiels, C. W. (2004). Moderate Temperatures Affect Escherichia coli Inactivation by High-Pressure Homogenization Only through Fluid Viscosity. *Biotechnology progress*, *20*(5), 1512-1517.

[170] Roach, A., & Harte, F. (2008). Disruption and sedimentation of casein micelles and casein micelle isolates under high-pressure homogenization. *Innovative Food Science & Emerging Technologies*, *9*(1), 1-8.

[171] Thiebaud, M., Dumay, E., Picart, L., Guiraud, J. P., & Cheftel, J. C. (2003). High-pressure homogenisation of raw bovine milk. Effects on fat globule size distribution and microbial inactivation. *International Dairy Journal*, *13*(6), 427-439.

[172] Sandra, S., & Dalgleish, D. G. (2005). Effects of ultra-high-pressure homogenization and heating on structural properties of casein micelles in reconstituted skim milk powder. *International Dairy Journal, 15(11), 1095−1104.*

[173] Hayes, M. G., & Kelly, A. L. (2003). High pressure homogenization of raw whole milk (a) effects on fat globule size and other properties. *Journal of Dairy Research, 70(3), 297−305.*

[174] Brookman, J. S. (1975). Further studies on the mechanism of cell disruption by extreme pressure extrusion. *Biotechnology and Bioengineering*, *17*(4), 465-479.

[175] Diels, A. M., & Michiels, C. W. (2006). High-pressure homogenization as a non-thermal technique for the inactivation of microorganisms. *Critical reviews in microbiology*, *32*(4), *201-216.*

[176] Donsì, F., Ferrari, G., Lenza, E., & Maresca, P. (2009). Main factors regulating microbial inactivation by high-pressure homogenization: Operating parameters and scale of operation. *Chemical Engineering Science*, *64*(3), 520-532.

[177] Innings, F., & Trägårdh, C. (2007). Analysis of the flow field in a high-pressure homogenizer. *Experimental Thermal and Fluid Science*, *32*(2*),* 345-354.

[178] Joscelyne, S. M., & Trägårdh, G. (2000).Membrane emulsification—a literature review. *Journal of Membrane Science*, *169(1), 107-117.*

[179] Iordache, M., & Jelen, P. (2003). High pressure microfluidization treatment of heat denatured whey proteins for improved functionality. *Innovative Food Science & Emerging Technologies*, *4*(4), 367-376.

[180] Kelly, W. J., & Muske, K. R. (2004). Optimal operation of high-pressure homogenization for intracellular product recovery. *Bioprocess and biosystems engineering*, *27*(1), 25-37.

[181] Gogate, P. R., Shirgaonkar, I. Z., Sivakumar, M., Senthilkumar, P., Vichare, N. P., & Pandit, A. B. (2001). Cavitation reactors: efficiency assessment using a model reaction. *AIChE Journal*, *47*(11), 2526-2538.

[182] Balasundaram B, and Harrison, S.T.L. (2006). Disruption of Brewers' yeast by hydrodynamic cavitation: process variables and their influence on selective release. Biotech Bioeng; 94(2).

[183] Keshavarz–Moore, E., Hoare, M., and Dunnill, P.(1990). Disruption of baker's yeast in a high–pressure homogenizer: New evidence on mechanism. *Enzyme Microbial Technol.* 12:764–770.

[184] Engler, C. R., & Robinson, C. W. (1981). Disruption of Candida utilis cells in high pressure flow devices. *Biotechnology and Bioengineering*, *23*(4), 765-780.

[185] Middelberg, A.P.J., O'Neill, B.K., and Bogle, I.D.L. 1991. A novel technique for the measurement of disruption in high–pressure homogenization: Study on *E. coli* containing recombinant inclusion bodies. *Biotechnol. Bioeng.* 38:363–370.

[186] Save, S.S., Pandit, A.B., and J.B. Joshi. (1994). Microbial cell disruption—role of cavitation. *Chem. Eng. J. Biochem. Eng. J.* 55:B67–B72.

[187] Miller, J., Rogowski, M., and Kelly, W. (2002). Using a CFD model to understand the fluid dynamics promoting *E. coli* breakage in a high-pressure homogenizer. *Biotechnol. Prog.* 18:1060–1067.

[188] Phipps, L. W. (1975). The fragmentation of oil drops in emulsions by a high-pressure homogenizer. *Journal of Physics D: Applied Physics*, *8*(4), 448.

[189] Kleinig, A. R., & Middelberg, A. P. (1996). The correlation of cell disruption with homogenizer valve pressure gradient determined by computational fluid dynamics. *Chemical Engineering Science*, *51*(23), 5103-5110

[190] Shamlou, P.A., Siddiqi, S.F., and Titicherner–Hooker, N.J. (1995). A physical model of high-pressure disruption of bakers' yeast cells. *Chem. Eng. Sci.* 50:1383–1391.

[191] Kleinig, A.R., Mansell, C.J., Nguyen, Q.D., Badalyan, A., and Middelberg, A.P.J. (1995). Influence of broth dilution of the disruption of *Escherichia coli*. *Biotechnol. Technol.* 9:759–762.

[192] Stevenson, M.J., and Chen, X.D. (1997). Visualization of the flow patterns in a high-pressure homogenizing valve using a CFD package. *J. Food Eng.* 33:151–165.

[193] Floury, J., Desrumaux, A., & Legrand, J. (2002). Effect of Ultra-high-pressure Homogenization on Structure and on Rheological Properties of Soy Protein-stabilized Emulsions. *Journal of food science*, *67*(9), 3388-3395. **[**194**]**

[194] Spiden, E. M., Scales, P.J., Kentish, S.E., Martin, G.J.O., (2013). Critical analysis of quantitative indicators of cell disruption applied to Saccharomyces cerevisiae processed with an industrial high pressure homogenizer. Biochemical Engineering Journal, 70, 120-126

[195] Shynkaryk, M.V., Lebovka, N.I., Lanoisellé, J.-L., Nonus, M., Bedel-Clotour, C., Vorobiev, E. (2009). Electrically-assisted extraction of bio-products using high pressure disruption of yeast cells (Saccharomyces cerevisiae). Journal of Food Engineering, 92, 189-195

[196] Yap, B.H.J., Dumsday, G.J., Scales, P.J., Martin, G.J.O. (2015). Energy evaluation of algal cell disruption by high pressure homogenisation. Bioresource Technology Journal, 184, 280-285.

[197] Spiden, E. M., Yap, B.H.J., Hill, D.R.A., Kentish, S.E., Scales, P.J. (2013). Quantitative evaluation of the ease of rupture of industrially promising Microalgae by high pressure homogenisation. Bioresource Technology Journal. 140, 165-171

[198] Braun R (2007). Anaerobic digestion: a multi-faceted process forenergy, environmental management and rural development. In: Ranalli P (ed) Improvement of crop plants for industrial end uses. Springer, Dordrecht pp. 335–415.

[199] Hammerschmidt, A., Boukis, N., Galla, U., Dinjus, E., & Hitzmann, B. (2011). Conversion of yeast by hydrothermal treatment under reducing conditions. *Fuel*, *90*(11), 3424-3432.

[200] Lamoolphak, W., Goto, M., Sasaki, M., Suphantharika, M., Muangnapoh, C., Prommuag, C., & Shotipruk, A. (2006). Hydrothermal decomposition of yeast cells for production of proteins and amino acids. *Journal of hazardous materials*, *137*(3), 1643-1648.

[201] Fernandez, V. E., Palazolo, G. G., Bosisio, N. A., Martínez, L. M., & Wagner, J. R. (2012). Rheological properties and stability of low-in-fat dressings prepared with high-pressure homogenized yeast. *Journal of Food Engineering*, *111*(1), 57-65.

[202] Mauri Product Limited. (Supplier: Dublin Food Sales). Pinnacle yeast, Hull HU7 0XW, England, UK. Available at: <www.abmauri.com >

[203] Enfors, S. O., Hedenberg, J., & Olsson, K. (1990). Simulation of the dynamics in the baker's yeast process. *Bioprocess engineering*, *5*(5), 191-198.

[204] Heredia-Arroyo, T., Wei, W., Ruan, R., & Hu, B. (2011). Mixotrophic cultivation of *Chlorella vulgaris* and its potential application for the oil accumulation from non-sugar materials. *Biomass and Bioenergy*, *35*(5), 2245-2253.

[205] Abreu, A. P., Fernandes, B., Vicente, A. A., Teixeira, J., & Dragone, G. (2012). Mixotrophic cultivation of *Chlorella vulgaris* using industrial dairy waste as organic carbon source. *Bioresource technology*, *118*, 61-66.

[206] Kong, W., Song, H., Cao, Y., Yang, H., Hua, S., & Xia, C. (2013). The characteristics of biomass production, lipid accumulation and chlorophyll biosynthesis of Chlorella vulgaris under mixotrophic cultivation. *African Journal of Biotechnology*, *10*(55), 11620-11630.

[207] Chlorella vulgaris. Culture collection of Algae Protozoa (CCAP), Scottish Marine Institute, Oban Argyll, PA37 1QA, Scotland, UK. <www.ccap.ac.uk >

[208] Characteristics of Deionised Water. Available at: <www.pro-analitika.hu/characteristics_of_deionized_water.pdf >(Accessed August, 2015)

[209] Protein Reagent and information. Available at: < www.Sigma-Aldrich.com> (Accessed August, 2015)

[210] Pierce protein biology products. Chemistry of protein assays. Available at: <http://www.piercenet.com/method/chemistry-protein-assays > (Accessed August, 2015)

[211] Montgomery, D. C. (1984), *Design and Analysis of Experiments.* (2nd ed.), John Wiley & Sons, New York.

[212] *Design-Expert software 8.0 user's guide.* (2010) Technical manual. ed., Stat-Ease Inc., Minneapolis, USA.

[213] Box, G. E. P., & Wilson, K. B. (1951). On the experimental attainment of optimum conditions. *Journal of the Royal Statistical Society. Series B (Methodological)*, *13*(1), 1-45.

[214] Khuri, A. I., & Cornell, J. A. (1996). *Response surfaces: designs and analyses* (Vol. 152). CRC press.

[215] Box, G. E., & Behnken, D. W. (1960). Some new three level designs for the study of quantitative variables. *Technometrics*, *2*(4), 455-475.

[216] Box-Behnken designs, Engineering Statistics Handbook. Available at: <http://www.itl.nist.gov/div898/handbook/pri/section3/pri3362.htm> (Accessed August, 2015)

[217] Montgomery, D. C., & Myers, R. H. (1995). Response surface methodology: process and product optimization using designed experiments. *Raymond H. Meyers and Douglas C. Montgomery. A Wiley-Interscience Publication*.

[218] Baldwin, C. V., & Robinson, C. W. (1994). Enhanced disruption of Candida utilis using enzymatic pretreatment and high-pressure homogenization. *Biotechnology and bioengineering*, *43*(1), 46-56.

[219] Vachon, J. F., Kheadr, E. Essier., Giasson, J., Paquin, P., & Fliss, I. (2002). Inactivation of foodborne pathogens in milk using dynamic high pressure. *Journal of Food Protection*, *65*(2), 345-352.

[220] Liu, D., Zeng, X. A., Sun, D. W., & Han, Z. (2013). Disruption and protein release by ultrasonication of yeast cells. *Innovative Food Science & Emerging Technologies*, *18*, 132-137.

[221] Delsa Nano C for Dynamic Light Scattering Measurement. Available online at: <https://ssl.arcor-secure.de/iuta.de/files/sop_dynamic_light_scattering.pdf.> (Accessed August, 2015).

[222] Floury, J., Desrumaux, A., Axelos, M. A., & Legrand, J. (2003). Effect of high pressure homogenisation on methylcellulose as food emulsifier. *Journal of Food Engineering*, *58*(3), 227-238.

[223] Delsa nano submicron particle size and zeta potential user's manual. Serial No: PN A54412AC (May 2011). Available online at: < www.beckmancoulter.com> (Accessed August, 2015)

[224] <www.seai.ie> (Accessed August, 2015).

[225] Benyounis, K.Y., Olabi, A. G., Hashmi, M. S. J., (2008). Multi-response optimization of CO2 laser-welding process of austenitic stainless steel. Opt Laser Technol; 40(1):76-87.

[226] Eltawahni, H. A., Olabi A. G., Benyounis, K. Y., (2010). Effect of process parameters and optimization of CO2 laser cutting of ultra high-performance polyethylene. Mater Des; 31(8):4029-38.

[227] Ekpeni, L. E. N., Benyounis, K. Y., Nkem-Ekpeni, Fehintola F., Stokes, J., Olabi, A.G., (2015). Underlying factors to consider in improving energy yield from biomass source through yeast use on high-pressure homogenizer (HPH), Energy, 81, 74-83. ISSN 0360-5442, *DOI:10.1016/j.energy.2014.11.038*

[228] Hetherington P. J., Follows, M., Dunhill, P., Lilly, M.D. (1971). Release of protein from bakers' yeast. Trans Inst Chem Eng; 49:142–148.

[229] Lovitt, R.W., Jones, M., Collins, S.E., Coss, G.M., Yau, C.P., Attouch C. (2000). Disruption of bakers' yeast using a disrupter of simple and novel geometry. Process Biochemistry. 36, 415–421.

[230] www.researchgate.net/publictopics.PublicPostFileLoader.html?id (jmp_DOE_guide) (Accessed August, 2015)

[231] *Design-Expert Software, Version 7,* (2005). User's Guide, Technical Manual‖, Stat-Ease Inc., Minneapolis, MN, USA.

Appendices

Appendix A:

Microalgae (Chlorella vulgaris) supply information

Strain Number:	**CCAP 211/11B**
Strain name:	*Chlorella vulgaris*
Author:	Beijerinck 1890
Synonyms:	
Collection place:	Freshwater; Delft, Holland
Isolated by:	Beijerinck 1892
Type material:	No
Other permanent collections:	SAG 211-11b; UTEX 259; IAM C-207; UTCC 111
Culture medium:	3N-BBM+V; EG:JM; Axenic. Media recipes are available on our website: www.ccap.ac.uk
Subculture interval:	
Culture conditions:	15°C ± 2°C (for faster growth, grow at 20-25°C; cool white fluorescent tubes about 10 cm from the culture, with an intensity of 30-40 µmol m-2 s-1; 12 hr light : 12 hr dark (for faster growth, use continuous light)

Liquid algae in tubes:
The algae should survive for at least 1-2 weeks, however it is advisable to subculture it as soon as possible. Normally, 2-5 ml of culture is inoculated into 50 ml of fresh sterile medium. Unless noted above, prior to despatch the culture will have been stored at 15°C - 20°C, cool white fluorescent lighting about 10 cm from the culture, with an intensity of approx. 40 $\mu mol\ m^{-2}\ s^{-1}$ (10-15 µmol for cyanobacteria); 12 hr light : 12 hr dark. If such facilities are unavailable, placing the tube in a north facing window at room temperature should suffice.

Algae on agar slopes:
Algae grown on agar slopes are sent as single tubes. Immediately before despatch, the cultures have been kept at CCAP under the following conditions (unless noted above): 15°C - 20°C, cool white fluorescent lighting about 10 cm from the culture, with an intensity of approx. 40 $\mu mol\ m^{-2}\ s^{-1}$ (10-15 µmol for cyanobacteria); 12 hr light : 12 hr dark. If such facilities are unavailable, placing the tube in a north facing window at room temperature should suffice. If maintained in suitable conditions, the culture should survive for about 4 weeks before it requires subculturing.

Special features:	recommended in ecotoxicity testing directive 87/302/EEC
Size in µm:	
Original designation:	
Other Information:	Syn. C. candida Shihira & Kraus

Please Note: There may be additional information available on certain strains which can be provided on application

CCAP (Culture Collection of Algae and Protozoa), Scottish Marine Institute, Oban, Argyll, PA37 1QA, UK
Tel: +44 (0)1631 559000 Fax: +44 (0)1631 559001 Email: ccap@sams.ac.uk Web: www.ccap.ac.uk

Hazard Group 1 Safety data sheet
To accompany organisms not assigned to hazard groups 2-4

Date of issue: March 1999

Information on supplied Cultures as required under COSHH regulations and HSW Acts 6(4)(c)

The culture(s) supplied (as listed on the enclosed Delivery Note) are not categorised as Risk Group 2, 3 or 4 under EU Directive 90/679/EEC; Classification of Biological Agents, and implemented in the UK through The Advisory Committee on Dangerous Pathogens, and therefore fall into Risk Group 1, i.e. a biological agent that is most unlikely to cause human disease. However, all microorganisms should be handled with care.

·   Avoid all contact with the organism, growth media or materials on which they have grown.

To avoid these possible hazards and reduce the risk in handling, normal aseptic microbiological techniques should be employed.

All parcels containing microorganisms should be opened in a laboratory with Containment Level 1 as described by the Advisory Committee on Dangerous Pathogens (*Categorisation of pathogens according to hazard and categories of containment*, 4 edition London HMSO) and summarised below.

CONTAINMENT LEVEL 1

Containment level 1 is suitable for work with organisms of hazard group 1. Laboratory personnel must have received instruction in the procedures conducted in the laboratory.

1.   The laboratory should be easy to clean. Bench surfaces should be impervious to water and resistant to acids, alkalis, solvents and disinfectants.

2.   If the laboratory is mechanically ventilated, it is preferable to maintain an inward airflow into the laboratory by extracting room air to the atmosphere.

3.   The laboratory must contain a wash-basin or sink that can be used for hand washing.

4.   The laboratory door should be closed when work is in progress.

5.   Laboratory coats or gowns should be worn in the laboratory and removed when leaving the laboratory suite.

6.   Eating, chewing, drinking, smoking, storing of food and applying cosmetics must not take place in the laboratory.

7.   Mouth pipetting must not take place.

8.   Hands must be disinfected or washed immediately when contamination is suspected, after handling viable materials, and also before leaving the laboratory.

9.   All procedures must be performed so as to minimise the production of aerosols.

10.   Effective disinfectants must be available for immediate use in the event of spillage.

11.   Bench tops should be cleaned regularly after use.

12.   Used laboratory glassware and other materials awaiting sterilisation must be stored in a safe manner. Pipettes if placed in disinfectant, must be totally immersed.

13. All waste material which is not to be incinerated should be rendered non-infective before disposal.

14. Materials for disposal must be transported in robust containers without spillage.

15. All accidents and incidents must be reported.

Opening cultures and ampoules : all parcels containing microorganisms must be opened in a laboratory by trained personnel and, ideally, in a cabinet that will prevent inhalation of aerosols.

Details of suitable media, incubation temperatures for the growth of the strains and any known special hazard are given with the strain(s) supplied.

Transport : if the materials are to be transported to another laboratory they should be packaged with enough absorptive material to absorb all contents of the containers in case of breakage. They should be placed in containers that will prevent breakage and all postal regulations of the recipient country must be followed

Disposal : all cultures, media and containers should be sterilised by autoclaving at 121°C for 15 min before disposal by suitable means such as incineration.

Procedures in case of spillage : if the culture is spilt or its container broken, thoroughly wet with a disinfectant, such as 4% sodium hypochlorite, and allow 30 min before swabbing up and transferring into a container for autoclaving.

Delivery Note No: 507611/1

Delivery Note Date:	26/05/2014
CCAP Order Number:	507611
Customer ID:	8283
Your VAT Number:	
Your Purchase Order:	

culturecollection
of algae and protozoa

SAMS Research Services Ltd
Scottish Marine Institute
Dunbeg, OBAN
Argyll PA37 1QA
Scotland

Tel:	+44 (0)1631 559000
Fax:	+44 (0)1631 559001
Email:	ccap@sams.ac.uk

VAT Reg No: GB 828 9579 61

Delivery To: Dublin City University
Sch of Mechanical & Manufacturing Engineering
Collins Avenue
Glasnevin
Dublin 9
Ireland
Attn: Mr L Ekpeni

Item	Description	Quantity
1 CCAP 211/11B	Chlorella vulgaris	4

Delivery Comments:

If any culture arrives in unsatisfactory condition it will be replaced free of charge if CCAP is informed within 14 days of receipt, preferably by returning the enclosed Customer Feedback Questionnaire.

Please note our payment terms are 30 days.

Intrastat Details for Cultures only:
Commodity Code : 30029050
Delivery Terms : CIF
Net mass : approx 40g
Mode of Transport : air
Country of Origin : United Kingdom

The Scottish Association of Marine Science (SAMS) is registered in Scotland as a Company Limited by Guarantee (SC009292) its registered office is Scottish Marine Institute, Oban, Argyll PA37 1QA. SAMS is a charity registered in Scotland (9206).

CCAP Customer Feedback Questionnaire

Feedback Form Date: 26/05/2014
CCAP Delivery Number: 507611/1
Customer ID: 8283
Your VAT Number:
Your Purchase Order:

culturecollection
of algae and protozoa

Department: UAD
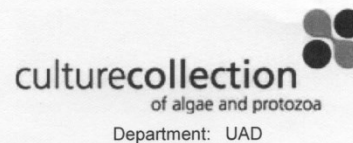
Return To:	Culture Collection of Algae and Protozoa
	SAMS Research Services Ltd
	Scottish Marine Institute
	Dunbeg, OBAN
	Argyll PA37 1QA
	Scotland

Tel: +44 (0)1631 559000
Fax: +44 (0)1631 559001
Email: ccap@sams.ac.uk

CCAP welcomes all feedback about customer orders, and we are pleased to hear any additional comments which may help us to improve the service we offer. If any culture arrives in unsatisfactory condition it will be replaced free of charge if CCAP is informed within 14 days of receipt. Please complete this questionnaire and return to the address above.

Item		Description	Quantity
1	CCAP 211/11B	Chlorella vulgaris	4

Date Despatched: 26/05/2014   **Carriage:** Int'l Tracked & Signed/Int'l Signed   **Date Received:** ....

1. Use for which the cultures have been purchased: ....
   ....

2. If research, please indicate line of research: ....
   ....

3. Was the volume of culture received sufficient for your purpose? ....
   ....

4. Was the condition of the culture satisfactory on arrival? ....
   ....

5. Other Comments: ....
   ....
   ....

Name: ....

Address (if different):....................................
....
....
....
.... Date:.....................

Despatched To: Dublin City University
Sch of Mechanical & Manufacturing Engineering
Collins Avenue
Glasnevin
Dublin 9
Ireland

Attention: Mr L Ekpeni

Appendix B:

Centrifuge user's guide and operation

⚠ These instructions are to be used only as a quick reference guide to centrifuge operation. We recommend that you read the centrifuge instruction manual thoroughly, particularly all WARNINGS and CAUTIONS, before operating the centrifuge.

Centrifuge Operation

1. Set the centrifuge power switch ON (the POWER light will illuminate).

2. *Prepare the rotor:* Load samples into the rotor and balance. Place the cover on the rotor. Secure the cover on fixed-angle rotors by turning the large cover locking knob counterclockwise.

3. Open the chamber door by pressing the DOOR button located just below the top deck. Install the rotor. Lock the rotor to the drive by turning the small rotor locking knob counterclockwise. Close the door.

4. Set the SPEED, TIME, and TEMPERATURE.

5. Set the BRAKE switch ON or OFF (the BRAKE switch is lit when BRAKE is ON).

6. Press the START switch (the switch will illuminate).

At the end of the run, the DOOR light on the control panel will come on to indicate the door can be opened. Press the DOOR button to open the door.

NOTE To stop a run in progress, turn the TIME dial to STOP (setting SPEED to 0 does not end a run).

Setting Temperature

The blue needle in the temperature meter selects the desired chamber temperature during a run. The red needle selects the chamber temperature while the timer is OFF (during standby or during run deceleration,), and selects maximum (overtemperature) during a run. To adjust the temperatures selected by the blue and red needles, turn the appropriate control knob (range is −20°C to +40°C).

The black needle indicates actual chamber temperature. During a run, the maximum chamber temperature allowed is +3° above the red needle setting; if the black needle exceeds this, the run will terminate.

NOTE Actual sample temperature may differ from the set or actual chamber temperatures depending on the rotor used, selected speed, ambient temperature, and efficiency of the refrigeration system. To guard against freezing or overheating samples, or when maintaining sample temperature is critical, follow the Rotor Speed/ Temperature Differential Compensation procedure in the centrifuge instruction manual.

Setting Speed

To set run speed, turn the SPEED dial to desired setting (range is 500 rpm to 21000 rpm). The speed meter indicates actual rotor speed.

Setting Time

To set run time, turn the TIME dial to the desired setting in minutes (up to 120 minutes) or to HOLD (for a continuous run). To stop a HOLD run, the dial must be turned to STOP.

Troubleshooting

If the run will not start:

- The chamber temperature is more than +3°C above the red temperature needle setting. Set the red needle to a temperature above the black needle or allow the centrifuge to cool before pressing START. OR

- The chamber door is open. OR

- The main power is OFF.

If the run terminates prematurely:

- A rotor imbalance occurred; the IMBALANCE light is on. Balance the rotor and restart. OR

- The chamber overtemperature was more than +3°C above the red temperature needle setting. Precool the rotor and centrifuge before restarting the run. If the problem still occurs, contact your service engineer. OR

- A power failure or interruption occurred. Restart the run when power is restored. OR

- No rotor was installed.

If the BRUSHES light is on: The motor brushes are worn and must be replaced. Replace brushes before starting a new run.

If the door will not open at the end of the run: Open door manually by pushing the door latch override button located next to the DOOR button with a pencil.

SORVALL®

●●Kendro
Laboratory Products

SUPERSPEED RCF CHART

These tables give the maximum RCF in g for all currently available SORVALL® rotors for superspeed applications up to 26,000 rpm.

To find the average or minimum RCF, consult your rotor instruction manual for the average or minimum radius, and use the formula given below:

$K = [2.53 \times 10^{11} \ln (R_{max}/R_{min})] / (rpm)^2$ $RCF = 11.17r \, (rpm/1000)^2$ where r = radius in centimeters

ROTOR: RADIUS, max.cm	SE-12 9.33	SA-300 9.67	SS-34 10.70	SM-24 inner 9.10	SM-24 outer 11.07	F-20/MICRO 11.51	SA-600 12.96	SLA-1000 11.77	GSA 14.56	GS-3 15.13	SLA-1500 13.59
RPM						**RCF**					
500	26	27	30	25	31	32	36	33	41	42	38
1,000	104	108	120	102	124	129	145	131	163	169	152
1,500	234	243	269	229	278	289	326	296	366	380	342
2,000	417	432	478	407	495	514	579	526	651	676	607
2,500	651	675	747	635	773	804	905	822	1,016	1,056	949
3,000	938	972	1,076	915	1,113	1,157	1,303	1,183	1,464	1,521	1,366
3,500	1,277	1,323	1,464	1,245	1,515	1,575	1,773	1,611	1,992	2,070	1,860
4,000	1,667	1,728	1,912	1,626	1,978	2,057	2,316	2,104	2,602	2,704	2,429
4,500	2,110	2,187	2,420	2,058	2,504	2,603	2,931	2,662	3,293	3,422	3,074
5,000	2,605	2,700	2,988	2,541	3,091	3,214	3,619	3,287	4,066	4,225	3,795
5,500	3,153	3,267	3,615	3,075	3,740	3,889	4,379	3,977	4,920	5,112	4,592
6,000	3,752	3,889	4,303	3,659	4,451	4,628	5,211	4,733	5,855	6,084	5,465
6,500	4,403	4,564	5,050	4,295	5,224	5,432	6,116	5,555	6,871	7,140	6,414
7,000	5,107	5,293	5,856	4,981	6,059	6,300	7,093	6,442	7,969	8,281	7,438
7,500	5,862	6,076	6,723	5,718	6,955	7,232	8,143	7,395	9,148	9,506	8,539
8,000	6,670	6,913	7,649	6,505	7,914	8,228	9,265	8,414	10,409	10,816	9,715
8,500	7,530	7,804	8,635	7,344	8,934	9,289	10,459	9,499	11,750	12,210	10,968
9,000	8,442	8,749	9,681	8,233	10,016	10,414	11,726	10,649	13,173	13,689	12,296
9,500	9,406	9,748	10,787	9,174	11,160	11,603	13,065	11,865	14,678	K = 4,203	13,700
10,000	10,422	10,801	11,952	10,165	12,365	12,857	14,476	13,147	16,264		15,180
10,500	11,490	11,909	13,177	11,207	13,633	14,174	15,960	14,495	17,931		16,736
11,000	12,610	13,070	14,462	12,299	14,962	15,557	17,516	15,908	19,679		18,368
11,500	13,783	14,285	15,806	13,443	16,353	17,003	19,145	17,387	21,509		20,076
12,000	15,007	15,554	17,211	14,637	17,806	18,514	20,846	18,932	23,419		21,859
12,500	16,284	16,877	18,675	15,882	19,321	20,089	22,619	20,542	25,412		23,719
13,000	17,613	18,254	20,199	17,178	20,897	21,728	24,465	22,219	27,485		25,654
13,500	18,993	19,686	21,782	18,525	22,536	23,431	26,383	23,961	K = 2,023		27,666
14,000	20,426	21,171	23,426	19,923	24,236	25,199	28,374	25,768			29,753
14,500	21,911	22,710	25,129	21,371	25,998	27,031	30,436	27,642			31,916
15,000	23,449	24,303	26,892	22,871	27,822	28,928	32,572	29,581			34,155
15,500	25,038	25,950	28,714	24,421	29,707	30,888	34,779	31,586			K = 1,475
16,000	26,679	27,652	30,597	26,022	31,655	32,913	37,059	33,657			
16,500	28,373	29,407	32,539	27,673	33,664	35,002	39,412	35,793			
17,000	30,118	31,216	34,541	29,376	35,735	37,156	41,837	K = 1,725			
17,500	31,916	33,079	36,603	31,129	37,868	39,374	K = 747				
18,000	33,766	34,997	38,724	32,934	40,063	41,656					
18,500	35,668	36,968	40,905	34,789	42,320	44,002					
19,000	37,622	38,993	43,146	36,695	44,638	46,413					
19,500	39,628	41,072	45,447	38,651	47,019	48,887					
20,000	41,686	43,206	47,808	40,659	49,461	51,427					
20,500	43,797	45,393	50,228	42,717	51,965	K = 187					
21,000	45,959	47,634	K = 714	K = 591	K = 434						
21,500	48,174	49,929									
22,000	50,441	52,279									
22,500	52,759	54,682									
23,000	55,130	57,139									
23,500	57,553	59,651									
24,000	60,028	62,216									
24,500	62,556	64,835									
25,000	65,135	67,509									
25,500	67,767	K = 573									
26,000	70,450										
	K = 335										

TO ORDER, CALL 1-800-522-SPIN (7746)

F-11

F

Only trained users are allowed to use the Sorvall RC-5B Centrifuge.
Rotors must be signed out on sheet provided in the prep. Lab.
All users should sign the logbook at the instrument and report any problems to the supervisor (Teresa Cooney/ Allison Tipping) at ext.5138/ 5771

Training

1.1 Training will be provided to all new users by the supervisor.
1.2 A demonstration of operation of the centrifuge will be given, working through the SOP. The new user will operate the instrument while being supervised and a training record sheet signed off when the supervisor is happy with the level of competency achieved.
1.3 All records of training are stored in the file labelled Training Records in XG51c.
1.4 Please contact Teresa Cooney / Allison Tipping at ext. 5138/5771 for training.

Centrifuge Operation

2.1 Set the POWER switch to ON.
2.2 Push the DOOR button and open the chamber door.
2.3 Load and balance the rotor.
2.4 Wipe surfaces clean before each operation to reduce the chance of the rotor sticking to the spindle.
2.5 Install the rotor. Lock to the drive by turning lid anti-clockwise.
2.6 Close the chamber door.
2.7 Set the TEMPERATURE needles to the desired settings.

> *NOTE*   If the chamber temperature is below room temperature and the rotor has not been precooled, allow time for the rotor to cool to the chamber temperature before locking it in place.

2.8 Turn the TIME dial to the desired run time setting.
2.9 Turn the SPEED dial to the desired run speed setting.
3.0 If you want the rotor to brake at the end of the run, set the brake ON by pressing the BRAKE. Press the switch so that the light is on.
3.1 Press the START switch. The centrifuge will accelerate to the selected speed and run for the selected time. The run will coast to a stop when the time expires.

NOTE   If it is necessary to stop the rotor before the selected time has elapsed, always turn the TIME control dial to STOP. DO NOT stop the rotor by turning the SPEED dial to 0 rpm.

3.2 When the rotor has decelerated below 100rpm, the DOOR light will turn on. The chamber door can then be opened by pushing the DOOR button and lifting the door handle. Remove the rotor.

Rotor Loading and Balancing

4.1 The rotor can be operated with either a full or less than full complement of tubes as long as the load is properly balanced.
4.2 Operating the rotor out of balance can cause damage to the centrifuge drive.
4.3 The load in each opposing rotor compartment, including adapters (where applicable), tube, and specimen must be properly balanced within five grams.
4.4 Centrifuge tubes should be no more than ¾ filled. Overfilled tubes will cause spillages.

Cleaning / Spillages

5.1 Wash the rotor with warm water and a mild soap once a week. It is particularly important to wash the rotor immediately after any spills have occurred..
5.2 Use 70% alcohol to disinfect the rotor and/or its components.

Storage

6.1 After the rotor has been cleaned and dried, it should be stored upside-down, with cover and tubes removed; this will prevent moisture from settling at the bottom of the tube compartments, and will allow air to circulate.

School of Biotechnology	E 10
Procedures Manual	Sheet 3 of 3
	Issue No:2
Section Title Equipment Operation Procedures	Issue Date: 28 April 2008
Operation of Sorvall RC- 5B Plus Centrifuge	Compiled by: T.Cooney / Allison Tipping Reviewed by: T.Cooney 19/7/2010

Maintenance

7.1 The Sorvall RC-5B is covered by a Preventative Maintenance Contract with Unitech. Calibration is carried out twice a year.

7.2 General maintenance is carried out by the supervisor on a monthly basis.

7.2 The centrifuge and rotors are washed with warm water and a mild soap.

7.3 All o-rings on rotors are checked and replaced if damaged.

7.4 The supervisor will conduct a test run of the instrument weekly to check for any faults.

Records

8.1 Service Reports are kept in the file Equipment Records in XG 51c.

Service and Repair

9.1 Contact Unitech 014048300

Manuals

10.1 For further information please refer to Sorvall operating instructions, kept in XG51c

Appendix C:

Water deionization information

WATERMAN DE-IONISING WATER PURIFICATION SYSTEM

De-ionisation or Ion exchange is a chemical process whereby charged impurities are taken into the ion exchange resin and replaced in solution by water molecules. The waterman system uses exchangeable mixed bed resins in its ion exchange process. The product water quality is better than 1 microsiemen/cm (Note:1 microsiemen/cm = 0.6 ppm of total dissolved solids)

Details of WP8 Waterman De-ionising unit

Flow rate	1.2 m³/hr
Capacity	5000 litres
Vessel size	8 x 25"
Inlet / outlet	¾"
Weight	26kg
Max. operating pressure	5 Bar

The exchangeable mixed bed resin needs changing when the resistivity meter indicator light turns red. A green light indicates that the resin quality is still good
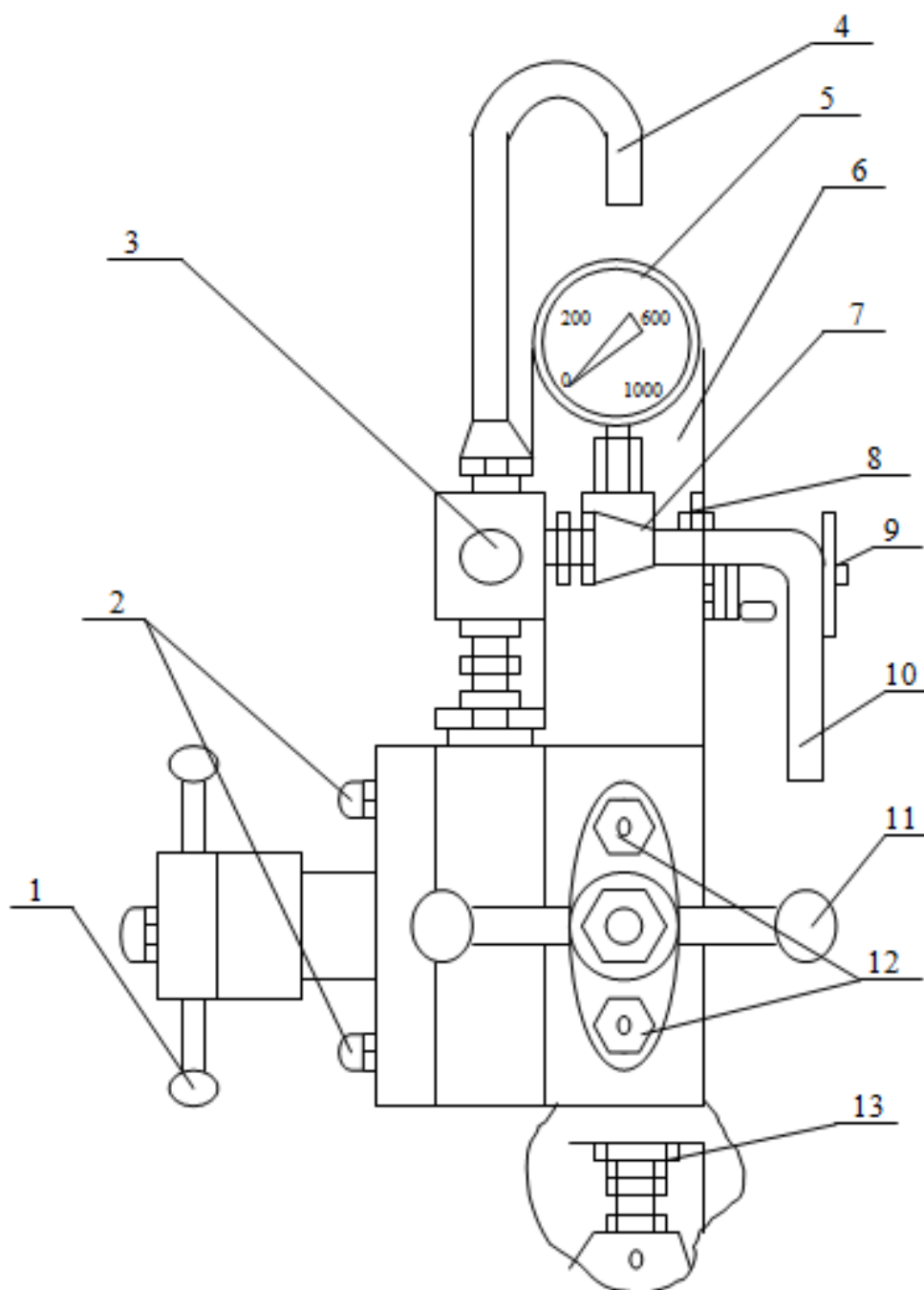
Resin change required

Resin quality good

Appendix D:

**The Outline Sketch of GYB40-10S/ GYB60-6S 2-Stage Homogenizing Valves of HPH**

1、2nd stage hand   2、Screw nut   3、Cross valve   4、Return pipe
5、Pressure gauge   6、Hopper   7、Screw nut   8、Screw nut
8、Relief lever   10、Discharge pipe   11、1st stage hand   12、Screw nut
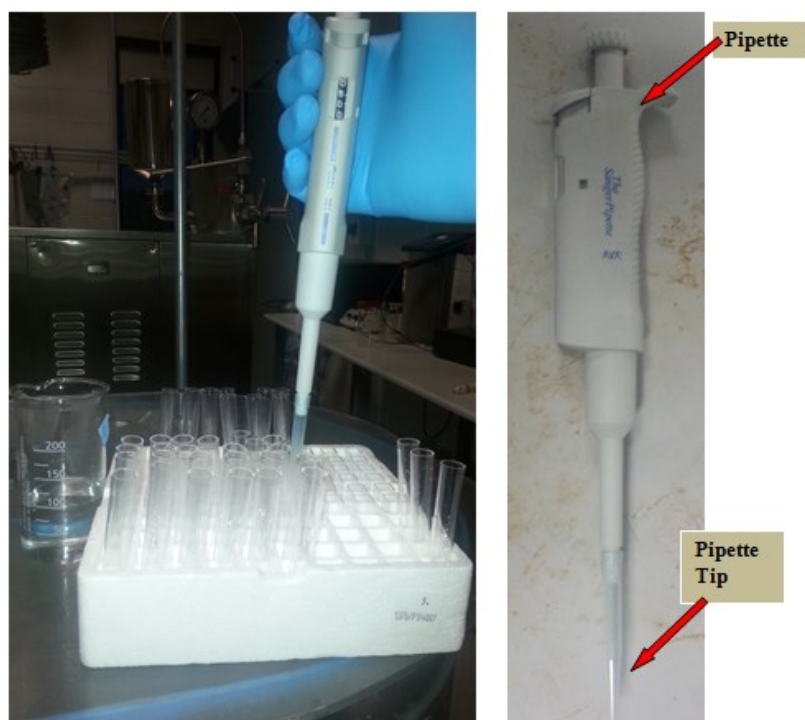13、Screw nut

Appendix E:
Laboratory Glassware

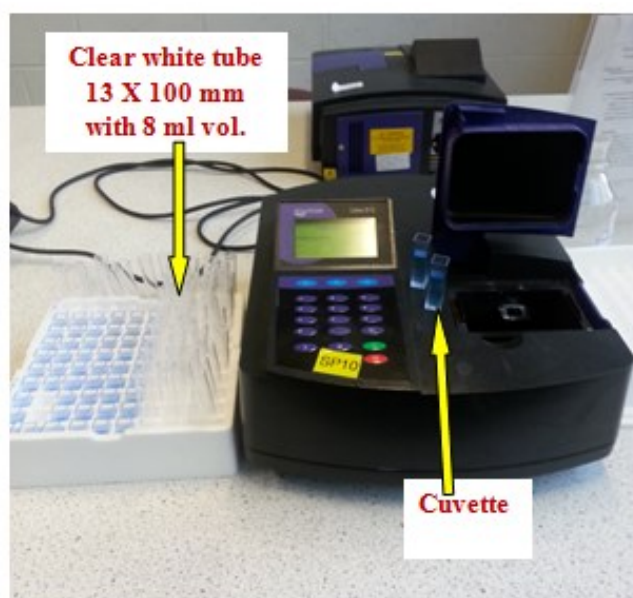**Figure E1:** Syringe and filter for particle separation from the centrifugated biomass substrates
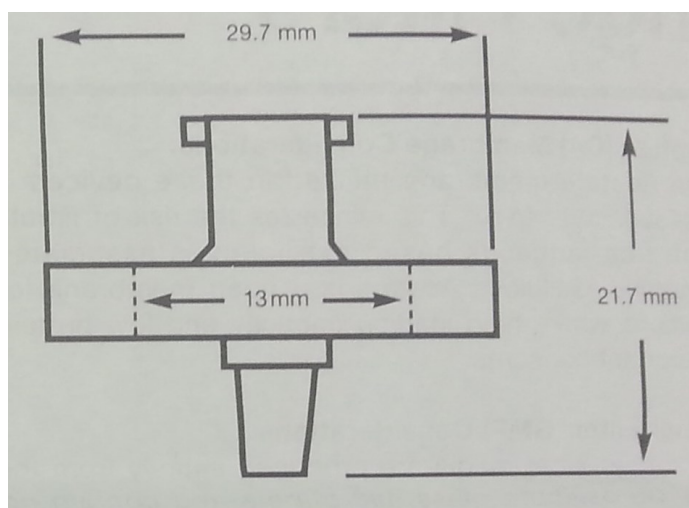
Figure E2: Schematic view of WHATMAN 0.2 μm PVDF filter

Figure E3: Pipette in measuring biomass solution into clear white tubes and cuvettes

Figure E4: showing cuvette with prepared solution in readiness to determine the protein concentration contained in the sample

Figure E5: 100 mL measuring cylinder for dilution ratio measurement and beaker with homogenized yeast
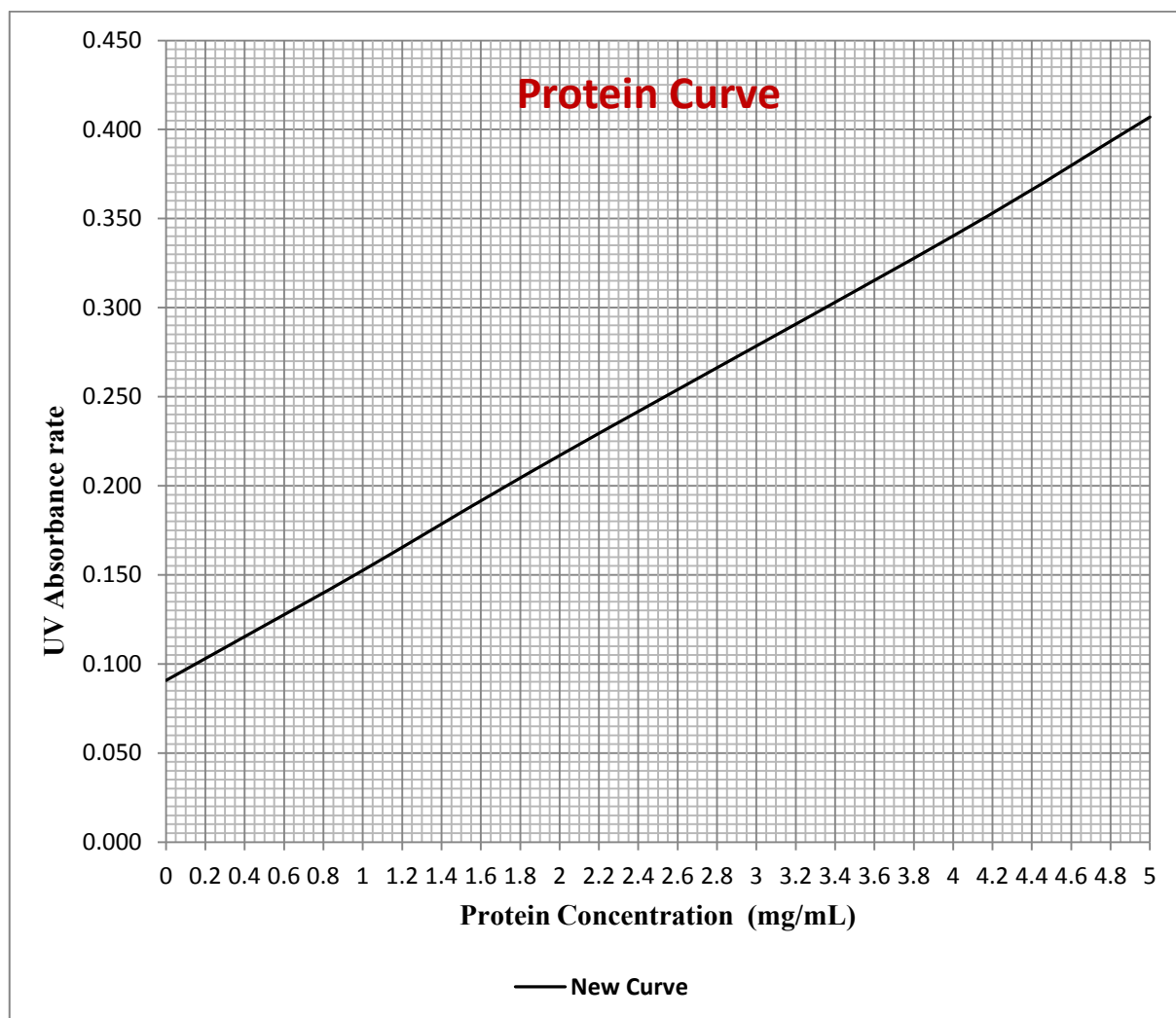

Figure E6: Round-bottom flask for measuring quantified solution in the preparation of buffer solution

Figure E7: pH 4.01 and 7.01 buffer solution (±0.01 pH @25 °C)

Appendix F:
Developed Protein Curve for Protein Analysis

Applying the linear graph equation; $y = MX + C$

Wherein;   y = Value on y-axis = (UV Absorbance rate)

   X = Value on x-axis = (Protein Concentration in mg/mL)

   M = Slope/Gradient = Change in y/Change in x = 0.062

   C = Intercept = (0.09)

Putting in the values implies;

(UV Absorbance rate) = 0.062 (Protein Concentration in mg/mL) + 0.09

(Protein Concentration in mg/mL) = [(UV Absorbance rate) – 0.09]/0.062

$$X = \frac{[y - C]}{M}$$

Appendix G:
Design of Experiment Equations

G1: Equations for Design Analysis

Sum of Squares –total =
$$SS_T = \sum_{i=1}^{n} (y_i - \bar{y})^2 \tag{3-9}$$

Sum of Squares- model =
$$SS_M = \sum_{i=1}^{n} (\hat{y}_i - \bar{y})^2 \tag{3-10}$$

Sum of Squares –Residuals =
$$SS_R = \sum_{i=1}^{n} (y_i - \hat{y}_i)^2 \tag{3-11}$$

Sum of Squares-Pure error =
$$SS_{PE} = \sum_{i=1}^{n_o} (y_i - \hat{y}_i)^2, \quad \text{only for centre points} \tag{3-12}$$

$$SS_{lof} = SS_R - SS_{PE} \tag{3-13}$$

$$SS_{b_i} = b_i \sum_{i=1}^{n} x_i y_i \tag{3-14}$$

$$SS_{b_{ij}} = b_{ij} \sum x_i x_j y_i \tag{3-15}$$

$$SS_{b_{ii}} = b_0 \sum_{i=1}^{n} y_i + b_{ii} \sum_{i=1}^{n} x_i^2 y_i - (\sum y_i)^2 / n \tag{3-16}$$

G2: Equation for Testing the Adequacy of the Developed Models

$$R^2 = 1 - \left[\frac{SS_R}{SS_R + SS_M} \right] \tag{3-19}$$

$$AdjR^2 = 1 - \left[\left(\frac{SS_R}{df_R} \right) \times \left(\frac{SS_R + SS_M}{df_R + df_M} \right)^{-1} \right] \tag{3-20}$$

$$\text{Pr}\,edR^2 = 1 - \left[\frac{PRESS}{SS_R + SS_M} \right] \tag{3-21}$$

$$PRESS = \sum_{i=1}^{n} (y_i - \hat{y}_{i,-i})^2 \qquad (3\text{-}22)$$

$$Adeq.precision = \left[\frac{Max(\hat{Y}) - Min(\hat{Y})}{\sqrt{\dfrac{p \times MS_R}{n}}} \right] \qquad (3\text{-}23)$$

Where:

p = Number of model parameters (including intercept b_0)
n = number of experiments

G3: Optimization through Desirability Approach Function

- *For goal of maximum, the desirability will define by:*

$$d_i = \begin{cases} 0 & , \quad Y_i \leq Low_i \\[2ex] \left(\dfrac{Y_i - Low_i}{High_i - Low_i} \right)^{wt_i} & , \quad Low_i \langle Y_i \langle High_i \\[2ex] 1 & , \quad Y_i \geq High_i \end{cases} \qquad (3\text{-}24)$$

- *For goal of minimum, the desirability will define by:*

$$d_i = \begin{cases} 1 & , \quad Y_i \leq Low_i \\[2ex] \left(\dfrac{High_i - Y_i}{High_i - Low_i} \right)^{wt_i} & , \quad Low_i \langle Y_i \langle High_i \\[2ex] 0 & , \quad Y_i \geq High_i \end{cases} \qquad (3\text{-}25)$$

- *For goal as a target, the desirability will define by:*

$$d_i = \begin{cases} \left(\dfrac{Y_i - Low_i}{T_i - Low_i}\right)^{wt_{1i}} & , \quad Low_i \langle Y_i \langle T_i \\[3mm] \left(\dfrac{Y_i - High_i}{T_i - High_i}\right)^{wt_{2i}} & , \quad T_i \langle Y_i \langle High_i \\[3mm] 0 & , \quad Otherwise \end{cases} \qquad (3\text{-}26)$$

- *For goal within range, the desirability will define by:*

$$d_i = \begin{cases} 1 & , \quad Low_i \langle Y_i \langle High_i \\[2mm] 0 & , \quad Otherwise \end{cases} \qquad (3\text{-}27)$$

$$D = \left(\prod_{i=1}^{n} d_i^{\,r_i}\right)^{\frac{1}{\sum r_i}} = \left(d_1^{\,r_1} \times d_2^{\,r_2} \times \ldots \times d_n^{\,r_n}\right)^{\frac{1}{\sum r_i}} \qquad (3\text{-}28)$$